

A GEOCHRONOLOGIC STUDY OF METAMORPHIC ROCKS
IN NORTHEASTERN MASSACHUSETTS

by

WILLIAM JOHN OLSZEWSKI, JR.

B.A., University of Pennsylvania
(1973)

SUBMITTED TO THE DEPARTMENT OF EARTH AND PLANETARY SCIENCES
IN PARTIAL FULFILLMENT OF THE REQUIREMENTS
FOR THE DEGREE OF
DOCTOR OF PHILOSOPHY

at the

MASSACHUSETTS INSTITUTE OF TECHNOLOGY

November, 1977

Signature of Author.....
Department of Earth and Planetary Sciences
Certified by.....
Thesis Supervisor
Accepted by.....
Chairman, Departmental Committee on Graduate Studies

Lindgren
WITHDRAWN
DEC 30 1977
FROM
LIBRARIES
MAIT LIBRARIES



Room 14-0551
77 Massachusetts Avenue
Cambridge, MA 02139
Ph: 617.253.5668 Fax: 617.253.1690
Email: docs@mit.edu
<http://libraries.mit.edu/docs>

DISCLAIMER OF QUALITY

Due to the condition of the original material, there are unavoidable flaws in this reproduction. We have made every effort possible to provide you with the best copy available. If you are dissatisfied with this product and find it unusable, please contact Document Services as soon as possible.

Thank you.

Due to the poor quality of the original document, there is some spotting or background shading in this document.

A GEOCHRONOLOGIC STUDY OF METAMORPHIC ROCKS
IN NORTHEASTERN MASSACHUSETTS

by

WILLIAM JOHN OLSZEWSKI, JR.

Submitted to the Department of Earth and Planetary Sciences,
November, 1977, in partial fulfillment of the requirements
for the Degree of Doctor of Philosophy

ABSTRACT

Northeastern Massachusetts geology is characterized by a sequence of interstratified metasediments and metavolcanics intruded by igneous rocks of Precambrian and Ordovician age. These units are cut by numerous strike-slip, thrust, and reverse faults. Metamorphic grade increases from the southeast to the northwest, then drops abruptly northwest of the Clinton-Newbury Fault Zone.

The metavolcanics are dominantly mafic and intermediate flows, tuffs, agglomerates and ash falls; the metasediments are reworked volcanics and volcanoclastics, quartzites, metapelites, calc-silicate rocks and occasional carbonates. The extreme southeastern and northwestern parts of the section appear to have been deposited in shallow marine shelf environments. The central part of the section is eugeosynclinal in character.

Previous geochronological work on the intrusive rocks has implied an Ordovician or older age for the stratified units. If a continuous sequence east of the Clinton-Newbury Fault Zone is assumed, a Precambrian age is likely, as the lower portion of the sequence is intruded by the Precambrian Dedham Granodiorite.

Zircons from a number of the units west of the Clinton-Newbury can be divided into two groups based on sample lithology, zircon morphology, U-Pb behavior and the ages of the zircons. The first group is a suite of euhedral and sub-

hedral zircons from the Fishbrook and Shawsheen Gneisses, which are interpreted as primary igneous zircons. Concordia plots of these zircons yield an upper intercept age of 742 m.y. The second group of zircons are rounded to subrounded grains of detrital origin from the Westboro Formation, Shawsheen Gneiss and possibly the Nashoba Formation. The upper Concordia intercept age for these zircons is 1.55 b.y., although scatter in the data suggests a range of 1.3-1.9 b.y.

Both groups underwent a final period of episodic lead loss about 275 m.y. ago. This age agrees with K-Ar dates and Pb- α and radiation damage ages from zircons in the plutonic rocks. Episodic lead loss was strongly controlled by the uranium and thorium induced radiation damage in the zircons.

Rb-Sr whole rock analyses show that the Rb-Sr systems were reset about 480 m.y. ago. This coincides with the beginning of a major period of metamorphism and igneous intrusion. The whole rock analyses fall into two groups of similar age but different initial Sr isotope ratios. The upper group (0.713-0.714) is composed mainly of metasediments, the lower group (0.705-0.707) is dominantly composed of metavolcanics. An upper mantle or lower crustal source for the volcanics is suggested.

The U-Pb and Rb-Sr data together with geologic information indicate the following history: Eugeosynclinal development in the late Precambrian (750-620 m.y.) with effusion of volcanics and deposition of sediments derived from an older source. Intrusion of igneous rocks and possibly partial cratonization in the latest Precambrian and earliest Cambrian (620-570 m.y.) was followed by deposition of Cambrian and Ordovician shallow marine sediments. The sequence was strongly metamorphosed and intruded 430-480 m.y. ago (Taconic Orogeny). A later, less intense thermal event is indicated for the Permo-Carboniferous (240-280 m.y.).

Thesis supervisor: Patrick M. Hurley

Title: Senior Lecturer in Geology

Acknowledgements

Despite the abysmal scientific content and potent ab-dominally disruptive qualities of this paper (conditions which, by necessity as well as being points of truth and honor, must be ascribed totally to the author), a number of people must be warmly thanked, as their comments, criticisms, and aid have prevented this promontory of agricultural by-product from becoming a disaster of astronomical proportions, as well as a crime against God and man.

First and foremost, I must thank my advisor, Prof. Patrick M. Hurley. This, of course, is an honor accorded to all advisors, but Prof. Hurley must be particularly applauded, not only for his intestinal stamina (and I truly believe, his gambling spirit) in taking the author on as his student, but also for allowing the author the freedom to make an extraordinarily large number of mistakes and, thereby, to learn a great deal in the process. His ability to stand by non-chalantly as I practiced a sort of "back of the comic book" knowledge of electronics and engineering on a rather sophisticated piece of analytical equipment never ceases to amaze me. It was a form of education which, though unstructured, swiftly pushed the author onto the exponential part of the learning curve (previously the author was on the linear part - with negative slope).

Next, I must thank Prof. Richard S. Naylor who provided transportation during early field trips, as well as providing a number of thin sections and a great deal of "inside" information. The author apologizes if some of this information has found its way, subconsciously of course, into this mighty tome without proper credit. The author has always believed, however, that plagiarism is the sincerest (if not the most dangerous) form of flattery.

In addition, I must thank Profs. S.R. Hart and H.E. Gaudette for reading the rough (a euphemism, to be sure) draft of this inelegant essay. The usefulness of their comments and criticisms was only exceeded by their ability to prevent regurgitation of their victuals during crucial (again euphemism) points in the narrative. Prof. Gaudette must also be thanked for removing the specter of unemployment following the author's termination (yes, I believe that to be the correct term) of activities at M.I.T. This has lightened considerably the burden of concocting (again the correct term) this study on the effects of vertigo.

A debt of gratitude goes to Donald C. Alvord and Kenneth G. Bell, formerly of the U.S.G.S. office in Boston, for providing a number of important samples, as well as lending guidance and advice during the early field work. The importance of this contribution is placed in proper context by the fact that the author's lack of navigational sense or ability is easily surpassed by his habit of unconsciously walking over outcrops that would shame even the edifice at Gibraltar.

Special thanks must go to Margaret E. Riggs, whose absence during the crucial summer in which this thesis was frantically composed allowed for its swift completion, as well as for its generally sober and humorless tenor. Needless to say, she has returned previous to the production of these words of gratitude.

Most sincere thanks and gratitude go to Carla W. Montgomery. Her impeccable drafting and flawless typing have lent credence, as well as scientific verification, to the old proverb that one can indeed make a silk purse, albeit an empty one, from a sow's ear. In addition, she has acted as an unwilling (you could tell by the look on her face) listener with an uncanny ability not to laugh at ideas which most assuredly deserved such treatment. This most civilized attitude is further highlighted by her unwillingness (most perplexing to the author) to engage in a ruthless and merciless vendetta against the author for his use of an extremely primitive form of comedy known as the pun. If this is not enough, her corrections of spelling, punctuation, grammar, sense and syntax have made this treatise, if not easier, at least more humane to read.

For financial recompense (in amounts, it must truthfully be stated, that far exceeded the author's contributions to science, art, or the betterment of mankind) the author wishes to thank the National Science Foundation Graduate Fellowships Program for financial support during his first three years at M.I.T. Although their support to the author has only dubious possibilities of furthering the development of the geologic sciences, it has greatly aided the cause of mental health, especially the author's, and is gratefully acknowledged. In addition, I would like to thank the Electron Microprobe Facility at M.I.T. whose contributions - made for other reasons, perhaps - supported the Research Assistantship which kept the author from becoming a computer programmer during his fourth year at M.I.T. The data that have been obtained by users of that facility will forever be marked by the uncertainty and inaccuracy characteristic of all of the author's best scientific endeavors. The author is, to say the least, philosophical in his belief that fame comes in many guises, although not necessarily the ones most divinely

cherished.

There are numerous other people - fellow graduate students, faculty, friends and relatives - who should also be thanked. However, because the legion of names is vast, and since the author believes the list of newly made enemies cited above to be already much too extensive to ensure his existence into old age, he would like to express his gratitude to them, without revealing names, for their comments, criticisms, help, encouragement and occasional financial support. Hopefully, I will be out of the country before you find out who you are.

Apologies and thanks to Ludwig von Beethoven, J.S. Bach, and Richard Wagner.

Table of Contents

<u>Subject</u>	<u>Page</u>
Abstract	2
Acknowledgements	4
Table of Contents	7
Index of Figures	9
Index of Tables	11
Chapter 1. Introduction	13
Chapter 2. Regional Geology	16
Chapter 3. Local Geology	26
Location of the Study Area	26
General Geology	30
Rocks east of the Bloody Bluff Fault Zone	35
Rocks between the Bloody Bluff Fault Zone and the Clinton-Newbury Fault Zone	39
Rocks west of the Clinton-Newbury Fault Zone	47
Fossiliferous Rocks in the Study Area	50
Chapter 4. Previous Geochronologic Work	53
Chapter 5. Present Study	67
Introduction	67
Sample Localities	67
Criteria for Sampling for Rb-Sr Whole Rock Work	70
Criteria for zircon sampling	72
Chapter 6. Results of U-Pb Analyses of Zircons	74
Sample Preparation and Zircon Separation	74
Zircon Yields	74
Zircon Morphologies	76
Interpretation of Zircon Morphologies	84
Zircon Dissolution, U-Pb Chemistry and Mass Spectrometry	89
U-Pb Results	90
Fishbrook Gneiss	91
Shawsheen Gneiss	98
Westboro Quartzite	104
Nashoba Formation	110
Lower-Quality Points	116

<u>Subject</u>	<u>Page</u>
Chapter 6. Results of U-Pb Analyses of Zircons (cont.)	
Common Lead	118
Detrital and Volcanic Trends	139
Continuous Diffusion	156
Summary	159
Chapter 7. Rb-Sr Whole Rock Results	161
Sample Preparation	161
Results	161
Fishbrook Gneiss	162
Nashoba Formation	166
Tadmuck Brook Schist	171
Worcester Formation	175
Shawsheen Gneiss	179
Middlesex Fells Volcanic Complex	183
Interpretation of Results	183
Premetamorphic History	203
Chapter 8. Microbomb Analyses	207
Introduction	207
Initial Experiments	207
Procedure	209
Blanks	213
Microbomb Results	214
Chapter 9. Interpretation of Results	217
Chapter 10. Summary	228
Appendix A. Rb-Sr Whole Rock Method	233
Appendix B. Zircon U-Pb Method	248
Appendix C. Sample Locations and Thin Section Descriptions	263
Appendix D. Statistics and Errors	271
References Cited	281

Index of Figures

(Page number refers to figure caption; figure will be found on following page(s).)

<u>Figure</u>	<u>Page</u>
1. Major structural features of New England, and area studied in this paper	17
2. Geologic sketch map of northeastern Massachusetts	27
3. Sample localities for this report	68
4. Photograph of zircons from Fishbrook Gneiss	78
5. Photograph of zircons from Fishbrook Gneiss	78
6. Photograph of zircons from Fishbrook Gneiss	78
7. Photograph of zircons from Shawsheen Gneiss	78
8. Photograph of zircons from Westboro Quartzite	78
9. Photograph of zircons from Nashoba Formation	78
10. Concordia plot, Fishbrook Gneiss zircons	94
11. Concordia plot, Shawsheen Gneiss zircons	100
12. Concordia plot, Westboro Quartzite zircons	107
13. Concordia plot, Nashoba Formation zircons	113
14. Pb^{204}/Pb^{206} of zircons vs. total radiogenic lead	126
15. Zircon sample weight vs. Pb^{204}/Pb^{206} of unspiked aliquot	130
16. Concordia plots, Fishbrook Gneiss zircons, corrected for different values of contamination lead isotopic ratios	135
17. Best Detrital Line	141
18. Resetting coefficient (C_r) vs. radiation damage coefficient (R_c)	149

<u>Figure</u>	<u>Page</u>
19. Concordia plot, Z-4 5M and R8311	154
20. Rb-Sr isochron plot, Fishbrook Gneiss	164
21. Rb-Sr isochron plot, Nashoba Formation	169
22. Rb-Sr isochron plot, Tadmuck Brook Schist	173
23. Rb-Sr isochron plot, Worcester Formation	177
24. Rb-Sr isochron plot, Shawsheen Gneiss	181
25. Rb-Sr isochron plot, Middlesex Fells Volcanic Complex	185
26. A. Rb-Sr isochron plot, all total rock samples	188
B. Histogram of initial ratios of $\text{Sr}^{87}/\text{Sr}^{86}$, all total rock samples	188
27. Best fit Rb-Sr isochrons for two groups of points in Figure 26A	192
28. Histogram of number of Rb-Sr analyses on upper and lower isochrons of Figure 27 for several formations	196
D-1. Fractional error of $\text{Pb}^{207}/\text{U}^{235}$ vs. fractional error of $\text{Pb}^{206}/\text{U}^{238}$ for zircon analyses	277

Index of Tables

<u>Table</u>	<u>Page</u>
1. Strike and dip of lineation, foliation, and layering of gneisses and schists	33
2. Isotopic ages for rocks of northeastern Massachusetts	54
3. Zircon analyses, Fishbrook Gneiss	92
4. Concordia intercepts and ages, Fishbrook Gneiss	96
5. Zircon analyses, Shawsheen Gneiss	99
6. Concordia intercepts and ages, Shawsheen Gneiss	102
7. Zircon analyses, Westboro Quartzite	105
8. Concordia intercepts and ages, Westboro Quartzite	109
9. Zircon analyses, Nashoba Formation	112
10. Concordia intercepts and ages, Nashoba Formation	115
11. Lower-quality zircon analyses	117
12. Lead contamination and radiogenic lead in zircons	121
13. Concordia intercepts and ages of the Best Detrital Line and Best Volcanic Line	144
14. Rb-Sr analyses, Fishbrook Gneiss	163
15. Rb-Sr analyses, Nashoba Formation	168
16. Rb-Sr analyses, Tadmuck Brook Schist	172
17. Rb-Sr analyses, Worcester Formation	176
18. Rb-Sr analyses, Shawsheen Gneiss	180
19. Rb-Sr analyses, Middlesex Fells Volcanic Complex	184
20. Results of microbomb analyses	215

Confusion will be my epitaph,
As I crawl a cracked and broken path....

- King Crimson

"Begin at the beginning," the King said, very gravely,
"and go on till you come to the end: then stop."

"Would you tell me, please, which way I ought to go
from here?"

"That depends a good deal on where you want to get to,"
said the Cat.

"I don't much care where - " said Alice.

"Then it doesn't matter which way you go," said the Cat.

" - so long as I get somewhere," Alice added as explanation.

"Oh, you're sure to do that," said the Cat, "if you
only walk long enough."

- Lewis Carrol, Alice's Adventures in Wonderland

Chapter 1

Introduction

Southeastern New England occupies an important position in understanding the geology and geologic history of the Appalachian system in New England, as well as for studying the development of the Appalachians as a whole. A number of authors (Wilson, 1966; Dixon, 1976; Cameron and Naylor, 1976) have commented on southeastern New England's unique characteristics and location in relation to other major structures and geologic areas in the New England region. In spite of this importance, southeastern New England has been sadly neglected by those working in New England geology. Only the barest outlines of the geology are known with any precision, and numerous theories of geologic history, some often contradictory, abound.

An interesting series of metavolcanics and metasediments crops out to the north and northwest of Boston in northeastern Massachusetts. They are highly variable and complex in terms of structure, lithology and metamorphism and as a result, they have not been studied closely until very recently. Yet this complexity suggests an equally complex history which has much to say about the geologic development of southeastern New England. However, a lack of fossils, absence of significant marker horizons, and the discontinuous nature of most units has hampered attempts at correlation and interpretation through the more classical methods such as field mapping and petrographic description. As a consequence, more sophisticated

techniques such as magnetic, gravity and seismic surveys, minor and trace element geochemistry and radioisotope geochronology have been brought to bear on the study of these Massachusetts rocks. Radioisotope age dating has been particularly useful in narrowing down the age ranges of many of these rocks and setting up a vague but useful chronology, but it has been largely confined to the intrusive rocks. However, the metavolcanic and metasedimentary rocks of northeastern Massachusetts record a significant series of events prior to the intrusion of the plutonic rocks. Knowledge about the ages of these rocks would go a long way towards helping the establishment of a geologic history and possible correlations with other areas.

The purpose of this paper is to present some radioisotope geochronologic data of a reconnaissance nature for the metavolcanics and metasediments of northeastern Massachusetts. The rubidium-strontium whole-rock method and uranium-lead analyses of zircons have been applied to these rocks in an attempt to discover their time of formation or deposition and the sequence of subsequent metamorphic events. Because much of the mapping and nomenclature is still uncertain and because of the lack of previous work on these rocks, this work must, of necessity, be a reconnaissance study. Thus the interpretations presented herein are general and the data open to alternate interpretation. An attempt will be made to suggest as many different models as the evidence allows, to present evidence both for and

against each model, and hopefully to decide on one interpretation that best fits the available data. In this way it is hoped that more specific problems and their solutions may be delineated and applied to the study of these rocks.

Chapter 2

Regional Geology

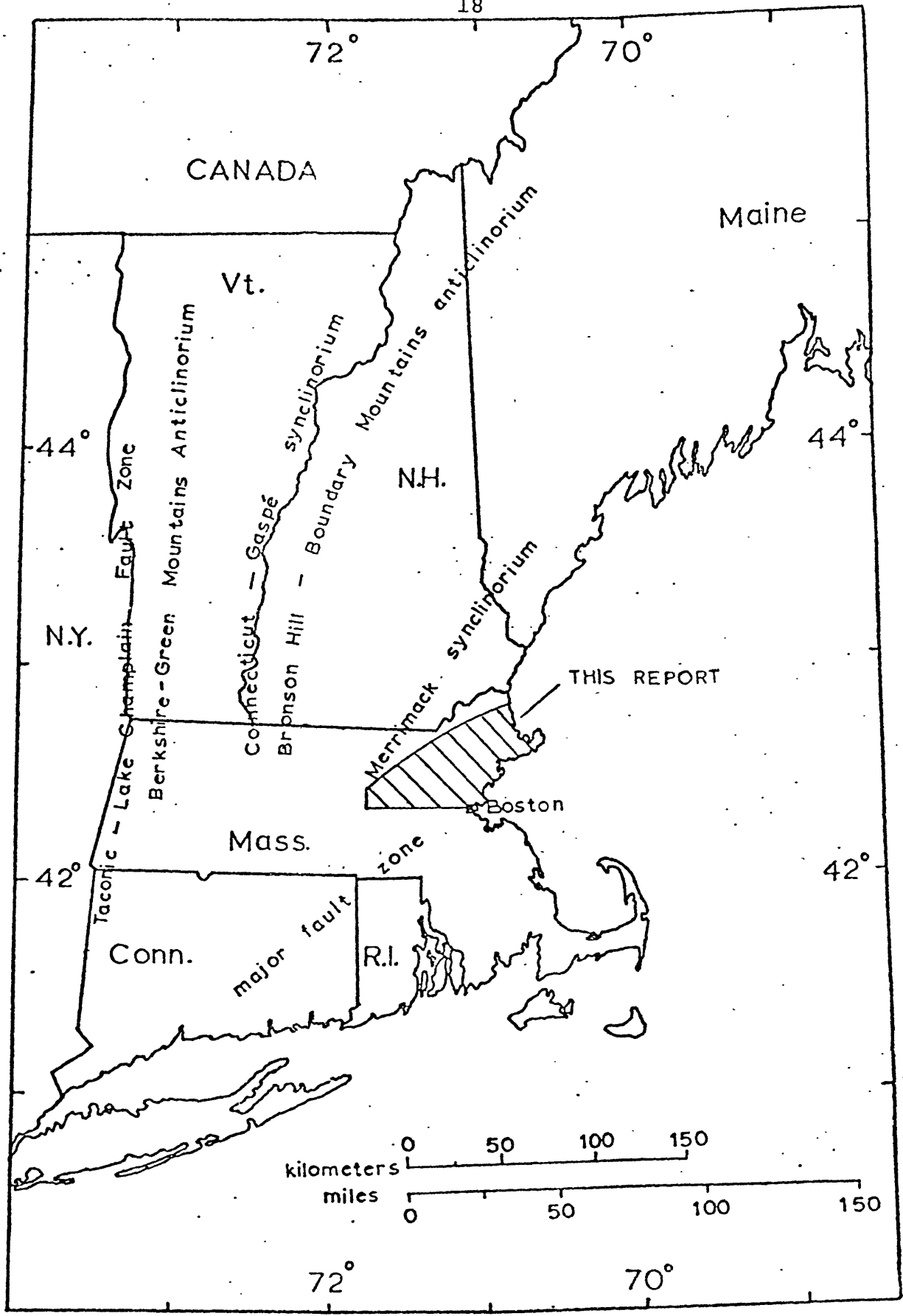
Although the data presented in this paper are of a local nature they may prove to be useful in a regional context. Therefore, some familiarity with the regional geology and structure of New England would be helpful. Excellent reviews of the regional framework and the lithologies, geology and structures of the major regional features have been given by Cady (1968), Zen (1968), Skehan (1969), Rodgers (1970), and Page (1976). Only a brief outline based on these reviews will be given here.

Figure 1 shows the major regional structures of New England and outlines the location for the study area of this report with respect to these structures. New England may be characterized geologically and structurally by a series of major stratigraphic and structural features that are parallel to sub-parallel across most of New England. These features strike approximately north-south in southern New England, where they are also the narrowest, the least recognizable and the most complex. To the north, in Vermont and New Hampshire, these structures gradually rotate to a northeast-southwest strike. In addition, they become wider and less complex. This general reduction in complexity (not often true locally) is a result of lower metamorphic grade, reduced deformation, and fewer complicating structural features.

The westernmost structural feature of New England is a

Figure 1

Major structural features of New England (after Page, 1976), and the area covered by this paper.



series of synclinoria (Middlebury, Hinesburg, St. Albans) that lie approximately along the New York - Vermont and New York - Massachusetts borders. Near the Massachusetts - Connecticut - New York triple point the strike becomes northeast-southwest following the general trend of the Appalachians. The synclinoria, essentially an extension of the Valley and Ridge province of the Appalachians to the south, are a foreland sequence of miogeosynclinal rocks, mostly quartzites, carbonates, and shales of Cambrian to Middle Ordovician age (Berry, 1968; Theokritoff, 1968). Deformation and metamorphism are variable but in general they increase from west to east. The synclinoria are further complicated by an extensive series of thrust and high-angle reverse faults that follow the same strike and affect most of the structures. Movement has apparently been from east to west on these faults (Zen, 1972). In addition, the southern half of the synclinal belt is overlain by a series of allochthons of Cambrian to Middle Ordovician age that apparently have come from the next structural unit to the east (Zen, 1972, 1976).

East of the miogeosynclinal sequence lies the Berkshire - Green Mountain Anticlinorium which comprises three major massifs composed of Precambrian crystalline rock (Ratcliffe and Zartman, 1976). The three massifs - the Hudson highlands of southwestern Connecticut and southeastern New York, the Berkshire massif of northwestern Connecticut and western Massachusetts, and the Green Mountain massif of western Vermont - are

composed of metasediments and metavolcanics probably deposited in a miogeosynclinal environment (Ratcliffe and Zartman, 1976), although a more volcanic environment to the south (Gates and Martin, 1976) suggests more eugeosynclinal conditions. The Precambrian rocks are intensely deformed and metamorphosed by a number of orogenic events. Lower Paleozoic rocks surround the massif but the contacts between the two are variable and often uncertain. The western sides of the massifs are probably a series of overlapping thrust faults which override the miogeosynclinal rocks to the west (Ratcliffe and Zartman, 1976), but locally an unconformity is indicated (Norton, 1976). The eugeosynclinal rocks to the east are thrust over the Precambrian basement of the massifs but also overlie the basement unconformably (Norton, 1976). The anticlinal structure continues in northern New England, although Precambrian basement is not exposed. Here the transition between the miogeosynclinal and eugeosynclinal rocks can be traced. In southwest New England the same transition may be a thrust fault contact, but correlations can still be made between the two groups of rocks (Norton, 1976; Hall, 1976).

To the east of the basement uplifts are a series of eugeosynclinal Paleozoic rocks which make up the Connecticut Valley - Gaspé Synclinorium, the southern part of which is covered by the rocks of the Triassic Newark Group of the Connecticut River Valley. The rocks are chiefly metasediments of various types (mostly mica schists and quartzites in the lower part; phyl-

lites become more common in the stratigraphically higher units) and metavolcanics (greenstone schists and amphibolites). Some carbonates appear in the upper units, suggesting a more miogeosynclinal environment. The west limb of the synclinorium is roughly a homoclinal sequence of Cambrian to Lower Devonian rocks (Schnabel, 1976). The center and east limb of the synclinorium are complicated by a series of domal structures cored by Ordovician (Schnabel, 1976) or possibly older rocks (Naylor, 1976). However, correlations can be made across the core of the synclinorium, and the sequence on the east limb is found to be similar to that on the west limb, although complicated by possible facies changes, recumbent folds, nappes, and a large post-metamorphic fault (the Ammonoosuc Fault).

To the east of the Connecticut Valley - Gaspé Synclinorium is a series of domes which constitute the core of the Bronson Hill - Boundary Mountain Anticlinorium that extends from central and northeastern Connecticut through central Massachusetts, western New Hampshire, and along the border between Canada and New Hampshire and Maine. The domes are composed of granitic and intermediate gneisses of probable Ordovician age (Naylor, 1968) which represent metamorphosed intrusives or volcanics apparently part of a volcanic arc (Naylor, 1976). The cores of some of the domes may be older, possibly Precambrian (Naylor et al., 1973). Where they are Ordovician the domes are mantled by Ordovician to Devonian rocks composed of metavolcanics, schists, and quartzites of various types, local carbonate

beds, calc-silicate units, slates, and phyllites. Where the cores are possibly Precambrian the mantling rocks are Cambrian to Ordovician metavolcanics and metavolcanoclastic rocks (Boudette and Boone, 1976). The domes are superimposed on large, extensive nappes and overturned folds that are characteristic of the Bronson Hill - Boundary Mountain Anticlinorium and the eastern part of the Connecticut Valley - Gaspé Synclinorium (Thompson et al., 1968). The nappes apparently involved rocks from Precambrian (?) to Devonian age and show overturning to the west and the east.

The Merrimack Synclinorium, which extends from northern and central Maine through eastern New Hampshire, east central Massachusetts and northeastern Connecticut, consists of a series of Ordovician (and possibly older) to Devonian eugeosynclinal sediments and volcanics and occasionally more shallow-water deposits (Hall et al., 1976). Rocks older than Ordovician crop out on the west and east limbs of the synclinorium (Boudette and Boone, 1976; Bickel, 1976; Brookins, 1976; this report) and possibly in the center of the synclinorium (Massachusetts Gneiss - Naylor et al., 1969; Bescanson et al., 1977). Much of the synclinorium is highly metamorphosed, especially at its center from northeastern Connecticut to southwest Maine (Thompson and Norton, 1968). As a result, correlations across the syncline are adequate only for central Maine (Ludman, 1976; Pankiwskyj et al., 1976). In addition, the geology of the syncline is further complicated by extensive igneous intrusions

of the White Mountain Magma Series and the New Hampshire Plutonic Series.

Although another major anticlinorial structure would be expected in easternmost New England, the coastline and the inherent complexity of the area make such a structure difficult to recognize. The Rockingham Anticline of southeast New Hampshire and the southeast coast of Maine, where possible Precambrian rocks are exposed (Bickel, 1976), may represent such a structure. But highly variable metamorphism and intense faulting and folding make regional trends difficult to discern. Southeastern New England, including eastern Massachusetts, Rhode Island, and southeastern Connecticut, is even more difficult to categorize. The general pattern is a series of large batholith-like masses of granitic and intermediate igneous rocks which intrude a series of metasedimentary and meta-volcanic eugeosynclinal rocks. The most important of these igneous rocks are the Dedham Granodiorite, the Northbridge Granite Gneiss, and the Milford Granite, all of which are late Precambrian in age (see Chapter 4). The Dedham Granodiorite is of singular importance in that it intrudes the lower part of the section covered by this paper (Bell and Alvord, 1976), and is the most intensely studied and best dated of the Precambrian intrusive rocks of southeastern New England (Kovach et al., 1977).

These intrusive and stratified rocks are in turn intruded by another series of granitic and intermediate rocks of Ordo-

vician (Handford et al., 1965; Zartman and Marvin, 1971) to Devonian (Lyons and Krueger, 1976) age.

A significant portion of southeastern New England is overlain by structural and topographic basins (the Boston, Norfolk, and Narragansett basins are the major ones) of Pennsylvanian (Oleksyshyn, 1976; Lyons et al., 1976) or probable Pennsylvanian (Billings, 1976) age. Deformation and metamorphism are intense and the area is cut by extensive faults with both strike-slip and thrust components to their motion (Bell, 1967; Barosh, 1972).

New England as a whole has undergone a number of significant orogenic, deformational, metamorphic, and thermal episodes. The Precambrian basement rocks record two or more episodes of Precambrian deformation and metamorphism, of which the chronology and stratigraphy have yet to be worked out. However, the Precambrian rocks of western New England do appear to record a different series of events from those in eastern New England (Naylor, 1976). The mid-Ordovician Taconic orogeny produced significant deformation and metamorphism in western New England and, as this paper will show, also in southeastern New England. The mid-Devonian Acadian orogeny is responsible for the intense deformation (nappes and domes) of central New England as well as the intrusion of extensive igneous bodies (New Hampshire Plutonic Series - Page, 1968). K-Ar mineral ages (Zartman et al., 1970) record a significant thermal event in eastern New England during Permian time. This episode may be related to

the extensive post-Pennsylvanian and pre-Cretaceous faulting in southeastern New England. Significant Mesozoic igneous activity is represented by the Triassic Newark Group of the Connecticut Valley area and the Jurassic to Cretaceous White Mountain Magma Series.

Chapter 3

Local Geology

Location of the Study Area

The area covered by this paper lies in northeastern Massachusetts to the north, northwest and west of Boston (Figure 1). Its eastern boundary is the Boston Basin and its associated boundary faults and a series of intrusive rocks (Cape Ann Granite, Salem Gabbro-Diorite and other smaller bodies) which make up the northeastern coast of Massachusetts. The southern limit is roughly the $42^{\circ}22'$ parallel which lies just south of Clinton and runs through Marlborough and Boston (see Figure 2). The western, northwestern and northern limit of the area is a curve running approximately from Clinton through Lawrence to Newbury on the coast.

Geologically the area of interest lies on the southeasternmost limb of the Merrimack Synclinorium in eastern Massachusetts and on the northwesternmost edge of what has come to be called the eastern block. The eastern block is the series of large intrusive bodies, stratified metamorphic rocks and non-marine sedimentary basins discussed in Chapter 2 and which are characteristic of southeastern New England. One of the conclusions of this paper will be that the stratified metamorphic rocks shown in Figure 2 are probably more closely related to the eastern block than they are to the Merrimack Synclinorium, thus further extending and delineating the

Figure 2

Geologic sketch map of northeastern Massachusetts showing major stratified units and faults. Except for the Andover Granite and the Dedham Granodiorite, intrusive rocks are not subdivided. Map after Bell and Alvord (1976).

Figure 2 - Legend

tb Tadmuck Brook Schist

Nashoba Formation:

nb	Beaver Brook member	ns	Spencer Brook member
nl	Long Pond Gneiss member	nbs	Billerica Schist member
nf	Fort Pond member	nbh	Bellows Hill member
nn	Nagog Pond Gneiss member	nbx	Boxford member
nnb	Nashoba Brook member	nu	Nashoba, member not identified
nt	Tophet Swamp member		

fg Fishbrook Gneiss

sg Shawsheen Gneiss

mu	Marlboro Formation, undivided	ms	Marlboro Formation, Sandy Pond Amphibolite member
----	----------------------------------	----	--

bf Burlington Formation

gf Greenleaf Mountain Formation

uqg1, uqg2 Remnants of unnamed quartzites and gneisses

mfv Middlesex Fells Volcanic Complex

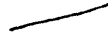
wf Westboro Formation


wyf Weymouth Formation


ag	Andover Granite	agqd	Andover Granite and Quartz Diorite
----	-----------------	------	---------------------------------------


Pcd Dedham Granodiorite

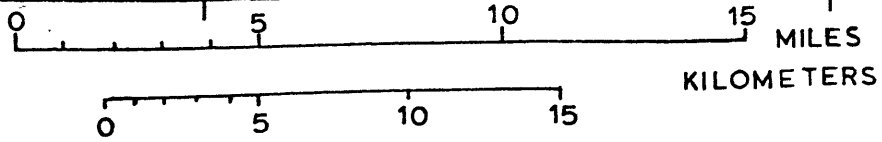
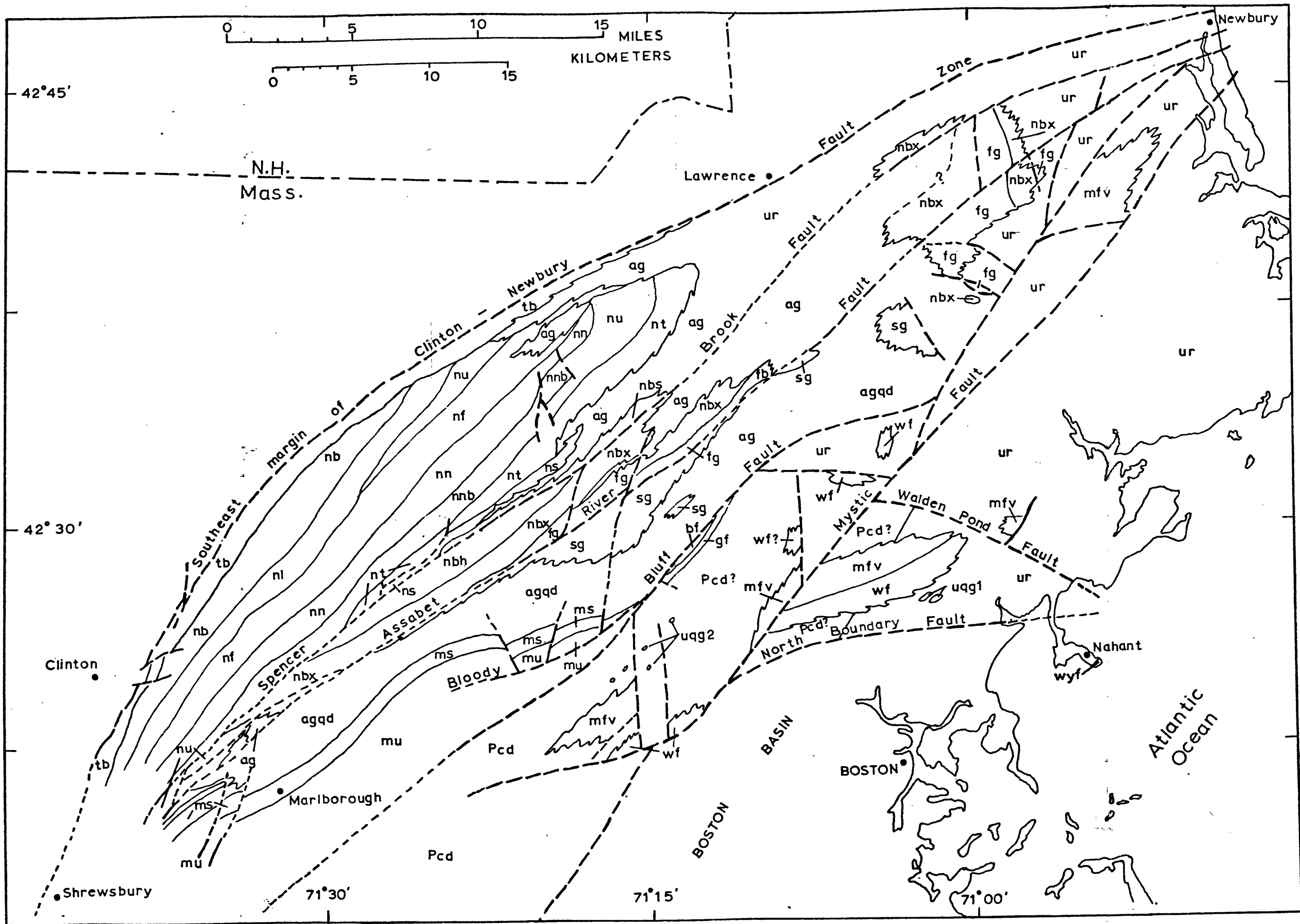
ur undivided intrusive rocks and stratified rocks of
Silurian or younger age

 Contact of stratified rock

 Intrusive contact

 Fault, mapped

 Fault, known from reconnaissance



42°45'

N.H.
Mass.

Lawrence

Newbury

42°30'

Clinton

Shrewsbury

Marlborough

71°30'

71°15'

BOSTON

Atlantic
Ocean

71°00'

eastern block.

General Geology

Figure 2 shows the geology of the stratified metamorphic rocks covered by this paper as well as important faults; intrusive rocks (except for the Andover Granite, ag and aggd, and the Dedham Granodiorite, Pcd) have not been divided but simply shown as "ur". This discussion of the general geology and the discussion of the specific geology to follow are based mainly on the work of Bell and Alvord (1976), Cameron and Naylor (1976), and Barosh et al. (1977). Other works also used although they cover smaller areas of the region or are somewhat out of date are: Emerson (1917), Clapp (1921), LaForge (1932), Hansen (1956), Jahns et al. (1959), Castle (1964, 1965a,b), Toulmin (1964), and Skehan (1968). More specific references will be noted where appropriate.

The stratified metamorphic rocks of northeastern Massachusetts are a sequence of metasediments and metavolcanics deposited for the most part in a eugeosynclinal environment. The predominant rock types are biotite-feldspar-quartz gneisses and schists, quartz-feldspar-biotite gneisses and schists, hornblende gneisses and schists, and amphibolites. Biotite-quartz granulites, calc-silicate granulites, marbles, quartzites, and muscovite schists and gneisses are also common and locally dominant (Skehan and Abu-Moustafa, 1976; Abu-Moustafa and Skehan, 1976). Metavolcanics and metavolcano-

clastic rocks predominate, but to the northwest and southeast terrigenous metasediments become more common, and to the extreme northwest and southeast they predominate.

Intrusive igneous rocks and their accompanying aplite dikes, pegmatites, and quartzofeldspathic veins are ubiquitous. For the most part, the intrusive rocks are calc-alkaline granites or intermediate rocks that range from granodiorite to quartz monzonite to monzonite. Along the coast, especially north of the Boston Basin, the dominant rock types are alkaline and peralkaline granites, diorites, and gabbros, and minor syenites which possibly are all related (Dennen, 1976). The intrusive rocks generally become more common and variable to the southeast. They become so extensive, in fact, that the stratified rocks become more like large "mega-xenoliths", completely surrounded by and intimately intruded by the igneous rocks. This can best be seen in the eastern and southeastern parts of the area in Figure 2.

The stratified rocks comprise a homoclinal sequence that dips to the northwest. Because of faulting and folding, the dips are highly variable but for the most part lie between 35° and 60° northwest. The strike of the units is more consistent. They are almost exactly northeast-southwest, although the strike of the units becomes slightly more northerly to the southwest. The lineations, foliation and layering in the schists and gneisses appear to follow these trends, although measurements made by the author suggest that

some of the blocks of stratified metamorphic rocks, in the northeast portion of the study area, have been rotated out of alignment with the more dominant trend. Table 1 shows these data. This rotation is probably the result of faulting or igneous intrusion, as these large blocks of stratified metamorphics are completely surrounded by faults or intrusive rocks.

All of the rocks of the study area are metamorphosed to one degree or another. For the stratified rocks the grade increases from southeast to northwest. However, as the Clinton-Newbury Fault Zone is crossed the grade drops abruptly. The major faults appear to control very strongly the relative placement of metamorphic isograds (Thompson and Norton, 1968). The highest grade is developed in the Nashoba Formation where sillimanite and potassium feldspar-bearing strata occur through much of the formation. Abu-Moustafa and Skehan (1976) estimate recrystallization temperatures and pressures for the Nashoba Formation of 625° to 675°C at 5 to 6 kb of pressure. This would be high amphibolite facies to amphibolite-granulite transitional facies (Turner, 1968). The lower grade rocks in the southeast are in the greenschist facies. Chlorite and epidote are common, although the existence of biotite and hornblende suggest a slightly higher grade which was later retrograded to chlorite-epidote grade. All of the formations show some signs of retrograding, mainly in the form of development of chlorite and epidote. The in-

TABLE 1

Strike and Dip of Lineation, Foliation, and Layering
of Gneisses and Schists

<u>Location</u> ¹	<u>Feature</u>	<u>Strike</u> ²	<u>Dip</u> ²
Z-1	foliation	N36W	55NE
Z-1	lineation	N55W	n.d. ³
Z-1	lineation	N73W	n.d.
Z-1	layering	N42W	n.d.
Z-2	foliation	N	57E
Z-3	lineation	N55E	n.d.
Z-4	lineation	N45E	n.d.

¹See Figure 3. Location refers to localities where samples were taken for zircon analysis; strike and dip measurements were made on the same outcrops.

²Average of three readings made across the width of the outcrop. Obvious folds and crenulations were avoided. All strike readings are declination corrected for magnetic north 15° W of geographic north (from U.S.G.S. Topographic Maps).

³n.d. = not determined

trusive rocks, except possibly for the Dedham Granodiorite, show little sign of thermal metamorphism. Some of the intrusives (most notably the Andover Granite) show foliated border phases, probably the result of flowage during intrusion and crystallization. All of the intrusions, however, do show the effects of dynamic metamorphism. Cataclasis, shearing, and fractured grains are common throughout the region. Only rocks of the Cape Ann Plutonic Series (Dennen, 1976) show few features of any type of metamorphism. Only the Dedham Granodiorite shows any significant contact metamorphic effects (Bell and Alvord, 1976). This suggests that the metamorphism of the stratified rocks is dominantly dynamothermal regional metamorphism rather than the effect of numerous igneous intrusions. This implies depths of burial of up to 20 km, or more for the Nashoba Formation (Abu-Moustafa and Skehan, 1976). The metamorphism is probably due to a single major Paleozoic metamorphic episode although an earlier Precambrian metamorphic episode is suggested in the southeastern part of the section.

Large scale folds (> 10 m in wavelength) are uncommon in the stratified rocks but smaller scale folds and intrastrata folds are quite common (Skehan, 1968). Most of the deformation in the area, however, appears to be in the form of faults. Figure 2 shows the major faults in the region. Actually, the major faults are fault zones composed of myriad smaller interlocking and anastomosing faults. When smaller more local

faults are considered the number of faults rises dramatically (Skehan, 1968; Barosh et al., 1977). The major fault zones show west over east thrust movement and right lateral strike-slip movement (Skehan, 1969; Barosh, 1976). Fault related features such as shears, mylonite, breccia, mineralization, silicified zones, and drag folds are common (Barosh, 1976). The major northeast striking faults (Figure 2) dip to the northwest usually at shallower angles than those of the stratified rocks (Skehan, 1968). To the southwest the major fault zones coalesce, then diverge again as the Lake Char and Eastford Fault Zones (Barosh, 1976). The faults also converge to the northeast but they may continue out into the Gulf of Maine (Ballard and Uchup, 1974).

The major fault zones divide the region into three main blocks wherein we may treat the lithologies, structure and metamorphism separately. Therefore in the following discussion of specific units and geological features, I will break the rocks into three divisions: those east of the Bloody Bluff Fault Zone, those between the Bloody Bluff Fault Zone and the Clinton-Newbury Fault Zone, and those northwest of the Clinton-Newbury Fault Zone.

Rocks East of the Bloody Bluff Fault Zone

Stratified Rocks - The two major stratified units east of the Bloody Bluff Fault Zone are the Westboro Formation and the Middlesex Fells Volcanic Complex. Remnants of these two for-

mations have been traced into northeastern Massachusetts and into Rhode Island where Bell and Alvord (1976) correlated them with the Blackstone Series of presumed Late Precambrian age.

The Westboro Formation consists mainly of massive and fine grained quartzites. The upper portion of the formation is mainly the massive quartzite. The lower portion of the formation contains much more fine grained quartzite plus significant amounts of fine grained gneiss, calc-silicate rocks and micaceous quartzite. Most of the quartzite bodies tend to be lenticular and show obscure sedimentary features such as lamination, cross-bedding, and graded bedding. The contact with the overlying Middlesex Fells Volcanic Complex is conformable or possibly a small unconformity. The environment of deposition was apparently shallow water marine to littoral. Sediments were mainly quartz sands with occasional fine grained silts and muds mixed with minor amounts of carbonates. The gneisses might be the result of airborne tuffs mixed with terrigenous clastic sediments.

The Middlesex Fells Volcanic Complex is a thick unit of mafic metavolcanics overlying the Westboro Formation. Like the Westboro Formation, the Middlesex Fells Volcanics often occur as blocks completely surrounded by faults or intrusive rocks. Nevertheless, some idea of the sequence of units is possible. The Middlesex Fells Volcanic Complex is a typical volcanic pile with flow rocks, coarse pyroclastics and fine grained tuffs. Discontinuous bodies of flow rocks occur throughout

the unit but are particularly common in the lower portion. Discontinuous lentils of coarse pyroclastics occur fairly evenly throughout the unit. Strata and lentils of fine grained tuffs are most common in the upper portion and as a whole constitute the most common lithology in the unit. Minor quartzites, calc-silicates and gneisses also occur, especially in the lower portion. Most of the volcanics are now amphibolites with biotite, chlorite, epidote and magnetite common due to retrograding. However, except in areas of intense retrograding, outlines of fragmental detritus, pillows, amygdules, and flow banding are easily discernible. All the volcanics are mafic except for a few rare dacitic lentils. Sub-aqueous deposition is indicated. An unconformity at the top of the Middlesex Fells Volcanic Complex is indicated by the lack of the top portion of the unit in some places.

A few smaller and less important rock units crop out east of the Bloody Bluff Fault Zone. A series of quartzites and gneisses that exist as xenoliths and pendants in the Dedham Granodiorite are thought to underlie the Westboro Formation conformably. No contact with the Westboro can be seen. The conformity is based on concordant attitudes between the Westboro and the quartzites and gneisses. Another series of similar gneisses and quartzites occur as xenoliths in the Salem Gabbro-Diorite (part of the Cape Ann Plutonic Series (?) - Dennen, 1976) northwest of the Mystic Fault. They are thought to overlie the Middlesex Fells Volcanic Complex unconformably

but no contact can be seen.

Two small units crop out just east of the Bloody Bluff Fault Zone and are truncated by it, and are surrounded by the Salem Gabbro-Diorite. The Greenleaf Mountain Formation is composed mainly of amphibolite and is thought to overlie the Middlesex Fells Volcanics although no contact is seen. Overlying the Greenleaf Mountain Formation is the Burlington Formation which consists of quartzite, gneiss, amphibolite, meta-arkose and metaconglomerate.

Intrusive Rocks - The two major groups of intrusive rocks east of the Bloody Bluff Fault Zone are the Dedham Granodiorite and associated rocks, and the Cape Ann Plutonic Series. The Dedham Granodiorite, occurring primarily to the south and west of the Boston Basin, is highly variable in composition and texture. It varies continuously from gabbroic to granitic phases and from extreme cataclasis and alteration to almost unaltered or undeformed rock. Generally, however, it is a granodiorite composed of andesine, quartz, potassium feldspar, hornblende, and other minor mafic minerals. Cataclasis and alteration of the mafic minerals is common. The Westboro Formation and the Middlesex Fells Volcanics are the only major units intruded by the Dedham Granodiorite. The late Precambrian age of the Dedham is fairly well documented (see Chapter 4) and suggests a late Precambrian age for the Westboro and Middlesex Fells.

The Cape Ann Plutonic Series is a complex group of intrusive rocks varying in composition from gabbro to peralkaline granite to syenite occurring mainly northwest, north and northeast of Boston. According to Dennen (1976), all of these phases are genetically related. If we accept this, plus the fact that the more sialic phases of the Series are probably Ordovician (Chapter 4), then an Ordovician or older age for all the stratified units east of the Bloody Bluff Fault Zone is implied, since they are all intruded by one or more phases of the Cape Ann Plutonic Series. This agrees with the Late Precambrian or older age established for the Westboro and Middlesex Fells.

Rocks between the Bloody Bluff Fault Zone and the Clinton-Newbury Fault Zone

Stratified Rocks — The stratified rocks between the Bloody Bluff Fault Zone and the Clinton-Newbury Fault Zone comprise the main northwest-dipping homoclinal sequence of eu-geosynclinal rocks in the region. The sequence is composed of five formations which from oldest to youngest are: the Marlboro Formation, the Shawsheen Gneiss, the Fishbrook Gneiss, the Nashoba Formation, and the Tadmuck Brook Schist. These units comprise an essentially continuous sequence of metavolcanics and metasediments. Metasediments generally become more common as we go up in the section, although in the Nashoba Formation the two lithologic types alternate in an almost cyclic fashion.

The Marlboro Formation is separated into two members. The lower unnamed member is a thick heterogeneous sequence of plagioclase-quartz-biotite-muscovite schist, amphibole-biotite-plagioclase-quartz gneiss, calc-silicate gneiss, marble, and amphibolite. The protoliths of the lower member were mafic tuffs and volcanoclastic material with an admixture of epiclastic sediments with rare carbonate sedimentation. A subaqueous marine environment is indicated.

The upper member of the Marlboro Formation - the Sandy Pond Member - is composed mainly of fine grained and massive amphibolites. The massive amphibolites are most common in the upper part of the section along with minor mica-quartz-plagioclase gneisses and schists. The member was presumably formed from subaqueous andesitic and basaltic tuffs and volcanoclastics interlayered with minor epiclastic and carbonate sediments.

The lower part of the Marlboro Formation is not seen since the bottom of the formation is cut out by the Bloody Bluff Fault Zone. The upper contact of the Marlboro is not seen because of intrusive rocks, but because the Sandy Pond section appears to be complete along its whole length, the contact with the overlying Shawsheen Gneiss is assumed to be conformable.

The Shawsheen Gneiss consists chiefly of medium grained muscovite-biotite-quartz-oligoclase gneisses interstratified with lenticular layers of amphibolite. Sillimanite-muscovite-

biotite-quartz schist is common in parts of the basal section of the unit. Occasional lenticular masses of agglomerate-like rocks are also seen. The protoliths of the unit are mainly submarine volcanic and volcanoclastic wackes of intermediate composition. These were mixed with small amounts of aluminous terrigenous silts and clays. Periods of more active volcanism produced mafic tuffs and/or flows now seen as amphibolites. Periods of little volcanic activity allowed deposition of terrigenous clays, muds and silts now seen as muscovite- and sillimanite-rich gneisses and schists. Neither the upper or lower contacts of the Shawsheen Gneiss are seen. The lower contact is stopped out by intrusive rocks and the upper contact is faulted. However, similarities between the top of the Shawsheen Gneiss and the bottom of the Fishbrook Gneiss suggests a conformable contact.

The Fishbrook Gneiss is predominantly a light colored plagioclase-biotite-quartz gneiss with occasional lenticular layers of amphibolite and biotite-hornblende-plagioclase schist and gneiss. The unit is well-bedded and, in general, very homogeneous. Its light color, due to almost complete lack of mafic minerals (< 10%) make it a very distinctive formation. Biotite is the most common mafic mineral although hornblende is sometimes common. Plagioclase of albite to oligoclase composition constitutes more than 50% of the dominant light colored gneissic facies. The protolith appears to have

been a very homogeneous volcanic wacke of felsic to intermediate composition. Occasional influxes of mafic tuffs and flows are now seen as amphibolites and mafic schists and gneisses. As discussed under the Shawsheen Gneiss the lower contact of the Fishbrook Gneiss is probably conformable with the Shawsheen Gneiss. The upper contact of the Fishbrook Gneiss with the overlying Boxford Member of the Nashoba Formation can be seen and is found to be conformable.

The Nashoba Formation is the thickest and most extensive formation in the area. It is a heterogeneous sequence of conformable yet completely interstratified metasedimentary and metavolcanic units. Approximately 50% of the Nashoba is a lenticularly bedded biotite-rich gneiss; about 15% is composed of evenly bedded diopsidic, amphibole- and biotite-rich gneisses and schists; 15% is variably textured amphibolites; 10% is sillimanite-rich mica schists; 19% is diopsidic calc-silicate gneisses and schists; and a small amount of the formation is composed of thin discontinuous lenticular masses of marble and quartzite. The Nashoba Formation is divided into ten lithostratigraphic members. This division is based on those parts of the formation which are dominantly composed of the distinctive biotite gneiss and schist, and amphibolite, as opposed to those composed of more heterogeneous rock types in addition to the biotite gneisses and schists, and amphibolites. For descriptions of the individual members and the various lithologic types found in the Nashoba, the reader is referred to Alvord

et al. (1976b) and Skehan and Abu-Moustafa (1976).

The Nashoba contains the highest grade rocks in the section. Sillimanite is ubiquitous in the more aluminous rocks. In rocks of appropriate composition, sillimanite and potassium feldspar are common, while muscovite is not often found. In spite of this high degree of metamorphism, relict sedimentary structures are evident, especially where faulting and igneous intrusion are absent. Stratification, current bedding with laminae and cross-bedding, ripple marks, graded beds, slumping, and concretions are found. Contacts between the individual members range from extremely sharp to completely gradational.

The protoliths and depositional environments for the biotite gneisses and schists, and amphibolites are probably the same as those for similar rock types found in the Shawsheen Gneiss. Influx of fine grained terrigenous sediments and carbonates was probably continuous throughout the deposition of the Nashoba Formation, but during periods of waning volcanic activity they became dominant. They are now seen as sillimanite-rich and calc-silicate-rich schists and gneisses. Magnesium- and calcium-rich volcanic wackes are now represented by the diopsidic amphibole- and biotite-rich gneisses and schists. The beds of marble and quartzite represent calcareous muds and quartzitic sands deposited during periods of little or no volcanic activity.

As discussed above the lower contact of the Nashoba Formation is conformable with the underlying Fishbrook Gneiss.

The upper contact appears to be conformable with the overlying Tadmuck Brook Schist in the southwestern part of the section. However, to the northeast the Tadmuck Brook Schist overlies successively older members of the Nashoba Formation which suggests a significant unconformity between the two. No evidence for a fault is seen, except locally (Alvord et al., 1976a).

The Tadmuck Brook Schist is the uppermost unit in the sequence of rocks between the Bloody Bluff and Clinton-Newbury Fault Zones. It is composed of aluminous schists interstratified with minor amphibolites and quartzites. The aluminous schists are composed of three sub-types: sillimanite-biotite-quartz-muscovite schist which weathers a rusty color; graphitic chlorite-quartz-biotite-sericite-muscovite-staurolite-andalusite phyllitic schist; and quartz-chlorite-biotite-sericite phyllite. Only gross sedimentary layering remains, fine details have been destroyed by recrystallization and tectonic shearing. The Tadmuck Brook Schist was derived mainly from terrigenous sediments deposited under generally euxinic conditions as sulfidic aluminous clays alternating with quartzose silty clays. Occasional quartz and greywacke sands interrupted deposition of clays, and both were in turn covered by andesitic and basaltic submarine flows and tuffs. The lower contact of the Tadmuck Brook Schist is discussed under the Nashoba Formation. The upper contact is not seen because of truncation by the Clinton-Newbury Fault Zone. The fault has put the Tadmuck Brook Schist in contact with the metasedimen-

tary rocks of the Merrimack Group and the intrusive rocks of the Ayer and Chelmsford Granites. Slivers of the Tadmuck Brook occur in the Clinton-Newbury Fault Zone (Gore, 1976a), but whether they come from a part of the unit no longer seen because of faulting, or whether they are part of the presently observed section of the Tadmuck Brook Schist is unknown.

Intrusive Rocks - The area between the Bloody Bluff and Clinton-Newbury Fault Zones is dominated by the Andover Granite. Essentially, it is a two-mica calc-alkaline granite, but its texture and lithology vary widely. Gneissic varieties with extensive cataclasis and shearing are found as well as varieties almost totally without such effects. The composition can occasionally approach granodioritic. The compositional and textural variations become even larger if we include into the Andover a number of smaller intrusive bodies found in the fault block. These include the Assabet Quartz Diorite and Gospel Hill Gneiss of Hansen (1956) and the Sharpners Pond Tonalite of Castle (1965a). Their calc-alkaline nature, proximity to the Andover Granite, and the pervasiveness of the Andover Granite throughout the fault block suggest that all of these intrusive bodies may be related.

The Andover Granite has produced major intrusive effects on the stratified rocks of the fault block. Contact metamorphic effects are rare because of the high grade of regional metamorphism in the stratified rocks. However, aplite dikes,

pegmatites, quartzofeldspathic veins and sills, and lenses and veins of the granite are present everywhere. Indeed, rare is the outcrop that does not show some signs of intrusive activity. This indicates the former presence of a large and extensive fluid phase associated with the intrusion of the Andover Granite that became pervasively and intimately associated with the stratified rocks.

The Andover Granite by itself appears to be Ordovician in age (Chapter 4), which implies an Ordovician or older age for the entire section of stratified metamorphic rocks in the Clinton-Newbury - Bloody Bluff fault block.

In the southwestern part of this fault block the Marlboro Formation and the Nashoba Formation are in contact with two older intrusive bodies - the Milford Granite and the Northbridge Granite Gneiss. Both of these igneous bodies are late Precambrian in age (Chapter 4). The contact with the Milford Granite is a fault contact, probably part of the Bloody Bluff Fault Zone. The contact with the Northbridge Granite Gneiss is also probably a fault but is less certain. Locally evidence for a fault contact between these two igneous bodies and the stratified rocks is not obvious, but neither is it evident whether the contact is intrusive or an unconformity. Thus, the relationship between the intrusive igneous rocks of definite late Precambrian age and the stratified metamorphic rocks is largely uncertain.

Rocks West of the Clinton-Newbury Fault Zone

Stratified Rocks - West and northwest of the Clinton-Newbury Fault Zone are a series of low grade metasedimentary rocks. The three major units are the Merrimack Quartzite, the Oakdale Formation, and the Worcester Formation. The Oakdale and Worcester have been separated into a number of smaller unnamed units by Peck (1976). The dominant lithologies are quartzites (especially in the Merrimack and Oakdale), phyllites, metasilstones, carbonaceous slates and phyllites, meta-greywackes, calc-silicates, and phyllites with chiastolite porphyroblasts. This last lithology is probably the result of contact metamorphic effects produced by the intrusion of the Chelmsford Granite (Peck, 1976). All of the other rocks are biotite grade or lower. The units dip west and northwest and strike more northerly relative to the units in the previous fault block. The lower part of the sequence is cut by numerous faults that are part of the Clinton-Newbury system, but the rest of the sequence appears to be continuous and relatively undeformed. Primary structures such as compositional layering, laminations, tabular and lenticular beds, cross-stratification and graded beds are still preserved (Peck, 1976). The Harvard Conglomerate was once considered to be a part of this sequence (Hansen, 1956) but recent evidence (Thompson and Robinson, 1976) shows it to be younger. It is probably related to the remnants of Pennsylvanian sediments found to the southwest in

the Worcester area (Grew, 1976). The protoliths of the rocks were evidently marine mudstones, siltstones, fine grained sandstones and limey sandstones. Grew (1971) and Peck (1976) have correlated these metasedimentary rocks northwest of the Clinton-Newbury Fault Zone with Silurian and Devonian rocks in New Hampshire and Maine based on lithologic similarities and geographic considerations. No fossils are found in these rocks. More recently these rocks have been designated Cambro-Ordovician (Barosh et al., 1977).

Intrusive rocks - The major intrusive rock northwest of the Clinton-Newbury is the Ayer Granite or Granodiorite. It is actually a heterogeneous collection of intrusive and possibly intrusive rocks that range in composition from granite to quartz diorite. Texture ranges from gneissic to cataclastic to porphyritic. Gore (1976a,b) has redefined the Ayer Granite as the Ayer Crystalline Complex to take into account these many variations. Gore recognizes two major phases of the Complex. One phase, the Clinton Quartz Monzonite, which occurs near the town of Clinton and in a large body near the Harvard-Littleton area, is a porphyritic, slightly foliated, coarse grained rock containing microcline, albite to sodic oligoclase, quartz, and biotite. This appears to be a true intrusive rock. It intrudes the lower part of the metasedimentary sequence described above.

The other phase, the Devens - Long Pond Gneiss, makes up most of the Ayer Crystalline Complex in the area of the town of

Ayer. The gneiss is composed of a porphyroblastic and equigranular gneiss composed of microcline (mostly in the porphyritic phase) with albite, quartz, biotite, and chlorite. Compositions range from quartz monzonite to granodiorite to quartz diorite. The Devens - Long Pond Gneiss is probably a mixture of intrusive rocks, metavolcanic and metasedimentary gneisses, and migmatites. Contact relations with the surrounding rocks are uncertain. Many contacts are sure to be faults but the contacts with the metasedimentary rocks of the Oakdale and Worcester Formations may be unconformities (Gore, 1976b). Gore (1976a) has also included the Chelmsford Granite in the Ayer Crystalline Complex. The Chelmsford Granite (Currier, 1937) is actually a quartz monzonite containing quartz, microcline, plagioclase, muscovite, biotite, and chlorite. It was included in the Ayer Crystalline Complex because of its proximity and mineralogic and textural similarities to the Clinton facies.

The Chelmsford Granite apparently intrudes the Devens - Long Pond facies. This implies that the Devens - Long Pond facies is probably the oldest unit of the complex. It also intrudes the upper units of Peck's (1976) sequence of metasedimentary units around Clinton where it also has produced significant contact metamorphic effects. Gore (1976b) has assigned the Clinton and Chelmsford facies a Devonian age and the Devens - Long Pond Gneiss an Ordovician or older age. Isotopic geochronology suggests an Ordovician or older age for

the entire Ayer Crystalline Complex (Chapter 4).

Fossiliferous Rocks in the Study Area

All of the stratified rocks discussed above are non-fossiliferous. In the discussion of the intrusive rocks an attempt has been made to outline the relationships between the igneous rocks and the stratified metamorphic rocks. This information combined with information on isotopic ages for the intrusive rocks does narrow down the ages of the stratified rocks. However, as the reader may have noticed, this approach is of little help. The best that can be said based on ages of the intrusive rocks is that the metasedimentary and metavolcanic rocks of this area are pre-Silurian, and possibly Precambrian depending on how we interpret the sequence.

However, a number of fossiliferous rocks do crop out within or near the area of interest. A number of small units of lower and middle Cambrian rock crop out to the southeast and south of Boston (Theokritoff, 1968; Bell and Alvord, 1976). The Cambrian rocks are a miogeosynclinal sequence of sandstones and shales which show few signs of deformation. Their use for age determinations is limited by the fact that all of their contacts with surrounding rocks appear to be faults or intrusive contacts.

A sequence of Siluro-Devonian volcanics - the Newbury Volcanic Complex (Shride, 1976a,b) - occurs north of Boston between the Spencer Brook Fault and the Bloody Bluff Fault

near the town of Newbury. The volcanics are a series of flows, tuffs, agglomerates, flow breccias and volcanoclastics with minor interlayered epiclastic terrigenous sediments. The upper part of the volcanic complex is mostly sedimentary: siliceous siltstones, sandy mudstones and calcareous mudstones. These volcanic and sedimentary units comprise an overturned homoclinal sequence almost totally undeformed and unmetamorphosed. Fossil ostracods found in the sedimentary units indicate a Silurian to possibly Devonian age. However, Shride (1976b) shows that the Newbury Volcanic Complex is completely fault bounded, although it has been tentatively correlated with the Lynn and Mattapan Volcanics around the Boston Basin and with volcanics along the coast of Maine and New Brunswick. The fact that the complex is fault bounded limits its usefulness in establishing ages.

A series of low grade metasediments of Pennsylvanian age (Grew, 1976) crops out in small isolated bodies from Worcester to Clinton. They are composed of conglomerates, arkoses, phyllites, and meta-anthracites which show signs of slight deformation. Fossil plants in the meta-anthracites indicate a Pennsylvanian age. However, most of the Pennsylvanian rocks are also fault bounded, although in some places the contacts may be unconformities (Thompson and Robinson, 1976). The Pennsylvanian rocks may be related to those in the nearby Norfolk and Narragansett Basins (Oleksyshyn, 1976; Lyons et al., 1976).

Overall, the fossiliferous rocks do not improve our knowledge concerning the ages of the unfossiliferous rocks.

Chapter 4

Previous Geochronologic Work

This chapter will attempt to present some of the significant isotope geochronologic work done on rocks in northeastern Massachusetts over the last twenty years. This review is not meant to be an exhaustive listing of geochronologic data, but rather a listing of the most recent data for each unit for each method applied to that unit.

Although there is no general summary of isotopic ages for northeastern Massachusetts, many of the ages reported in the literature are included in a number of summaries of ages from New England, eastern North America or all of North America. The earliest such summary was by Rodgers (1952); other compilations are: Gheith (1958), Goldsmith (1964), Tilton (1965), Lyons and Faul (1968), Faure and Powell (1972), and Naylor (1976).

Table 2 is a listing of isotopic ages for rocks within the area of this paper, as well as a number of rocks which have important relations to the study area but lie outside of it. Age data are given separately for the conventional K-Ar and Rb-Sr methods and various U-Th-Pb methods. In this way the reader may compare the behavior of each system relative to the others for each unit. In addition, one can compare the quality and consistency of the data. Where the method was applied to a single mineral, the name of the min-

TABLE 2

Isotopic Ages for Rocks of Northeastern Massachusetts

Unit	Method	Age, m.y. ¹	Reference
Andover Granite	K-Ar (muscovite)	239 ± 8	Zartman <u>et al.</u> , 1970
	"	278 ± 10	"
	"	306 ± 9	"
	Rb-Sr	460 ± 23 0.7050 ± .0020	Handford <u>et al.</u> , 1965
Ayer Granite (Ayer Crystalline Complex of Gore, 1976a, 1976b)	K-Ar (muscovite)	327 ± 17	Zartman <u>et al.</u> , 1970
	Rb-Sr	460 ± 150 0.710 ± .005	Heath, 1965 (thesis)
	Pb-α (zircons)	410 - 520	Zartman <u>et al.</u> , 1965
	U-Th-Pb (zircons)	425 ± 10	Zartman, 1976 (written comm. to Grew, 1976; see also Peck, 1976)

¹Where available, the initial ratio of Sr⁸⁷/Sr⁸⁶ is also given for Rb-Sr data.

TABLE 2 (CONT.)

Unit	Method	Age, m.y. ¹	Reference
Beverly Syenite (part of Cape Ann Plutonic Series of Dennen, 1976)	Rb-Sr	330 ± 30 0.705 ± .005 (assumed)	Fairbairn <i>et al.</i> , 1966
Blue Hills Aporhyolite ²	Rb-Sr	235 - 420	Bottino <i>et al.</i> , 1970
Blue Hills Granite Porphyry ³	Rb-Sr	282 ± 8 0.717 ± .002	Bottino <i>et al.</i> , 1970
Brimfield Schist (high to medium grade metasediment within Merrimack Synclinorium; see Peck, 1976, and Peper and Pease, 1976)	K-Ar (biotite) " Rb-Sr	252 ± 8 316 ± 9 421 ± 41 0.717 ± .002	Zartman <i>et al.</i> , 1970 " Brookins and Methot, 1971

²(devitrified felsic volcanics associated with Quincy Granite; see Kaktins, 1976, and Naylor and Sayer, 1976)

³(chilled border phase of Quincy Granite; see Naylor and Sayer, 1976)

TABLE 2 (CONT.)

Unit	Method	Age, m.y. ¹	Reference
Cape Ann Granite	K-Ar (amphibole)	374 - 397	Zartman and Marvin, 1971
	Rb-Sr	435 ± 6 0.703	"
	Pb ²⁰⁷ /Pb ²⁰⁶ (zircon)	452 ± 10	"
Chelmsford Granite (part of Ayer Crystalline Complex?; Gore, 1976a, 1976b)	K-Ar (muscovite)	327	Fairbairn <u>et al.</u> , 1967a
	Rb-Sr	364 ± 71 0.7190 ± .0180	Handford <u>et al.</u> , 1965
Dedham Granodiorite	Rb-Sr	608 ± 17 0.7065 ± .0011	Kovach <u>et al.</u> , 1977
	Pb-α (zircon)	365	Webber <u>et al.</u> , 1956

TABLE 2 (CONT.)

Unit	Method	Age, m.y. ¹	Reference
Milford Granite	K-Ar (biotite)	244 ± 13	Hurley <u>et al.</u> , 1960
	Rb-Sr	614 ± 24	Zartman and Naylor, 1972 (ages reported in Cam- eron and Naylor, 1976)
	Pb ²⁰⁷ /Pb ²⁰⁶ (zircon)	630	" "
	Pb-α (zircon)	355	Webber <u>et al.</u> , 1956
Millstone Hill Granite (possibly related to Ayer or Chelms- ford Granites; see Hepburn, 1976)	Rb-Sr	380 ± 15	Zartman, 1976 (written comm. to Grew, 1976)
	Rb-Sr (muscovite)	360 ± 10	Zartman <u>et al.</u> , 1965
	K-Ar (muscovite)	245 ± 12	"
Newbury Volcanic Complex	Rb-Sr	345 ± 10 0.709 ± .001	Fairbairn <u>et al.</u> , 1967a

TABLE 2 (CONT.)

Unit	Method	Age, m.y. ¹	Reference
Newburyport Quartz Diorite	K-Ar (biotite)	321 ± 10	Zartman <u>et al.</u> , 1970
Northbridge Granite Gneiss	K-Ar (biotite)	247 ± 13	Hurley <u>et al.</u> , 1960
	Rb-Sr	569 ± 4 0.7058 ± .0005	Fairbairn <u>et al.</u> , 1967b
	Pb-α (zircon)	260	Webber <u>et al.</u> , 1956
Peabody Granite	K-Ar (amphibole)	350 - 403	Zartman and Marvin, 1971
	Rb-Sr	367 ± 24 0.708	"
	Pb ²⁰⁷ /Pb ²⁰⁶ (zircon)	435 ± 12	"
	"	445 ± 22	"

TABLE 2 (CONT.)

Unit	Method	Age, m.y. ¹	Reference
Quincy Granite	K-Ar (amphibole)	430 - 458	Zartman and Marvin, 1971
	Rb-Sr	313 ± 22 0.731	"
	Pb ²⁰⁷ /Pb ²⁰⁶ (zircon)	437 ± 32	"
Rattlesnake Pluton (alkalic pluton intruding Dedham Granodiorite; see Lyons and Krueger, 1976)	K-Ar (amphibole)	366 ± 9	Lyons and Krueger, 1976
	K-Ar (biotite)	308	"
	"	254	"
	K-Ar (whole rock, on trachyte)	342	"
Salem Gabbro- Diorite	Rb-Sr	360? 0.704?	Fairbairn <u>et al.</u> , 1967a
	He ratio (magnetite)	>330	Rodgers, 1952

TABLE 2 (CONT.)

Unit	Method	Age, m.y. ¹	Reference
Sharpners Pond Diorite	K-Ar (hornblende)	329 ± 18	Zartman <u>et al.</u> , 1970
unnamed coarse- grained diorite southeast of Newbury Volcanic Complex; see Shride, 1976)	K-Ar (hornblende)	640	Zartman, 1972 (oral comm. to Shride, 1976)

eral will be given; if no mineral name is given, a whole rock analysis is assumed.

No attempt has been made to correct for the various values of radioactive half-lives, isotopic ratios and elemental abundances which different authors use. For this reason, the original references are given in Table 2 so that the reader may refer to those works in order to compare the differing values for the abovementioned parameters.

Changes in rock unit nomenclature will be mentioned where appropriate, but since such changes have been quite varied and subtle through time, any analyzed rock unit may include samples no longer considered part of that rock unit. Thus, redefinitions of rocks or changes in nomenclature for the units of Table 2 of which the author is not aware are not unlikely.

Comments on the Data in Table 2

As the data in Table 2 show, most of the major intrusive igneous bodies in eastern Massachusetts have been investigated by one or more isotopic methods. Two extrusive volcanic units (Blue Hills Aporhyolite and the Newbury Volcanic Complex) and a metasedimentary-metavolcanic sequence (Brimfield Schist) have also been investigated. The major reasons for this emphasis on the intrusive rocks in the area are their overall favorable chemistry, mineralogy and grain size, as well as lack of major regional metamorphic effects and defor-

mation. In spite of this, the data for the intrusive rocks have proved to be highly variable and difficult to interpret.

The data in Table 2 immediately show that discordancy between the various geochronologic methods is common to all of the units in the area. This is not surprising for K-Ar ages and ages obtained by older U-Pb methods (Pb- α and He) where daughter loss occurs easily and is difficult to correct for. Zartman et al. (1970) have noted a significant thermal event in eastern New England during the Permian which has reset or partially reset K-Ar ages. Lyons and Krueger (1976), however, argue that K-Ar ages they have obtained for the Rattlesnake Pluton southwest of Boston are the true ages of the pluton. If true, it would make the Rattlesnake Pluton distinctly younger than any other similar alkalic pluton in eastern Massachusetts. They present arguments that suggest that the ages of these other alkalic plutons may be incorrect. They suggest two periods of alkalic intrusion - one in the Ordovician, another in the Devonian. Geochemical data (Buma et al., 1971; Dennen, 1976) favor the idea that the alkalic plutons of eastern Massachusetts are all related and thus roughly contemporaneous, as suggested by the isotopic work. In addition, as Table 2 shows, where K-Ar ages are backed up by Rb-Sr whole rock ages or U-Th-Pb ages on zircons, the K-Ar ages are nearly always the youngest. Thus, until proved otherwise by data obtained from other methods, it is felt that K-Ar ages from this area should always be viewed with

suspicion.

Most of the units in Table 2 have been analyzed by the Rb-Sr whole rock method, but few of them have been backed up by U-Th-Pb analyses on zircons. In cases where Rb-Sr whole rock and U-Th-Pb zircon analyses have been made on the same unit, a few (Peabody and Cape Ann Granites) show discordance between the two methods. As Naylor and Sayer (1976) have pointed out, this is probably due to increased mobility of radiogenic Sr^{87} . Because these plutons are alkali-rich, much of the Sr^{87} produced radiogenically is in alkali-rich phases. Small thermal events may cause rapid release of radiogenic Sr^{87} ; in fact, it may diffuse continuously. Since there are few phases in these alkalic plutons which readily accept Sr, such as plagioclase, apatite, and epidote, the radiogenic Sr^{87} probably diffuses completely out of the rock. This is probably not as great a problem with the more calc-alkaline and intermediate rocks in the area, although many of them are in the higher grade parts of the section and as a result have undergone more intense thermal and deformational events.

A similar problem seems to occur in the Rb-Sr analyses of volcanic rocks, although for different reasons. Their usual fine grain size and high content of glass, which later devitrifies, makes them highly susceptible to Rb and Sr loss. This would explain the observations that Rb-Sr whole rock ages on volcanics are usually lower than the ages determined

by fossils or other isotopic methods (Brookins, 1976; Naylor, 1976). The data for the Blue Hills Aporhyolite and the Newbury Volcanic Complex show this effect quite well. The Rb-Sr age for the Newbury Volcanic Complex determined by Fairbairn et al. (1967a) gives an early Carboniferous age for the Complex. This is younger than the Siluro-Devonian age deduced from fossils (Shride, 1976). The data for the Blue Hills Aporhyolite are quite scattered but the upper limit of 420 m.y. is in good agreement with the age of 437 ± 32 m.y. determined by Zartman and Marvin (1971) for the Quincy Granite by Pb^{207}/Pb^{206} analyses of zircons. The Blue Hills Aporhyolite is probably an extrusive phase of the Quincy Granite according to Naylor and Sayer (1976). Kaktins (1976) sees a direct relationship between the apparent ages of samples from the Aporhyolite and the characteristics of the flow from which the samples came. Most of the flows are ash flows and apparently the greater the induration and welding of the flow the greater is the apparent age. The greatest age (420 m.y.) is for a true flow of rhyolitic composition. The rhyolite flow was probably more homogeneous and cooled and devitrified more quickly than the ash flows. In spite of the fact that the rhyolite probably contained as much glass as the ash flows, it probably remained a closed system over a longer period of time than the ash flows.

Despite these problems and the variability shown by the ages in Table 2, a number of significant intrusive and meta-

morphic events can be recognized. U-Th-Pb results on zircons distinctly show two major intrusive episodes. The first episode is a late Precambrian or early Cambrian one (650 to 565 m.y.), often called the Avalonian orogeny, represented by the Dedham Granodiorite, Milford Granite and Northbridge Granite Gneiss. These rock units make up the so-called eastern basement of New England and represent a basement sequence distinctly different in age from the basement in western New England.

The second episode is an Ordovician to early Silurian event (490 to 420 m.y.) that has been correlated with the Taconic Orogeny of western New England. The major units of this intrusive event are the alkalic plutons of eastern Massachusetts - the Quincy, Cape Ann, and Peabody Granites - and the calc-alkaline plutons in the western part of the study area - the Andover and Ayer Igneous Complexes. These last two units intrude the major sections of stratified rocks in the area. This suggests that the major period of regional metamorphism slightly predates the intrusion of the Ayer and Andover Complexes because both show few signs of regional metamorphic effects.

The Permian thermal event which has affected K-Ar ages has been mentioned above.

The existence of the Devonian Acadian Orogeny in this area is difficult to discern based on the information in Table 2. A number of ages fall within the proper range for

the Acadian (350 to 400 m.y.), but these ages are from K-Ar analyses or Rb-Sr whole rock ages that are either not backed up by U-Th-Pb analyses, or show older ages from such analyses. It would seem that if the Acadian Orogeny had any major effects on the region, it manifested itself as a locally variable thermal or hydrothermal event rather than a distinct period of deformation and metamorphism.

Chapter 5
Present Study

Introduction

In order to gain more information about the geologic history of the area, a combined Rb-Sr whole rock and zircon U-Pb study of the stratified metamorphic rocks was proposed. The complex interlayering of metavolcanics and metasediments with highly variable compositions and lithologies means a high degree of difficulty in interpreting the data, but it also means that a great deal more information can be obtained from a small area.

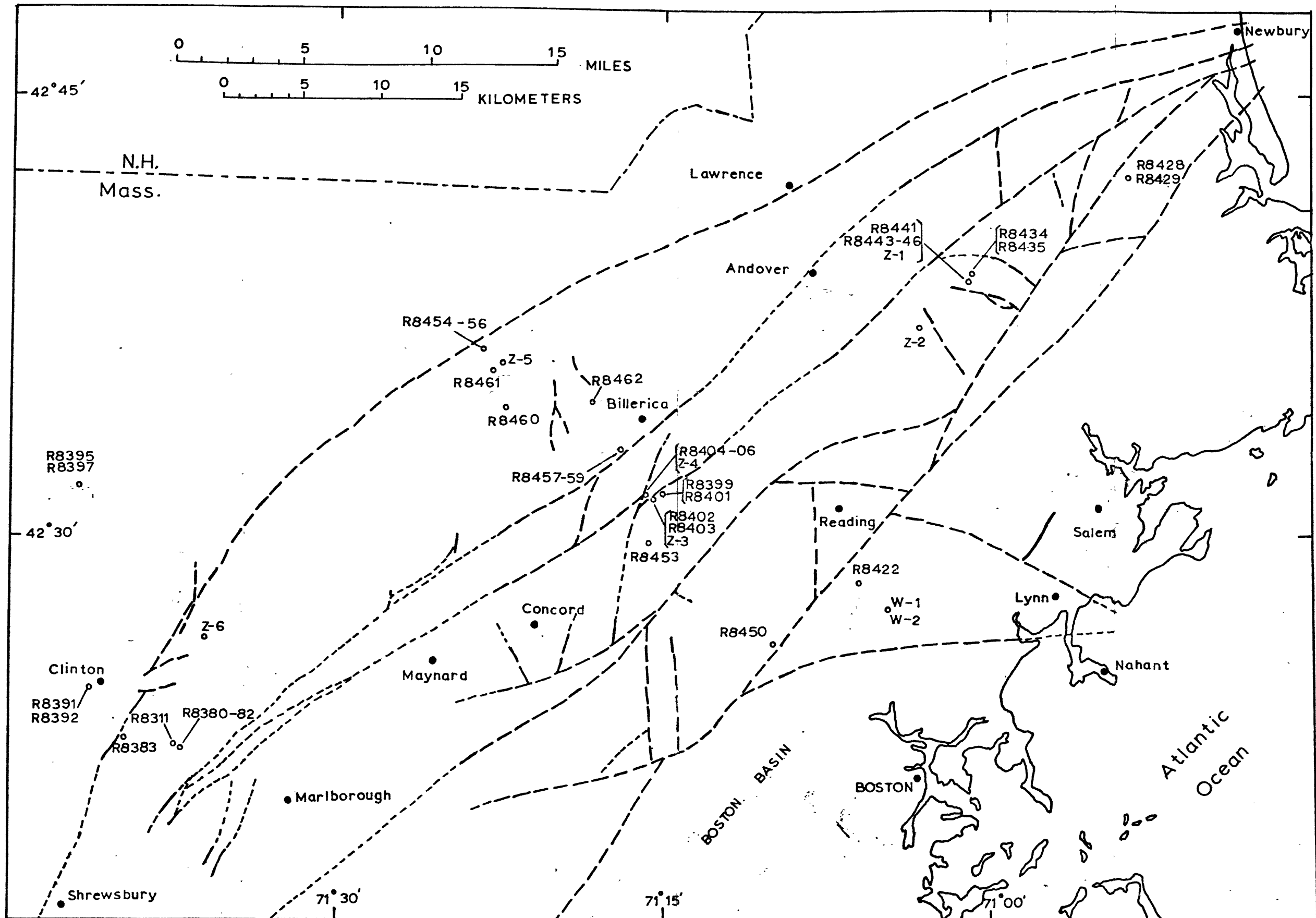
The reasoning for this approach is that U-Pb Concordia plots of zircon analyses from volcanics and sediments would provide information on the ages of deposition for the various units and the continuity of the rock sequence, as well as information about the source areas of the sediments. The whole rock Rb-Sr data would either confirm the zircon results or, more likely, provide information about the major metamorphic episodes in the area and how the different rock types responded to the metamorphism.

Sample Localities

Figure 3 shows the locations of samples collected and analyzed for this report. Samples collected for the Rb-Sr whole rock method are indicated by and R followed by four

Figure 3

Sample localities for this report. (Map after
Bell and Alvord, 1976.)



digits. Samples for zircon analysis are indicated by a single letter followed by a single digit. A few Rb-Sr samples were also used for zircon analyses. In order that stratigraphic names and lithologic descriptions remain consistent, the nomenclature of Bell and Alvord (1976) will be used for the stratified units east of the Clinton-Newbury Fault Zone. The nomenclature of Peck (1976) will be used for the units studied west of the Clinton-Newbury around Clinton, Massachusetts; although when grouped together the name Worcester Formation will be used.

Samples for Rb-Sr work were collected in the fall of 1975 by the author with the help of K. Bell and D. Alvord, formerly of the U.S.G.S. office in Boston. Some samples were also provided by Alvord. Short sample descriptions are given in Chapter 7. General sample locations are shown in Figure 3. Detailed sample locations and thin section descriptions are given for selected samples in Appendix C.

Samples for zircon analyses were collected by the author in the spring of 1976. General sample locations are given in Figure 3. Short hand-sample descriptions are given in Chapter 6. Detailed sample locations and thin section descriptions are given for all the zircon samples in Appendix C.

Criteria for Sampling for Rb-Sr Whole Rock Work

The rocks in this part of Massachusetts share two characteristics in common. One is intense weathering, often

reaching half of a meter or more into a rock. Its major effects are sericitized feldspars and iron staining from weathered biotite and hornblende and oxidized magnetite. Because weathering can significantly affect Rb-Sr whole rock ages (Bottino and Fullagar, 1968), attempts were made to avoid weathering wherever possible. Where this was not entirely possible to do during sampling, weathered material was removed during sample preparation. Although it is believed that the effects of weathering have been minimized, it is doubtful that they have been completely removed.

The second common characteristic is the pervasive effect of hydrothermal activity. Small dikes, veins, apophyses and pods of granite, aplite, quartzofeldspathic and quartzose material are almost everywhere. Veins and pods of epidote-zoisite are common also, especially in the greenstones east of the Bloody Bluff Fault Zone. Such things were avoided as much as possible, but an outcrop clear of such phenomena does not insure that they do not exist some small distance below the surface of the outcrop. The effect of hydrothermal activity on the Rb-Sr whole rock ages is uncertain. Much of the activity appears to be low temperature in nature, probably the result of very late stage igneous activity or retrograde metamorphism. Some of the activity, however, such as the dikes and veins of granite and aplite, appears to be associated with the main period of igneous activity.

Sample size was determined by the grain size of the

rock. For most samples, the sample size was 50 to 100 or more times the average grain size. For some of the coarse grained gneisses this would have meant samples of a very large size. So these samples were chosen so that sample size was ten or more times the average grain size. It is believed this is large enough to insure a homogeneous sample.

Mineralogic criteria were also applied to the sampling. Samples rich in carbonate, epidote and zoisite were avoided even if veins of such material were not present. The more mafic greenstones and amphibolites were also avoided because of low rubidium content. A few quartzites were sampled (W-1, W-2, R8311), but only one (R8311) had a sufficient rubidium content for analysis.

Deformational criteria were taken into consideration also. Samples with signs of extensive cataclasis, shearing or faulting were avoided.

Criteria for Zircon Sampling

The qualifications for zircon samples were essentially the same as those used for Rb-Sr samples. Weathering, hydrothermal, mineralogic, and deformational criteria were exactly the same. Sample sizes were 30 kg or larger to insure that the zircon separates obtained from them would be large enough to be useful. Because the Rb-Sr work was done before zircon sampling, this sampling was guided somewhat by the Rb-Sr results.

Wherever possible zircon samples were taken from the same outcrop as Rb-Sr samples or as close as possible to an outcrop used for Rb-Sr work. This would insure close control between the two methods. Samples without Rb-Sr control are W-1, W-2, Z-2, and Z-6. In order to maximize this control between Rb-Sr whole rock data and U-Pb zircon data, zircons were also separated from a few samples used for Rb-Sr work (R8311, R8422, R8441, R8453, R8458).

All of the major units east of the Clinton-Newbury Fault Zone were sampled except for the Marlboro Formation. The Marlboro was not sampled because suitable outcrops could not be found. All five of Peck's (1976) units were sampled although only three (Units 2, 3, and 5) were later found suitable based on rubidium and strontium content (Appendix A).

Chapter 6

Results of U-Pb Analyses of Zircons

Sample Preparation and Zircon Separation

Samples were crushed and ground to less than 20 mesh and sieved to obtain the 60 to 325 mesh range of grain sizes. Zircons were separated using standard heavy liquids and magnetic separation techniques. The zircons were split according to magnetic properties and grain size following the zircon suite method of Silver and Deutsch (1963). A detailed description of sample preparation and zircon separation is given in Appendix B.

Zircon Yields

Amounts of zircons recovered from the samples varied widely as would be expected from the wide variation in composition of the samples. The highest yields of zircons came from two Nashoba samples: a feldspathic quartzite (R8311) and a biotite-feldspar-quartz gneiss (Z-5). They both yielded about 13 to 14 mg of zircons per kg of sample. The next highest yield also came from a biotite-feldspar-quartz gneiss (R8453) but from the Shawsheen Gneiss. It produced about 10 mg/kg. A large gap exists between these samples and the samples giving the next highest yields. The three Fishbrook Gneiss samples (Z-1, Z-4, R8441) gave about 4 to 5 mg/kg. A sample of the Nashoba (R8458) also gave a

zircon yield in the same range. All four samples were feldspar-quartz-biotite gneisses. A number of samples gave a yield between 1 and 2.5 mg/kg. This included quartzites (W-1 and W-2), a feldspar-quartz-biotite gneiss (Z-6), and a biotite-feldspar-quartz gneiss (Z-3). The lowest yield (approximately 0.6 mg/kg) came from an amphibolite from the Shaw-sheen Gneiss.

Absolute amounts of zircons recovered depended on sample size, amount processed, efficiency of separation and zircon concentration. This accounts for the variation in the number of splits of zircons for each sample. The samples initially used for Rb-Sr work were small - 1 to 2 kg - but were separated by centrifuging (see Appendix B) which is somewhat more efficient than the method used for the samples chosen specifically for zircon work. Nevertheless, only 1 or 2 splits could be obtained from these samples except for R8311 where a number of splits have been obtained because of the high yield. For the samples chosen just for zircon work, the two Fishbrook Gneiss samples gave the largest number of splits since they were also the largest samples processed (>30 kg). Z-5 and Z-6 had only one split apiece because the amounts of sample processed were small (2-3 kg).

The amount that could be processed efficiently and quickly was determined somewhat by the composition. Samples rich in biotite and hornblende were difficult to work with since these minerals had to be removed by magnetic separation

in order to avoid using outrageous quantities of heavy liquids. The magnetic separation is an inherently inefficient and time-consuming process, especially when dealing with large amounts of rock material. This is another reason for the small sizes of some samples.

It can be seen from the zircon yields that these rocks are basically poor in zircons. Even assuming only a 50% recovery rate, most of these rocks are still much poorer in zircons than typical granitic rocks where much higher yields would be expected. This general poverty in zircons is not surprising considering the overall composition of this sequence of rocks. It does mean that various factors, such as mixing of different zircon populations and analytical problems of small zircon samples, become more important.

Zircon Morphologies

Because the rocks under consideration represent a complex mixture of sediments and volcanics, the possibility of mixing of various populations of zircons is highly probable. For this reason a short study of the characteristics of the zircons was made in order to ascertain whether various populations of zircons were present.

The broadest generalization that can be made from observations of the zircons from all the rocks analyzed is that there are two basic populations. The first population is a euhedral to subhedral suite of zircons which are generally

clear and translucent although darker (pink and reddish) grains that transmit less light are not uncommon. These grains are usually well-faceted, doubly terminated crystals or angular broken fragments of crystals showing significant portions of euhedral crystal faces. The second population is a rounded to subrounded, occasionally subhedral, suite. The zircons are significantly darker in color, ranging from yellow to red to brown. Very few zircons of this suite were pink or pinkish-red in color, and no clear zircons were found. These zircons showed signs of frosting and only occasional overgrowths of limited extent were found. Both populations showed signs of resorption. Pitting, embayments, and occasional badly corroded grains were seen.

Fishbrook Gneiss - The three samples of the Fishbrook Gneiss (Z-1, Z-4, and R8441) are very similar and will be described together. Figures 4, 5, and 6 show photographs of zircons taken from sample Z-1; they are generally typical of all the other zircons taken from the Fishbrook Gneiss. The zircons are also typical of the first suite described above. They are generally euhedral to subhedral and quite clear or translucent (see Figure 6). Colors are clear, light pink and occasionally reddish (most common in Z-4). Faces and terminating prisms are usually fairly well developed although many grains appear to be slightly rounded at the edges. It is impossible to tell whether this is the result of transporta-

Figures 4, 5, 6, 7, 8, and 9

Photographs of zircons from Fishbrook Gneiss, sample Z-1 (Figs. 4, 5, 6); Shawsheen Gneiss, R8453 (Fig. 7); Westboro Formation, W-1 (Fig. 8); and Nashoba Formation, R8311 (Fig. 9). Designations after sample number are magnetic and size fraction designations explained in Appendix B. Scale is given next to each photograph. Note differences in grain morphology, color, and surface textures between the zircons in Figures 4, 5, and 6 and those in Figures 7, 8, and 9.

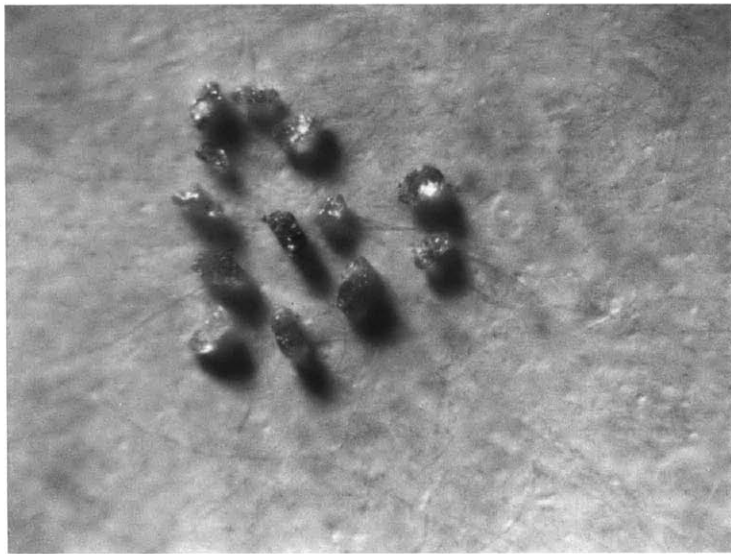


Figure 4

Z-1 2°M

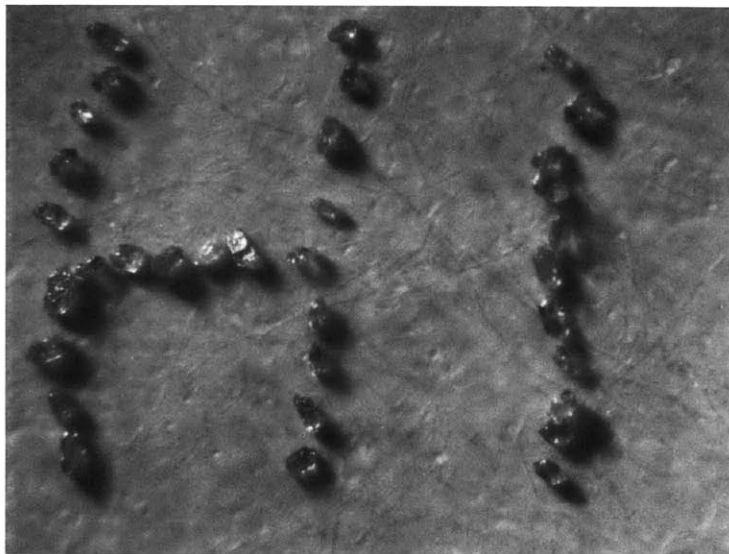
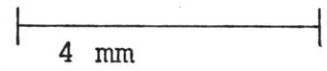
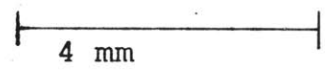


Figure 5

Z-1 1M
-150+200



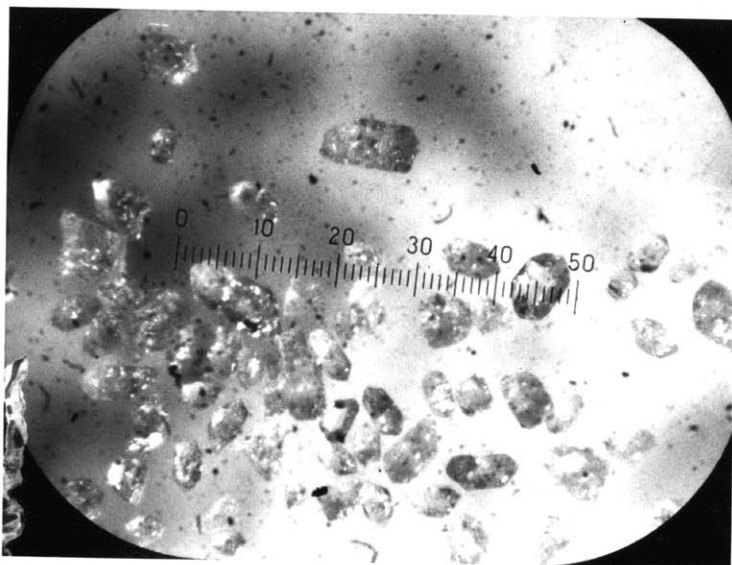


Figure 6

Z-1 2°M

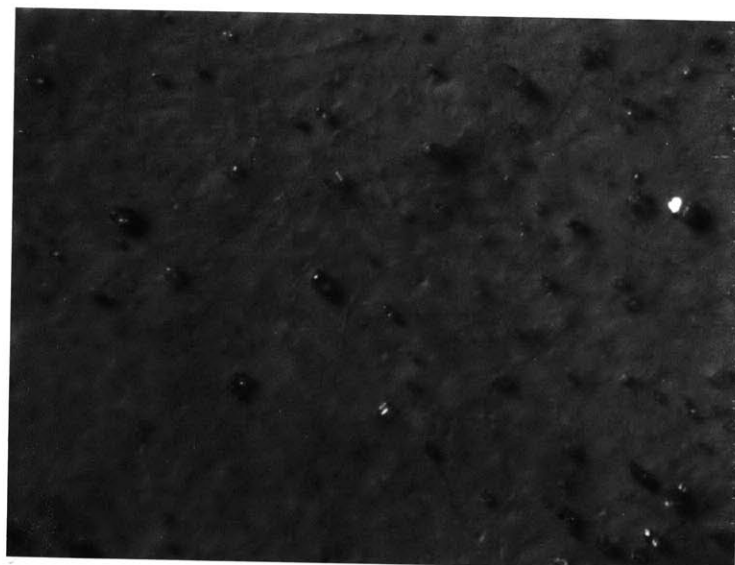
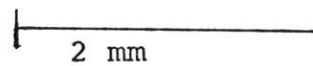
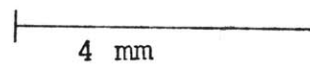


Figure 7

R8453 10NM



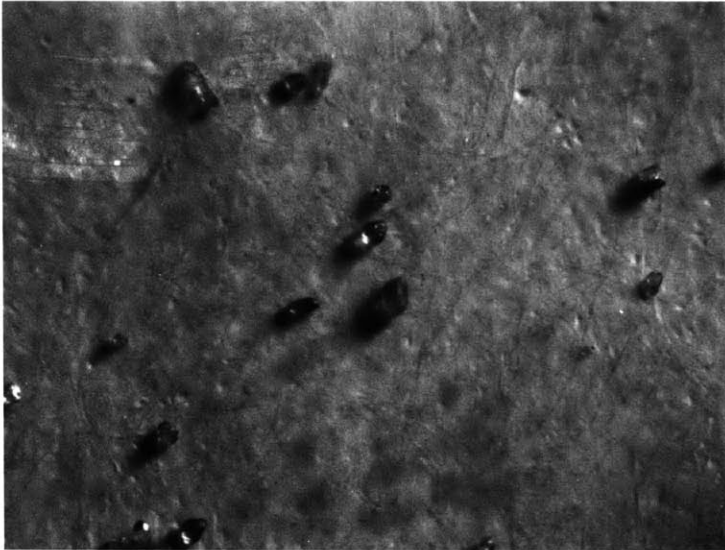


Figure 8

W-1 1M

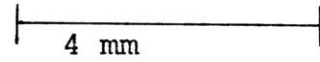
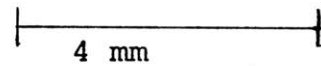


Figure 9

R8311 0.58NM



tion or resorption. Many grains show signs of embayment and corrosion especially in the larger and darker grains. As grain size decreases the zircons become clearer, more euhedral and more inclusion-free. A very magnetic fraction of the Fishbrook Gneiss which was not analyzed because it contained other minerals, contained mostly large, dark red zircons that were badly corroded and broken, yet still clearly showed sharp faces, edges and terminations.

Shawsheen Gneiss - The three samples of the Shawsheen Gneiss showed examples of both populations. Z-2, an amphibolite sample, gave a low yield of small (<150 mesh) zircons that were very euhedral and a uniform light pink in color. Grains were well faceted, almost universally doubly terminated and very elongated (elongation coefficient >3.0). Z-3 and R8453, however, contrast very sharply with this (see Figure 7). Both samples were well rounded to subrounded although occasional subhedral grains were found. Color is generally red to dark red to brown with a few yellow grains, especially in Z-3. Surfaces were generally frosted and commonly pitted. No signs of overgrowth or refaceting could be seen.

Westboro Quartzite - Both the samples of the Westboro Quartzite, W-1 and W-2, were very similar. Figure 8 shows some grains from W-1. In general, both samples were well rounded to subrounded with occasional euhedral grains (see top portion of Figure 8). Colors were yellow, red, dark red, and brown.

The zircons of W-2 were distinctly darker although they covered the same range. Both samples showed large numbers of frosted and pitted grains. Color became lighter and grain size generally decreased as magnetic susceptibility decreased. In fact, the most non-magnetic fractions of both samples showed a large number of clear to pink, euhedral grains.

Nashoba Formation - Of the four Nashoba samples, three (R8311, R8458, and Z-5) are similar to one another in morphology, surface features and color. Grains of these three samples are well rounded, crystal faces and edges are almost totally lacking. Their density and refractive indices were the only way of identifying them as zircons. All were darkly colored. Brown, dark red and reddish yellow zircons were the most common. Only the least magnetic fraction of R8311 showed a significant amount of light colored, more euhedral zircons. All the grains showed cloudy, frosted surfaces and pitting. Figure 9 shows typical grains of R8311. Zircons from this sample were the largest and darkest and were very magnetic. No signs of overgrowth could be seen.

Z-6, however, contained mainly euhedral and subhedral crystals that were pink and red in color. Grains were quite elongated, well faceted and doubly terminated. A few (<10%) small, partially rounded grains were also present.

Middlesex Fells Volcanic Complex - R8422 produced a small amount of zircons less than 200 mesh in size. These were clear, euhedral, well faceted, doubly terminated crystals. The grains were very elongate, inclusion-free, and showed no signs of resorption or overgrowth.

Interpretation of Zircon Morphology

The clear-cut separation of the zircons into two populations with distinctly different morphologies, surface textures and grain elongation conforms closely with Poldervaart's (1955, 1956) observation that detrital zircons are distinct from primary igneous zircons. Many of the characteristics of the zircons listed above are considered by Poldervaart to be typical of either detrital or primary igneous zircons, even after undergoing metamorphism.

The zircons of W-1 and W-2 are a clear-cut detrital population. The rock compositions and the zircon morphology and surface texture agree exactly with that interpretation. That detrital zircons can retain their rounded appearance and frosted surface texture well into high grade metamorphism has been observed by a number of authors (Eckelman and Kulp, 1956; Gastil et al., 1967; Pidgeon et al., 1970; Köppel and Grünenfelder, 1971; Gebauer and Grünenfelder, 1976). In fact, evidence indicates (Gastil et al., 1967) that detrital zircons only begin to refacet and lose their detrital characteristics near the beginning of partial melting. This argues strongly

for a detrital origin for the other zircons which also show similar characteristics (Z-3, Z-5, R8311, R8453, R8458). As will be shown later, the U-Pb data coincide with this interpretation. The rock compositions for some of these samples also back up this interpretation: R8311 is a feldspathic quartzite and R8458 is a biotite-muscovite gneiss.

A more difficult question to answer about the detrital zircons is whether or not they represent more than one population. There is some evidence for a probable metamorphic population. As noted above, many of the samples with detrital grains show a small population of clear to pink euhedral grains, especially in the least magnetic fractions. Saxena (1966) presents evidence for the growth of new zircons during diagenesis and low grade metamorphism, especially by the dissolution of more metamict grains. Saxena also points out that where overgrowths occur the detrital core can usually be discerned and the overgrowth usually takes on the shape of the pre-overgrowth zircon. The lack of rounded cores and the very euhedral, elongate morphology of the least magnetic fraction of the detrital samples suggests that they are a metamorphic population rather than a detrital population. The fact that these euhedral grains are clear or pink in color hints at a low uranium content. Saxena points out that the newly formed population will have a low uranium content.

The possibility also exists that there are a number of different populations within the detrital grains themselves.

Variations in color, grain size and morphology all appear to be continuous. Thus, no separation into different populations was possible except for the obvious dichotomy between the detrital and metamorphic populations. But the possibility of different detrital populations is evident and must be kept in mind when interpreting the data.

The more euhedral zircons of the other samples suggest an igneous origin based on the criteria of Poldervaart (1956). For some of these samples the composition also indicates an igneous origin. Z-2 is an amphibolite and R8422 is an intermediate volcanic agglomerate. It might be argued that these zircons represent a metamorphic population, but the high uranium content of some of the samples (Z-2, Z-4, Z-6, R8441), the very elongate crystals of some, and the large variation in grain size indicates otherwise.

Based on this I interpret the zircons of Z-1, Z-2, Z-4, Z-6, R8422 and R8441 to be igneous zircons of volcanic origin. An alternative explanation is that they represent detrital zircons that have been completely recrystallized. There are a number of points against this hypothesis, however:

- (1) Zircons from widely different areas, different metamorphic grades, different rock compositions, and different size and magnetic fractions still retain their detrital grain morphologies with almost no sign of refaceting, overgrowth, or layering evident. Yet, the samples with the igneous population are often from the same formation or within a short

distance of samples with definite detrital populations. Z-3 and Z-4 are two good examples (see Figure 3) of zircon populations widely different in morphology, yet they are at the same metamorphic grade and less than one kilometer from one another. R8422, W-1 and W-2 also manifest this difference. Although they are few kilometers from one another, they are part of a continuous section in a single fault block at the same metamorphic grade. These observations agree with the studies of Eckelman and Kulp (1956). They found that even in high grade granitic paragneisses, zircons retain their detrital morphologies even over great distances. However, concordant and discordant granitic orthogneisses still retain their euhedral, elongate igneous morphologies.

(2) All the evidence favors a process of dissolution and resorption of metamict zircons and the growth of new, metamorphic zircons from the mobilized zirconium according to the processes outlined by Saxena (1966). Evidence of resorption and corrosion is especially evident in the igneous suite where the sharp, angular zircon faces and edges reveal even small amounts of corrosion.

Magnetic susceptibility is directly related to the degree to which the zirconium have become metamict (Silver, 1963) and indeed, most of the resorption is seen in the most magnetic fractions, such as the 5° magnetic fraction of the Fishbrook Gneiss mentioned above. The evidence for overgrowth or recrystallization of an old detrital population is

meager.

(3) The metamorphic grade is in general too low to cause significant recrystallization of zircons. Gastil et al. (1967) and Eckelman and Kulp (1956) note that it is difficult to completely recrystallize and reset zircons even under high grade metamorphism. Only during intense granitization (Kögl and Grünenfelder, 1971) or near anatexis conditions (Gastil et al., 1967) do recrystallization or refaceting occur. Such conditions are approached locally in the Nashoba Formation, yet samples from various parts of that formation still retain clear-cut detrital characteristics. Some of the slight rounding seen in some of the Z-1 and Z-4 zircons (see Figure 4) could be detrital, but an alternative explanation is that it is due to corrosion and resorption. Poldervaart (1956) indicates that rounding of zircons due to corrosion is common in effusive igneous rocks.

(4) As will be seen later, the igneous suite and the detrital suite fall on two different trends of U-Pb Concordia data. Although these might be interpreted as two detrital lines, one would have to explain why one trend includes zircons from an amphibolite (Z-2) and a volcanic agglomerate (R8422) which are almost certainly igneous in origin.

Taking all these things into consideration it is clear that there are two populations of zircons: an igneous population and an older detrital population. A younger metamorphic population may be mixed with both of these but it can

not be clearly delineated except possibly in the detrital population. The possibility of mixing of the igneous and detrital populations must be considered. Although the evidence presented above suggests that the two populations are well separated, petrographic evidence suggests mixing is highly probable. Bell and Alvord (1976) note that the vast majority of metavolcanic rocks in the area are subaqueous and usually reworked. They consist of volcanic wackes, volcanic sands, waterlain tuffs and occasional subaqueous flows. Mixture with a detrital zircon fraction can not be discounted, and the data presented above do not allow for a quantitative estimate of mixing. But lack of any observable zircons of clear-cut detrital origin in the volcanic suite suggests that the mixing is slight.

Zircon Dissolution, U-Pb Chemistry and Mass Spectrometry

Appendix B describes the dissolution, U-Pb separation and mass spectrometric procedures used. The technique of Krogh (1973) was used with some minor variations. Appendix B also discusses the nature of spike calibrations, blanks, and replicate analyses. All Pb^{204} observed was assumed to be contamination. A discussion of the possibility of inherited common lead in the zircons follows the presentation of the data. Both Pb and U were run using the silica gel method. The usual Ta_2O_5 technique used by Krogh for uranium was not found to be suitable for small quantities of uranium

(Montgomery, 1977) whereas the silica gel method was found to produce good results. A discussion of the reasons for this change are given in Appendix B.

All values (i.e. weights of spikes, concentrations of spikes, isotopic ratios, etc.) were measured a number of times to produce a standard error of measurement. These errors were propagated through all calculations. All errors quoted in this paper are \pm one standard deviation of the mean unless otherwise noted. A discussion of the error and statistics used in this paper are given in Appendix D.

U-Pb Results

The U-Pb results for each formation studied follow, as well as short petrologic descriptions of the samples used. Half-lives of U^{235} , U^{238} , and the isotopic ratios used are given in Appendix B. Pb^{207}/U^{235} and Pb^{206}/U^{238} ratios were calculated and plotted on Concordia diagrams (Wetherill, 1956). Pb^{207}/Pb^{206} , Pb^{207}/U^{235} , and Pb^{206}/U^{238} ages were taken from the tables of Stacey and Stern (1973). Any samples in which total contamination Pb (spiked and unspiked aliquots) was two or more times the total radiogenic Pb (i.e. Pb^{204}/Pb^{206} ratios less than 53) were discarded as were samples in which the errors of the final Concordia points were greater than 5%. These "bad" points will be discussed separately. Chords for the discordant zircons were determined using the linear least squares cubic regression equations of

York (1966, 1967, 1969). A discussion of the errors, error correlation coefficients and other parameters used in the regressions is given in Appendix D. Intercepts with Concordia were determined by an iterative process until consecutive values for the intercept were within 0.01% of one another.

Fishbrook Gneiss - The Fishbrook Gneiss zircons came from three samples:

Z-1: Light colored plagioclase-quartz-biotite gneiss. Medium to coarse grained, surfaces are fresh except for some iron staining associated with biotites. Foliation poorly developed, except where biotite is occasionally clumped.

Z-4: Similar to Z-1 but more biotite rich. Small amount of muscovite developed. Slightly weathered and badly iron stained.

R8441: Similar to Z-1 but foliation better developed. From same outcrop as Z-1.

See Figure 3 for outcrop localities.

U-Pb isotopic data for the Fishbrook Gneiss are shown in Table 3. Data are plotted on a Concordia diagram and shown in Figure 10. Some least squares regression lines are also shown in Figure 10. Intercepts and ages of these and other chords for the Fishbrook Gneiss samples are given in Table 4.

The scatter for individual samples is quite large. Whether this difference in slopes between the different samples is real or reflects the limited sampling and range of

TABLE 3

Fishbrook Gneiss

Sample	Split	Pb*, ppm ¹	U, ppm	$\frac{\text{Pb}^{206}}{\text{Pb}^{204}}$	$\frac{\text{Pb}^{207^2}}{\text{Pb}^{206}}$	$\frac{\text{Pb}^{208^2}}{\text{Pb}^{206}}$
Z-1	3M +150	34.04	468.6	110.0	0.06248	0.12400
	3M -150	28.12	464.2	1186	0.05551	0.10908
	2M	23.32	375.6	2457	0.05652	0.11740
	1M +150	24.85	276.1	96.96	0.06133	0.48195
	1M -200+250	24.81	275.3	151.1	0.05985	0.23313
	1M -250	24.38	336.1	1972	0.05783	0.12113
	1NM +150	26.02	249.3	199.3	0.06380	0.29602
	1NM -150+250	35.56	242.3	178.3	0.06023	1.0573
	1NM -250	35.77	285.3	251.4	0.06823	0.65293
Z-4	5M	81.69	1608	337.8	0.05531	1.3489
	4M	85.67	1342	337.5	0.05620	0.12015
	3M	88.39	1373	235.0	0.05914	0.11824
	2M	N.D.	N.D.	267.7	0.05593	0.11427
	1M	17.30	291.2	655.7	0.05878	0.15748
	1NM	31.65	1161	1161	0.05932	0.098818
R8441	4M	65.92	1153	543.8	0.05711	0.13405
	4NM	41.36	625.8	1445	0.05647	0.12954

¹Pb* = radiogenic lead²corrected for contamination;
see Appendix B

TABLE 3 (CONT.)

Sample	Split	Apparent ages, m.y.				
		$\frac{\text{Pb}^{207}}{\text{U}^{235}}$	$\frac{\text{Pb}^{206}}{\text{U}^{238}}$	$\frac{\text{Pb}^{207}}{\text{U}^{235}}$	$\frac{\text{Pb}^{206}}{\text{U}^{238}}$	$\frac{\text{Pb}^{207}}{\text{Pb}^{206}}$
Z-1	3M +150	.6131±.0094	.0712±.0003	486	444	691
	3M -150	.4629±.0024	.0605±.0002	386	379	433
	2M	.4791±.0029	.0615±.0003	398	385	473
	1M +150	.5721±.0080	.0677±.0005	460	423	651
	1M -200+250	.6682±.0104	.0810±.0009	528	503	598
	1M -250	.5704±.0050	.0715±.0005	458	445	524
	1NM +150	.7842±.0071	.0892±.0006	588	551	735
	1NM -150+250	.6666±.0204	.0823±.0003	519	510	612
	1NM -250	.7945±.0068	.0845±.0004	594	523	876
Z-4	5M	.1866±.0029	.0245±.0003	174	157	425
	4M	.4890±.0047	.0631±.0003	404	395	460
	3M	.5184±.0046	.0636±.0004	424	398	572
	2M	.4994±.0035	.0648±.0002	411	405	450
	1M	.4600±.0046	.0568±.0003	384	357	558
	1NM	.5863±.0030	.0717±.0003	469	446	579
R8441	4M	.4393±.0027	.0558±.0003	370	350	496
	4NM	.5043±.0029	.0648±.0003	415	405	471

Figure 10

Concordia plot of U-Pb data from the Fishbrook Gneiss showing the last two best fit chords of Table 4. Ages are millions of years with \pm one standard deviation of the mean error.

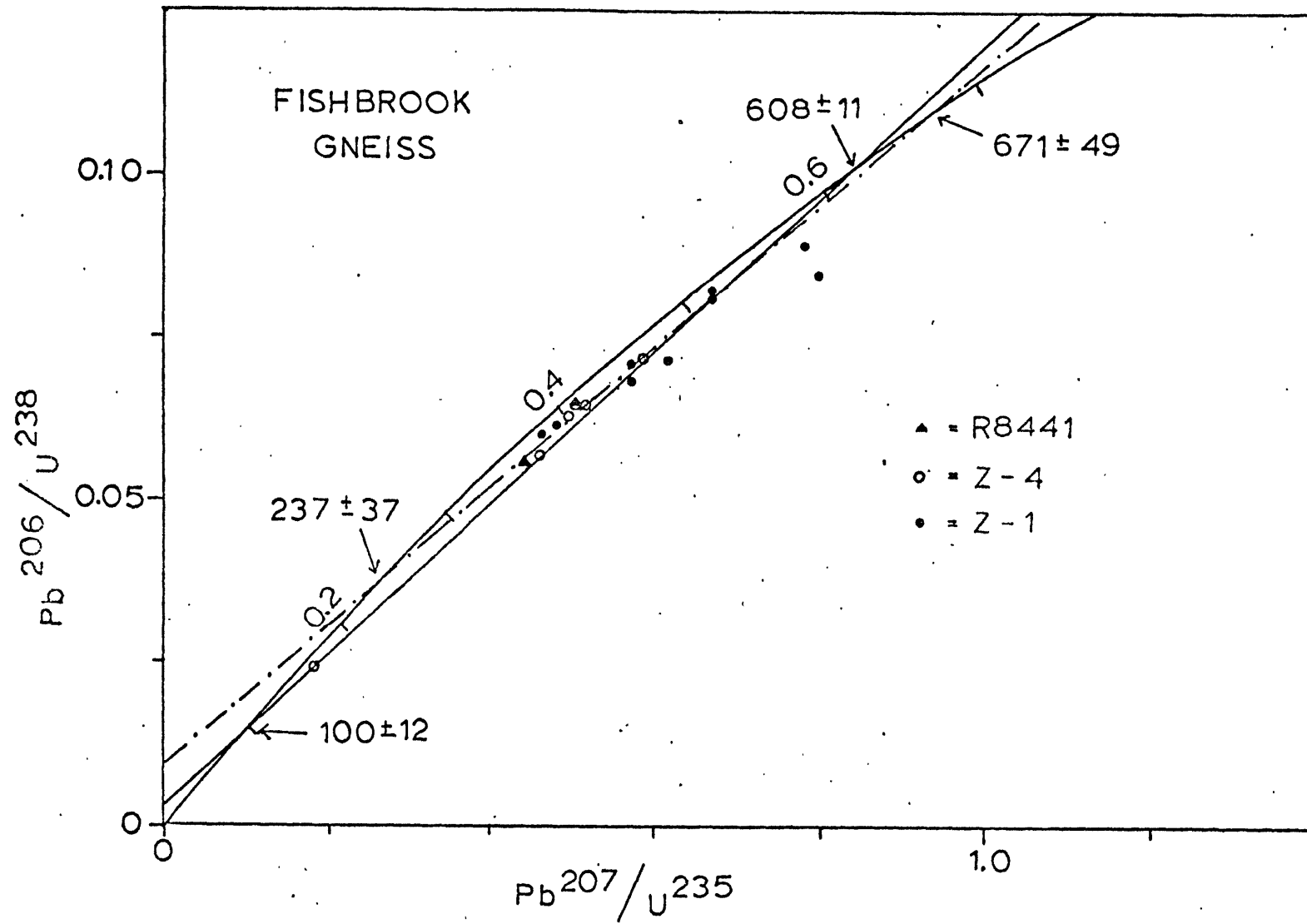


TABLE 4

Concordia Intercepts and Ages of Fishbrook Gneiss

Sample	Upper Intercept			Lower Intercept			Comments
	$\frac{\text{Pb}^{207}}{\text{U}^{235}}$	$\frac{\text{Pb}^{206}}{\text{U}^{238}}$	Age	$\frac{\text{Pb}^{207}}{\text{U}^{235}}$	$\frac{\text{Pb}^{206}}{\text{U}^{238}}$	Age	
Z-1	1.597	0.1622	969 ± 57	0.3978	0.0542	340 ± 15	
Z-4	0.7037	0.0875	541 ± 18	0.0515	0.0079	51 ± 19	
Z-4	0.7216	0.0893	552 ± 98	0.0886	0.0135	86 ± 172	without 5M
R8441	0.6073	0.0776	482	0	0	0	line from origin through mean of two points
All points	0.8205	0.0990	608 ± 11	0.1030	0.0156	100 ± 12	
All points without Z-1 1NM-250 and Z-4 5M	0.9363	0.1097	671 ± 49	0.2629	0.0375	237 ± 37	

$\text{Pb}^{207}/\text{U}^{235}$ and $\text{Pb}^{206}/\text{U}^{238}$ ratios is not completely evident. Evidence suggests, however, that the scatter is not a reflection of differences in the ages of the samples but rather a result of the limited sampling. R8441 consists of only two splits and thus no errors could be determined for the line passing through them. The Z-4 chord is determined mainly by one point (Z-4 5M) and even when this point is removed we are left with three closely grouped points, the fourth point again determining the slope. Thus errors in 2 or 3 points can contribute significantly to errors in the slope which are not revealed completely in the statistics.

Except for Z-4 5M all the points lie very close to one another and along a similar, fairly well defined trend. Because of this, together with the similarities in zircon morphology, and the fact that the samples come from the same formation which is quite homogeneous and distinctive, the points have been grouped together to produce a single chord. However, because Z-4 5M is very far from the main group of points it still has a significant effect on the slope, especially in determining the lower intercept. For this reason, and as will be shown later because Z-4 5M appears to have undergone significant Pb loss via continuous diffusion, it was removed from the regression along with a Z-1 point (Z-1 1NM -250) which fell outside the 2σ limits for the fifth line of Table 4). This leaves 15 closely related points which produce the last regression line of Table 4.

The anchoring effect of Z-4 5M is seen in the higher intercept ages and increased errors of the new line. In spite of this, the excellent grouping of the points, together with similarities to data which follows and facts about the nature of resetting, suggest this to be the best line for the Fishbrook Gneiss. Assuming the zircons from the Fishbrook Gneiss to be a volcanic suite, this implies an original age of 671 ± 49 m.y. for the Fishbrook Gneiss and a lower, possibly metamorphic, age of 237 ± 37 m.y.

Shawsheen Gneiss - The zircons of the Shawsheen Gneiss come from three samples:

Z-2 Dark biotite-ferrohornblende amphibolite schist, medium grained with poorly developed foliation. Plagioclase makes up less than 25% of the rock and is usually badly weathered on the surface. Magnetite and pyrite are common.

Z-3 Dark colored biotite-plagioclase-quartz-muscovite gneiss. Well developed gneissic texture defined by feldspar-quartz rich layers. Homogeneous medium grain size except for occasional irregular quartz-feldspar segregations.

R8453: Black and pink banded biotite-plagioclase-quartz gneiss of medium grain size with a well developed gneissic texture. Dark biotite rich bands are discontinuous and irregular. Sample is from the lower middle portion of the Shawsheen Gneiss.

U-Pb data for these samples are shown in Table 5. Figure 11 shows the data plotted on a Concordia diagram along

TABLE 5
Shawsheen Gneiss

Sample	Split	Pb*, ppm ¹	U, ppm	$\frac{\text{Pb}^{206}}{\text{Pb}^{204}}$	$\frac{\text{Pb}^{207}{}^2}{\text{Pb}^{206}}$	$\frac{\text{Pb}^{208}{}^2}{\text{Pb}^{206}}$
Z-2	4NM	123.8	1446	263.4	0.05726	0.62667
Z-3	4NM	46.58	342.1	57.09	0.08356	0.39968
	4NM -150 +250	42.66	270.3	259.5	0.09725	0.13690
	4NM -250	44.85	329.5	483.8	0.08745	0.13125
R8453	10NM	50.95	505.4	311.5	0.07339	0.09000

Sample	Split	Apparent ages, m.y.				
		$\frac{\text{Pb}^{207}}{\text{U}^{235}}$	$\frac{\text{Pb}^{206}}{\text{U}^{238}}$	$\frac{\text{Pb}^{207}}{\text{U}^{235}}$	$\frac{\text{Pb}^{206}}{\text{U}^{238}}$	$\frac{\text{Pb}^{207}}{\text{Pb}^{206}}$
Z-2	4NM	.4654±.0042	.0590±.0003	388	370	502
Z-3	4 M	1.228 ±.024	.1065±.0006	814	653	1282
	4NM -150 +250	1.993 ±.013	.1486±.0007	1114	894	1572
	4NM -250	1.565 ±.011	.1298±.0007	957	787	1370
R8453	10NM	1.020 ±.009	.1007±.0007	714	618	1024

¹Pb* = radiogenic lead

²corrected for contamination;
see Appendix B

Figure 11

Concordia plot for the U-Pb data from the Shawsheen Gneiss along with two best fit chords from Table 6. Ages in millions of years.

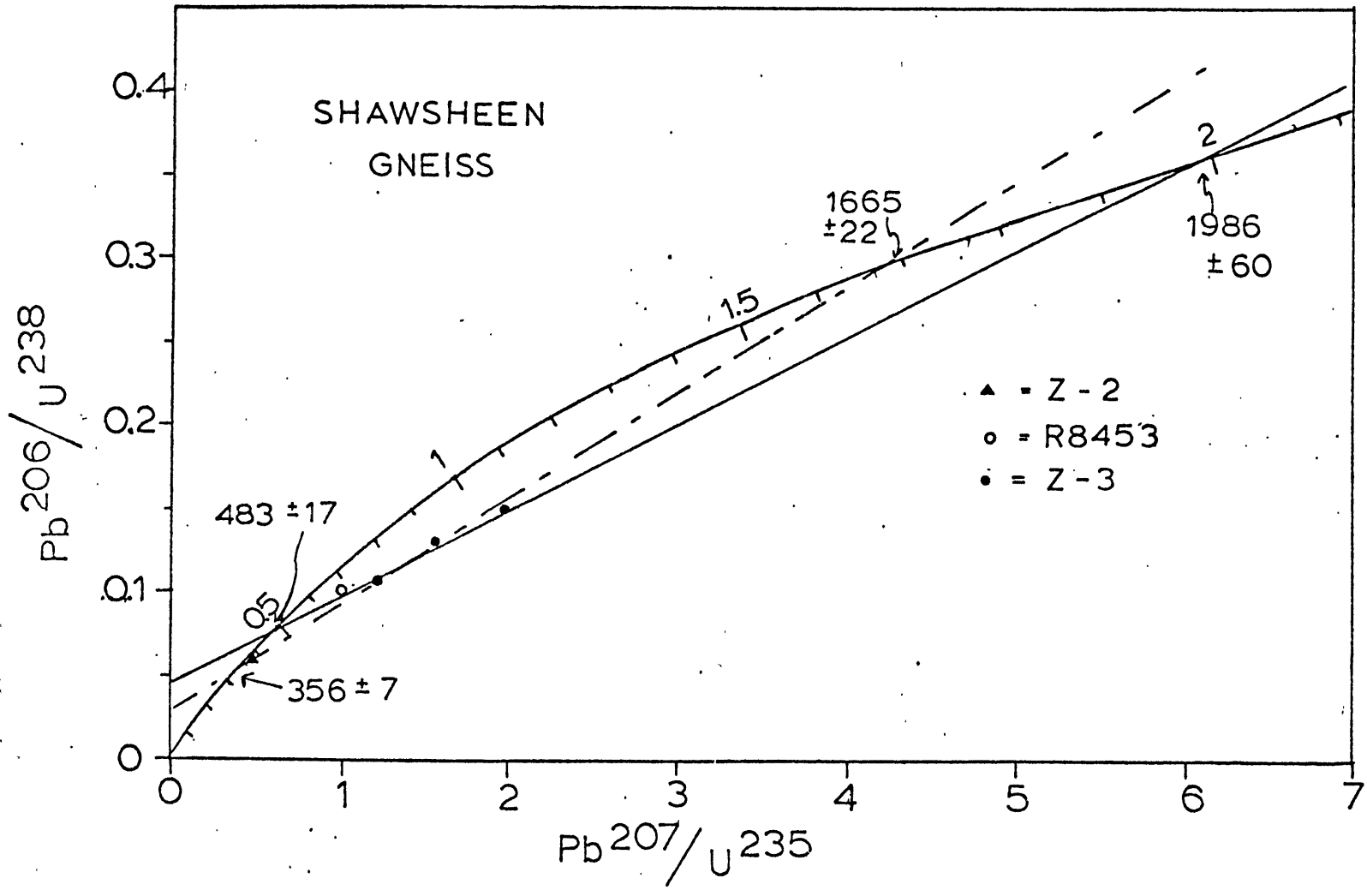


TABLE 6

Concordia Intercepts and Ages of Shawsheen Gneiss

Sample	Upper Intercept			Lower Intercept			Comments
	$\frac{\text{Pb}^{207}}{\text{U}^{235}}$	$\frac{\text{Pb}^{206}}{\text{U}^{238}}$	Age	$\frac{\text{Pb}^{207}}{\text{U}^{235}}$	$\frac{\text{Pb}^{206}}{\text{U}^{238}}$	Age	
Z-3	5.177	0.3321	1849 ± 76	0.5022	0.0662	413 ± 36	
All points	4.152	0.2946	1665 ± 22	0.4206	0.0569	356 ± 7	
Z-3 and R8453	6.069	0.3607	1986 ± 60	0.6084	0.0777	483 ± 17	without Z-2

with various least squares lines. The intercepts and ages for these lines are shown in Table 6.

Four of the zircon splits of the Shawsheen Gneiss appear to be significantly older than the fifth (Z-2) as well as being significantly older than the Fishbrook Gneiss zircons. This agrees with the observations on zircon morphology which suggest that the zircons from Z-3 and R8453 are an older detrital population. Z-2 may belong to this detrital group but it is unlikely for a number of reasons. First, although the number of points is small, Z-3 forms a fairly well defined chord. The addition of R8453 changes the chord only slightly, whereas the addition of Z-2 causes a very significant change. Secondly, the zircon morphology and rock composition of Z-2 are significantly different from Z-3 and R8453. Thirdly, the Z-2 point falls well within the grouping of Fishbrook Gneiss points and is clearly more closely related to them than to the other Shawsheen Gneiss points. This agrees with the interpretation of the Fishbrook Gneiss zircons as an igneous suite since the Z-2 zircons are almost certainly igneous.

Z-3 and R8453 imply a very old source area for the detrital zircons of the Shawsheen Gneiss. The upper intercept suggests a source area as old as 2.0 b.y. However, because of the limited number of points and their great discordance, it is difficult to ascertain how accurate this age is even though they form a very good line. Detrital zircons from the Westboro Formation (see below) suggest a source area of

younger age. The lower intercept of 483 m.y. is close to, although somewhat older than, the time usually assigned to the Taconic Orogeny (Lyons and Faul, 1968).

Westboro Formation - Two samples:

W-1: Fine grained, sugary, grey quartzite with small amounts of biotite, magnetite and feldspar. Massive and homogeneous in texture with few signs of weathering. The sample is from a quartzite lens surrounded by metavolcanics

W-2: From outcrop about 50 ft. east of W-1. Massive, homogeneous, coarse grained steel-grey colored quartzite. Biotite, magnetite, feldspar and pyrite are common. The biotite gives the rock a distinct foliation. Rock is relatively unweathered but is cut by extensive joints.

Table 7 gives the U-Pb data for W-1 and W-2. The data are shown plotted on the Concordia diagram in Figure 12.

Table 8 gives the intercepts and ages of the discordia lines.

The first observation that can be made about the results from these zircons is the obvious difference in the behavior of the samples: there is a distinct separation between the zircons of each group. There is no doubt that these two samples are from the same formation; indeed, they are essentially at the same stratigraphic level and thus at the same grade of metamorphism. Their different behavior must be due to some factor internal to the zircons rather than to external conditions. This distinction appears to be correlated with the

TABLE 7
Westboro Quartzite

Sample	Split	Pb*, ppm ¹	U, ppm	$\frac{\text{Pb}^{206}}{\text{Pb}^{204}}$	$\frac{\text{Pb}^{207}{}^2}{\text{Pb}^{206}}$	$\frac{\text{Pb}^{208}{}^2}{\text{Pb}^{206}}$
W-1	4M	56.08	301.8	248.7	0.08352	0.09319
	3M	61.81	342.4	506.3	0.10068	0.11986
	2M	66.48	329.2	1385	0.09131	0.12068
	1M	60.91	270.5	909.1	0.09795	0.13708
	1NM	61.78	211.2	165.9	0.09432	0.33273
W-2	5M	82.08	1263	223.5	0.07395	0.11359
	3M	84.10	1146	462.5	0.07740	0.07296
	1.5M	54.44	758.7	499.5	0.06955	0.07044
	1.5NM	47.92	483.6	644.7	0.07436	0.10390

¹Pb* = radiogenic lead

²corrected for contamination; see Appendix B

TABLE 7 (CONT.)

Sample	Split	Apparent ages, m.y.				
		$\frac{\text{Pb}^{207}}{\text{U}^{235}}$	$\frac{\text{Pb}^{206}}{\text{U}^{238}}$	$\frac{\text{Pb}^{207}}{\text{U}^{235}}$	$\frac{\text{Pb}^{206}}{\text{U}^{238}}$	$\frac{\text{Pb}^{207}}{\text{Pb}^{206}}$
W-1	4M	2.114 ±.016	.1836±.0010	1154	1087	1282
	3M	2.387 ±.017	.1719±.0008	1239	1023	1637
	2M	2.438 ±.024	.1937±.0018	1254	1142	1454
	1M	2.862 ±.017	.2119±.0010	1372	1239	1585
	1NM	3.095 ±.043	.2380±.0025	1432	1376	1515
W-2	5M	.6487±.0073	.0636±.0004	508	398	1040
	3M	.7918±.0077	.0742±.0005	592	462	1132
	1.5M	.7019±.0078	.0732±.0008	540	456	915
	1.5NM	1.003 ±.007	.0978±.0005	706	602	1052

Figure 12

Concordia plot of U-Pb data and the best fit chords
for the Westboro Formation. Ages in millions of
years.

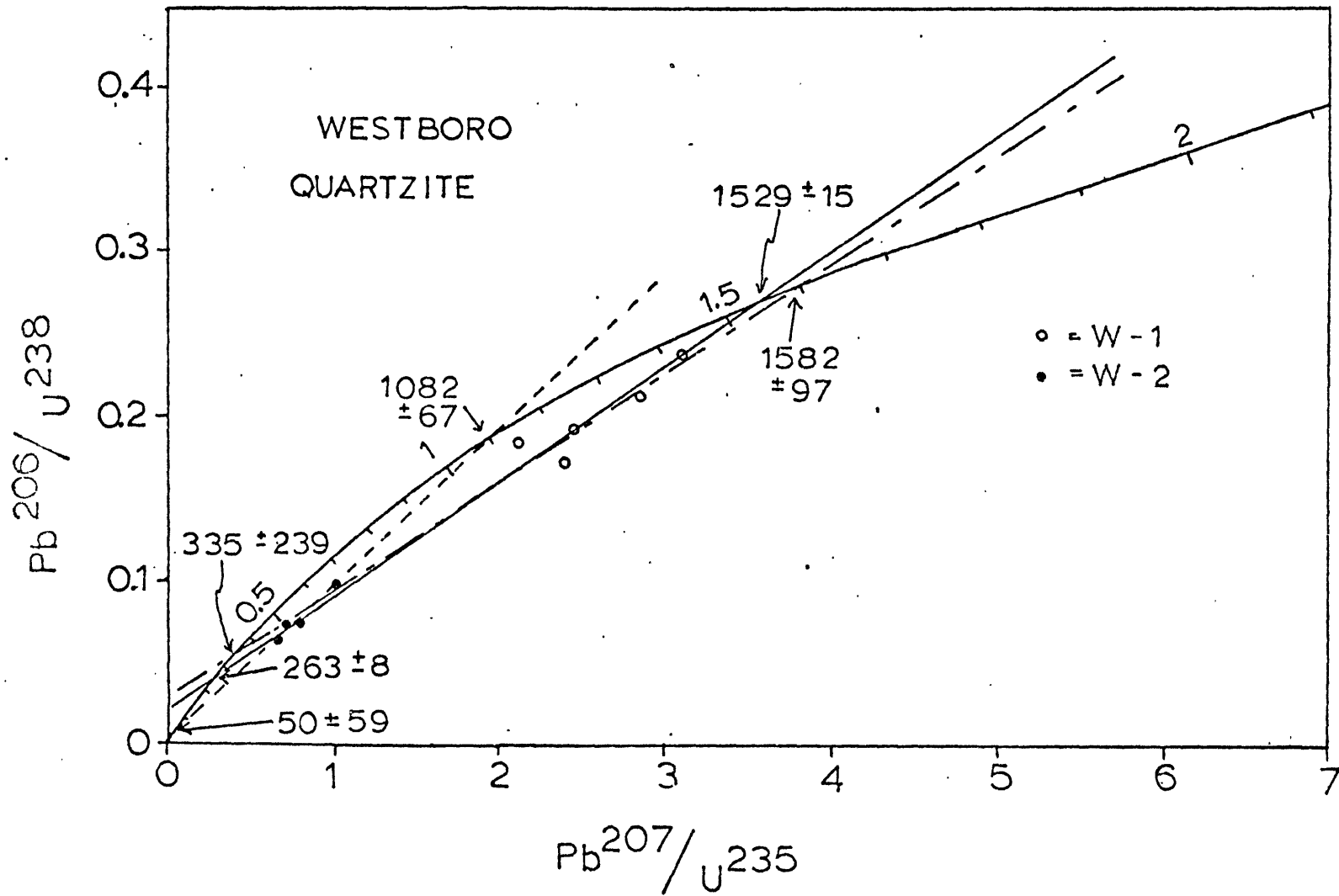


TABLE 8

Concordia Intercepts and Ages of Westboro Quartzite

Sample	Upper Intercept			$\frac{\text{Pb}^{207}}{\text{U}^{235}}$	$\frac{\text{Pb}^{206}}{\text{U}^{238}}$	Age
	$\frac{\text{Pb}^{207}}{\text{U}^{235}}$	$\frac{\text{Pb}^{206}}{\text{U}^{238}}$	Age			
W-1	3.750	0.2782	1582 ± 97	0.3902	0.0533	335 ± 239
W-2	1.902	0.1827	1082 ± 67	0.0507	0.0078	50 ± 59
All points	3.509	0.2677	1529 ± 15	0.2957	0.0417	263 ± 8

uranium content of the zircons. The more discordant W-2 zircons have a distinctly higher uranium content. This correlation will be discussed in detail later.

The best fit lines for W-1 and W-2 produce significantly different slopes and intercepts. However, because of the scatter in the W-1 points and the closeness of the W-2 points, it is hard to judge whether these differences are significant. As will be discussed later, I believe the behavior of the W-2 points to possibly be the result of continuous diffusion superimposed on episodic lead loss. This hypothesis is lent further credence by the very low (50 m.y.) intercept of the W-2 points. In addition, the slope of the line for W-2 is strongly controlled by a single point (1.5 NM) which is not significantly off the trend defined by W-1 and W-2. Taken together W-1 and W-2 indicate an old source area for their detrital zircons similar to, but significantly younger than, the zircons from the Shawsheen Gneiss. The lower intercept of 263 m.y. is similar to the lower intercept of the Fishbrook Gneiss points.

Nashoba Formation - Zircons of the Nashoba Formation come from two samples:

Z-5: Dark biotite-plagioclase gneiss with subordinate amounts of quartz. Quartz is locally abundant as small lenses. Massive, well foliated with a well developed gneissic texture. Some weathering, especially in the feldspars, is

evident. Magnetite is common.

R8311: Grey, medium grained quartzite with abundant biotite and feldspar. Homogeneous and massive, no foliation discernible. Some weathering of feldspars. Highly recrystallized with complex interlocking of quartz, biotite and feldspar grains.

Both samples are from the upper portion of the formation.

Table 9 gives the U-Pb data for these samples. The Pb^{207}/U^{235} and Pb^{206}/U^{238} ratios are plotted on the Concordia diagram of Figure 13. Various regression lines, their intercepts and ages are shown in Table 10.

The most noticeable aspect of the data from the Nashoba Formation is the very young lower intercepts that result no matter how we arrange the data. Although R8311 and Z-5 are most certainly a detrital suite they appear to be more closely related to the zircons from the Fishbrook Gneiss. However, the very young intercepts at the low end of the lines and the distinct curvature to the points taken together suggest loss of lead through a continuous diffusion process. R8311 1AmpNM agrees closely with the zircons of W-2, which implies that the Nashoba zircons may represent an extension of the detrital trend defined by W-1, W-2, Z-3, and R8453. This is further substantiated by the fact that the R8311 zircons at the low end of the line fall close to Z-4 5M, which, as mentioned above, also appears to have recently lost lead. On the other hand, the R8311 and Z-5 points at the upper end of the curve

TABLE 9

Nashoba Formation

Sample	Split	Pb*, ppm ¹	U, ppm	$\frac{\text{Pb}^{206}}{\text{Pb}^{204}}$	$\frac{\text{Pb}^{207}{}^2}{\text{Pb}^{206}}$	$\frac{\text{Pb}^{208}{}^2}{\text{Pb}^{206}}$
Z-5	5NM	38.79	670.9	351.1	0.06806	0.06454
R8311	1Amp NM	32.43	359.1	145.1	0.06910	0.14968
	.63Amp NM	435.9	3147	1302	0.05585	2.9075
	.60Amp NM	185.2	3203	4950	0.05947	2.8841
	.58Amp NM	200.4	3028	1096	0.05609	2.5262

Sample	Split	Apparent ages, m.y.				
		$\frac{\text{Pb}^{207}}{\text{U}^{235}}$	$\frac{\text{Pb}^{206}}{\text{U}^{238}}$	$\frac{\text{Pb}^{207}}{\text{U}^{235}}$	$\frac{\text{Pb}^{206}}{\text{U}^{238}}$	$\frac{\text{Pb}^{207}}{\text{Pb}^{206}}$
Z-5	5NM	.5571±.0101	.0594±.0004	451	372	870
R8311	1Amp NM	.8206±.0095	.0861±.0004	609	532	902
	.63Amp NM	.3111±.0047	.0404±.0006	275	255	446
	.60Amp NM	.1389±.0028	.0169±.0003	132	108	584
	.58Amp NM	.1652±.0015	.0214±.0002	155	137	456

¹Pb* = radiogenic lead

²corrected for contamination; see Appendix B

Figure 13

Concordia plot of U-Pb data from the Nashoba
Formation.

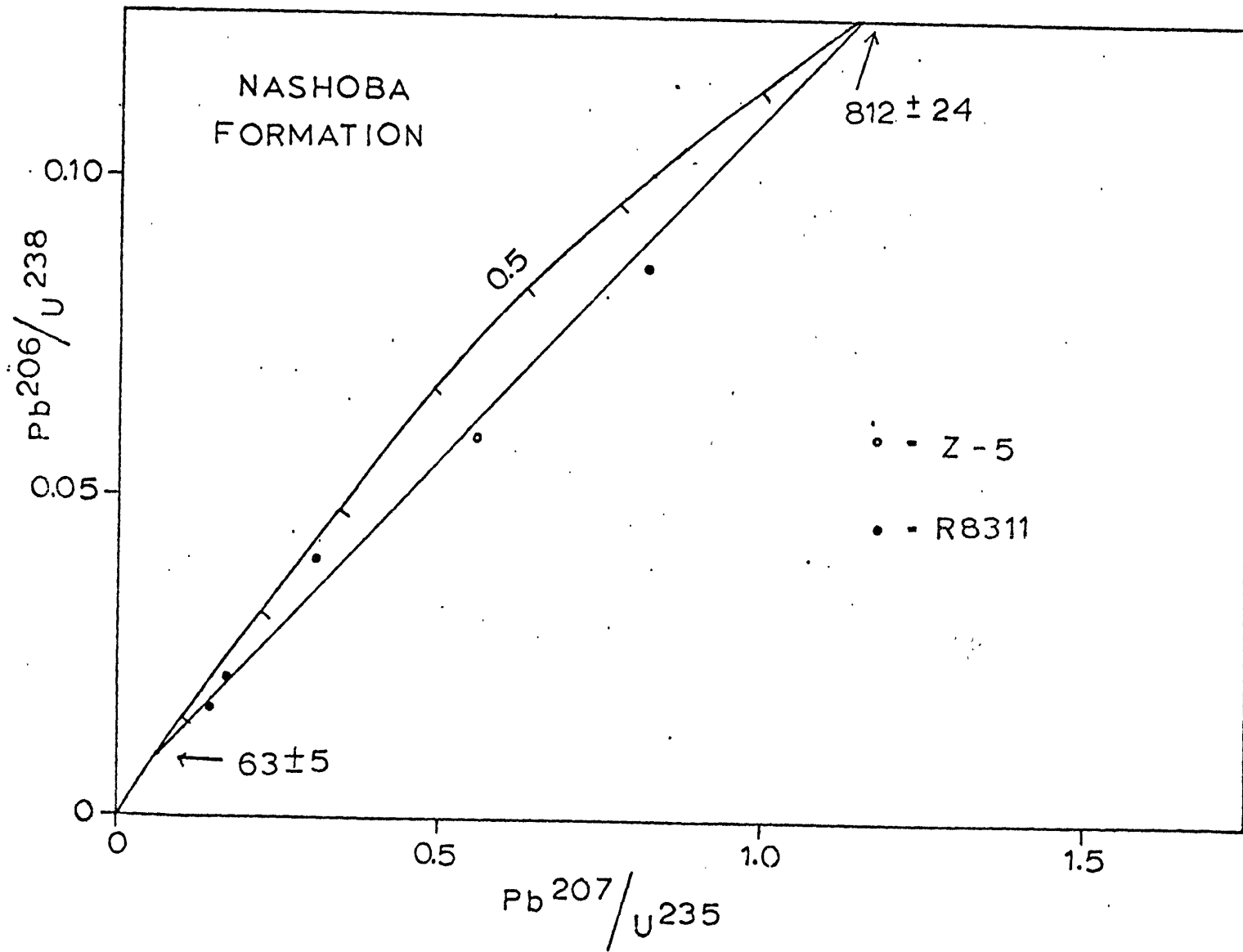


TABLE 10

Concordia Intercepts and Ages for the Nashoba Formation

Sample	Upper Intercept			Lower Intercept			Comments
	$\frac{\text{Pb}^{207}}{\text{U}^{235}}$	$\frac{\text{Pb}^{206}}{\text{U}^{238}}$	Age	$\frac{\text{Pb}^{207}}{\text{U}^{235}}$	$\frac{\text{Pb}^{206}}{\text{U}^{238}}$	Age	
R8311	1.061	0.1207	734 ± 30	0.0539	0.0083	53 ± 7	
R8311 without 1Amp NM	0.6545	0.0825	511	0	0	0	Line from origin through mean of three points
R8311 and Z-5	1.225	0.1343	812 ± 24	0.0637	0.0098	63 ± 5	

fall to the right of the main Fishbrook Gneiss trend. If continuous diffusion is a prime determinate of the Pb/U ratios of the zircons, then the intercepts with Concordia probably have no meaning.

Again a correlation between distance along the best fit chord (shown in Figure 13) and uranium content appears, just as with the W-1 and W-2 points. The two lowest R8311 points have the highest uranium contents (> 3100 ppm). Each successively higher point has a correspondingly lower uranium content. This correlation between uranium content and the amount of resetting will be dealt with quantitatively in a later section.

Low Quality Points

Because of large amounts of contamination in some samples, they were not included in the data presented above. However, in spite of this, most agree remarkably well either with other points from the same formation or with other zircons from the same morphologic suite.

Five zircon analyses were considered too contaminated for inclusion into the data above. The results of the U-Pb analyses for these zircons are shown in Table 11.

All of the samples except Z-1 1M -150+200 agree well with related points. Z-3 4NM +150 lies just slightly above the trend established by the other Z-3 points. Z-6 and R8422 are almost concordant and lie at opposite ends of the

TABLE 11

Lower-Quality Points Omitted from Previous Tables

Sample	Split	Pb*, ppm ¹	U, ppm	$\frac{\text{Pb}^{206}}{\text{Pb}^{204}}$	$\frac{\text{Pb}^{207}{}^2}{\text{Pb}^{206}}$	$\frac{\text{Pb}^{208}{}^2}{\text{Pb}^{206}}$
Z-1	1M -150+200	30.46	288.7	45.16	0.11421	0.39404
Z-3	4NM +150	29.37	205.3	41.46	0.08742	0.09550
Z-6 (Nashoba)	10NM	41.80	900.3	39.43	0.05172	0.15937
R8422 (Middle- sex Fells)	20NM	18.62	141.7	36.26	0.05811	0.62585
R8458 (Nashoba)	5NM	14.20	250.0	52.81	0.06756	0.07416

Sample	Split	Apparent ages, m.y.				
		$\frac{\text{Pb}^{207}}{\text{U}^{235}}$	$\frac{\text{Pb}^{206}}{\text{U}^{238}}$	$\frac{\text{Pb}^{207}}{\text{U}^{235}}$	$\frac{\text{Pb}^{206}}{\text{U}^{238}}$	$\frac{\text{Pb}^{207}}{\text{Pb}^{206}}$
Z-1	1M -150+200	1.279 ±.031	.0812±.0006	836	504	1867
Z-3	4NM +150	1.695 ±.038	.1406±.0009	1006	848	1370
Z-6	10NM	0.3178±.0127	.0446±.0002	280	281	273
R8422	20NM	0.7249±.0302	.0905±.0009	554	558	534
R8458	5NM	0.5389±.0100	.0578±.0002	438	362	856

¹Pb* = radiogenic lead²corrected for contamination; see Appendix B

line established by the zircons of the Fishbrook Gneiss. In fact, Z-6 agrees quite well with the lower intercept of the best Fishbrook Gneiss chord (last line, Table 4). R8422 lies somewhat to the left of the main Fishbrook Gneiss trend, but the large errors for this point mean that it could still lie well within the main group of Fishbrook Gneiss points. R8458 agrees well with the other Nashoba points and lies close to the Z-5 point on the curving trend established by Z-5 and R8311. Z-1 LM -150+200, however, does not agree with any other group of points. It lies well to the right of the other Fishbrook Gneiss points and below the main group of detrital points. Its singular behavior suggests that it is truly a "bad" point, the result of analytical problems (non-equilibration of spike and sample; fractionation of uranium and lead prior to spiking; etc.) or measurement errors (errors in weights of spike; error in measurements of ratios; etc.).

Common Lead

It has been assumed in all of the above discussion that all of the Pb^{204} observed is due to laboratory contamination. However, the possibility exists that a significant portion of this Pb^{204} is the result of common lead incorporated into the zircons during the original crystallization or during metamorphism. A number of facts suggest that common lead is not a significant contribution to the Pb^{204} of these zircons, al-

though they do not entirely discount the existence of common lead in the zircons.

First: The good agreement between analyses with highly variable Pb^{206}/Pb^{204} ratios, including the samples very badly contaminated, implies that the lead contamination ratios used to correct the raw lead data are approximately correct. The influence of a small amount of common lead may explain some of the remaining scatter, but this can also be easily explained by other factors. Natural "geologic scatter", diffusion, multiple metamorphic events and possibly weathering could increase the scatter.

Second: Large amounts (>1 ppm) of common lead are not usually found in zircons. Silver and Deutsch (1963) and Doe (1970) note that zircons in general do not incorporate significant quantities of common lead, and that the major portion of Pb^{204} observed comes from reagents and other laboratory contamination. The quantitative studies done by Krogh (1973) indicate that zircons of low magnetic susceptibility usually contain less than 0.75 ppm of common lead. More magnetic zircons tend to contain slightly higher concentrations of common lead (a few ppm) but the higher concentrations of uranium in more magnetic zircons will slightly counteract this increased concentration of common lead. In the same paper, Krogh suggests that these are maximum values and that true concentrations of common lead are probably lower.

Third: The evidence from zircon morphology, which sug-

gests mainly resorption of zircons rather than overgrowths, implies that common lead has probably not been added to the zircons during metamorphism. Annealing and recrystallization tend to expel lead rather than incorporate it (Gebauer and Grünenfelder, 1976). Zircons formed during metamorphism may incorporate common lead, but the evidence on this is ambiguous. Zircons formed under high grade conditions seem to incorporate high concentrations of trace elements (Köppel and Grünenfelder, 1971), while those formed during diagenesis and low grade metamorphism appear to have lower trace element concentrations (Saxena, 1966). Either way, the evidence presented in the section on zircon morphology shows that a metamorphic population is not common or widespread in these zircons, except possibly in a few splits. Since the metamorphic populations, if they exist, seem to be mostly in the least magnetic fractions, this implies a more ordered crystal lattice and thus a lower concentration of trace elements. This further decreases the possibility of incorporated common lead.

Fourth: Table 12 shows all the zircon samples analyzed, along with the calculated total amount of lead contamination, radiogenic lead and sample weight. There does not appear to be any significant correlation between any of these numbers, but it should be noticed that there is a significant variability in the amounts of contamination. A similar variation occurs in the blanks given in Appendix B. The amounts of contamination are high enough in most cases that if common lead

TABLE 12

Total¹Lead Contamination and Total Radiogenic Lead in Zircons

<u>Sample</u>	<u>Split</u>	<u>Pb^{con}, ng²</u>	<u>Pb*, ng³</u>	<u>Sample wt, mg</u>
Z-1	3M +150	125.1	191.3	5.62
	3M -150	41.2	549.8	19.55
	2M	15.0	468.9	20.11
	1M +150	90.5	141.6	5.70
	1M -200+250	45.8	144.9	5.84
	1M -250	16.8	421.3	17.28
	1NM +150	25.8	78.1	3.00
	1NM -150+250	33.8	208.4	5.86
	1NM -250	27.1	191.7	5.36
	Z-2	4NM	76.5	398.6
Z-3	4M	30.8	19.1	0.41
	4NM -150+250	45.6	160.4	3.76
	4NM -250	45.1	328.7	7.33
Z-4	5M	55.6	750.8	9.19
	4M	62.9	320.4	3.74
	3M	12.2	39.8	0.45

¹ total contamination in spiked + unspiked aliquots²Pb^{con} = contamination lead³Pb* = radiogenic lead

TABLE 12 (CONT.)

<u>Sample</u>	<u>Split</u>	<u>Pb^{con}, ng¹</u>	<u>Pb*, ng²</u>	<u>Sample wt, mg</u>
Z-4	2M	18.3	64.4	6.90
	1M	18.9	162.4	9.39
	1NM	14.6	217.4	6.87
<hr/>				
Z-5	5NM	196.8	1099	28.32
<hr/>				
W-1	4M	46.1	215.9	3.85
	3M	32.1	230.5	3.73
	2M	19.2	412.8	6.21
	1M	18.8	340.5	5.59
	1NM	88.2	180.4	2.92
<hr/>				
W-2	5M	102.4	334.1	4.07
	3M	80.6	497.9	5.92
	1.5M	606.0	529.1	9.72
	1.5NM	43.6	421.7	8.80
<hr/>				
R8311	1AmpNM	39.6	106.1	3.27
	.63AmpNM	33.0	2044	4.69
	.60AmpNM	83.2	2481	13.40
	.59AmpNM	89.9	1577	7.87

TABLE 12 (CONT.)

<u>Sample</u>	<u>Split</u>	<u>Pb^{con}, ng¹</u>	<u>Pb*, ng²</u>	<u>Sample wt, mg</u>
R8441	4M	22.4	204.4	3.10
	4NM	18.4	393.8	9.52
<hr/>				
R8453	10NM	144.2	524.8	10.30
<hr/>				

represented a significant fraction of this contamination, it would imply exceedingly high concentrations of common lead, approaching in some cases 20 ppm. It is interesting that the range covered by the contamination of the zircon samples is, within a factor of 2, similar to the range found for the blanks. In addition, although specific correlations between contamination, radiogenic lead and sample weight are not apparent, there does seem to be a slight positive correlation of contamination lead with radiogenic lead. It is by no means an exact correlation, but along with the other facts mentioned above, it lends credence to the explanation given in Appendix B for this large variability. Basically, the idea is that we are dealing with a fixed amount of contamination which is introduced largely (>80%) at the time of sample loading. A variable amount of radiogenic lead is then loaded on top of this fixed amount of lead contamination. Thus the Pb^{204}/Pb^{206} ratio and the amount of lead contamination will depend on the ratio of contamination lead to radiogenic lead loaded on the filament. The amount of lead contamination will depend essentially on the concentration of lead in the loading reagents (mostly silica gel), while the amount of radiogenic lead loaded onto the filament depends on a number of factors: sample weight, Pb^{rad} concentration, efficiency of column separation of Pb, efficiency of dissolution of the final lead concentrate in the phosphoric acid loading agent (probably the major factor affecting the amount of lead load-

ed) and the amount of phosphoric acid solution actually loaded. This means that two samples may have similar Pb^{204}/Pb^{206} ratios because the amount of lead loaded on the filament was the same for both samples. If the concentration of lead in one sample is twice that of the other, the amount of contamination will appear to be twice as high.

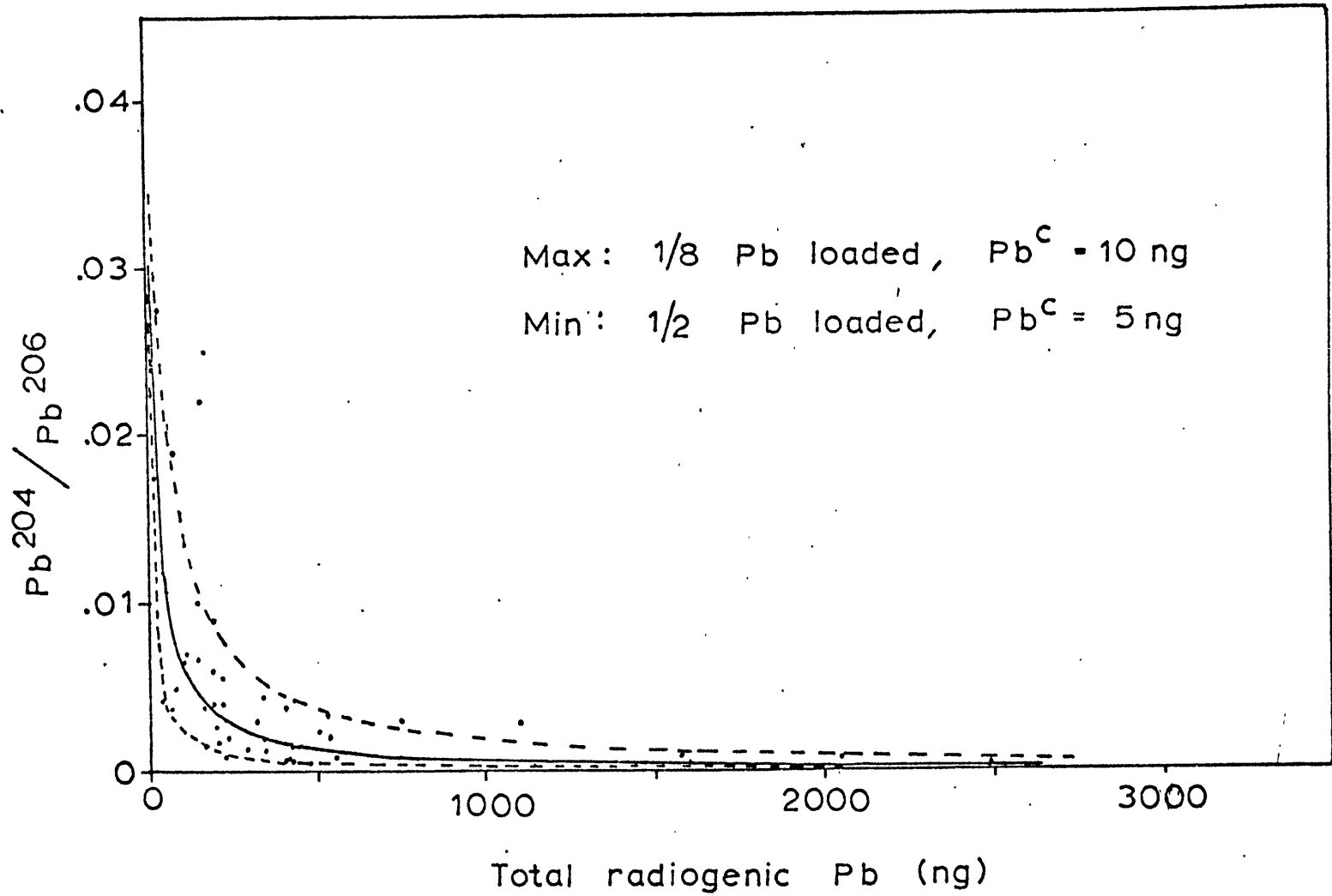
Fifth: If common lead is the major factor affecting the Pb^{204}/Pb^{206} ratios of the samples, then the Pb^{204}/Pb^{206} ratio observed should not be dependent on the total amount of radiogenic lead in the sample. This is because a sample with a large amount of Pb^{rad} may also have a large amount of common lead. The amount of common lead in the zircon will depend on whatever factors determine the incorporation of lead into the zircon structure. However, when observed Pb^{204}/Pb^{206} ratios are plotted against total Pb^{rad} (Figure 14), there is a distinct correlation between the two. In fact, it is just the effect that would be expected. As we add more radiogenic lead to a fixed amount of contamination, the Pb^{204}/Pb^{206} ratio should drop off quickly and then asymptotically approach zero at high Pb^{rad} values. This is the case in Figure 14. Scatter around the trend is most likely due to the variable loading of Pb^{rad} mentioned above. We can theoretically establish a relationship between the Pb^{204}/Pb^{206} ratio and the total Pb^{rad} in the sample that is dependent on the amount of Pb contamination. The relationship is:

Figure 14

Plot of the observed $\text{Pb}^{204}/\text{Pb}^{206}$ ratios for the unspiked aliquots of all the U-Pb analyses made, including points with high $\text{Pb}^{204}/\text{Pb}^{206}$ ratios.

----- Maximum and minimum limits of the $\text{Pb}^{204}/\text{Pb}^{206}$ ratios based on lead contamination of 5 to 10 ng and a loading factor of 1/2 to 1/8 of the total radiogenic lead.

———— Average trend line: $\text{Pb}^{\text{con}} = 7.5 \text{ ng}$,
 Pb^{rad} loaded = 1/4 of total Pb^{rad} .



$$\frac{\text{Pb}^{204}}{\text{Pb}^{206}} = \frac{0.023 \text{ Pb}^{\text{con}}}{\text{Pb}^{\text{rad}} + 0.467 \text{ Pb}^{\text{con}}}$$

where:

Pb^{con} = lead contamination, in ng and

Pb^{rad} = radiogenic lead loaded onto filament, in ng.

The constants merely convert total amounts of lead in ng to amounts of Pb^{204} and Pb^{206} in moles. This introduces some errors since the conversion of total Pb^{rad} to $\text{Pb}^{206, \text{rad}}$ depends on the $\text{Pb}^{207}/\text{Pb}^{206}$ and $\text{Pb}^{208}/\text{Pb}^{206}$ ratios in the zircon, but this is a small effect except for some zircons. Assuming that Pb^{con} varies between 5 and 10 ng and the amount of Pb^{rad} loaded onto the filament is 1/2 to 1/8 of the total Pb^{rad} , we can establish maximum and minimum limits for the $\text{Pb}^{204}/\text{Pb}^{206}$ ratios. These curves are shown in Figure 14. It can be seen that these curves follow the trend of the data quite closely and contain most of the analyzed points between them. Only three points lie well outside of the band defined by the maximum and minimum curves. Of these three points, two of them are among the group of badly contaminated points left out of all the Concordia plots.

The average curve lying between the maximum and minimum curves would represent a Pb^{con} of 7.5 ng and a Pb^{rad} loaded of 1/4 the total Pb^{rad} . A Pb^{con} of 7.5 ng is close to the minimum contamination (5-6 ng) found for the procedure blanks, and a Pb^{rad} loading factor of 1/4 is about average since the total sample was split roughly in half to get a spiked and

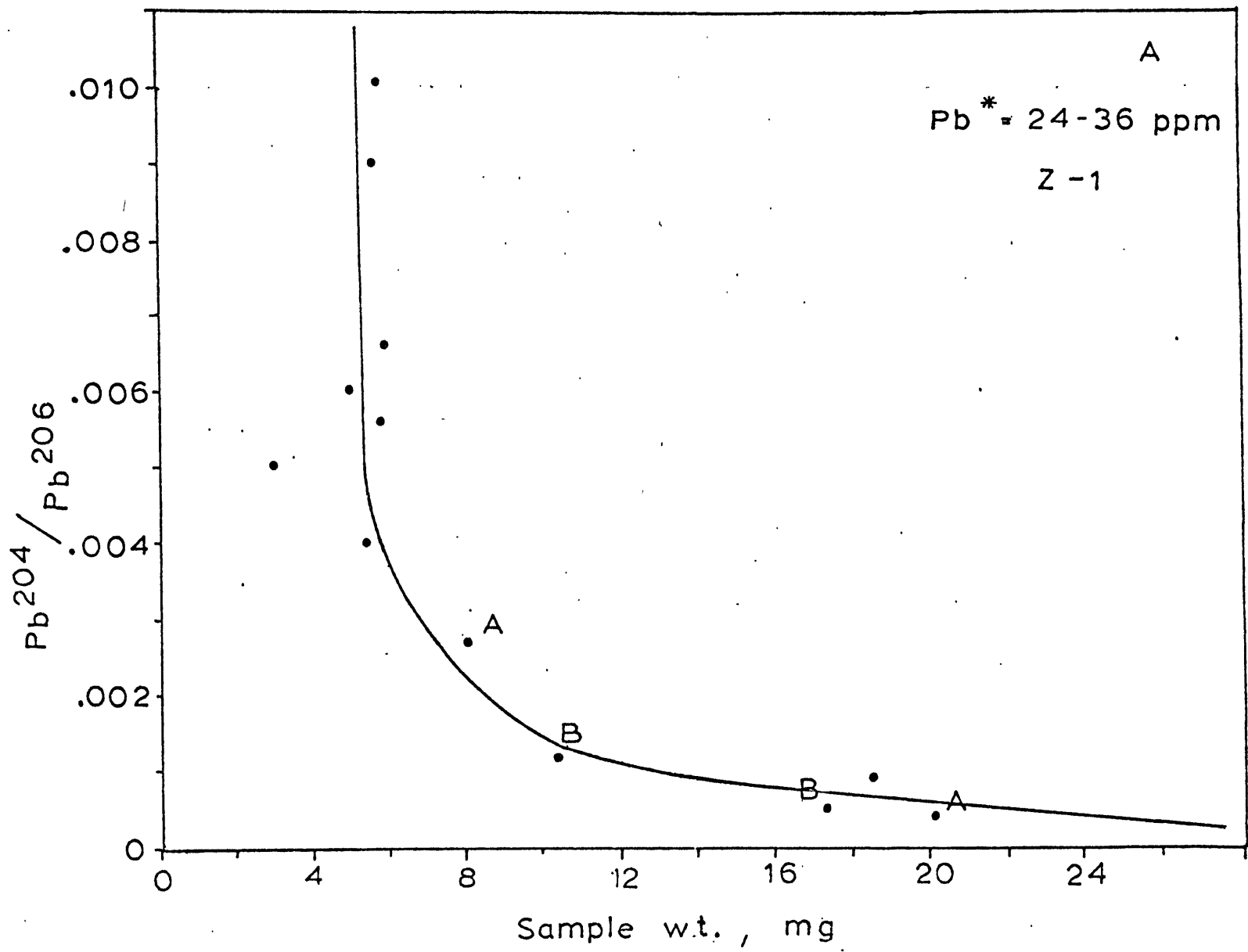
unspiked aliquot, and only about 1/2 of each aliquot was loaded onto the filament. In fact, ignoring the three points mentioned above, 50% of the samples fall above this average line while 50% fall below.

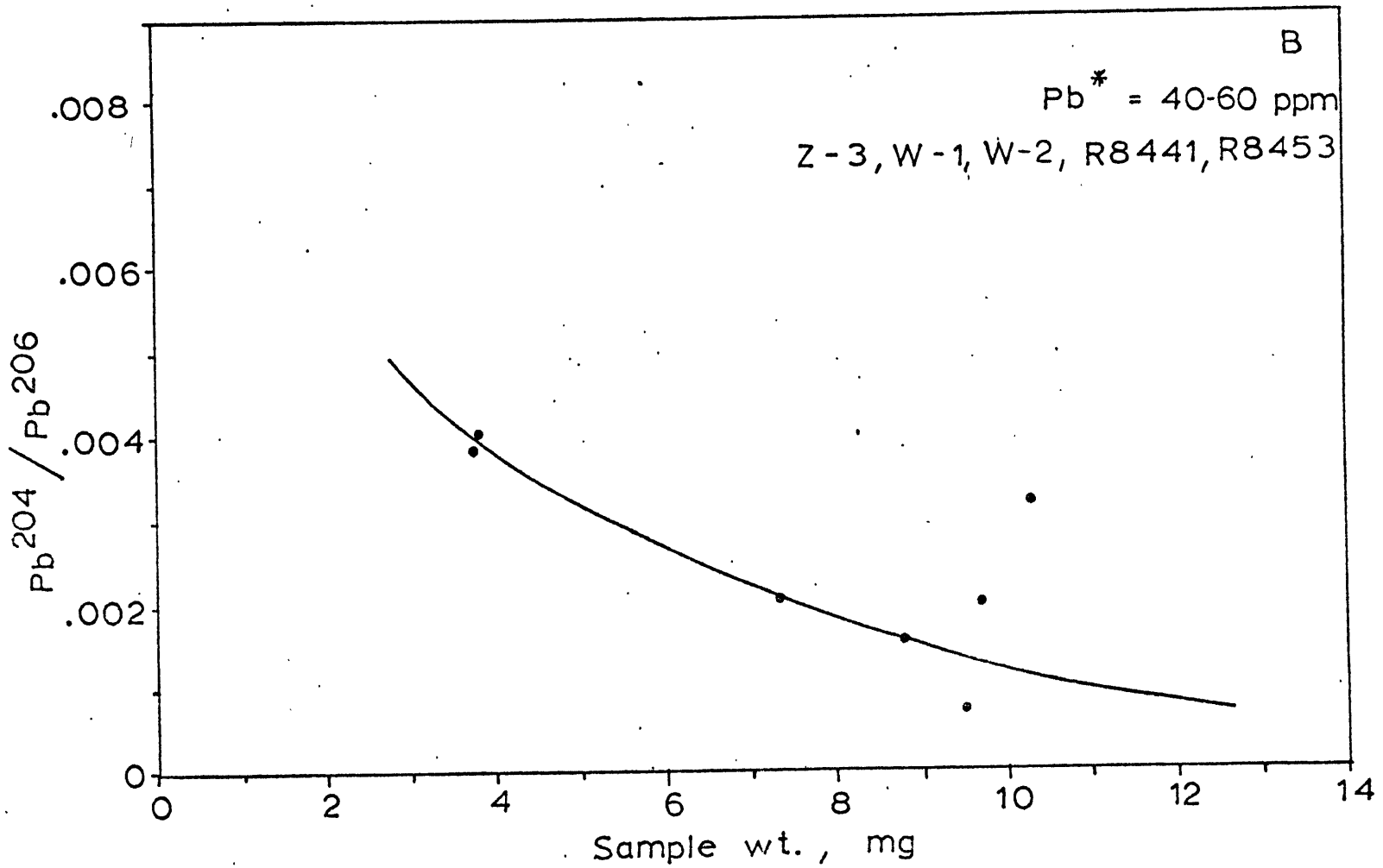
It might, of course, be argued that instead of a relatively constant amount of laboratory contamination, we are really dealing with a relatively constant amount of common lead. If this is the case, then zircons with similar Pb^{rad} concentrations would also have fairly similar common lead concentrations. As a result, there should be little or no variation of Pb^{204}/Pb^{206} ratio with sample weight, since as the sample weight increases both the Pb^{rad} and Pb^{common} will increase. But, as seen in Figure 15, this is not the case. Figure 15 A-C shows three different groups of zircons with approximately similar Pb^{rad} concentrations. The data are necessarily limited since few zircons fall within any reasonably narrow range of concentrations. Figure 15A shows the best group of points. They fall within a very limited range of concentrations. When the Pb^{204}/Pb^{206} ratios are plotted against sample weight, we see a curve similar to that seen in Figure 14. Again this is exactly the behavior expected from a variable amount of Pb^{rad} superimposed on a fixed amount of lead contamination. The data in Figure 15B are more scattered and less well defined, but show the same trend as Figure 15A. Figure 15C also shows the same trend. If the Pb^{204}/Pb^{206} ratios were determined to a large extent

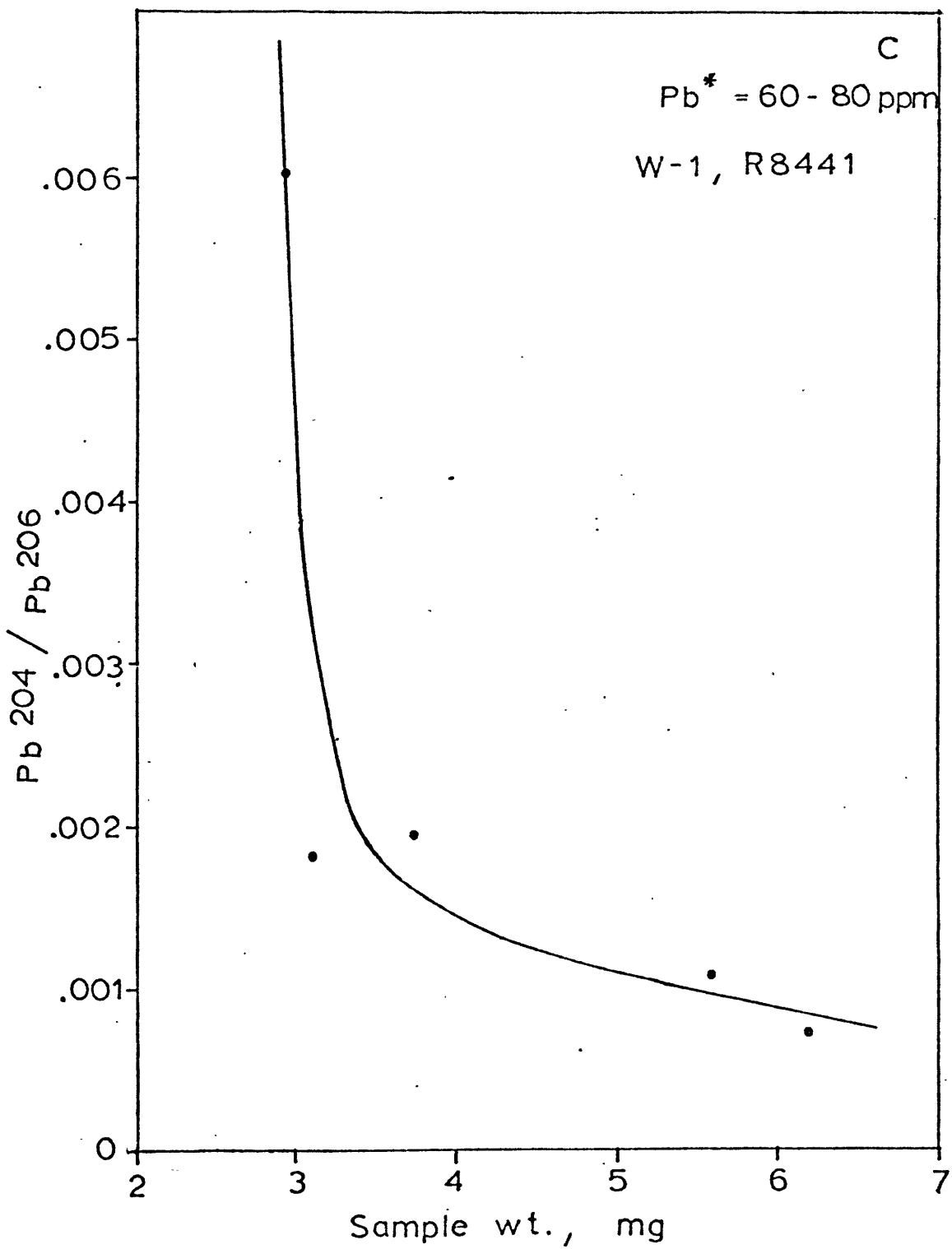
Figure 15

Plots of sample weight versus $\text{Pb}^{204}/\text{Pb}^{206}$ ratios for the unspiked aliquots of three groups of zircons with narrow ranges of Pb^{rad} concentrations.

- A: Pb^{rad} concentrations of 24 to 36 ppm for zircons from Z-1. A and B on the diagram are replicates for two of the splits; A is Z-1 2M, B is Z-1 1M -250.
- B: Pb^{rad} concentrations of 40 to 60 ppm.
- C: Pb^{rad} concentrations of 60 to 80 ppm.







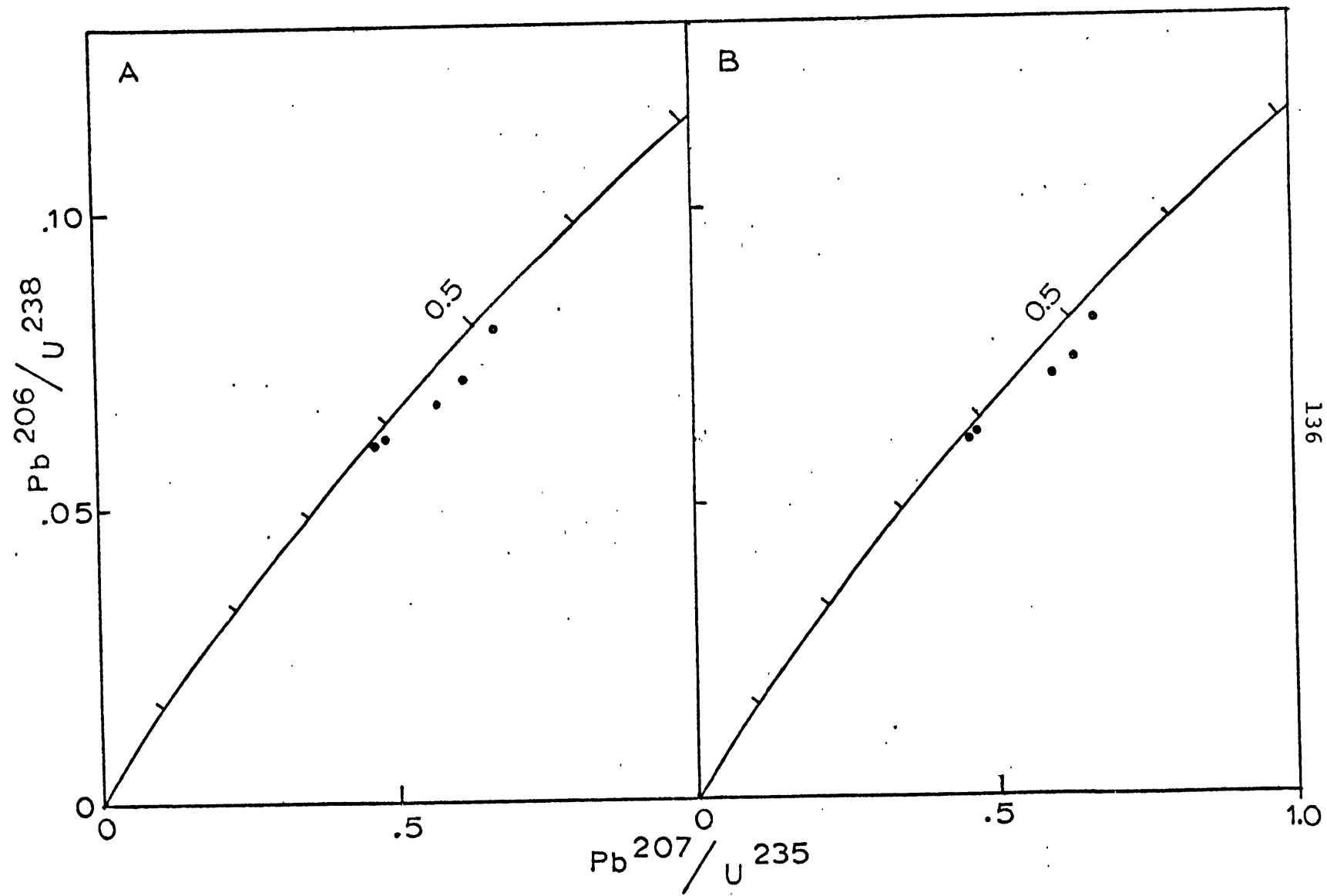
by common lead within the zircons, then there should be no significant correlation between Pb^{204}/Pb^{206} ratios and sample weight. This is strong evidence for a roughly constant amount of lead contamination introduced externally.

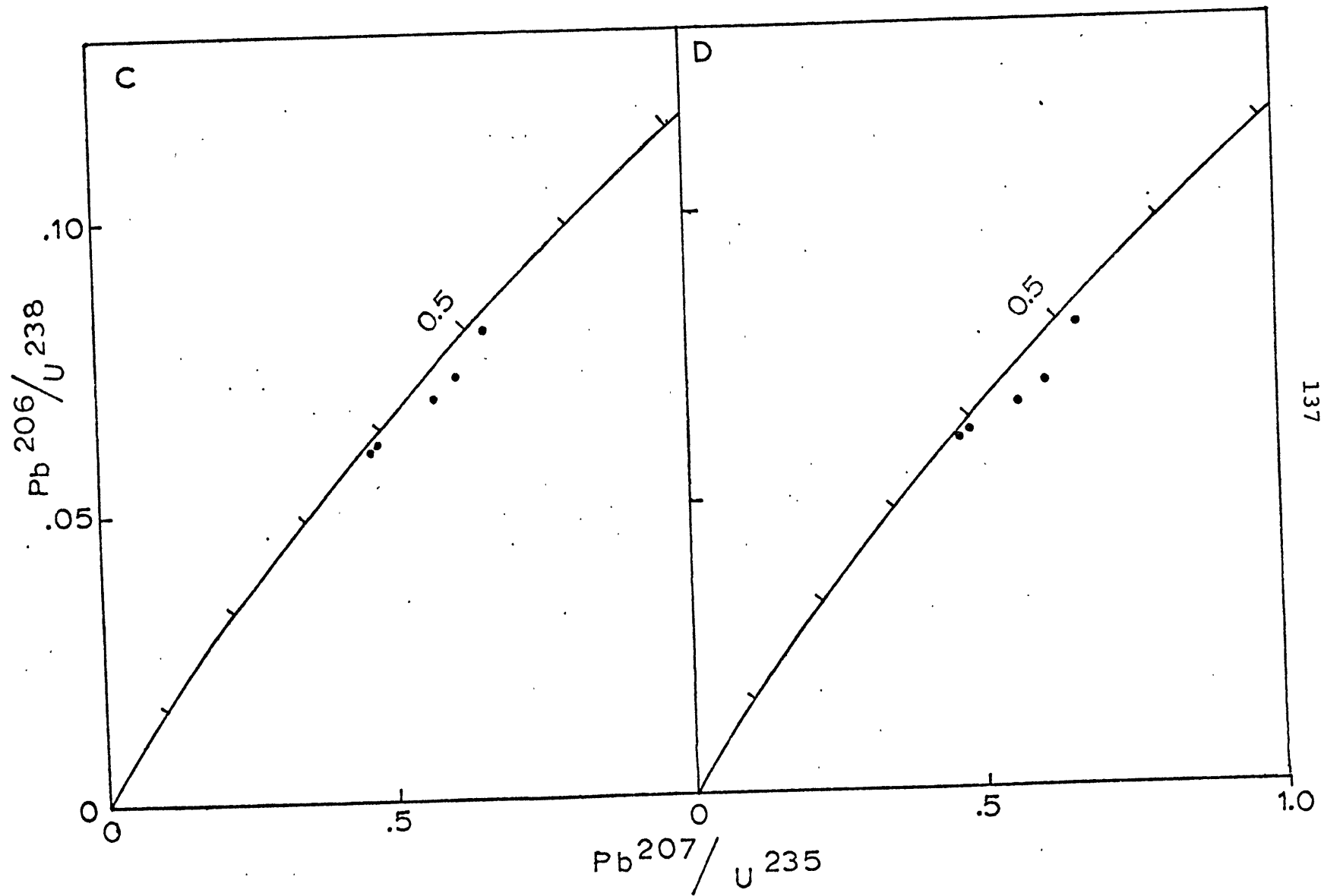
Lastly, even if we assume the worst case, i.e. that all the Pb^{204} is common lead, and correct the zircon data for various values of common lead, the points do not shift position significantly. Figure 16A shows five Fishbrook Gneiss points from Figure 10. These points were used because they lie close to Concordia, they show the general trend of all the Fishbrook Gneiss points and cover a wide range of Pb^{204}/Pb^{206} ratios. As a consequence, these points would show the effects of changes due to common lead more clearly than other points. Figures 16 B, C, and D show the same points corrected for three different values of common lead taken from Doe's (1970) compilation of common lead values. B and C are single stage lead ore values: B is from metamorphosed rocks 1.6 and 1.7 b.y. in age; C is from middle Ordovician rocks. Specific references are given in the figure caption. D is whole rock common lead from gneiss of Llano, Texas, chosen because it is significantly different from B and C and because its Pb^{204}/Pb^{206} , Pb^{207}/Pb^{206} , and Pb^{208}/Pb^{206} values are below those of A, while those of B and C are above A in value. Although these values of common lead do change the positions of the points slightly, the overall trend and discordia lines are not changed significantly. In

Figure 16

Concordia plots of five Fishbrook Gneiss points corrected for six different values for the isotopic ratios of the contamination.

- A: $\text{Pb}^{204}/\text{Pb}^{206} = 0.0496$, $\text{Pb}^{207}/\text{Pb}^{206} = 0.7843$,
 $\text{Pb}^{208}/\text{Pb}^{206} = 1.9579$; see Appendix B.
- B: $\text{Pb}^{204}/\text{Pb}^{206} = 0.0620$, $\text{Pb}^{207}/\text{Pb}^{206} = 0.9640$,
 $\text{Pb}^{208}/\text{Pb}^{206} = 2.2370$; Kollar et al. (1960).
- C: $\text{Pb}^{204}/\text{Pb}^{206} = 0.0547$, $\text{Pb}^{207}/\text{Pb}^{206} = 0.8628$,
 $\text{Pb}^{208}/\text{Pb}^{206} = 2.1063$; Ostic et al. (1967).
- D: $\text{Pb}^{204}/\text{Pb}^{206} = 0.0453$, $\text{Pb}^{207}/\text{Pb}^{206} = 0.7191$,
 $\text{Pb}^{208}/\text{Pb}^{206} = 1.909$; Zartman (1965).
- E: $\text{Pb}^{204}/\text{Pb}^{206} = 0.0618$, $\text{Pb}^{207}/\text{Pb}^{206} = 0.9395$,
 $\text{Pb}^{208}/\text{Pb}^{206} = 2.2009$; calculated by the author using $\text{U}^{238}/\text{Pb}^{204} (\mu) = 9.0$, $\text{Th}^{232}/\text{Pb}^{204} (\mu \cdot K) = 36$, the uranium decay constants of Jaffey et al. (1971), the thorium decay constant of LeRoux and Glendenin (1963), primordial lead ratios compiled by Doe (1970), and assuming the common lead was separated out 1.5 b.y. ago.
- F: $\text{Pb}^{204}/\text{Pb}^{206} = 0.0566$, $\text{Pb}^{207}/\text{Pb}^{206} = 0.9230$,
 $\text{Pb}^{208}/\text{Pb}^{206} = 2.1002$; same as E, except that $\text{U}^{238}/\text{Pb}^{204} = 11$ and $\text{Th}^{232}/\text{Pb}^{204} = 44$.





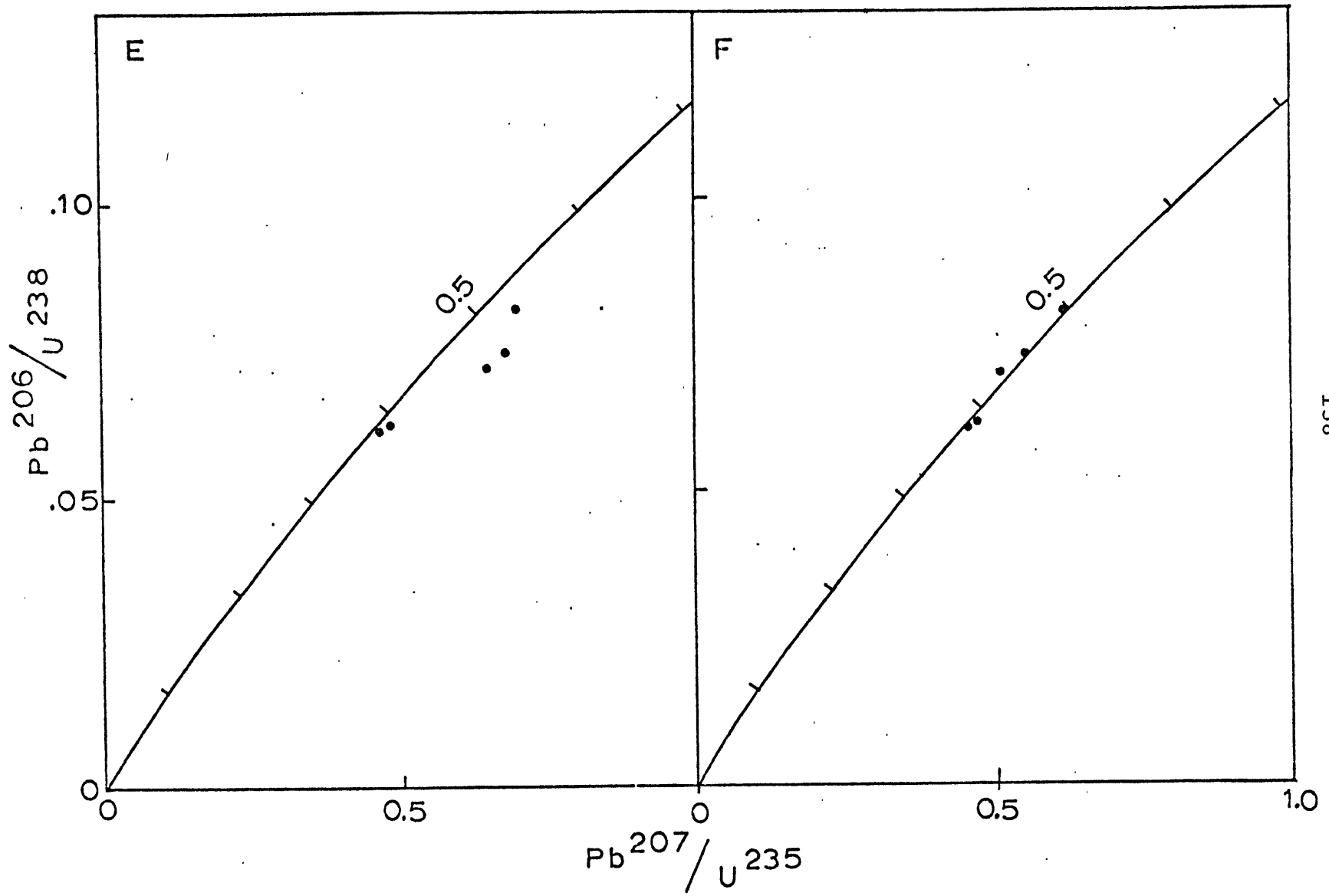


Figure 16E, single-stage lead ratios for 1.5 b.y. ago were calculated using average primordial lead ratios given by Doe (1970) and U^{238}/Pb^{204} and Th^{232}/Pb^{204} ratios of 9.0 and 36.0 respectively. These calculated ratios were then used to correct the points of Figure 16A. The points are shifted somewhat to the right, but the scatter of the points is significantly increased. In Figure 16F the same correction has been made except that the common lead ratios are based on $U^{238}/Pb^{204} = 11$ and $Th^{232}/Pb^{204} = 44$. Here the points become concordant or fall to the left of Concordia.

Taking these diagrams together, it can be seen that if common lead is a significant contaminant, it either has little effect or must be derived from a system confined to narrow values of U^{238}/Pb^{204} (μ) and Th^{232}/Pb^{204} ($\mu \cdot K$); otherwise, the corrected points will fall to the left of Concordia or will be scattered to a larger degree.

Although the arguments presented above are given to show that common lead is not a significant part of the contamination, this by no means implies that there is no common lead in the contamination. A small amount of common lead combined with a larger and more significant amount of laboratory contamination may account for some (but not all) of the scatter in the data.

Detrital and Volcanic Trends

The zircons or W-1, W-2, Z-3 and R8453 are most certain-

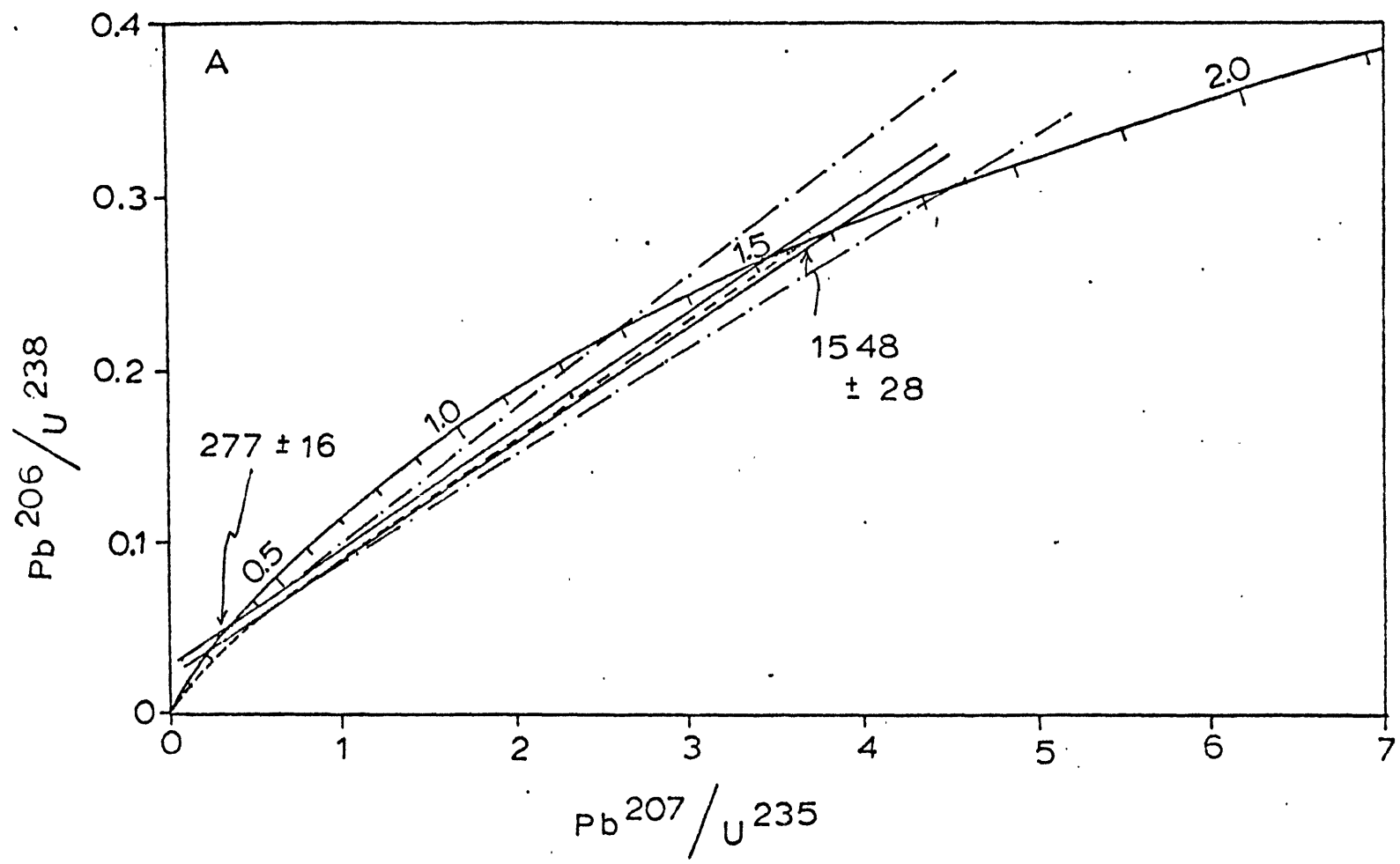
ly of detrital origin, and although the individual groups give different chords and intercepts, taken together the points appear to lie on a single trend, although with a great deal of scatter. Since there is no compelling evidence from zircon morphology and characteristics or from field relations to suggest otherwise, it has been found convenient to combine these points into a single chord designated as the Best Detrital Line (BDL). Figure 17 shows the BDL and its error limits ($\pm 2\sigma$ of the mean). Table 13 shows the intercepts, their ages and their errors. Because of the large spread in ratios and significant number of points (13), the BDL is fairly well defined; the only question is whether these points represent a single population. That they might not represent a single population is suggested by the scatter in the points. If we use the lower intercept of the BDL (277 m.y.) as a common tie point, lines bounding all of the detrital points can be drawn to form a wedge outlining the area covered by the detrital points (see Figure 17A). This suggests that the detrital zircons may be a mixture of populations from 1.3 to 1.75 b.y. in age. This difference is small enough, however, to deal with them as a single group without changing the basic interpretation significantly. As will be seen below, there is evidence, besides the similarity of the points, to suggest that they represent a single group.

Because the BDL is fairly well defined, and the nature of the zircons in these rocks is relatively certain, I will

Figure 17

Best Detrital Line

- A: Best Detrital Line (BDL) and its error bounds ($\pm 2\sigma$ of the mean). The BDL is made up of W-1, W-2, Z-3, and R8453. The two solid lines indicate the area covered by the BDL. Also shown: a time-dependent continuous diffusion curve for 1.55 b.y. (Wasserburg (1963), corrected for new decay constants; dashed line); and a wedge outlining all of the detrital points (dashed-dotted lines, which cross at the lower intercept of the BDL, at 277 m.y.).
- B: BDL (solid line) and the ($\text{Pb}^{207}/\text{U}^{235}$, $\text{Pb}^{206}/\text{U}^{238}$) points for the analyses from W-1, W-2, Z-3, R8453, Z-5, and R8311. Dashed lines show time-dependent continuous diffusion curves (Wasserburg, 1963) for 1.3 and 1.55 b.y. old zircons (short and long dashes respectively).



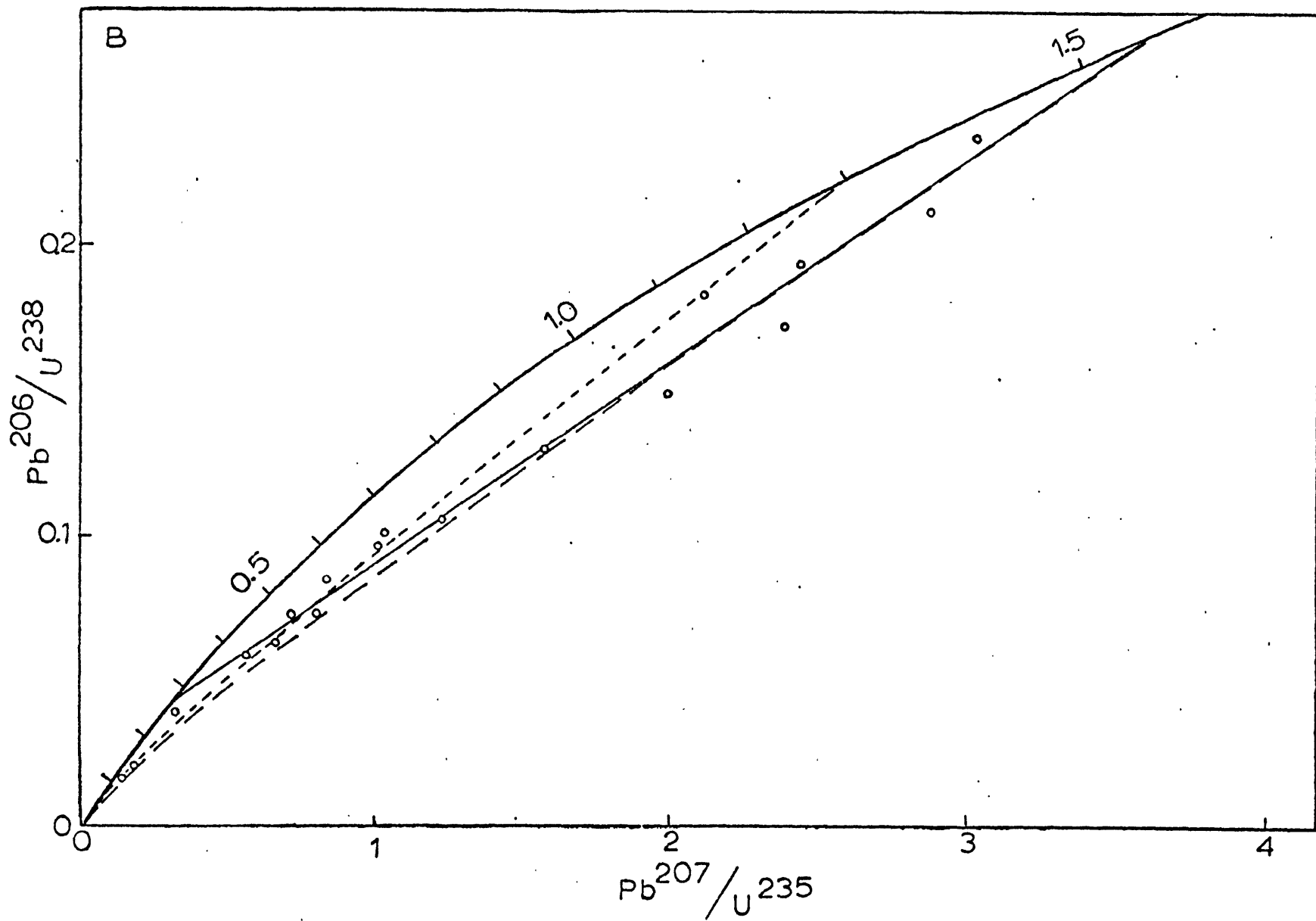


TABLE 13

Intercepts and Ages of the Best Detrital and Best Volcanic Lines

Line	Upper Intercept			Lower Intercept			Comments
	$\frac{\text{Pb}^{207}}{\text{U}^{235}}$	$\frac{\text{Pb}^{206}}{\text{U}^{238}}$	Age, m.y.	$\frac{\text{Pb}^{207}}{\text{U}^{235}}$	$\frac{\text{Pb}^{206}}{\text{U}^{238}}$	Age, m.y.	
Best Detrital	3.590	0.2713	1548 ± 28	0.3136	0.0439	277 ± 16	composed of all W-1, W-2, Z-3, and R8453 points
Best Volcanic	1.076	0.1220	742 ± 91	0.3067	0.0430	272 ± 47	composed of Z-1 (except 1NM-250), Z-2, Z-4 (except 5M), and R8441

144

Errors quoted on ages above are ± two standard deviations of the mean.

use the BDL as a reference line against which we can compare the other points in terms of age, behavior and quality.

The first question that arises is whether the Fishbrook Gneiss and the other volcanic zircons represent an entirely different trend or whether they are really detrital zircons that have been almost completely reset. Evidence given under the zircon morphology section strongly suggests that they are a different group. Evidence concerning the nature of the resetting of the detrital zircons also suggests the same thing.

The detrital zircons seem to have been affected by an episodic Pb loss event at approximately 277 m.y. The resetting of these zircons does not appear to have been strongly affected by continuous diffusion. A time-dependent continuous diffusion curve of Wasserburg (1963) for 1.55 b.y. old zircons is shown in Figure 17. In Figure 17B, it can be seen that the majority of the points at the low end of the BDL lie above the diffusion curve which suggests that time-dependent diffusion has not been a major factor in resetting these points. A volume diffusion curve (Tilton, 1960; not shown) would lie slightly above the time-dependent curve but would still leave most of the points above it at the low end. A time-dependent continuous diffusion curve for zircons 1.3 b.y. in age is also shown in Figure 17B. This fits the lower points (W-2, R8311) more closely but misses the points from W-1 and Z-3. A diffusion curve for 1.4 b.y. old zircons (not shown) fits the data points somewhat better but still leaves the points some-

what skewed relative to the curve. The points with $\text{Pb}^{207}/\text{U}^{235}$ ratios greater than 1.0 still lie below the the 1.4 b.y. old curve, while points with $\text{Pb}^{207}/\text{U}^{235}$ ratios less than 1.0 lie, in general, above it. In addition, as will be shown later, the lower intercept of the detrital line is geologically meaningful in southeastern New England.

Accepting episodic lead loss as the major contributing factor to resetting, we must next determine the mechanisms which control resetting. Even though grade of metamorphism exercises some control (Gastil *et al.*, 1967), it can not be the only factor since W-1 and W-2 show distinctly different behaviors even though they are at exactly the same metamorphic grade. It was noted above that W-1 and W-2 do have distinctly different uranium contents. A number of authors (Silver, 1963; Gastil *et al.*, 1967; Gebauer and Grünenfelder, 1976) have noted that radiation damage due to decay of radioactive elements within the zircons exercises a strong control over the amount of resetting during episodic lead loss. Gebauer and Grünenfelder (1976) have shown that the lead loss can occur at fairly low temperature (300-400°C) as a result of annealing and recrystallization of radiation damaged zircons.

In order to test whether this has been the mechanism of resetting for the detrital zircons of this report, two parameters must first be defined. The first parameter measures the amount of resetting of an individual point. This was done by drawing a line perpendicular to the BDL from the individual

point. The distance from the intersection of this line and the BDL to the upper intercept was measured and then divided by the total length of the BDL from the upper to the lower intercept. Thus, an unreset concordant zircon would have a coefficient of resetting (C_r) of zero, while a completely reset zircon would have a C_r of 1. The second parameter is a measure of radiation damage. Wasserburg (1963) suggested that a good measure of radiation damage would be $U^{238} + 0.23 \text{ Th}^{232}$. Th^{232} was not measured for this paper, but we can approximate its value by first assuming that the Th-Pb and U-Pb systems have behaved similarly, which is approximately correct (Doe, 1970). Since we know the original age of the zircons, the $\text{Pb}^{208}/\text{Pb}^{206}$ ratio and the amount of uranium in the zircons, we can calculate approximately the Th^{232} content. As a result we obtain the following measure of radiation damage:

$$R_c = U \cdot (1 + 0.75 [\text{Pb}^{208}/\text{Pb}^{206}])$$

where

R_c = radiation damage coefficient,

U = uranium content in ppm, and

$\text{Pb}^{208}/\text{Pb}^{206}$ = $\text{Pb}^{208}/\text{Pb}^{206}$ ratio of the zircons, corrected for contamination.

Now, strictly speaking, R_c is really a measure of the rate of radiation damage. Two zircons with similar values of R_c can have different amounts of total radiation damage if

they are different in age. But for a group of zircons that are of the same age, R_c will be proportional to the total radiation damage. Since R_c is time-independent, it is useful for comparing two groups of zircons in order to ascertain whether they are of the same age but have been reset to different degrees, or whether they are in fact two different groups of zircons with different ages.

C_r and R_c were calculated for the 13 best detrital points and are plotted in Figure 18A. It can be readily seen that they form a well defined curve in exactly the manner expected. This represents a clear-cut case of episodic lead loss controlled by radiation damage. Continuous diffusion would, of course, produce the same trend (except at the low end) but the lines shown in Figure 17B show that continuous diffusion curves do not fit the observed data well, except possibly for R8311 and Z-5 (see the next section).

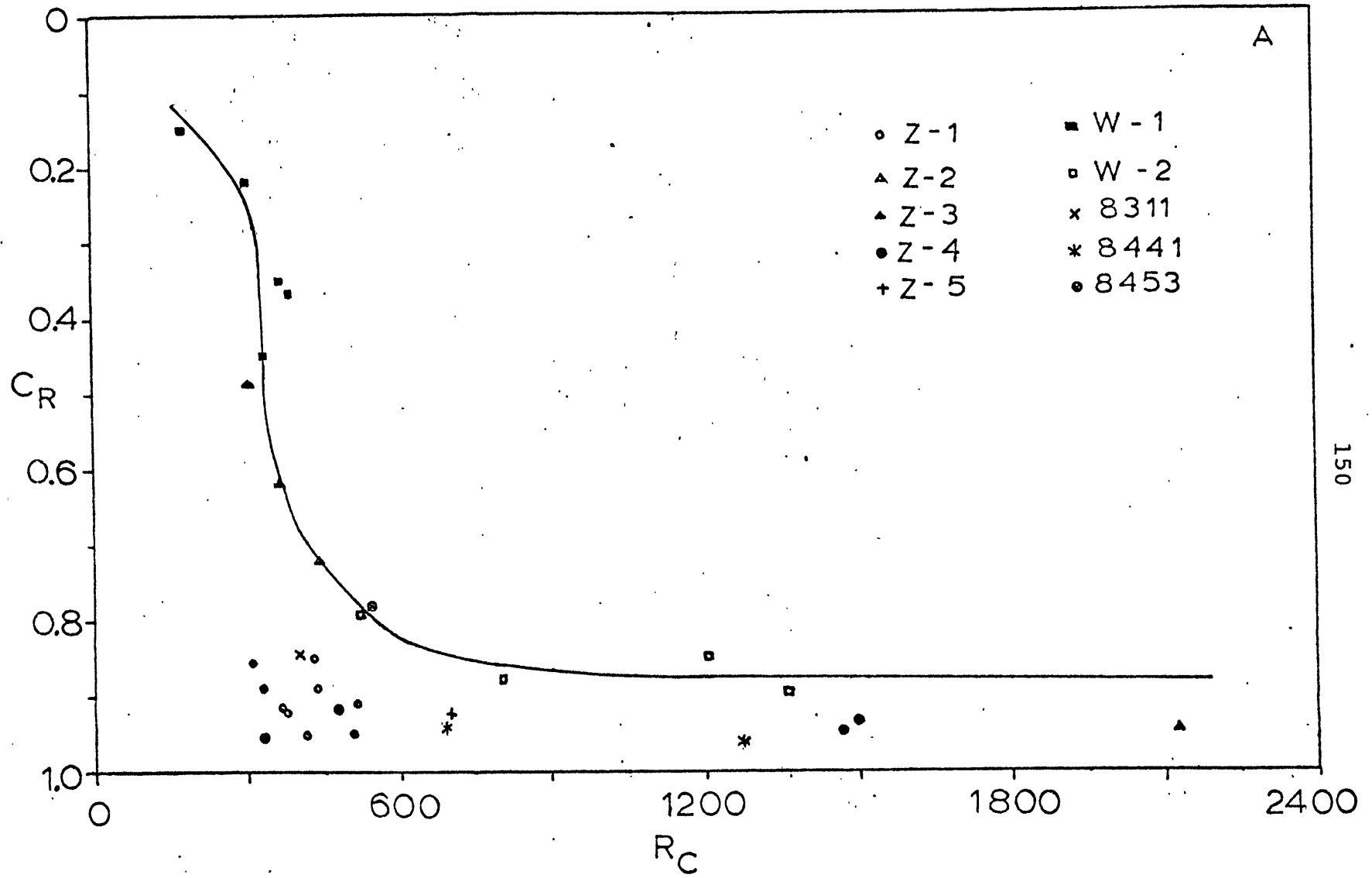
The scatter is remarkably small considering the number of assumptions involved. The "best fit" line drawn through the detrital points in Figure 18A points out a number of other interesting facts. Below a certain R_c (< 300) there appears to be little resetting. One explanation for this would be that small amounts of radiation damage anneal spontaneously or at least, anneal over a time period shorter than the time it would take for Pb to diffuse out of the zircon.

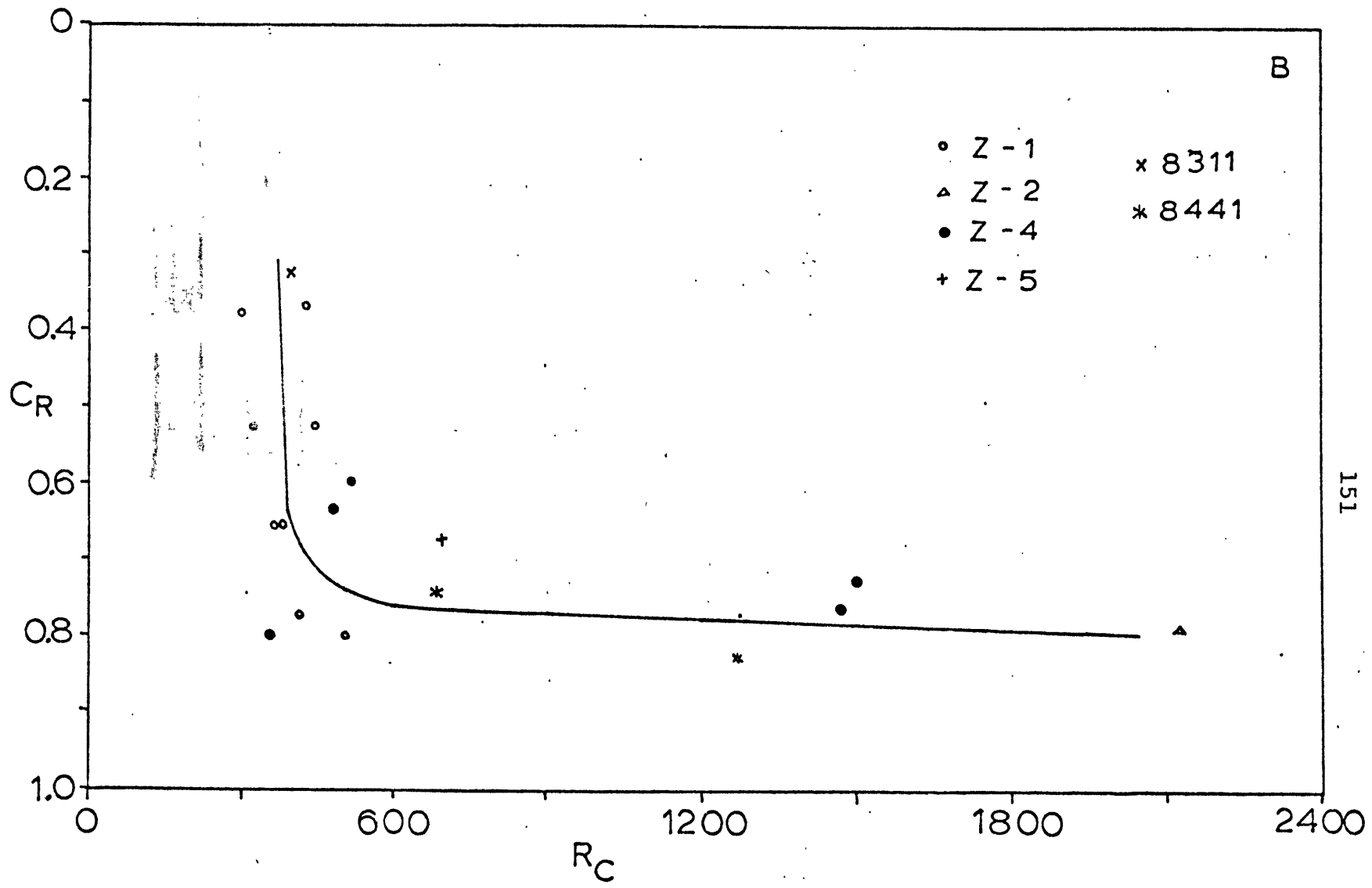
For R_c values between 300 and 500 resetting occurs over a wide range (0-80%). This probably represents the region

Figure 18

Plots of the resetting coefficient (C_r) versus the radiation damage coefficient (R_c) for the zircons analyzed in this paper.

- A: C_r versus R_c for all the points analyzed, except for three R8311 points and Z-4 5M, which give C_r values greater than 1.0 . The solid line is the "best fit" line for the trend established by the detrital points made up of W-1, W-2, Z-3, and R8453.
- B: C_r versus R_c for the volcanic points made up of Z-1, Z-2, Z-4, R8441, plus Z-5 and R8311 1Amp NM, whose affiliations are uncertain.





151

B

where radiation damage exists over a time period longer than the rate of diffusion of lead during an episodic event. The increased diffusion rates that would occur during an episodic thermal event, would allow lead to diffuse out of the zircon only if enough radiation damage were present, such that annealing occurred over a time period on the same order as the time for Pb to diffuse out of the zircon. This appears to be the case between 300 and 500 on the R_c axis.

At higher R_c values, a kind of saturation seems to occur. This is not surprising since there will always be sites in the zircon that have annealed spontaneously prior to the episodic event, or which anneal more quickly during the event than the diffusion rate of Pb. Thus, a residue of 10-15% of the total radiogenic lead is tightly held and is probably not released except at very high R_c values and high metamorphic grades. At high R_c values it must also be remembered that many radioactive decays will occur in areas that have already been radiation damaged. Thus, added increments of R_c will be reflected as less real radiation damage in the zircon. So at very high R_c values very little extra real radiation damage occurs. In addition, inhomogeneities in the distribution of radioactive elements in the zircon will mean that some areas of the zircon may have very low R_c values, although the zircon as a whole may have a high value. All of these factors combine to explain the leveling off seen at high R_c values.

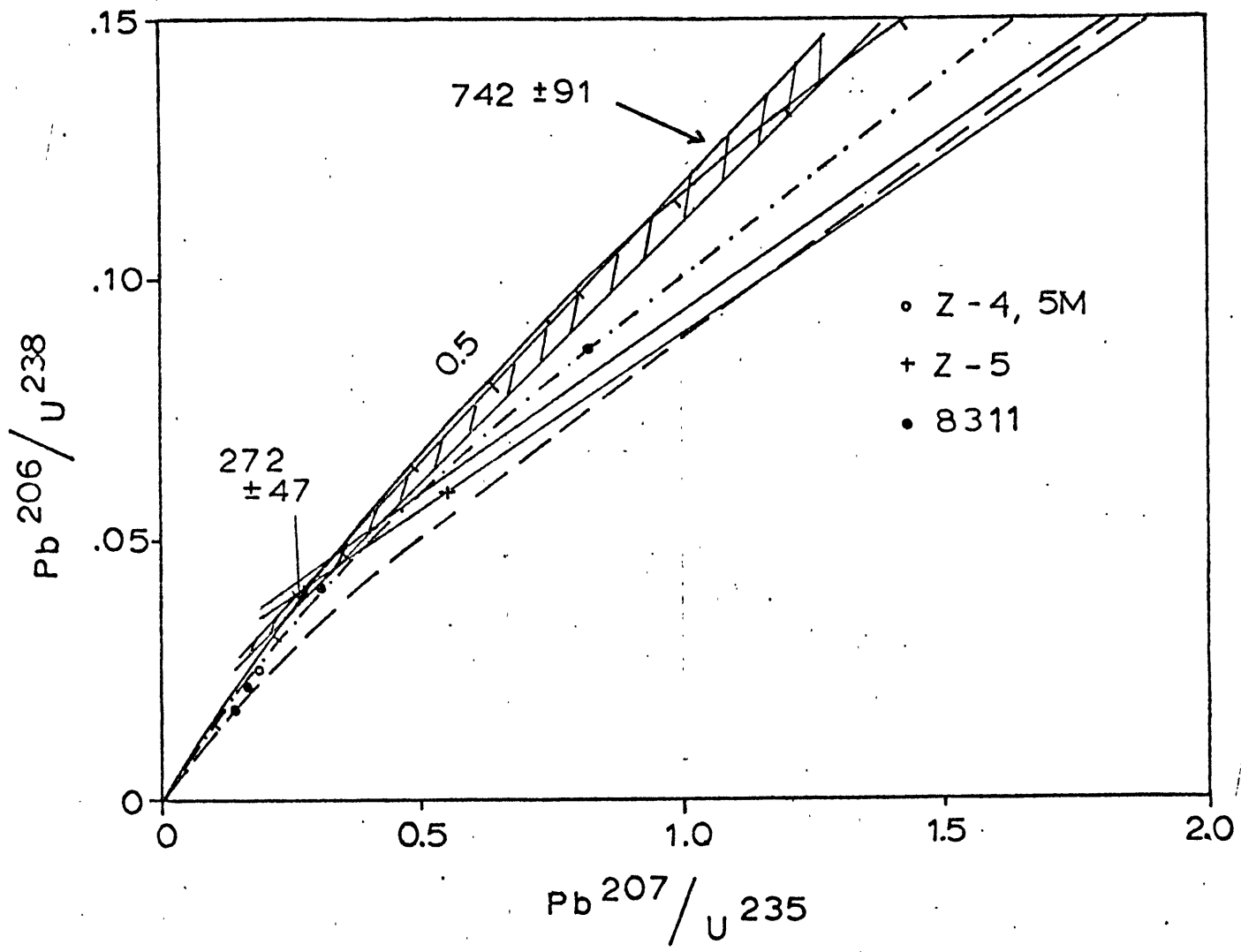
The curve in Figure 18A also implies that the zircons of W-1, W-2, Z-3 and R8453 are behaving as a single, well-defined group. There appears to be no overall difference in behavior between any of these zircons. This strongly suggests that the detrital zircons are derived from a single source area, or from a well mixed combination of source areas which remained essentially constant from the time of deposition of the Westboro Formation to the deposition of the Shawsheen Gneiss.

When the volcanic zircons are plotted on Figure 18A using the BDL as a reference line, it can be seen that they fall well off from the main curve of the detrital points. The volcanic zircons cover almost the same range of R_c values, yet all appear excessively reset compared to the detrital zircons. This implies that they are in fact not completely, or almost completely, reset detrital points, but rather represent a different group altogether.

If a best fit line (BVL) for the volcanic points is calculated (Table 13; Figure 19) and the same type of analysis is carried out we get the plot shown in Figure 18B. Although the scatter is much larger, the same type of curve is obtained as with the detrital points. In fact, the curves are very similar in shape and position. The conclusion that is reached from this analysis is that we are definitely dealing with two different groups of zircons. The first group is a population of detrital zircons approximately 1.55 b.y. in age. The second is a population of volcanic zircons approximately

Figure 19

Concordia plot of anomalous points Z-4 5M and R8311. Also shown are the Best Detrital Line (BDL, area between the two parallel solid lines), the Best Volcanic Line (BVL, cross-hatched area), a time-dependent continuous diffusion curve for 1.55 b.y. old zircons (dashed line) and a similar curve for 1.25 b.y. old zircons (dashed-dotted line). The diffusion curves are after Wasserburg (1963), corrected by the author for the new decay constants (see Appendix B). The areas outlined for the BDL and BVL are the boundaries marked by plus or minus two standard deviations of the mean line (see Appendix D). Ages shown are the intercepts of BVL with Concordia; they are in millions of years, also $\pm 2\sigma$ of the mean.



740 m.y. in age. Both have undergone episodic lead loss at about the same time (note the similarity in the lower intercepts of BDL and BVL in Table 13). This lead loss has been controlled mainly by the amount of radiation damage produced in the zircons.

There are two detrital points (Z-5 5NM and R8311 1Amp NM) which do not fit the detrital curve of Figure 18A, although they fall within the detrital trend of Figure 17. As seen in Figure 18B, they are more similar to the volcanic points than the detrital points. There are two explanations for this behavior. One is that they may contain a metamorphic population of zircons which makes them appear more reset than they really are. The other possibility is that they are more strongly controlled by metamorphism. They are from the highest grade part of the section and this may have caused them to be more reset (by increased diffusion rates) than zircons at lower grades but with similar values of R_c .

Continuous Diffusion

A few points (Z-4 5M, R8311 except for 1Amp NM) have been ignored in the above analysis mainly because their lower intercepts suggest recent lead loss more strongly than any of the other points. But this recent loss also appears to be strongly controlled by radiation damage. All four points have R_c values greater than 3000. Enough radiation damage has probably been produced to allow continuous diffusion to

occur. Figure 19 shows the BDL and BVL along with R8311, Z-5 and Z-4 5M plotted on a Concordia diagram. Also shown is the time-dependent continuous diffusion curve of Wasserburg (1963) for 1.55 b.y. old zircons. It can be seen that all of these points lie above the diffusion curve. This could possibly be due to the fact that they represent a different population of zircons. In fact, as Figure 19 shows a continuous diffusion curve for 1.25 b.y. old zircons agrees very closely with the Nashoba points (R8311 and Z-5; Z-4 5M will be left out of the following analysis, but the same arguments hold, except that its continuous diffusion curve originates within the Fishbrook Gneiss group). But there is no other evidence to suggest that they are a different population; in fact, the geologic evidence (Bell and Alvord, 1976) suggests a continuous sequence from the Shawsheen Gneiss up through the Nashoba Formation. In addition, the strong evidence for episodic lead loss suggests that R8311 and Z-5 are the result of continuous diffusion superimposed on episodic lead loss.

The following model can be advanced. First, the increased diffusion rates caused by the higher grade of metamorphism of the Nashoba Formation would cause the resetting curve of Figure 18A to shift over to lower values of R_c and possibly cause the amount of resetting in the saturation region to rise (90-95%).

Second, during the major period of metamorphic activity

(430-470 m.y. by Rb-Sr whole-rock data; see Chapter 7), the Nashoba zircons would have been reset to the maximum limit (90-95%). Subsequent, less intense metamorphic episodes (Acadian, approximately 380 m.y.; Permo-Carboniferous, approximately 270 m.y.) would have affected only those zircons that had built up enough radiation damage.

Finally, the three Nashoba Formation zircons with high R_c values will continue to lose Pb by continuous diffusion up to the present, because of large amounts of radiation damage.

As Figure 19 shows, this is the trend we find. R8311 1Amp NM, which has the lowest R_c value of the Nashoba points, lies farthest up the diffusion curve. Its R_c value lies roughly in the region where resetting occurs over a wide range (Figure 18) for lower metamorphic grades. Thus, its amount of resetting will depend strongly on other, less well known, factors. It seems to have been affected by a later event somewhere between 350 and 400 m.y., as a chord drawn through the point and the upper intercept of the BDL reveals. The 270 m.y. event seems not to have affected this zircon split, however. Z-5, on the other hand, because of its slightly higher R_c value, was affected by all the metamorphic events and now lies on the main detrital trend. The remaining three R8311 points probably did not lie too far from Z-5, but since then have followed a continuous diffusion curve to the present.

As a result, the U-Pb data - both the trends and the

scatter - can be explained as the result of three effects:

(1) Continuous diffusion of U and Th rich zircons superimposed on radiation damage controlled episodic Pb loss;

(2) Annealing, recrystallization and increased Pb diffusion rates caused by three or possibly four metamorphic or thermal events;

(3) Variable behavior of zircons due to variations in radiation damage, variations in metamorphic grade during metamorphic events, variations in the overall strength of each metamorphic event, and other external conditions, especially in the range where resetting occurs over a wide range.

Summary

The geochronologic data that come from the U-Pb results can be summarized in a number of major points:

(1) There is a volcanic suite of zircons that is 742 ± 91 m.y. old.

(2) There is a detrital suite of zircons that is 1.55 ± 0.03 b.y. old, which may actually represent a well mixed combination of a number of different detrital populations.

(3) Both suites underwent their last major period of lead loss and annealing 270 m.y. ago, but were also probably affected by previous metamorphic events, especially at 450 to 470 m.y. ago.

(4) This 270 m.y. event is geologically reasonable. It agrees with ages of zircons from plutonic rocks in the area based on radiation damage measurements (Fairbairn and Hurley, 1957) which average about 250 m.y. Many Pb- α ages also fall into this range (Webber et al., 1956).

This age also agrees well with many K-Ar mineral ages in the region (Zartman et al., 1970) which have been ascribed to a thermal resetting event. The correlation between K-Ar mineral age resetting and zircon resetting is further strengthened by the fact that K-Ar ages in micas approach complete resetting in the temperature range of 300-400°C (Dalrymple and Lanphere, 1969), just the temperature range that Gebauer and Grünenfelder (1976) suggest is the range where zircon U-Pb systems become open due to radiation damage. Thus, radiation damage ages and K-Ar ages would both record the last event to occur in this temperature range.

(5) Similarities between the detrital zircons suggest that the sedimentary sequence from the Westboro Formation to the Shawsheen Gneiss shared the same source area or areas. This implies a continuous sequence, or at least one in which unconformities do not represent significant periods of time. Geologic evidence and similarities in the zircons suggest that the sequence may be continuous up through the Nashoba Formation. For the present, the evidence favors a continuous sequence of essentially the same age throughout (742 m.y.).

Chapter 7

Rb-Sr Whole Rock Results

Sample Preparation

Appendix A outlines the procedures used for preparing and dissolving samples, separating and purifying Rb and Sr, mass spectrometry, and data analysis for the Rb-Sr whole rock analyses. Analyses of standards, spike calibrations, replicates, and blanks are also given in Appendix A as well as various isotopic ratios used. The decay constant used for all age calculations is $1.39 \times 10^{-11} \text{ y}^{-1}$. Slopes of isochrons were determined using the linear least squares cubic regression equations of York (1966, 1967). Multiple measurements were taken of all ratios to determine statistics and all errors were propagated through all calculations. Errors are given as ± 1 standard deviation of the mean except where noted otherwise. Samples with errors in $\text{Rb}^{87}/\text{Sr}^{86}$ greater than 5% or in $\text{Sr}^{87}/\text{Sr}^{86}$ greater than 0.5% were removed from consideration.

Results

The following discussion gives the results of rubidium-strontium whole rock analyses. Calculated $\text{Sr}^{87}/\text{Sr}^{86}$ and $\text{Rb}^{87}/\text{Sr}^{86}$ ratios are plotted on standard isochron diagrams (Faure and Powell, 1972). Concentrations of Rb and Sr are also given. The data will be presented for each formation along with short descriptions of hand samples. Selected thin

section descriptions are given in Appendix C. Concentrations of Rb and Sr given in the tables are probably accurate to about 2%.

Fishbrook Gneiss - Data for the Fishbrook Gneiss is composed of ten samples:

R8404-R8406: Same as Z-4.

R8434-R8435: Medium to coarse grained light colored gneiss with quartz, feldspar, biotite, and other unidentified mafic minerals. Well developed gneissic layering.

R8441, R8443: Same as R8441 in Chapter 6.

R8444-R8445: Granitic gneiss; medium grained, pinkish white in color, with quartz, feldspar, biotite. Poorly developed foliation.

R8446: Medium grained biotite, quartz, feldspar, amphibole schist with quartzofeldspathic segregations.

The data for these samples is shown in Table 14. Points are plotted in Figure 20. Except for R8443 the points form a fairly well defined line. The reason for the large difference between R8443 and the other points is unknown. It is exactly similar to R8441 in every respect. However, because it leads to large errors in the age and intercept (line 1, Figure 20) and is quite obviously off the main trend in the data it will be left out of the following discussion.

Without R8443 an age of 400 m.y. and initial ratio of 0.708 is indicated. R8406 has a large residual with respect to this line (line 2). A regression done without this point

TABLE 14

Rb-Sr Results for Fishbrook Gneiss

<u>Sample</u>	<u>Rb, ppm</u>	<u>Sr, ppm</u>	<u>Rb⁸⁷/Sr⁸⁶</u>	<u>Sr⁸⁷/Sr⁸⁶</u>
R8404	36.06	75.85	1.342 ±.006	.71430 ±.00007
R8405	56.32	69.48	2.312 ±.024	.72163 ±.00099
R8406 ¹	65.39	83.38	2.216 ±.010	.72304 ±.00017
R8434	23.98	124.0	0.5382±.0009	.71040 ±.00028
R8435 ¹	21.70	147.1	0.4151±.0058	.71103 ±.00012
R8441	8.51	37.89	0.6187±.0079	.71126 ±.00015
R8443	5.33	31.60	0.4502±.0028	.72111 ±.00006
R8444	43.24	43.06	2.828 ±.042	.72294 ±.00016
R8445	65.20	35.75	5.222 ±.053	.73640 ±.00017
R8446	46.22	180.6	0.7266±.0039	.71123 ±.00032

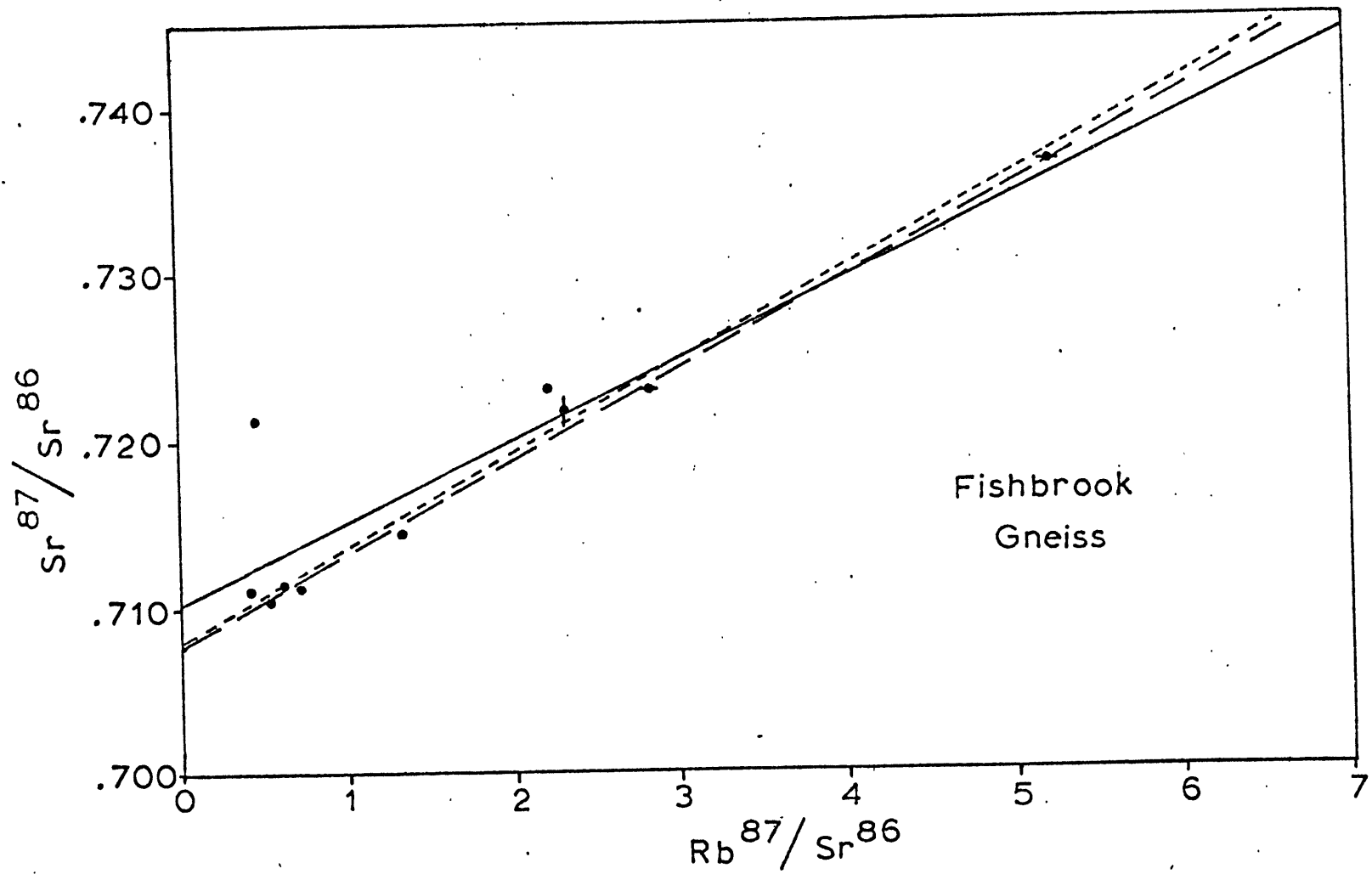
¹Composite of two replicates; see Appendix A.

Figure 20

Rb^{87}/Sr^{86} and Sr^{87}/Sr^{86} plot of whole rock samples from the Fishbrook Gneiss.

Data for the regression lines:

- Age 354 ± 64 m.y.; initial ratio
of $Sr^{87}/Sr^{86} = 0.7101 \pm .0018$.
- Without R8443. Age 403 ± 23 m.y.;
 $Sr^{87}/Sr^{86}_o = 0.7079 \pm .0007$.
- - - - - Without R8443 and R8406. Age
 394 ± 14 m.y.; $Sr^{87}/Sr^{86}_o =$
 $0.7078 \pm .0004$.



changes the line very little, reducing the age to 394 m.y. and leaving the initial ratio essentially unchanged (line 3). There is still some scatter about this line, however, and the slope is determined for the most part by only a few points which suggests that the age may not be as well determined as the errors imply. In fact the points lower than 2.5 in Rb^{87}/Sr^{86} value suggest a slightly higher slope. Although no regression was calculated for these points, their ages and intercepts will still probably lie within the error limits (at $\pm 2\sigma$) suggested by the other lines. Thus, no matter how the data are arranged an age about 400 m.y. and initial ratio about 0.708 still remain the most probable.

Nashoba Formation - The Nashoba Formation data consist of ten samples:

R8311: Described in Chapter 6.

R8380: Two feldspar - biotite - muscovite - quartz gneiss. Poorly developed gneissic texture. Biotite mostly clumped in irregular patches. Coarse grained, light pink in color; may be segregation or an injection of igneous material.

R8381: Dark black biotite-plagioclase-quartz gneiss. Well developed gneissic texture and foliation. Contains numerous small (3-10 mm) quartz-rich segregations.

R8382: Similar to R8381, but lighter in color with more quartz and feldspar.

R8457: Silver grey strongly folded and banded medium

to coarse grained muscovite-biotite-feldspar-quartz gneiss. Feldspar, quartz and some biotite mostly in small lenses and augen.

R8458: Similar to R8457 but with more quartz and feldspar and much less muscovite; some garnets in felsic bands.

R8459: Dark colored fine grained biotite-feldspar-quartz gneiss. Banding indistinct but well developed foliation. Occasional quartz-feldspar rich lenses.

R8460: Fine to medium grained biotite-quartz-feldspar gneiss.

R8461: Fine to medium grained, poorly foliated biotite-feldspar schist.

R8462: Medium to coarse grained well banded and foliated biotite-muscovite-feldspar-quartz gneiss. Quartz-feldspar rich veins are very coarse and tend toward lenses.

Using the nomenclature of Bell and Alvord (1976), R8311 is from the Beaver Brook Member. R8380-R8382 are from the Fort Pond Member, as is R8460. R8457-R8459 are from the Billerica Schist Member. R8461 is from the unidentified Nashoba Member and R8462 is from the Tophet Swamp Member.

Rb-Sr results are shown in Table 15 and the Sr_{87}/Sr_{86} - Rb_{87}/Sr_{86} points are plotted in Figure 21.

As with the Fishbrook Gneiss there is some scatter and the slope is essentially determined by a few points. There is also a similarity in ages although the initial ratio of the Nashoba Formation appears distinctly higher.

TABLE 15

Rb-Sr Results for the Nashoba Formation

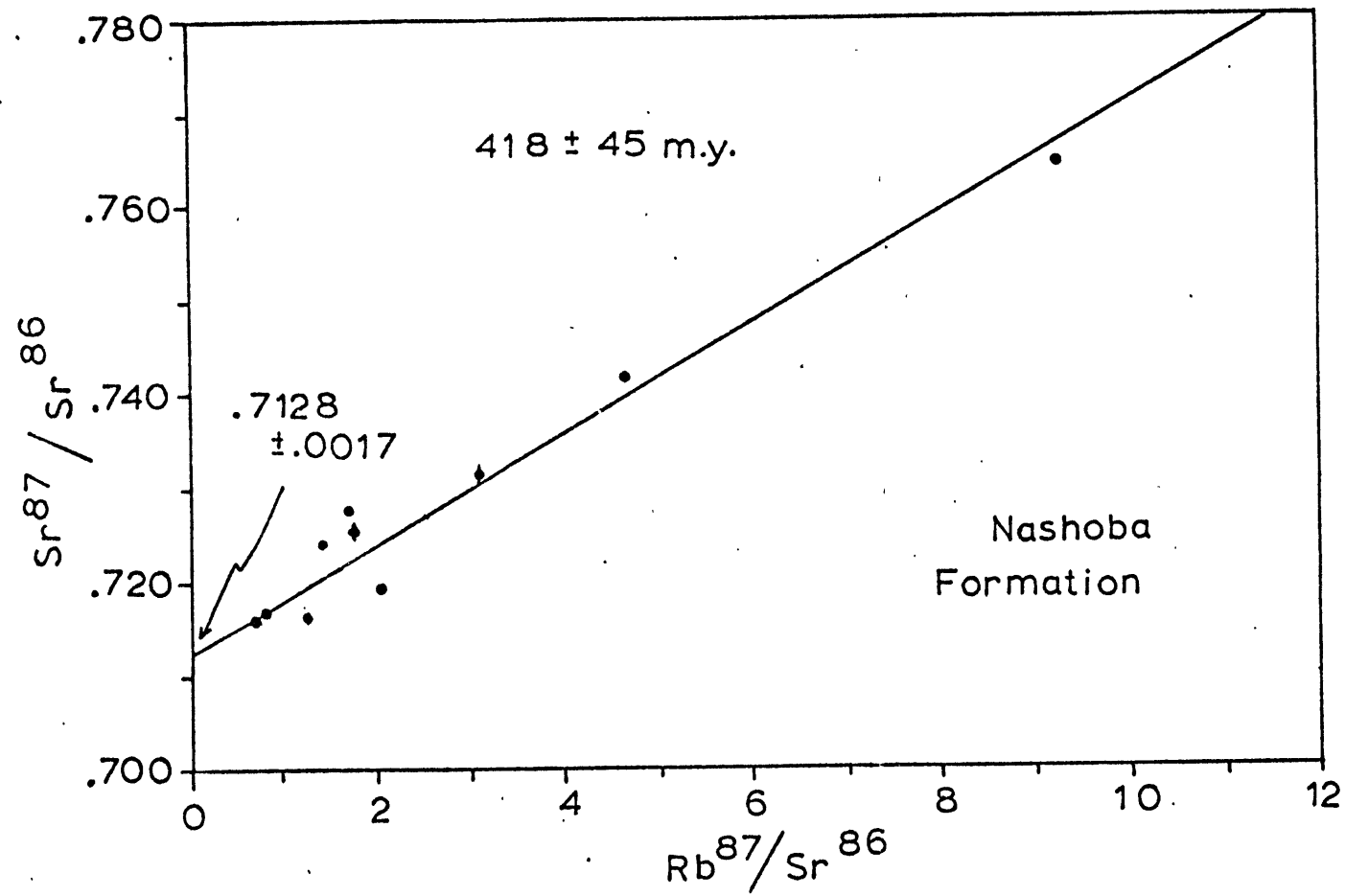
<u>Sample</u>	<u>Rb, ppm</u>	<u>Sr, ppm</u>	<u>Rb⁸⁷/Sr⁸⁶</u>	<u>Sr⁸⁷/Sr⁸⁶</u>
R8311 ¹	151.0	255.0	1.697 ±.002	.72740 ±.00009
R8380	90.16	372.7	0.6866±.0024	.71608 ±.00053
R8381	157.2	357.8	1.259 ±.008	.71614 ±.00029
R8382	117.9	191.9	1.754 ±.009	.72550 ±.00077
R8457 ²	205.2	63.87	9.254 ±.012	.76433 ±.00007
R8458 ²	152.4	93.71	4.670 ±.005	.74173 ±.00063
R8459 ²	257.8	241.0	3.092 ±.026	.73135 ±.00080
R8460 ²	90.98	301.0	0.8582±.0325	.71700 ±.00028
R8461 ²	158.0	220.2	2.057 ±.009	.71939 ±.00017
R8462 ²	130.2	260.2	1.431 ±.010	.72408 ±.00009

¹Collected by L. Schutts; analysis by A. Kovach; calculations by the author.

²Sample provided by D. Alvord.

Figure 21

$\text{Rb}^{87}/\text{Sr}^{86}$ versus $\text{Sr}^{87}/\text{Sr}^{86}$ plot of whole rock samples from the Nashoba Formation. Best fit regression line is also shown.



Although these samples originate from a number of different members of the Nashoba there does not appear to be any correlation between the positions of the points and particular members.

Tadmuck Brook Schist - Four samples:

R8383: Dark silver grey phyllitic schist. Fine to coarse grained. Only discernible mineralogy is large muscovite flakes parallel to foliation; some biotite, feldspar and quartz observable.

R8454: Grey fine to medium grained muscovite-biotite-quartz-feldspar schist. Contains small quartz-feldspar lenses.

R8455: Grey-black coarse grained biotite-muscovite schist with some quartz and feldspar.

R8456: Silver grey coarse muscovite-biotite schist. Almost no quartz or feldspar apparent.

Rb-Sr data are shown in Table 16 and the isochron plot in Figure 22. Although the data are limited there is a similarity in age with the Fishbrook Gneiss and the Nashoba Formation. The initial ratio is distinctly higher than both although it is closer to that of the Nashoba Formation. Again the data are scattered but this is not unexpected since the Tadmuck Brook Schist is almost certainly a terrigenous metasediment (Chapter 3) and scatter of Rb-Sr data for such rocks is well documented (Whitney et al., 1961; Gebauer and Grünenfelder, 1974, 1976; Cordani et al., 1976). The higher initial ratio is also consistent with this interpretation

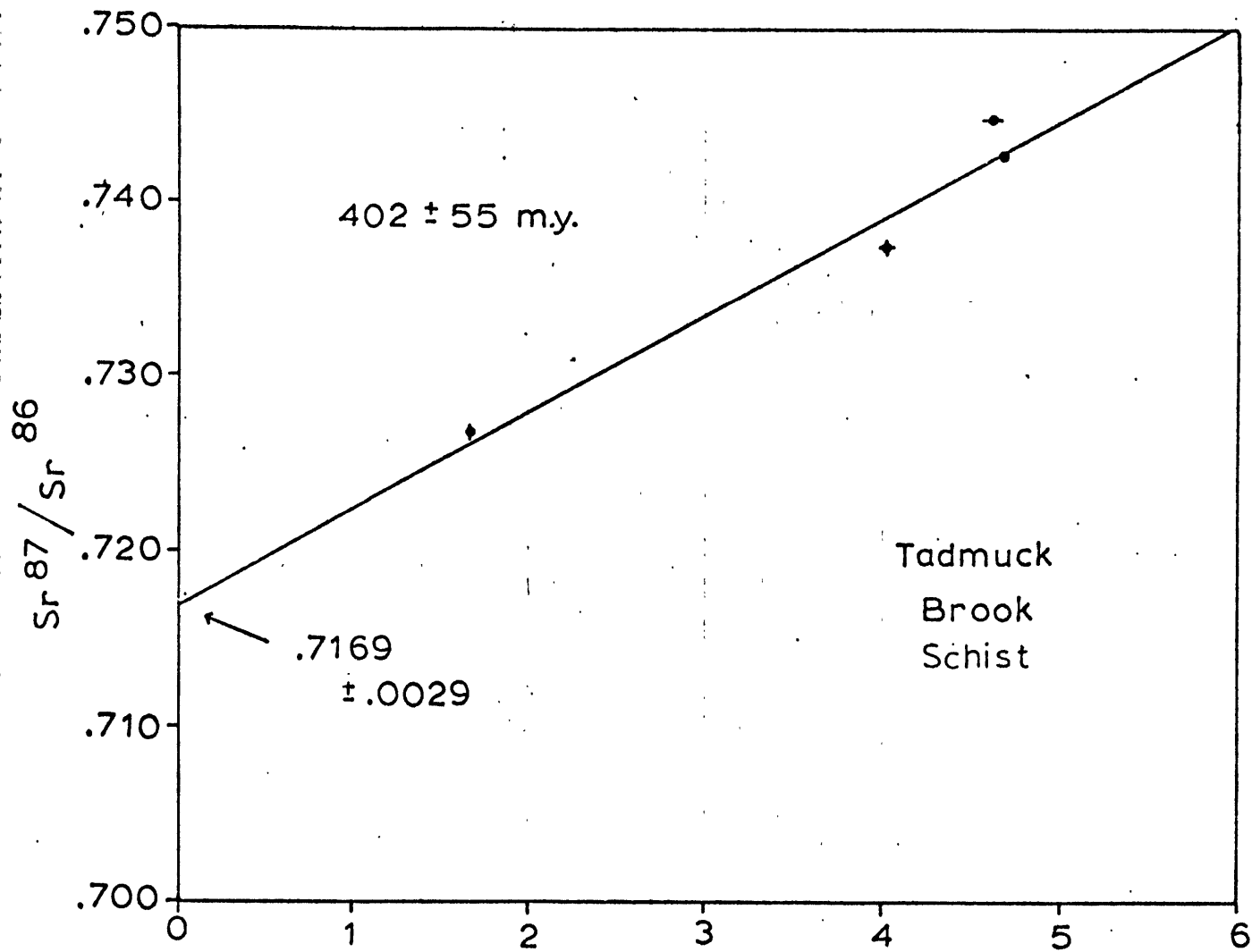
TABLE 16
Rb-Sr Results for the Tadmuck Brook Schist

<u>Sample</u>	<u>Rb, ppm</u>	<u>Sr, ppm</u>	<u>Rb⁸⁷/Sr⁸⁶</u>	<u>Sr⁸⁷/Sr⁸⁶</u>
R8383	190.2	136.1	4.019 ±.030	.73729 ±.00037
R8454 ¹	174.7	297.8	1.684 ±.006	.72671 ±.00039
R8455 ¹	240.6	150.4	4.616 ±.047	.74467 ±.00006
R8456 ¹	238.6	146.9	4.683 ±.011	.74268 ±.00029

¹Sample provided by D. Alvord.

Figure 22

$\text{Rb}^{87}/\text{Sr}^{86}$ versus $\text{Sr}^{87}/\text{Sr}^{86}$ plot for whole rock samples from the Tadmuck Brook Schist. Also shown is the best fit regression line.



(Whitney et al., 1961; Cordani et al., 1976).

Worcester Formation - The data for the Worcester Formation consist of four samples:

R8391: Unit 2 of Peck (1976). Silty phyllite with clay interlayers. Muscovite and pyrite the only discernible mineralogy. Well developed slaty cleavage.

R8392: Unit 3 of Peck (1976). Slate or phyllite with occasional silty layers. Muscovite only discernible mineral.

R8395: Unit 5 of Peck (1976). Fine to medium grained dark grey quartz-biotite-plagioclase metasilstone, slightly foliated.

R8397: Unit 3 of Peck (1976). Purple-black muscovite phyllite with good slaty cleavage, very fine grained.

Data for the Rb-Sr analyses are shown in Table 17. Ratios are plotted in the isochron diagram of Figure 23.

The Worcester Formation points form a fairly well defined isochron with little scatter in spite of their obvious sedimentary origin. The isochron age is distinctly older than the previous formations although when the errors are extended to \pm two standard deviations it does overlap the Nashoba Formation and the Tadmuck Brook Schist in age.

The initial ratio is similar to that of the Nashoba Formation and at \pm 2 standard deviations the Worcester and Tadmuck Brook Schist initial ratios overlap. However, since the number of points is limited it is difficult to tell whether

TABLE 17

Rb-Sr Results for the Worcester Formation

<u>Sample</u>	<u>Rb, ppm</u>	<u>Sr, ppm</u>	<u>Rb⁸⁷/Sr⁸⁶</u>	<u>Sr⁸⁷/Sr⁸⁶</u>
R8391 ¹	118.1	159.9	2.109 ±.025	.72580 ±.00027
R8392 ²	120.8	74.03	4.669 ±.012	.74441 ±.00024
R8395 ³	85.73	179.1	1.358 ±.022	.72145 ±.00034
R8397 ²	201.7	117.8	4.933 ±.012	.74503 ±.00042

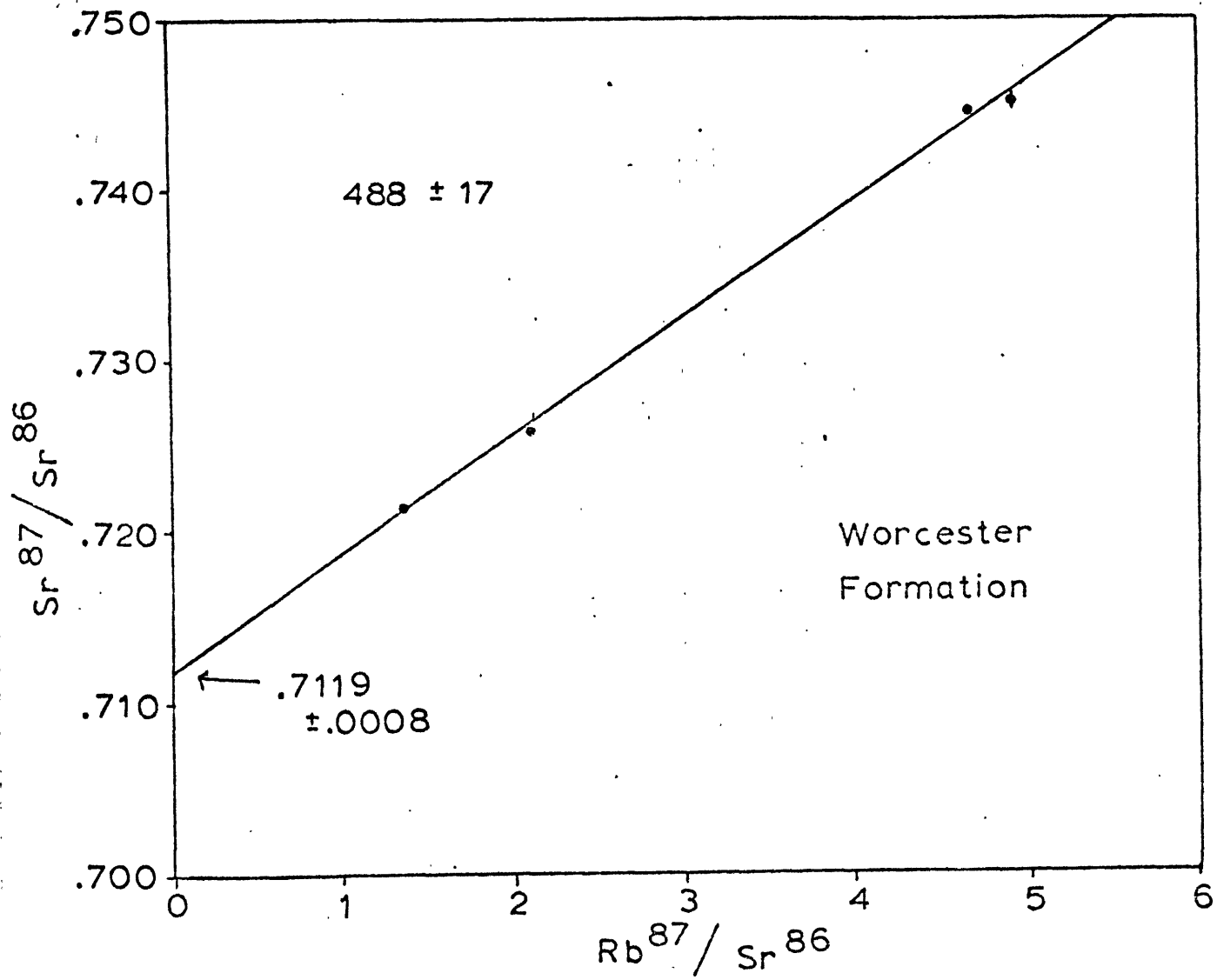
¹Unit 2 of Peck, 1976.

²Unit 3 of Peck, 1976.

³Unit 5 of Peck, 1976.

Figure 23

Rb^{87}/Sr^{86} versus Sr^{87}/Sr^{86} plot of whole rock samples from the Worcester Formation. Solid line is the best fit regression isochron.



the high quality of this line is real or merely coincidental.

Shawsheen Gneiss - Five samples:

R8399, R8401: Fine grained grey to black quartz-feldspar-biotite-calc-silicate gneiss, with significant amounts of epidote. R8401 is somewhat coarser grained and contains less epidote than R8399.

R8402-R8403: Dark quartz-feldspar-biotite-muscovite gneiss of medium grain with occasional lenses of quartz. R8403 contains almost no muscovite and much less biotite than R8402.

R8453: Described in Chapter 6.

Isotopic results are shown in Table 18 and plotted in Figure 24.

As the isochron plot shows, there is a great deal of scatter in the data, and for this reason regression lines were not calculated. Reference isochrons have been drawn on Figure 24 at initial ratios of 0.705 and 0.710 to suggest possible ranges of age. Since the formations already discussed generally tend to agree in age (400-500 m.y.), we might expect the Shawsheen Gneiss to give an age in the same range if the scatter was less. This implies that the initial ratio is between 0.705 and 0.710, probably closer to 0.707. This suggests that the Shawsheen Gneiss is more closely related to the Fishbrook Gneiss in terms of initial ratio.

There does not appear to be any strong correlation of the positions of the points with rock type or geographic

TABLE 18

Rb-Sr Results for the Shawsheen Gneiss

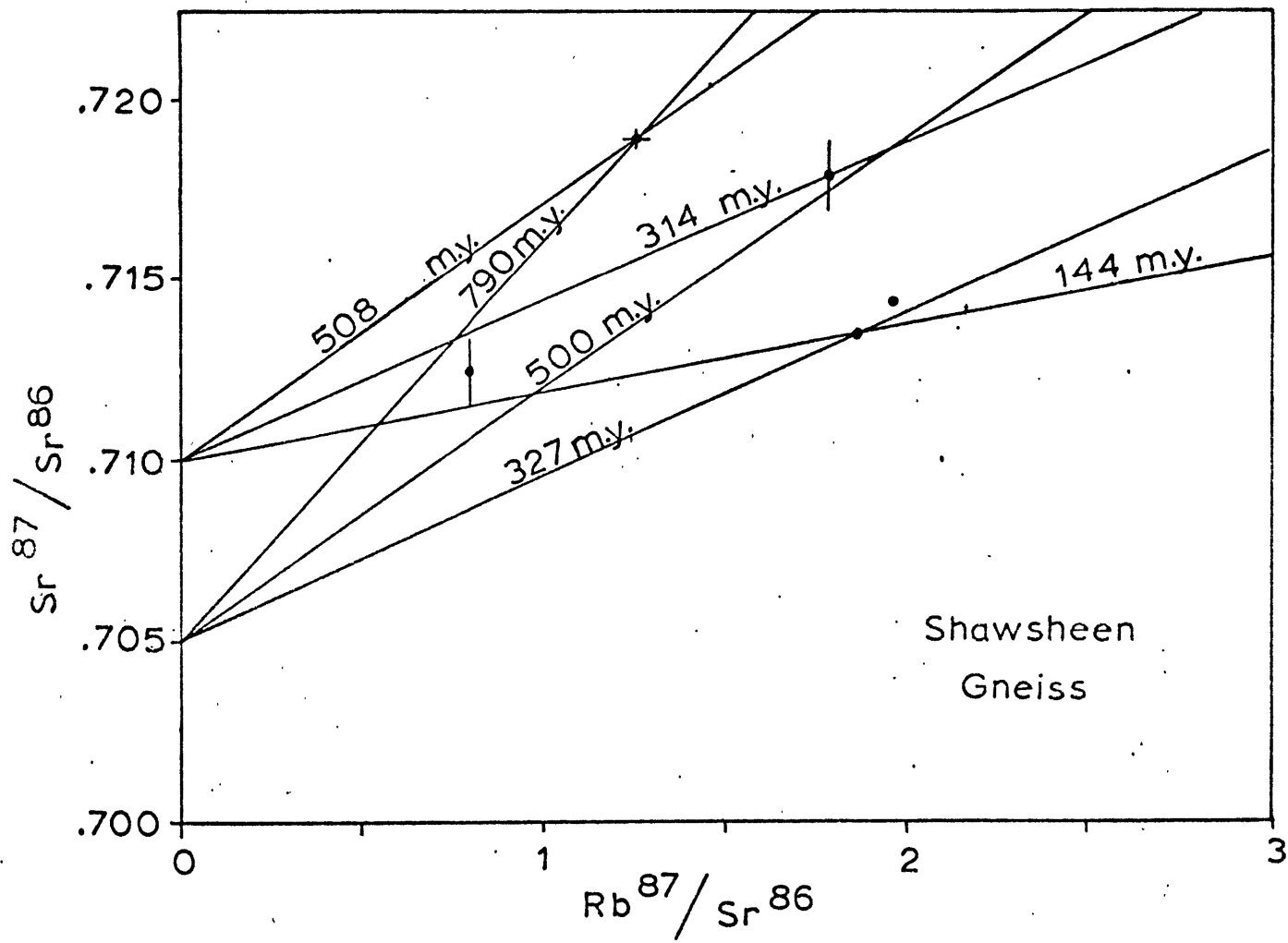
<u>Sample</u>	<u>Rb, ppm</u>	<u>Sr, ppm</u>	<u>Rb⁸⁷/Sr⁸⁶</u>	<u>Sr⁸⁷/Sr⁸⁶</u>
R8399	192.7	280.5	1.971 ±.005	.71435 ±.00005
R8401	178.1	273.1	1.865 ±.048	.71350 ±.00010
R8402 ¹	91.67	207.2	1.264 ±.041	.71895 ±.00030
R8403	68.29	238.8	0.8010±.0052	.71237 ±.00099
R8453 ²	97.40	155.6	1.781 ±.008	.71778 ±.00100

¹Composite of two replicates; see Appendix A.

²Sample provided by D. Alvord.

Figure 24

Rb^{87}/Sr^{86} versus Sr^{87}/Sr^{86} plot of whole rock samples from the Shawsheen Gneiss. Solid lines are model isochrons based on assumed initial ratios of 0.705 and 0.710.



locality, although the point with the highest $\text{Sr}^{87}/\text{Sr}^{86}$ ratio also has a high content of muscovite.

Middlesex Fells Volcanic Complex - Data for this formation came from four samples:

R8422: Light colored coarse grained, porphyritic, agglomerate facies with very fine grained matrix. Phenocrysts are feldspar and unidentified mafic minerals.

R8428-R8429: Very fine grained grey intermediate facies, no observable mineralogy.

R8450: Light colored fine grained felsic (?) facies, no observable mineralogy.

Data are given in Table 19 and plotted in Figure 25.

Again the data are very scattered and show no useful trends. No regression lines were calculated but reference isochrons with an initial ratio of 0.705 are shown for each point. In the case of the Middlesex Fells points as well as the other formations which show large scatter it is not possible to determine whether the scatter is due to weathering, metamorphism, or inherent in the rocks themselves. Evidence presented below suggests all three effects.

Interpretation of Results

An interesting aspect of the data presented above is that there appears to be a difference in initial ratios between the Fishbrook Gneiss, Shawsheen Gneiss and Middlesex Fells Volcanic Complex on the one hand, and the Nashoba For-

TABLE 19

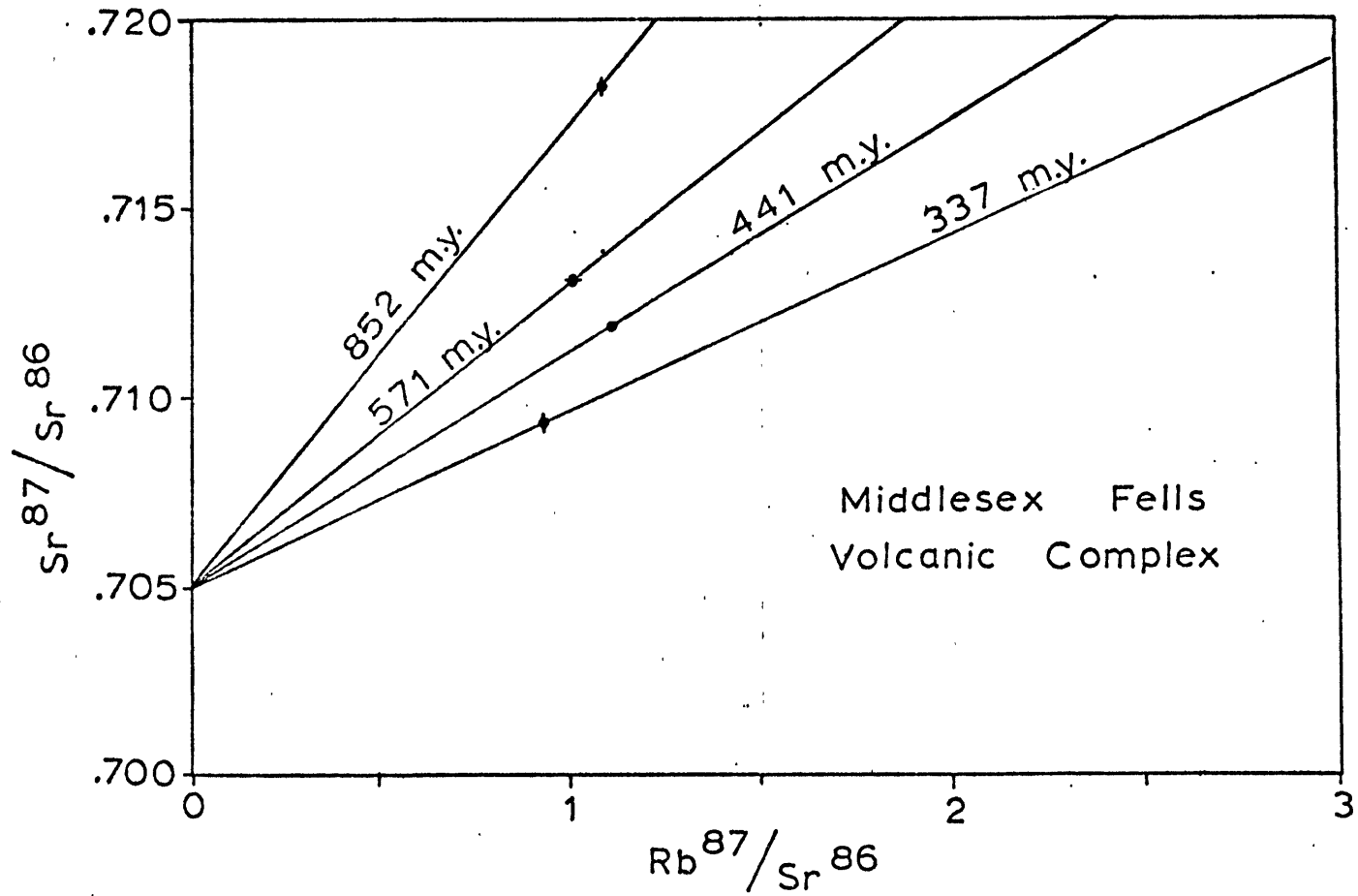
Rb-Sr Results for the Middlesex Fells Volcanic Complex

<u>Sample</u>	<u>Rb, ppm</u>	<u>Sr, ppm</u>	<u>Rb⁸⁷/Sr⁸⁶</u>	<u>Sr⁸⁷/Sr⁸⁶</u>
R8422 ¹	79.55	222.8	1.007 ±.016	.71303 ±.00003
R8428	22.90	69.00	0.9297±.0019	.70937 ±.00029
R8429	28.67	72.61	1.106 ±.002	.71182 ±.00019
R8450	95.66	248.6	1.094 ±.003	.71818 ±.00024

¹Composite of two replicates; see Appendix A.

Figure 25

$\text{Rb}^{87}/\text{Sr}^{86}$ versus $\text{Sr}^{87}/\text{Sr}^{86}$ plot of whole rock samples from the Middlesex Fells Volcanic Complex. A model isochron for each point is shown based on an assumed initial ratio of $\text{Sr}^{87}/\text{Sr}^{86}$ of 0.705.



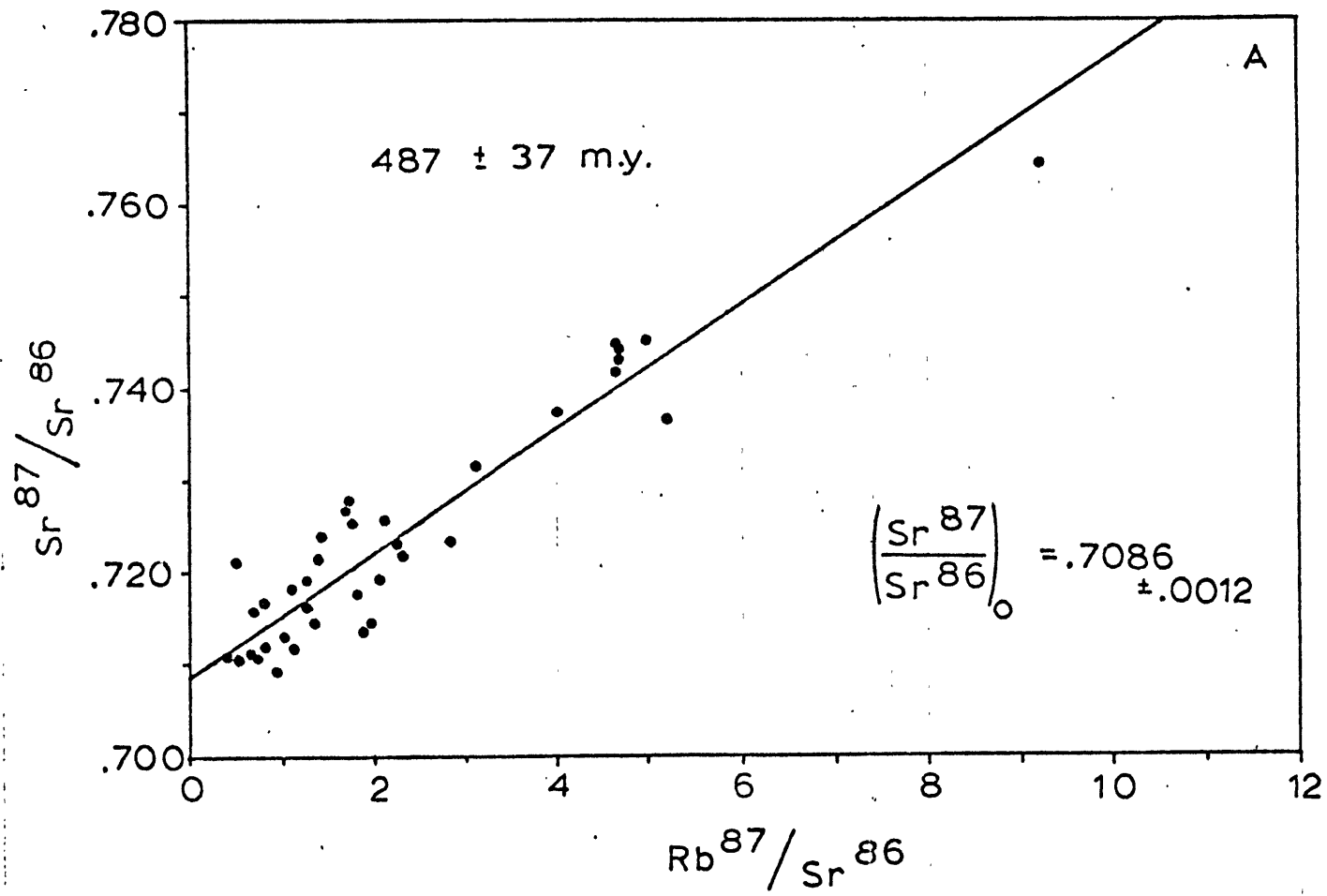
mation, Worcester Formation, and Tadmuck Brook Schist on the other. The former have initial ratios that probably range between 0.705 and 0.709 while the latter have initial ratios of 0.711 or larger. This dichotomy in initial ratios becomes more pronounced when we plot all of the data together on a single plot. Figure 26A shows such a plot as well as the best fit isochron for the points. It can readily be seen that the points fall into two groups above and below the line with very few points falling on or near the line, even within the errors attached to individual points. In fact, even when the errors for individual points are extended to two standard deviations very few points overlap the best fit line. It appears as if there are two separate trends in the data; both have similar slopes and thus similar ages but have significantly different initial ratios. This bimodal distribution is strongly revealed when initial ratios for each point are calculated using the slope of the best fit line of Figure 26A. When the initial ratios are plotted as a histogram of number of points within successive 0.002 increments in initial ratio, starting at 0.700, we get the results shown in Figure 26B. There are two distinct peaks in the data, one at 0.707, the other at 0.711, with a sharp gap between the two, although above and below these peaks the ratios drop off more gradually. These peaks still remain when the errors in the initial ratios are considered, although the peaks become smaller, wider, and less clearly separated.

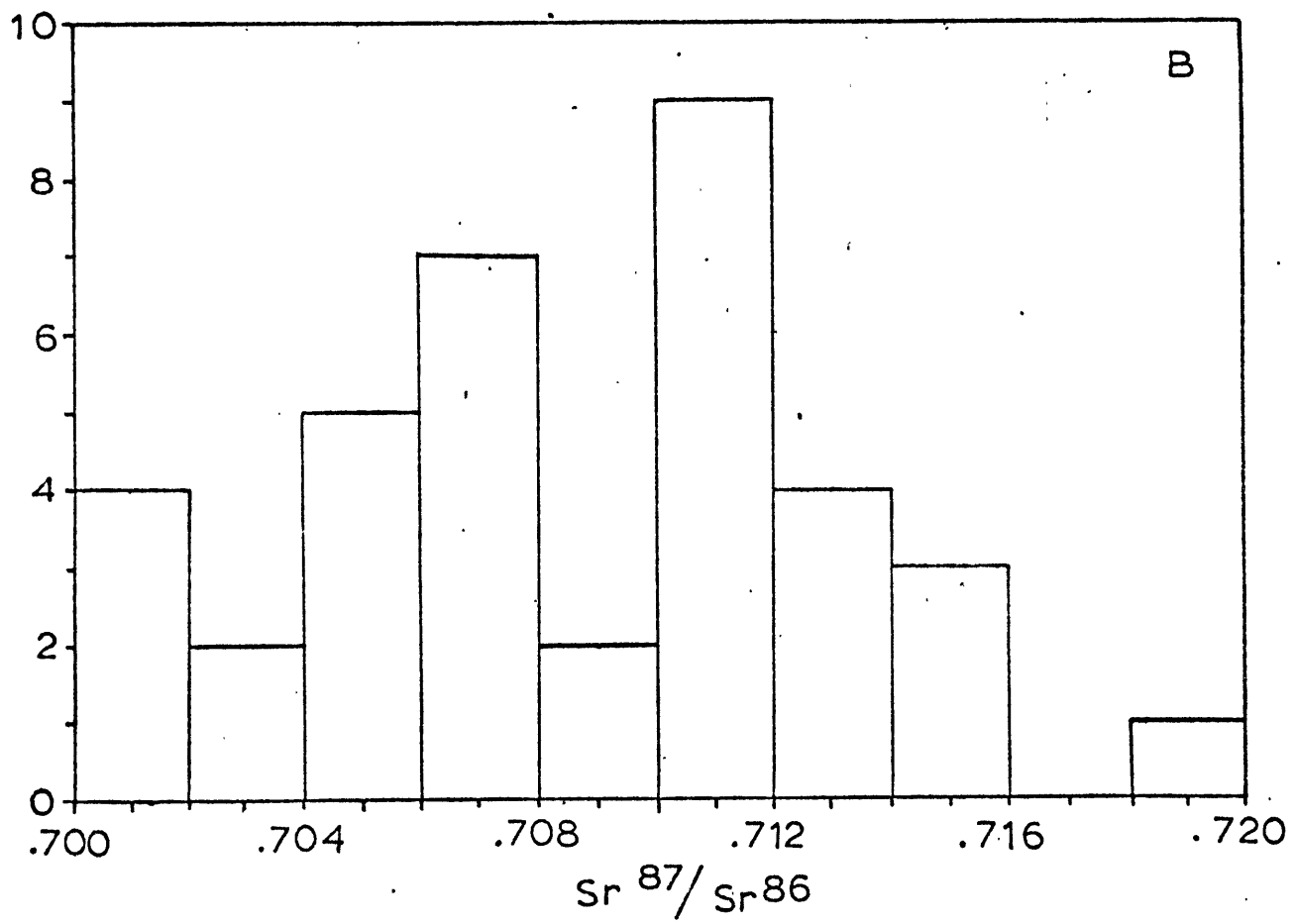
Figure 26A

$\text{Rb}^{87}/\text{Sr}^{86}$ versus $\text{Sr}^{87}/\text{Sr}^{86}$ plot of all the whole rock samples used in this paper. Solid line is the best fit regression isochron.

Figure 26B

Histogram of initial ratios for the points in Figure 26A based on an assumed isochron for each point with the same slope as that shown in Figure 26A.





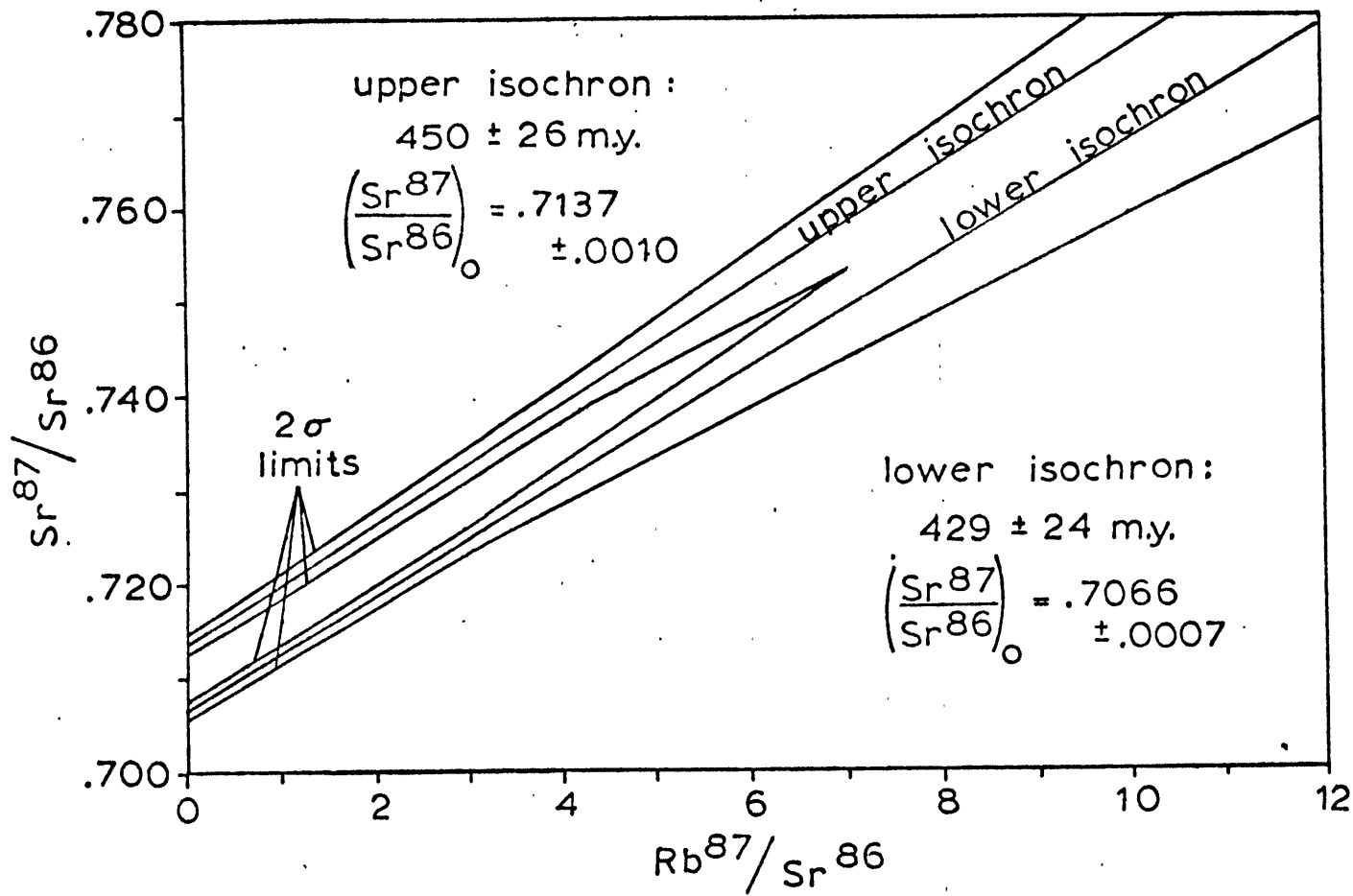
If we separate the points into two groups - those above the best fit line of Figure 26A and those below - the two groups are composed of the following points:

<u>Upper group</u>	<u>Lower group</u>
R8383	R8399
R8454	R8401
R8455	R8403
R8456	R8453
R8391	R8381
R8392	R8457
R8395	R8461
R8397	R8404
R8402	R8405
R8311	R8406
R8380	R8434
R8382	R8435
R8458	R8441
R8459	R8444
R8460	R8445
R8462	R8446
R8443	R8422
R8450	R8428
	R8429

Regressions were calculated for each of these groups. The results are shown in Figure 27. Individual points are not plotted but the two standard deviation error limits of the mean for each line are shown. The similar ages but different initial ratios are readily seen. Although the lower isochron appears slightly younger the errors are such that the ages overlap down to 0.42 standard deviations of the mean, whereas the initial ratios do not overlap until 4.2 standard deviations. The slightly younger age of the lower line may also be explained by the fact that its slope is determined to a great extent by two points (R8457, R8445).

Figure 27

Best fit regression isochrons for the two groups of points defined by the isochron in Figure 26A. Also shown are the 2σ mean limits of both lines and the ages and intercepts of both lines with 1σ of the mean errors.



Since weathering tends to lower the ages of samples (Bottino and Fullagar, 1968) by loss of Sr or selective loss of radiogenic Sr^{87} from Rb-rich minerals, samples with high $\text{Rb}^{87}/\text{Sr}^{86}$ ratios are bound to show the greatest effects from weathering. Both R8457 and R8445 are among the four samples showing the lowest initial ratios in the histogram of Figure 26B. When these two points are removed and a new regression calculated, an age of 495 m.y. and initial ratio of 0.7053 result. Although now older than the upper isochron, removing R8457 and R8445 just about doubles the errors in age and intercept of the new line. So either way the ages still overlap significantly while the initial ratios remain significantly different. In addition, when R8443 is left out of the upper isochron (it has the largest residual), the new regression line gives an age of 480 m.y. and an intercept of 0.7124, further indicating the similarity in age and difference in initial ratio. Thus an average age about 487 m.y., close to that given by the best fit isochron of Figure 26A, seems reasonable for both isochrons. Initial ratios of 0.7124 and 0.7053 are then assigned to the upper and lower isochrons respectively.

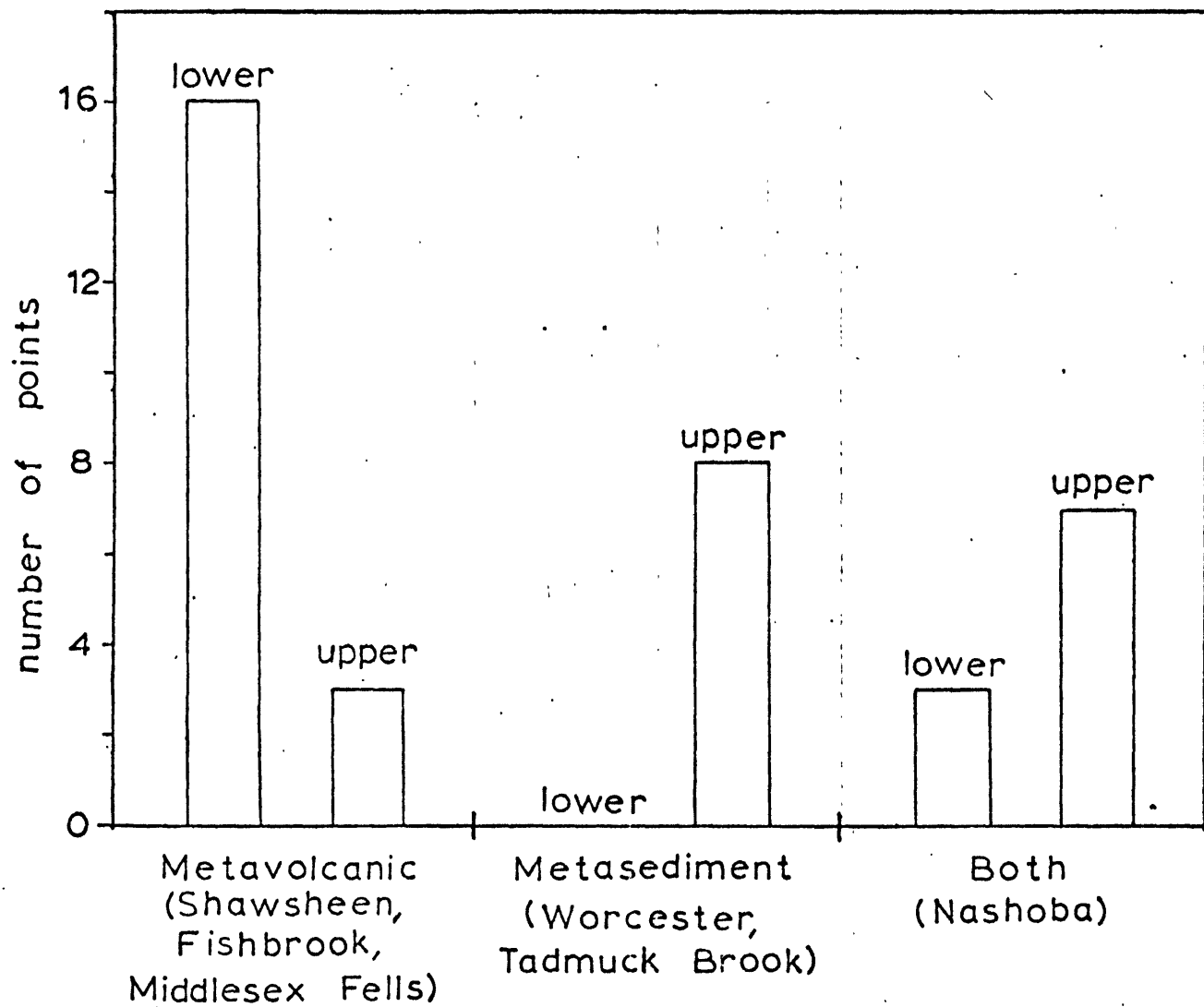
Having established that there are two separate isochrons we must determine what they represent. One obvious correlation which was established above is that certain formations are confined to one isochron or the other. The Fishbrook Gneiss, Shawsheen Gneiss, and Middlesex Fells Volcanic Com-

plex are almost totally on the lower isochron, while the Worcester Formation and Tadmuck Brook Schist are completely on the upper isochron and the Nashoba Formation is split between the two but with most of the points on the upper isochron. According to the work of Bell and Alvord (1976), Abu-Moustafa and Skehan (1976), Skehan and Abu-Moustafa (1976), and Peck (1976), the Fishbrook Gneiss, Shawsheen Gneiss, and Middlesex Fells Volcanic Complex are dominantly volcanic or volcanoclastic material; the Tadmuck Brook Schist and the Worcester Formation are mainly terrigenous sediments, while the Nashoba Formation is probably both although terrigenous sediments dominate. Figure 28 shows a histogram of the number of points on each isochron from volcanic, sedimentary, and Nashoba samples. There appears to be a strong correlation between protolith of the metamorphic rock and the initial ratio. This correlation fits with what would be expected in general concerning the behavior of these broad rock types. The metasediments, because their source area is bound to be older and have high $\text{Sr}^{87}/\text{Sr}^{86}$ values, will have a higher initial ratio in agreement with the value of 0.714 shown in Figure 27.

This separation into two isochrons is also similar to the results found in thin-slice Rb-Sr whole rock analyses (Montgomery et al., 1977) where equilibration of strontium isotopes occurs over distances of a few centimeters or larger. Different equilibrated domains give separate isochrons de-

Figure 28

Histograms of the number of whole rock Rb-Sr analyses that fall on the upper and lower isochrons of Figure 27 versus the probable protoliths for the formations from which the samples were taken.



pending on the average $\text{Sr}^{87}/\text{Sr}^{86}$ ratio of the domain. If such a process is at work here, then strontium isotopic equilibration over larger distances (i.e. 0.5 meters or greater) is indicated. This aspect will be discussed in greater detail below.

The question of what these isochron ages mean must still be answered. It is highly unlikely that they represent true ages of deposition although Rb-Sr dating of sediments has met with limited success (Whitney et al., 1961; Whitney and Hurley, 1964; Cordani et al., 1976). The high grade of metamorphism of many samples, the agreement between samples of varying lithology, geography and metamorphic grade, the similarity in ages between the stratified rocks, the intrusive rocks and a period of major metamorphism (see Chapter 4), and most importantly of all the evidence from the zircon analyses (Chapter 6) which gives an older age for the section all imply that the Rb-Sr isochrons represent reset isochrons. The evidence of Gebauer and Grünenfelder (1974, 1976) indicates that sediments can be easily reset during diagenesis and low grade metamorphism and are more likely to record a period of major metamorphism rather than a depositional age although with much scatter due to inherited radiogenic Sr^{87} and the effects of later metamorphism. Volcanics have always been controversial when Rb-Sr whole rock techniques have been applied to them (Brookins, 1976; Naylor, 1976). Their usual fine grain size and the high content of

glasses in volcanics makes them susceptible to loss of Rb and Sr. They may not become closed Rb-Sr systems until recrystallized by a metamorphic event.

The exact method of resetting can probably not be determined even with a more detailed petrographic and isotopic study, but a number of models can be suggested. In the following models a number of assumptions are made. First, the entire sequence is assumed to be 742 ± 92 m.y. in age based on the zircon data. Next, the sequence is assumed to be essentially continuous (also based on zircon data and the work of Bell and Alvord (1976)), although their present relative positions may be significantly different than they were when first deposited because of faulting and folding which is often significant (see Chapter 3). Third, when deposited the rocks did not have a spread of Rb^{87}/Sr^{86} ratios greater than presently seen (0-10) and in fact it was probably less (0-5). Fourth, although mixing of sediments and volcanics is probably widespread, it is probably only significant locally and in general sediments and volcanics retained their individual characteristics during deposition. Lastly, the present differences between the two isochrons are the result of pre-metamorphic differences in the rock rather than the result of some metamorphic effect. This is reasonable since metamorphism would tend to homogenize and smear isotopic differences rather than establish them.

Four models of resetting are proposed:

Model 1 - In this model we assume that Sr isotope equilibrium has occurred over a large distance on the order of the size of formations or larger. This would explain why samples from widely different parts of the same formation agree (Jäger, 1970), but it does not explain why individual formations have not equilibrated with one another. This can be explained by the many large and small scale faults recognized and inferred for the area (Barosh et al., 1977). The number of unrecognized small faults and shears may be even larger. The faults and shears would be responsible for juxtaposing rocks which have not equilibrated with one another because they were once more widely separated. However, this just returns us to the problem of why samples from different parts of the same formation agree but occasionally samples from the same outcrops do not.

Model 2 - In this case Sr isotopic homogenization occurred over a much smaller distance on the order of hand sample size. In addition it is assumed that Rb^{87}/Sr^{86} ratios prior to metamorphism were more restricted than at present (± 0.5 around the average). The present range of Rb^{87}/Sr^{86} values would be the result of metamorphic differentiation. In other words just prior to metamorphism all the volcanics would have a roughly similar Rb^{87}/Sr^{86} ratio of approximately 1.4 and thus have a similar Sr^{87}/Sr^{86} ratio of approximately 0.705. The same can be said for the sediments but their Rb^{87}/Sr^{86} ratio would be somewhat higher (2.2) and their

$\text{Sr}^{87}/\text{Sr}^{86}$ ratio would be higher (0.713). Metamorphism would spread out the $\text{Rb}^{87}/\text{Sr}^{86}$ ratios and cause some Sr isotopic homogenization but since the isotopic differences within a formation were small to begin with, the now variable Rb/Sr values would be starting from roughly the same $\text{Sr}^{87}/\text{Sr}^{86}$ ratios. Since isotopic homogenization occurred only over hand sample distances, locally variations in Rb/Sr and in $\text{Sr}^{87}/\text{Sr}^{86}$ would be retained. This explains why most samples from the same formation are in agreement but why anomalies occur. It also explains the results from the Nashoba Formation which is the most heterogeneous of the units. Against this model is the fact that it assumes special conditions about the Rb/Sr and $\text{Sr}^{87}/\text{Sr}^{86}$ ratios at the time of deposition. This may be a sampling problem but the chemistry of the volcanics (mafic and intermediate for the most part) implies a small range of Rb/Sr values, and the natural mixing of detritus in a sedimentary environment would make a small range in Rb/Sr value likely in a sediment.

Model 3 - Here I assume that not only were the Rb/Sr ratios limited in range but were also very low in value (<1). As a result between 740 and 490 m.y. no significant amount of radiogenic Sr was produced. At the time of metamorphism, significant quantities of Rb were introduced from outside producing a variation in $\text{Rb}^{87}/\text{Sr}^{86}$ ratios. Thus the present initial ratios are essentially the same as those at the time of deposition and later metamorphism. Evidence for this

model is that the initial ratio of the volcanics is similar to that of many of the nearby Late Precambrian plutons (see Chapter 4) suggesting a similar origin and relationship. Also, the numerous aplite dikes, pegmatite veins and quartzofeldspathic veins which are intimately related with the stratified rocks would provide a vehicle for the introduction of Rb (Jäger, 1970). This would also explain why the initial ratios of the two groups of rocks have been retained, since little isotopic homogenization is needed to explain the observed results. Against this model is the fact that it implies input of massive amounts of Rb. The only source of Rb would be the plutonic rocks which intrude the section, but many of these are calc-alkaline intermediate rocks with low contents of Rb (< 200 ppm). Also the Worcester Formation, Tadmuck Brook Schist and Middlesex Fells Volcanic Complex show fewer signs of intrusion of igneous material than the other formations, but even the Fishbrook Gneiss which shows significant signs of intrusion of igneous material has a Rb content under 70 ppm.

Model 4 - This model is similar to Model 3 but instead of an input of Rb, the igneous intrusions supply a source of Sr with low initial ratio (about 0.705). Isotopic exchange with the Sr of the stratified rocks would lower the $\text{Sr}^{87}/\text{Sr}^{86}$ ratios of the stratified rocks especially those with higher $\text{Rb}^{87}/\text{Sr}^{86}$ ratios. As a result the ages would be lowered as would the initial ratios. Evidence for this is that many of

the intrusive rocks are rich in Sr. But against it are many of the disadvantages of Model 3 especially that some localities show few effects of igneous intrusion (especially in the Worcester Formation). In addition this process is likely to smear and homogenize the differences between the initial ratios.

Of these models I think the evidence and assumptions favor Model 2 or possibly a combination of Models 2 and 3. Model 2 tends to be simpler and does not involve long distance transport of Rb and Sr and chemical or isotopic equilibration over large distances. Models 2 and 3 also have the advantage that they are less likely to destroy the original difference in initial ratio. There is also the possibility that all four models have worked to one extent or another locally contributing to the observed scatter.

Pre-Metamorphic History

If Model 2 was the main process of resetting it allows us to make some rough estimate of pre-metamorphic $\text{Sr}^{87}/\text{Sr}^{86}$ ratios. Assuming the zircon age of 740 m.y. is correct and that the major period of metamorphism which reset the Rb-Sr systems began about 487 m.y. (from Figure 26A), if we take the present initial ratio of 0.7053 (without R8457 and R8445) for the volcanics as the average ratio 487 m.y. ago we can calculate the $\text{Sr}^{87}/\text{Sr}^{86}$ ratio at 740 m.y. Using the average $\text{Rb}^{87}/\text{Sr}^{86}$ ratio of 1.4 gives a $\text{Sr}^{87}/\text{Sr}^{86}$ ratio at 740 m.y.

of 0.7003. Two standard deviations increase (833 m.y.) in the zircon age even with a similar increase in the Rb-Sr age leads to ridiculously low ratios (< 0.700). Two standard deviations lower in the zircon ages (651 m.y.) gives an initial ratio of 0.7021. The possibility exists that the ratio of 0.7053 may be slightly low, as Figure 27 shows a value around 0.706-0.707 which may be more accurate. Taking all the errors into account a wide range in $\text{Sr}^{87}/\text{Sr}^{86}$ ratios occurs - 0.697 to 0.705 - but a value somewhere between 0.701 and 0.703 seems most probable. The major problem is that sampling necessities lead to a higher estimate of $\text{Rb}^{87}/\text{Sr}^{86}$ ratios than is true for the volcanics as a whole since mafic volcanics were avoided.

Even so, Models 2 and 3 suggest a subsialic source for the volcanics because of the low $\text{Sr}^{87}/\text{Sr}^{86}$ ratios (Faure and Hurley, 1963; Faure and Powell, 1972). Model 3 suggests slightly higher initial ratios which imply a source somewhat richer in Rb than upper mantle material. An oceanic basalt source or continental contamination are two possibilities. Slightly higher initial ratios seem to be common for continental volcanics (Hurley et al., 1965; Faure and Powell, 1972). The lower initial ratios obtained from Model 2 suggest an upper mantle source (Faure and Powell, 1972; Hurley et al., 1965; Faure and Hurley, 1963).

The same analysis carried out for the metasediments suggests a range from 0.700 to 0.710. Since values below 0.706

are unlikely for sediments of terrigenous origin (Hurley et al., 1965; Cordani et al., 1976) the most probable values for the sediment initial ratios are 0.706 to 0.710, but the possibility of admixed volcanic material lowering the initial ratio is possible. This range of values does cover the values for sea water that might be expected even at that time (Peterman et al., 1970; Faure and Powell, 1972; Veizer and Compston, 1974, 1976). Sampling biases also suggest that the average $\text{Rb}^{87}/\text{Sr}^{86}$ used may be too high.

As far as the metamorphism is concerned, the Rb-Sr data indicate a significant metamorphic event between 490 and 400 m.y. ago with a more probable range between 480 and 450 m.y. The complete resetting of the Rb-Sr whole-rock systems while the zircons show mainly the effects of later metamorphism suggests that these later metamorphisms were much different in character. They were mainly thermal events, lacking significant amounts of igneous intrusion, mobile fluid phase or important redistribution of major elements. A fluid phase appears to be very important in the diffusion of Rb and Sr (Hoffman and Giletti, 1970; Jäger, 1970; Lancelot et al., 1976). This agrees with geological data (Bell and Alvord, 1976) and isotopic evidence (Zartman et al., 1970; Zartman and Marvin, 1971; Naylor, 1976). As a result the Rb-Sr systems remained essentially closed during later metamorphic episodes except possibly for the introduction of some scatter. A similar situation was found by Jäger (1970) in the Alps,

and by Lancelot et al. (1976) in Africa.

Chapter 8

Microbomb Analyses

Introduction

Because of the possibility of more than one population of zircons existing in the detrital suite described in Chapter 6 as well as mixing of detrital and volcanic zircons and because of the low yields and small zircon samples that resulted from the zircon separation, an attempt was made to analyze small zircon samples using the single zircon technique of Lancelot et al (1973, 1976). A number of problems prevented the work from being completed. As a result no analyses of the detrital zircons were made but two analyses of zircons from the Fishbrook Gneiss yielded results in good agreement with the samples analyzed using the Krogh (1973) method. For this reason it is believed the procedure outlined below is useful for small (about 0.5 mg) zircon samples, which can easily and rapidly be hand picked, and which have small amounts of lead (less than 100 ppm).

Initial Experiments

Two problems became apparent almost instantly: contamination and detectability. The blanks for the reagents given in Appendix B are too high to be useful for the small amounts of lead that were encountered (< 30 ng). A second step of two-bottle subboiling distillation (Mattinson, 1971, 1972)

appeared to solve the problem for HF, HCl and HNO₃. Blanks for these reagents showed non-detectable levels of lead after the second distillation step. Taking into account errors in measurement this indicates that the lead content of these reagents is less than 0.1 ppb. As noted in Appendix B the H₂O and H₃PO₄ used are already clean enough. The major contamination problem, however, came from the silica gel used for loading the lead sample on the rhenium filament according to the method of Cameron et al (1969). The silica gel used for the Krogh (1973) technique had a blank (about 400 ppb) usable for that technique but definitely not usable for the microbomb technique. Preparation of new silica gel with various types of washing in ultrapure H₂O and HCl did not significantly improve the blank of the silica gel. Attempts were made to run the lead in the spectrometer without silica gel but it was found that the sample burned off much too quickly and peak heights were low. Even a very small amount of silica gel was found to improve peak heights by a factor of two and run times by a factor of five. Finally it was decided to dilute the silica gel used for the Krogh method to one-half its usual concentration with ultrapure H₂O. This reduced the contamination somewhat without diluting the silica gel to an unusable concentration.

As outlined in Appendix A, the mass spectrometer used in this study is outfitted with a vibrating reed electrometer to detect and amplify the signal from the Faraday cup at the

detector end of the spectrometer. Although such a device has a theoretical detectability of 10^{-17} amps, signal-to-noise and response time considerations limit the lowest usable signal to about 10^{-14} amp for the largest peak in a mass spectrum. Tests made by running known but variable amounts of standard lead (NBS 983) indicate a lower limit of 1 ng can be run with any degree of success. This 1 ng is the amount of lead directly loaded on the filament. Taking into account run-time considerations (at least 1 hour is needed), signal-to-noise considerations and the necessity of keeping contamination corrections low, 5 ng directly loaded onto the filament is more reasonable and 10 ng is preferred. Since twice this much is needed for a complete analysis of a spiked and unspiked aliquot and since the microbomb will not handle more than 1 mg of zircon, we are thus limited to zircons of 20 ppm lead concentration or greater. But this does represent an improvement since the Krogh technique as practiced in this laboratory would require at least 5 mg of zircons to be useful at that lead concentration level, because of the large loading blanks. The modifications made to the Krogh technique for this study (Appendix B) allow 2-3 mg to be used at that concentration level, although 1 mg samples may be used if higher contamination corrections are deemed acceptable.

Procedure

Zircons were separated and cleaned as outlined in Chapter

6 and Appendix B. Zircons were then hand picked; attention was paid to picking zircons that were similar in shape, size and color to obtain a sample as close to a single population as possible. The number of zircons picked was variable but 50 to 75 zircons of +200 mesh size usually insured a sample weight of 0.5 mg or higher.

After picking the zircons were washed in ultrapure H_2O , dried and weighed on an electronic microbalance. Samples were then placed in the Teflon capsules of the microbombs. For a description of the microbombs, see Hull (1976). Twice distilled 48% HF was then added (0.04 ml) with a 0.01 ml micro-pipette which was used to input and extract all reagents from the microbomb. The plastic pipette tips were rinsed with ultrapure H_2O between each use, except for the pipette used to load the samples onto the filament. Here a new pipette tip was used for each sample load. These tips were cleaned in a similar manner to those used for the Krogh method. Liquid input to the capsule from the pipette was done by depositing the reagent against the upper portion of the walls of the capsule's working volume. The pipette was never allowed to come into contact with the sample or liquid at the bottom of the capsule except when an aliquot was removed for mass spectrometry. All input and output of reagents was done in a laminar flow hood equipped with ultrapurity filters.

After adding the HF, the bombs were sealed and heated at 250°C for 48 hours in a drying oven. The bombs were then

removed, allowed to cool and then opened. Microscopic examination of the liquid revealed no remaining solids in all the samples that were examined (5 out of 10 samples prepared). The remaining HF was evaporated off under a heat lamp in the laminar flow hood. After the HF was completely evaporated, 0.04 ml of double distilled 3.1 N HCl was added and evaporated to take up any insoluble fluorides. After the HCl is evaporated, 0.02 ml of double distilled concentrated HNO₃ is added and evaporated off. The HNO₃ is added because it was found that loading the sample as a nitrate seemed to improve peak heights by as much as a factor of two. Cameron et al. (1969) also used an aqueous nitrate solution for loading the lead for their silica gel technique. The author believes this increase in efficiency is due to increased solubility of the nitrates of most metals relative to their chlorides and phosphates (developed when adding phosphoric acid). Thus when an aliquot of the sample is removed more is dissolved in the liquid than if it was taken up as a chloride in phosphoric acid as is done in the Krogh method. These problems with insoluble compounds are further discussed in Appendix B.

After the nitric acid is evaporated, 0.02 ml of ultrapure H₂O is added and the capsule is warmed under a heat lamp with the top of the capsule on to avoid evaporation. Then 0.01 ml of the liquid is removed with a micropipette. In this was a rough 1:1 aliquoting of the sample is done which allows a calculation of the total amount of Pb and U to be done although

this is not necessary to obtain a Concordia point. The 0.01 ml of liquid removed is loaded onto a filament (already loaded with 0.01 ml of dilute silica gel), dried and 0.01 ml of 0.5 N H_3PO_4 is loaded on top of this and dried. This is run in the spectrometer to obtain $\text{Pb}^{208}/\text{Pb}^{206}$, $\text{Pb}^{207}/\text{Pb}^{206}$, and $\text{Pb}^{204}/\text{Pb}^{206}$ ratios.

The remaining liquid portion is weighed in the capsule and 0.1 ml of dilute mixed spike (Pb^{208} and U^{235}) is added and weighed. The spikes were prepared by diluting the more concentrated spikes used in the larger bombs to 1/50 to the concentrated values. The two spikes (Pb^{208} and U^{235}) were then mixed together to form a composite spike. These were calibrated in the same manner as the concentrated spikes in Appendix B using NBS 983 for lead and NBS 950a for uranium. The calibration of the spikes yielded the following data:

Dilute mixed spike -

$$\text{Pb}^{208} = 1.0946 \pm .0015 \times 10^{-9} \text{ moles/g}$$

$$\text{Pb}^{204}/\text{Pb}^{208} = 0.000037 \pm .000001$$

$$\text{Pb}^{206}/\text{Pb}^{208} = 0.010615 \pm .000075$$

$$\text{U}^{235} = 2.0916 \pm .0029 \times 10^{-10} \text{ moles/g}$$

$$\text{U}^{238}/\text{U}^{235} = 0.000830 \pm .000004$$

The concentration of the U^{235} is somewhat lower than needed; a concentration at or slightly above the concentration of the Pb^{208} would be more useful. Double distilled 3.1 N HCl is used to dilute the spikes.

The spike in the capsule is then taken down to dryness. Next 0.01 ml of the HNO_3 is added and again taken to dryness. Finally 0.01 ml of ultrapure H_2O is added, warmed and completely removed and loaded in a similar manner to the unspiked aliquot. Lead and uranium are run on the same filament, lead first because it comes off at a slightly lower temperature.

The procedure is essentially designed for rapid and efficient sample analysis by dispensing with lead and uranium separation and using a minimum of laboratory apparatus. Also, by keeping the sample in the Teflon capsule during all procedures and opening the capsule and transferring reagents only in a laminar flow hood, it is believed that environmental contamination is kept to a minimum.

Blanks

A number of procedure blanks were run by following the same procedure as outlined above but without a zircon sample. Because of the small amount of lead in the blank it was not possible to run an unspiked portion to obtain the isotopic ratios of the contamination. What little data was obtained indicated that the contamination ratios are similar to those found for the larger bombs. For this reason the contamination ratios given in Appendix B were used to correct the microbomb analyses. Contamination in the two procedures may be different but probably not significantly different since the con-

tamination in both cases is coming principally from the same source, i.e. the silica gel.

Blanks ran poorly and the scatter in data was great, but averages suggest a total lead blank of 3 to 6 ng for the total procedure (spiked and unspiked aliquots). Uranium blanks were not run since blanks run for the larger bombs suggest insignificant amounts of U contamination.

Microbomb Results

Ten zircon samples were dissolved in the microbombs and analyzed. However, because of unstable signals, inefficient ion production or unacceptable amounts of contamination, only two of the ten samples produced usable data. These two samples and their U-Pb results are shown in Table 20. Unfortunately both samples do not have good analyses done with the Krogh technique in order to make a useful comparison. Sample Z-1 1M -150+200 was analyzed using the large bombs but because of contamination was left out of all the Concordia plots and is included in Table 11. In fact it is the only one of the low-quality points that does not agree with the higher quality points from the same formation. Sample Z-1 5M is a very magnetic split which contained many zircons which could be easily hand picked for the microbombs. In both cases, the largest, clearest, most euhedral zircons were picked for analysis.

If the Pb^{207}/U^{235} and Pb^{206}/U^{238} ratios of Table 20 are

TABLE 20

Results of Microbomb Analyses

	Z-1 5M	Z-1 1M -150+200
Sample wt., mg	0.63	0.91
Pb ²⁰⁶ /Pb ²⁰⁴	180.1	221.1
Pb ²⁰⁷ /Pb ^{206*}	0.06041	0.06820
Pb ²⁰⁸ /Pb ^{206*}	0.08934	0.34223
Pb ^{radiogenic} _{total} , ng	58.8	30.0
Pb ^{contamination} _{total} , ng	24.7	8.2
Pb ^{radiogenic} _{total} , ppm	93.3	33.0
U _{total} , ppm	893.7	322.7
Pb ²⁰⁷ /U ²³⁵	.8798 ± .0453	.7914 ± .0178
Pb ²⁰⁶ /U ²³⁸	.1056 ± .0053	.0842 ± .0005
Apparent ages, m.y.:		
Pb ²⁰⁷ /U ²³⁵	641	592
Pb ²⁰⁶ /U ²³⁸	647	521
Pb ²⁰⁷ /Pb ²⁰⁶	618	876

*corrected for contamination

compared with the other Fishbrook Gneiss points of Table 3 and Figure 10, it can be seen that they agree quite well with the other Fishbrook Gneiss points. In keeping with the nature of the zircons chosen the points lie at the upper end of the Fishbrook Gneiss chord and further strengthen the late Precambrian age obtained from the points of Table 3.

Z-1 5M lies slightly above Concordia, although it is concordant within the errors quoted. This slight reverse discordance can be ascribed to two major effects. The first is non-equilibration of spike and sample, especially with regard to uranium. A similar problem was observed and discussed by Krogh (1973). A second problem is that the ratios for laboratory contamination are not adequately known for this technique. The errors quoted in Table 20 take this uncertainty into account as the errors attached to the contamination isotopic ratios found for the Krogh technique (Appendix B) were doubled for the correction of the microbomb samples.

Even though a much more thorough analysis and comparison between the two procedures is needed, the data shown above suggest that the procedure given in this chapter is usable. It allows rapid and efficient analyses of small amounts of carefully selected zircons to be carried out within reasonable limits of error. Some refinements, such as a clean silica gel and a better mass spectrometer detector system, would improve the procedure immensely.

Chapter 9

Interpretation of Results

The existence of a suite of volcanic zircons in the Fishbrook Gneiss, Shawsheen Gneiss and Middlesex Fells Volcanic Complex which agree quite closely and give an age of 742 ± 91 m.y. suggests that this is the age of deposition for most of the sequence studied. The conformable relationships between the Westboro and Middlesex Fells, between the Shawsheen and Fishbrook, and between the Fishbrook and Nashoba are further evidence that the sequence from the Westboro up to the Nashoba is probably a continuous stratigraphic sequence with only minor unconformities. This fits with the data from the detrital zircons which suggest that the Westboro and Shawsheen contain a similar although possibly not identical population of old (1.55 b.y.) zircons. The possibility exists that the Nashoba also contains a similar population. This is not definite but it would agree with interpretations based on the volcanics.

The agreement with the geologic data is good. The Westboro and Middlesex Fells are intruded by the late Precambrian Dedham Granodiorite which is probably not older than 620 m.y. Once the general continuity of the sequence is accepted it implies that most of the sequence is older than 620 m.y. which is in good agreement with both zircon suites. Whether the Tadmuck Brook Schist and rocks west of the Clinton-Newbury Fault Zone are of the same age is unknown. A significant un-

conformity may exist between the Tadmuck Brook and the Nashoba but for the moment I think it best to include the Tadmuck Brook Schist with the other units east of the Clinton-Newbury until more evidence is available. As for the rocks west of the Clinton-Newbury, the Rb-Sr data argue for an Ordovician or older age if we accept the Rb-Sr data as recording a metamorphic event. Such an assumption is quite reasonable considering that the rocks of the Worcester are mainly fine grained aluminous sediments which evidence indicates (Gebauer and Grünenfelder, 1974) are quite easily reset at low metamorphic grades. Based on the difference in strike and dip, metamorphic grade, different overall lithology and geographic position I am inclined to call the rocks to the west of the Clinton-Newbury Cambro-Ordovician in age. This agrees with the fact that they are intruded by the Ayer Granite, also of Ordovician age. This is compatible with the age assignment of Barosh et al. (1977) but is somewhat older than the age (Siluro-Devonian) assigned by Peck (1976). The rocks to the west of the fault zone represent a thick sequence of Cambrian to Ordovician terrigenous sediments, in fact the Merrimack Quartzite (Emerson, 1917) and other quartzites (Hepburn, 1976) which underlie the Worcester (Barosh et al., 1977) may represent basal Cambrian quartzites similar to those seen in other parts of New England.

The recognition of a large late Precambrian sequence of stratified rocks expands the area of Precambrian rocks recog-

nized in southeastern New England. Such ages had formerly been confined to intrusive rocks. To the south of this area the Westboro Quartzite and other rocks similar to those studied in this paper have been described by Nelson (1974) and correlated with rocks in Rhode Island (the Blackstone Group - Quinn, 1971) and Connecticut (Plainsfield and Quinnebaug Formations - Dixon, 1976; Goldsmith, 1976). If such correlations are correct they imply that most of the high grade metamorphic rocks east, southeast, and south of the Clinton - Newbury - Lake Char - Honey Hill Fault System are Late Precambrian. This indicates not only a significant period of Late Precambrian intrusive activity but also sedimentation and volcanism covering most of southeastern New England. The obvious conclusion is that the intrusive activity and sedimentation and volcanism are related; the massive intrusive bodies (Dedham, Milford, and Northbridge Granites) representing the later stage of eugeosynclinal development represented by the sediments and volcanics. This sequence may have been partially cratonized by the Cambrian since fossiliferous Cambrian shelf facies rocks are found in eastern Massachusetts which overlie the Dedham (Fairbairn *et al.*, 1967b) and the probable Cambro-Ordovician rocks of the Worcester are also a shallow water facies. But the evidence from the Rb-Sr data implies that these rocks were still undergoing significant metamorphism and intrusion in the Ordovician and thus were still part of the Appalachian orogenic system

at this time. Such repeated activity over an extended period of time seems to be characteristic of the Appalachians and other similar orogenic systems (Fairbairn and Hurley, 1970; Hurley, 1974).

Whether or not such late Precambrian rocks extend to the northwest is unknown but there is evidence to suggest they do. The Massabesic Gneiss near Manchester, New Hampshire is an ortho- and paragneiss formerly mapped with the Fitchburg Granite (Emerson, 1917) in the center of the Merrimack Synclinorium. Zircon ages (Bescanson et al., 1977) from the orthogneiss (which appears to intrude the paragneiss) give an age of 620 m.y. This age is based on a discordia line which is determined by a single zircon split with low Pb^{207}/U^{235} and Pb^{206}/U^{238} ratios which suggests recent Pb loss. The other points are too well grouped to form a good line without this single point but an older age does seem likely. In fact the field relations, lithologies, and positions of zircon points on the Concordia plot for the Massabesic Gneiss show a great similarity to the Shawsheen Gneiss - Fishbrook Gneiss part of the section covered in this report. Data are still too scanty to suggest a real correlation.

One interesting correlation is suggested by Rb-Sr whole rock ages obtained by Cormier (1969) on the Coldbrook Volcanics of New Brunswick. An extrusion age of 750 ± 80 m.y. was obtained for the volcanics. This is remarkably close to the

age obtained for the volcanics in this paper. Similarities of these volcanics with others in Maritime Canada (Fairbairn et al., 1966) mean that a significant period of late Precambrian volcanism and sedimentation is probably common to the entire eastern half of the northeastern Appalachians.

More definite correlations cannot be made, but the pattern from northeastern Massachusetts of a late Precambrian sequence of extrusives, intrusives and sediments overlain by shallow water Cambrian and Ordovician rocks is also seen in Newfoundland (Williams, 1964). The implication is that the eastern block probably extends from southern Connecticut through Rhode Island and eastern Massachusetts to Newfoundland. The limits to the northwest are unknown, but they may extend as far as the Bronson Hill Anticlinorium. The eastern block thus forms a single continuous tectonic unit distinct from the Precambrian rocks of western New England and of the western Appalachians in general. Such a conclusion has been reached by other authors based on other data (Wilson, 1966; Schenk, 1971).

Returning once again to more local aspects of the data, the recognition of a late Precambrian sequence of sediments and volcanics leads to the question of what was the basement on which these rocks were deposited. The remnants of gneisses and schists found by Bell and Alvord (1976) under the Westboro Formation hint at a possible older sialic basement. There is no evidence of an ensimatic basement.

The question of the basement for these rocks next leads to the question of the source area of the detrital zircons. The same problems which plagued the analysis of these zircons in Chapter 6 also plague any answer to this question. The major problem is the extent to which the detrital zircons represent a mixture of populations with different ages. The data as shown in Chapter 6 are ambiguous. The difference in trend between the Shawsheen Gneiss and Westboro Quartzite points and the large overall scatter suggest multiple populations, whereas similarity in resetting behavior and position of points on the Concordia diagram suggest a single population or well-mixed combination of populations. But for the purposes of discerning possible source areas only general age ranges are really needed since a source area of a single well defined age is highly unlikely. From the data presented in Chapter 6 a maximum range of ages for the source area of 1300 to 1900 m.y. is most likely. Significant amounts of zircons younger or older than this could easily be discerned except under special conditions which are highly unlikely.

This age range of 1300 to 1900 m.y. is not a common one for nearby old North American rocks (Stockwell, 1968). Ages in the range 1600 to 1800 m.y. are common for the Churchill Province of Canada (Stockwell, 1968), but its vast geographic distance and intervening large areas of older (Superior) and younger (Grenville) rocks makes it a highly unlikely source. Rocks in this range are common on other continents (Hurley

and Rand, 1969; Semenenko, 1970) but the consensus among many workers (Wilson, 1966; Bird and Dewey, 1970; Schenk, 1971) has been that Africa is the continent most likely to have been interacting with this part of North America at that time. This conclusion agrees with available paleomagnetic evidence (Schutts et al., 1976).

The age range given above is exactly the range of ages found in the Precambrian rocks of the Anti-Atlas of Morocco (Charlot, 1976; Hurley et al., 1976). Based on geological evidence (Schenk, 1971) and possible continental fits (Bullard, 1965), the Anti-Atlas would be the closest source of Precambrian material to this part of New England. An event of granite intrusion and mineral age resetting occurred in the Anti-Atlas from 1750 to 1500 m.y. (Charlot, 1976) where a significant unconformity occurs. In the west and central parts of the Anti-Atlas especially, a period of orogeny and granite and granodiorite intrusion occurred between 1550 and 1450 m.y. (Charlot, 1976; Schenk, 1971). The westernmost part of the Anti-Atlas would be the closest part of northwest Africa to this part of New England.

Further evidence comes from the High Atlas and Moroccan Meseta to the north of the Anti-Atlas. Here a significant period of late Precambrian sedimentation and volcanism began about 750 to 800 m.y. ago as a geosynclinal environment began to develop at the present position of the High Atlas (Schenk, 1971; Hurley et al., 1974). These late Precambrian rocks are

seen to overlie the older Precambrian rocks in many places (Charlot, 1976; Schenk, 1971) and so there is no doubt that the mid-Precambrian rocks could have acted as a source for the rocks of the Meseta. This depositional period was apparently climaxed by a period of intrusion beginning at about 650 m.y. ago (Charlot, 1976; Hurley et al., 1976). The parallels with northeastern Massachusetts are very strong.

Another interesting parallel is the fact that igneous zircons from Upper Paleozoic and Triassic sandstones from the northwestern Meseta (Hull, 1976) give a primary age of about 1.6 b.y. and a lower resetting age of 270 m.y. which is remarkably close to the detrital zircons of this paper. However, the data from those zircons was limited and the possibility of contamination from Lower Paleozoic rocks exists.

The metamorphic history as revealed by the isotopic data indicates two major periods of increased temperature during which isotope systems were affected. The first major period probably occurred over a range of about 60 years from 490 to 430 m.y. ago. This range is based on the scatter of data from the Rb-Sr whole rock analyses of Chapter 7. Activity may have continued up to 400 m.y. or younger since ages from many aplites (Cameron and Naylor, 1976; U.S.G.S., 1967) associated with the Andover granite give ages that low. Almost all the isotopic evidence for an orogenic episode at this time is seen in the Rb-Sr data. There is no clear cut evidence for it in the zircon data although it is likely they were affected

by it. The Rb-Sr system was apparently completely reset at that time. This implies not only high temperature but also considerable influence from a pervasive fluid phase. This agrees well with geologic and other isotopic evidence which indicates that the major period of metamorphism and igneous activity in the Paleozoic for this area was during the Ordovician. Similar Rb-Sr results from rocks west of the Clinton-Newbury Fault Zone are interpreted as evidence that they underwent regional metamorphism at the same time even though their grade is significantly lower and their style of deformation is different.

The ages of the intrusive rocks (about 470 to about 430 m.y.) are slightly younger than what might be considered the peak of Rb-Sr whole rock resetting (about 490 m.y.) based on the data in Chapter 7. This agrees with geologic evidence that suggests the intrusives were emplaced in the waning stages of regional metamorphism and deformation. The intrusives are only deformed and show gneissic textures in some places while they are relatively unaffected in others.

The second event appears to have been mainly a thermal event which partially reset the zircons. Lower temperatures and lack of a fluid phase left the Rb-Sr system virtually intact. Geologic evidence for a Permian episode of intrusion and deformation is minimal in this part of southeastern New England, which is in agreement with K-Ar data (Zartman et al., 1970) and radiation damage ages (Fairbairn and Hurley, 1957)

which suggest a simple thermal event. This early Permian event may be related to the more intense and significant period of late Pennsylvanian metamorphism and intrusive activity seen farther to the south (Quinn, 1971; Hurley et al., 1960) but the evidence is not clear cut.

Evidence for a Devonian "Acadian" event is not significant. Some of the zircons may have been affected at that time but it is not definite. The lack of significant intrusive activity and lack of effects on the Rb-Sr whole rock system further accentuate the absence of an event at this time. The only evidence for activity at this time are the Siluro-Devonian volcanics of the Newbury Volcanic Complex (Shride, 1976a, 1976b). Isolated in downdropped fault blocks, they are relatively unmetamorphosed and undeformed. In addition, they contain significant amounts of silicic and intermediate volcanics interlayered with shallow water fossiliferous sediments, and isotopic data (Bottino, 1963) gives an initial $\text{Sr}^{87}/\text{Sr}^{86}$ ratio that is somewhat high (0.708-0.710). All of these facts together indicate that by the Silurian the late Precambrian sediments and metasediments of northeastern Massachusetts were fairly well cratonized and acted as a stable area except for occasional epeirogenic movements (early Permian). The major processes at work would have been deposition of shallow water sediments and continental volcanism or erosion during periods of uplift.

Evidence for a period of late Precambrian regional meta-

morphism is also meager in spite of the large amount of intrusive activity that has been identified at that time. Contact metamorphic effects are associated with these intrusives (Bell and Alvord, 1976; Cameron and Naylor, 1976). Regional metamorphism may have occurred but was later wiped out by the intense Ordovician event.

These unrecognized events may be responsible for some of the scatter observed in the U-Pb and Rb-Sr data presented in this paper.

Chapter 10

Summary

The conclusions reached in this paper can be summarized as follows:

(1) Two basically different populations of zircons can be recognized in the metasediments and metavolcanics of northeastern Massachusetts: a volcanic population and a detrital population. These two populations are differentiated on the basis of lithology of host rock, grain morphology and color, different primary ages and discordia trends, and different resetting behavior.

(2) The volcanic zircons yield an age of 742 ± 91 m.y. which implies a late Precambrian age for all of the regionally metamorphosed stratified rocks east of the Clinton-Newbury Fault Zone.

(3) The detrital zircons yield a primary age of 1.55 ± 0.03 b.y. This may be the result of mixing of zircon populations 1300 - 1900 m.y. in age although positions on the Concordia diagram and resetting behavior suggest that they are a single population or a well-mixed combination of populations.

(4) Although a single source area for the detrital zircons cannot be definitively delineated, similarity in ages suggests a northwest African source, probably the Anti-Atlas of Morocco. Other similarities, such as similar ages of depo-

sition, volcanism and igneous intrusion, similar ages of zircons and their time of resetting from Paleozoic and Mesozoic sandstones of the Moroccan Meseta and similar tectonic environments further enhance the correlation.

(5) The resetting of both zircon suites was largely controlled by radiation damage. The amount of radiation damage is dependent on the U and Th content of the zircons. Some radiation damage controlled continuous diffusion also seems to have occurred.

(6) The major period of regional metamorphism, deformation and igneous intrusion began about 490 m.y. ago, continued through the Ordovician, but began to taper off at the end of the Ordovician. It probably continued sporadically through the Silurian. During this orogenic period the Rb-Sr whole rock systems were completely reset, possibly due to a combination of high temperature, a widespread mobile fluid phase and an initial narrow range of Rb/Sr ratios in the rocks. Large scale transport and input and output of Rb and Sr is also a possibility.

(7) The Rb-Sr whole rock systems were largely unaffected by later metamorphisms due to their lower temperatures and lack of a fluid phase.

(8) The last event to affect the zircons was a thermal event of late Carboniferous or early Permian age.

(9) The Rb-Sr data separate into two trends with roughly the same age but different initial ratios. This separation

correlates well with the protoliths of the rocks: metasediments give high initial ratios while the volcanics give low initial ratios.

(10) Extrapolations of initial ratios back to the time of deposition imply a lower crust or upper mantle source for the volcanics regardless of the resetting model used (except Model 4). Similar analyses for the sediments give a range of values expected for seawater although the value for a particular geologic period cannot be defined.

(11) Lithologic correlations appear to give a late Precambrian age to most of the high grade stratified rocks east and south of the Clinton - Newbury - Lake Char - Honey Hill Fault system. Possible chronostratigraphic correlations with similar volcanic and sedimentary sequences in New Brunswick and Newfoundland are also apparent.

(12) Rocks west of the Clinton-Newbury Fault Zone are probably Cambro-Ordovician in age and were metamorphosed by the same events as the rocks to the east.

(13) A crude, and by no means the only, geologic history of the area can be established:

750-650 m.y.: geosynclinal development with deposition of volcanics and sediments on an unknown basement, possibly mid-Precambrian in age.

650-570 m.y.: large scale igneous intrusion, uplift and partial cratonization of the area.

600-450 m.y.: deposition of Cambro-Ordovician shal-

low water shelf sediments.

490-400 m.y.: major period of metamorphism, deformation and intrusion with the area becoming almost completely cratonized.

400 m.y. to the present: area is fairly stable except for epeirogenic movement and significant period of strike-slip and thrust faulting probably in the late Paleozoic or early Mesozoic.

(14) A usable method of rapidly and efficiently analyzing small zircon samples (about 0.5 mg) in microbombs has been worked out and should prove useful for population studies and small sample reconnaissance analyses.

Suggestions For Further Research

Needless to say this work still leaves many questions unanswered. Even the data presented here need to be refined. More work is needed to establish definitely the volcanic and detrital trends and learn whether the detrital suite is a mixture of populations. Variations within the sequence are also possible and should be sought.

Outside of the area similar studies should be applied to the rocks of Rhode Island and eastern Connecticut and to the areas west of the Clinton-Newbury Fault Zone. The lithostratigraphic correlations should be tested and expanded. The nature of the source areas for these sediments should also be investigated.

Most importantly of all, the basement on which these metasediments and metavolcanics were deposited should be sought. The nature of this basement would reveal much about the true nature of the tectonic environment which existed in this area at that time.

Appendix A

Rb-Sr Whole Rock Method

Because the procedures used in this study to prepare, dissolve, and process samples for Rb-Sr whole rock analyses are not standard, they will be given in detail here.

Initial Preparation

Large hand samples were broken with a sledgehammer into pieces about 9 to 10 inches or less in size. Weathering rinds and veins or apophyses of foreign material were removed if possible. These pieces were then crushed in a large jaw crusher to fist size or less. Any remaining weathered pieces or material not belonging to the country rock were removed. A small fresh piece was also removed for thin sectioning. The remaining pieces were then run through a small jaw crusher to centimeter or less sizes. A small portion (about 5 g) of the -100 mesh portion of this crushed material was then removed.

This small portion of the samples was analyzed by X-ray fluorescence to make a rough determination of the content of Rb and Sr. The unknown Rb $K\alpha$ and Sr $K\alpha$ peaks were compared against those of standard whole rocks: G-1, G-2, GSP-1, AGV-1, BCR-1, and W-1. Scans were made over the Rb and Sr peaks only once for both standards and unknowns and no matrix corrections were made. An exact determination of Rb and Sr concentrations was not necessary. Approximate values are enough to guide sample selection and spiking. Differences between the XRF-

determined concentrations and the isotope dilution concentrations were highly variable; sometimes very good agreement could be obtained, other times they would disagree by as much as 100%.

Criteria used for selecting samples for further processing were as follows: samples with greater than 20 ppm of Sr and Rb by XRF were used. Samples with less than this would have problems with contamination and significant amounts (about 1 g) would have to be processed to get enough Rb and Sr. Also, only samples with Rb/Sr ratios greater than 0.1 were used.

Based on the XRF data, calculations were then made to determine the amount of Rb⁸⁷ and Sr⁸⁴ spikes needed. The calculations were based on a sample weight of 0.2 to 0.8 g and a Rb⁸⁵/Rb⁸⁷ (spike + sample) ratio of approximately 1 and an Sr⁸⁴/Sr⁸⁶ (spike + sample) ratio of approximately 0.5.

Amounts of spikes used usually ranged between 2 and 8 ml and were rounded to the nearest ml to make pipetting easier.

About 1 kg of the crushed material was then removed from those samples selected to further processing. This 1 kg aliquot was then ground in a disc grinder to less than 20 mesh. This ground material was then homogenized by mixing and rolling on a large sheet of paper. A 5 to 10 g split was then made by passing the homogenized material through an aluminum splitter or by removing small aliquots at random with an aluminum spatula. This 5 to 10 g split was then placed in the stainless steel cannister of a Pica Blending Mill. The split

was run in the blending mill for 15 to 20 minutes to reduce its grain size to less than 325 mesh. The sample was removed and stored in a labeled polyethylene vial.

All grinding and crushing equipment was cleaned between samples to reduce cross-contamination.

Spiking, Dissolution and Rb and Sr Separation

All laboratory ware which comes in contact with the sample, spikes or radioactive tracer was cleaned by washing with nitric acid and rinsing with tap water, demineralized water and ultrapure H₂O.

The sample was weighed out of the polyethylene vial onto powder paper to approximately the amount calculated as described above. Exact weights were not necessary since they did not enter into the calculation of a $Rb^{87}/Sr^{86} - Sr^{87}/Sr^{86}$ diagram point. The sample was then dumped into a Pt dish. The calculated amounts of spikes were then volumetrically pipetted in. (Pipettes were decontaminated by pipetting and discarding a few aliquots of spike.) One ml of ultrapure HClO₄ was then added along with 10 ml of ultrapure HF. The Pt dishes were then placed on a steam bath, covered with Teflon covers, and heated for 1 to 2 hours.

Even after 2 hours on the steam bath most samples still retained an undissolved residue. Examination of some of them revealed two components: a greyish white amorphous material, probably silica gel and insoluble fluorides, and a refractory mineral component, mainly graphite, zircon, aluminosilicates

and occasionally garnets. Except for garnets the refractory minerals are very low in Rb and Sr.

After dissolution the Teflon covers were removed and the HF was allowed to evaporate until only the HClO_4 remained. A few ml of ultrapure 2 N HCl was then added and the dishes warmed on the steam bath to help dissolve the fluorides by conversion to soluble chlorides. The Pt dishes were then removed from the steam bath and allowed to cool. The residue was filtered out on filter paper previously washed with ultrapure 2 N HCl and H_2O .

The filtered liquid was collected into a Vycor evaporating dish and covered with a Pyrex watch glass. At this point a few drops of dilute radioactive Sr^{85} tracer were added. The radiation count was checked on a proportional counter. Enough tracer was added to get a minimum count rate of 150 cps (background was less than 10 cps). Because of decay more tracer had to be added through time but never more than 1 ml was ever added because of contamination.

The Vycor dishes were placed on a hot plate and the liquid allowed to evaporate until only the HClO_4 remained (signalled by white fumes). A few ml of ultrapure 6N HCl were then added, the dishes were covered and then allowed to sit overnight. Allowed to sit for a few hours at room temperature in acid conditions alkali perchlorates (including Rb perchlorate) slowly precipitate out as long thin needle-like crystals. The liquid with precipitated perchlorates was washed with ul-

trapure 6N HCl into 15 ml centrifuge tubes and centrifuged for a few minutes at moderate speeds. After centrifuging the liquid was decanted back into the Vycor dishes which had been rinsed with ultrapure H₂O. (The centrifuge tubes are checked on the proportional counter to make sure no Sr has been caught up in the alkali perchlorates. If the perchlorates do have a count significantly above background, the solid is washed back into the Vycor dish with ultrapure 2N HCl, the dish is returned to the hot plate and the perchlorate separation repeated.) The solid remaining in the centrifuge tube was made into a slurry by adding ultrapure 2 N HCl and stirring with a glass rod. This slurry was poured into a 5 ml Vycor beaker. The centrifuge tube was washed once with the 2 N HCl and the washings were poured into the Vycor beaker with the slurry. The Vycor beaker was placed on a hot plate under a heat lamp and the liquid evaporated to dryness. Then 1-2 ml of ultrapure 7 N HNO₃ were added and also taken to dryness to convert the perchlorates to nitrates. The Vycor beaker was removed, allowed to cool and covered with Parafilm.

The dishes with decanted liquid were then returned to the hot plate and evaporated to the perchloric acid. They were removed from the hot plate, a few ml of ultrapure 2 N HCl was added and then allowed to cool.

The liquid was poured through filter paper and a funnel into a 65 cm long Vycor column (1.0 cm inside diameter) filled 4/5 of its length with Dowex 50X8-400 cation exchange resin.

After the sample liquid has completely entered the resin the column was filled with ultrapure 2 N HCl and attached to an overhead reservoir of the 2 N HCl. The pressure from the reservoir increased the flow of HCl through the column, thus reducing the separation time.

The resin was previously cleaned by passing a column length of the 2 N HCl through it. The separation of cations in the column is essentially a dynamic one. They separate based on how fast they move through the column which is a function of cation size and valence, as well as other things. Since most of the rubidium has already been removed it is only necessary to separate the Sr from the other cations.

The first 125 ml of HCl to pass through the column was collected and checked on the counter. If only background was found this liquid was discarded; if the count rate was high, the Sr had already passed through the column and the sample had to be restarted from the beginning of the procedure. This happened only rarely. The liquid then passing through the columns was then collected 5 ml at a time in 15 ml polyethylene beakers. Each 5 ml aliquot was checked on the counter. Most of the radioactive Sr⁸⁵ tracer should be in 3 or 4 of the beakers.

The liquid in these few beakers was returned to the rinsed Vycor dishes and taken down to dryness. The residue was taken up with 2-3 ml of the 2 N HCl and poured in a 5 ml Vycor beaker. The radiation count was again checked to make

sure that most of the Sr had been recovered. The liquid was then taken down to dryness and converted to nitrate in a similar manner to the Rb sample.

Mass Spectrometry

Samples were loaded by adding about 0.05 ml of ultrapure 7 N HNO_3 to the Vycor beakers and mixing the sample and acid with a tapered glass rod. A drop of the nitrate solution was taken up with the glass rod and placed on the filament. The drop was taken down to dryness by heating with a heat lamp and by passing a small current (0.5 amp) through the filament.

The filaments were made of 0.00075" thick, 0.015" wide zone-refined tantalum ribbon. The filament was previously coated with a thin layer of Ta_2O_5 by heating it briefly in air at a pressure of about 100 microns. This coating improved ion emission and provided better adhesion for the drop of sample during loading.

Samples were analyzed in a 12-inch, 60° Nier type programmable mass spectrometer at the M.I.T. Geochronology Laboratory. Accelerating voltage was 4.5 kv and the detector was a Cary 31 vibrating reed electrometer. The electrometer was always set for 300 mV output. The output went to a scale expander and an integrating digital voltmeter. Output from the scale expander went to a strip chart recorder. The voltmeter was controlled by a PDP-8 computer with 4K memory. The computer controlled data acquisition and output from the volt-

meter as well as controlling switching of mass peaks. This switching was done through a series of relays that controlled an array of resistors. The resistors controlled the output from the regulated power supply for the magnet.

The computer was programmed to read all the strontium peaks in order from 84 to 88 plus the baseline ($85\frac{1}{2}$ position) and the mass 85 peak. Baseline was subtracted from all peaks. Then the 87 peak was corrected for natural Rb^{87} by subtracting approximately 1/3 of the 85 peak from the 87 peak. The 84/86, 87/86 and 88/86 ratios were then calculated and printed out. Up to 42 such measurements could be made. Usually an average of 30 to 40 such cycles were taken.

The rubidium in the strontium sample was checked during degassing of the sample. The filament current was turned up to just below the point at which Sr came off to allow volatile material to burn off. A quick scan was made of the 85 and 87 peaks. For most samples only natural Rb contamination was found, but in a few some spiked whole rock Rb had gotten through the perchlorate and column separation. In this case the strontium could not be run until the Rb had burned off completely.

The Rb sample was loaded and run in a similar manner, except that the computer was programmed to read only two peaks, correct them for background and print out a single ratio. Usually 20 readings were taken. The Rb sample was loaded on a filament previously used for a Sr run since all

the Rb was already burned off and the Sr did not come off at the low temperature at which Rb was run.

Reagents and Reagent Blanks

- HF: Reagent grade 48% HF, sub-boiling distilled in Teflon 2-bottle still (Mattinson, 1971, 1972).
Blanks: Rb = 2.6 ng/ml; Sr = 8.4 ng/ml.
- HClO₄: Commercially prepared, double Vycor distilled.
Blanks: Rb = 0.8 ng/ml; Sr = 2.3 ng/ml.
- HCl: 12 N reagent grade HCl, single Vycor distilled, then diluted with ultrapure H₂O to 6N and 2N.
Blanks: 6N - Rb = 0.08 ng/ml; Sr = 1.2 ng/ml;
2N - Rb = 0.11 ng/ml; Sr = 0.14 ng/ml.
- H₂O: Tap water distilled, then passed through mixed-bed high capacity resin exchange column and distilled in Vycor. Blanks: Rb = 0.04 ng/ml; Sr = 0.07 ng/ml.
- . 7N HNO₃: 14 N reagent grade HNO₃ diluted with ultrapure H₂O to 7N, then distilled in Vycor. Blanks:
Rb = 0.03 ng/ml; Sr = 0.1 ng/ml.
- Sr⁸⁵ tracer: Sr⁸⁵Cl₂ diluted to 1 liter with 2 N HCl (ultrapure) to give final count rate of about 1 µc/ml.
Blanks: Rb = 146 ng/ml; Sr = 43 ng/ml.

Spikes

- Rb⁸⁷: Rb⁸⁷NO₃ diluted in 2N HCl to give about 10 µg/ml of Rb⁸⁷. 20-30 ml of this solution was removed, dried down, converted to nitrate and run on the mass spectrometer to get the isotopic ratios. No correction for fractionation was made.

The observed Rb⁸⁵/Rb⁸⁷ ratio was 0.00788 ± 0.00023.

Concentration of spike solution was calibrated by mixing a known amount of spike solution with NBS Standard Reference Material 607 K-feldspar and processing it through the procedure outlined above. NBS 607 contains 523.90 ± 1.01 ppm Rb.

The observed spike solution concentration was:

$$\text{Rb}^{87} = 1.13403 \pm 0.00028 \times 10^{-7} \text{ moles/ml (9.87 } \mu\text{g/ml)}.$$

Sr^{84} : $\text{Sr}^{84}(\text{NO}_3)_2$ diluted with ultrapure 2 N HCl to approximately $0.5 \mu\text{g/ml}$ of Sr^{84} . Like the Rb^{87} spike, an aliquot was removed and run on the mass spectrometer to obtain isotopic results. These were corrected for fractionation by assuming the isotopic ratio data supplied with the spike were correct and that any change from these values was due to contamination from dilution and fractionation. An iterative correction gave the following values:

$$\text{Sr}^{86}/\text{Sr}^{84} = 0.000760 \pm 0.000030$$

$$\text{Sr}^{87}/\text{Sr}^{86} = 0.5856 \pm 0.0060$$

$$\text{Sr}^{88}/\text{Sr}^{86} = 2.378 \pm 0.002$$

Concentration of the spike solution was also calibrated against NBS 607 in the same manner as the Rb^{87} spike. NBS 607 contains 65.485 ± 0.320 ppm of Sr with and $\text{Sr}^{87}/\text{Sr}^{86}$ ratio of 1.20039 ± 0.00020 .

The observed spike concentration was:

$$\text{Sr}^{84} = 5.74822 \pm 0.00184 \times 10^{-9} \text{ moles/ml (0.48 } \mu\text{g/ml)}.$$

Procedure Blanks

Procedure blanks were done by following the procedure given above but without a sample. Because the perchlorate separation could not be done without a sample to provide sufficient alkalis, the Rb and Sr blanks were prepared separately. The Rb blank was simply taken to dryness at the perchlorate separation step, converted to nitrate and analyzed. The Sr blank went through the whole procedure.

An average of two blanks gave the following data:

$$\text{Rb}^{87} = 1.249 \pm 0.042 \times 10^{-9} \text{ moles (390 ng total Rb)}$$

$$\text{Sr}^{86} = 3.103 \pm 0.079 \times 10^{-10} \text{ moles (276 ng total Sr)}$$

$$\text{Sr}^{87}/\text{Sr}^{86} = 0.72163 \pm 0.00184.$$

These values were used to correct all Rb and Sr data for contamination. It can be seen that nearly all of this contamination can be accounted for by the contamination in the reagents. For the sample sizes and Rb and Sr concentrations involved in this work this contamination represents 1 to 2% of the rock Rb and Sr.

Constants Used in Calculations

Natural $\text{Rb}^{85}/\text{Rb}^{87} = 2.6510$ (mole percent; Friedlander et al., 1964).

Atomic weight of Rb = 85.548 g/mole (Friedlander et al., 1964).

Rb^{87} decay constant = $1.39 \times 10^{-11} \text{ y}^{-1}$. (This has been the standard value used at the M.I.T. Geochronology Laboratory; to correct ages to a value of $1.42 \times 10^{-11} \text{ y}^{-1}$, multiply ages by 0.979; to correct to a value of $1.47 \times 10^{-11} \text{ y}^{-1}$, multiply ages by 0.946.)

Natural $\text{Sr}^{86}/\text{Sr}^{88} = 0.1194$ (mole percent; Faure and Powell, 1972).

Natural $\text{Sr}^{84}/\text{Sr}^{86} = 0.0570$ (mole percent; Faure and Powell, 1972).

Atomic weights (from Friedlander et al., 1964):

$$\text{Rb}^{85} = 84.912$$

$$\text{Rb}^{87} = 86.909$$

$$\text{Sr}^{84} = 83.913$$

$$\text{Sr}^{86} = 85.909$$

$$\text{Sr}^{87} = 86.909$$

$$\text{Sr}^{88} = 87.906$$

No errors were attached to any of the constants used.

Fractionation

No correction was made for fractionation of the Rb.

The strontium ratios were corrected for fractionation by using the standard $\text{Sr}^{86}/\text{Sr}^{88}$ ratio of 0.1194. An iterative procedure was used in which the Sr^{86} and Sr^{88} contributed by the spike was also taken into account. Iteration was stopped when successive values of $\text{Sr}^{87}/\text{Sr}^{86}$ were within 0.01% of each other. The corrections were then applied to the $\text{Sr}^{84}/\text{Sr}^{86}$ ratio. The fractionation corrected $\text{Sr}^{87}/\text{Sr}^{86}$ ratio was then corrected for the contributions of Sr^{87} and Sr^{86} from the spike. This gave the $\text{Sr}^{87}/\text{Sr}^{86}$ ratio for the sample. The fractionation corrected $\text{Sr}^{84}/\text{Sr}^{86}$ ratio was used to calculate the amount of Sr^{86} .

Standards

No rubidium standards were run.

The Eimer and Amend Standard Strontium Carbonate (Lot # 492327) was run 12 times (40 ratios measured each time) during the course of the Rb-Sr work. The average value obtained was $\text{Sr}^{87}/\text{Sr}^{86} = 0.70816 \pm 0.00016$ (± 2 standard deviations of the mean of 12 runs each containing 40 ratio measurements). Each measurement of $\text{Sr}^{87}/\text{Sr}^{86}$ ratio was individually corrected for fractionation.

This value is very close to the accepted value of 0.7080 but is slightly high. A similar value and error were found by Gebauer and Grünenfelder (1974) which they ascribed to non-

linearity in the electrometer. This seems to be the case here also. When the Rb-Sr work was first begun, measurements of the standard gave a very low value (0.7065 ± 0.0010). When the vacuum tubes of the electrometer were replaced the values began to average the value given above.

No correction of the Sr data has been made for this slight difference between the observed and accepted values of the standard.

Replicates

Four samples were each re-analyzed in order to check the accuracy of the results and the quality of the chemical procedures and various corrections made. Each replicate analysis was put through the entire chemical procedure. Mass spectrometer analyses and corrections for contamination were the same for all replicates. The results of the replicate analyses are:

<u>Sample</u>	<u>Run</u>	<u>Sr⁸⁷/Sr⁸⁶</u>	<u>Rb⁸⁷/Sr⁸⁶</u>
R8402	1	0.71825 ± 0.00073	1.366 ± 0.018
	2	0.71864 ± 0.00044	1.174 ± 0.005
R8406	1	0.72296 ± 0.00023	2.208 ± 0.010
	2	0.72338 ± 0.00025	2.228 ± 0.003
R8435	1	0.71093 ± 0.00014	0.412 ± 0.007
	2	0.71106 ± 0.00017	0.424 ± 0.001
R8422	1	0.71311 ± 0.00007	1.066 ± 0.011
	2	0.71482 ± 0.00413	0.979 ± 0.004

It can be seen that the Sr⁸⁷/Sr⁸⁶ ratios agree quite well within the limits of error. The Rb⁸⁷/Sr⁸⁶ ratios, how-

ever, do not agree very well with one another. The differences are variable; R8406 and R8453 do agree with one another when the errors are extended to two standard deviations but R8402 and R8422 are 10% or more off in their replicates.

A number of reasons can explain this behavior. Sample inhomogeneities, non-equilibration of sample and spike, lack of fractionation correction for Rb, and variable amounts of contamination could cause the $\text{Rb}^{87}/\text{Sr}^{86}$ ratios to be different. The exact reason for the discrepancies is not known but they suggest that the errors of the $\text{Rb}^{87}/\text{Sr}^{86}$ ratios are somewhat larger than those quoted in Chapter 7, where only precision errors are given.

The data which are given in Chapter 7 for the four samples above are composites of the two replicates for each sample.

Appendix B

Zircon U-Pb Method

Sample Preparation

Samples were crushed and ground in the same manner as the Rb-Sr samples described in Appendix A. XRF analyses were skipped and the samples went immediately from the small jaw crusher to the disc grinder. The resulting powder was sieved to recover the -60 to +325 mesh fraction. The +60 mesh fraction was re-ground in the disc grinder and re-sieved until nearly all the sample passed through a 60 mesh sieve.

Zircon Separation

The exact method of separation depended on the lithology of the rock. For large samples of quartz and feldspar rich rocks, the -60 +325 mesh fraction was placed into a large separatory funnel filled with acetylene tetrabromide (density =2.96), stirred thoroughly and then allowed to settle for a few hours with occasional light stirring to increase separation efficiency.

The minerals which sank were drained off and washed thoroughly with acetone to remove the tetrabromide. Magnetite was removed with a hand magnet at this point. The remaining material was passed through a Frantz Isodynamic Magnetic Separator at 30° forward slope and 20° side slope. The material was successively passed through the separator at 0.5, 1.0, and 1.5 amps. This removed most of the biotite, hornblende, ilmenite,

and other dense highly magnetic minerals.

The non-magnetic minerals remaining from the magnetic separation were placed in a small (100 ml) separatory funnel filled with methylene iodide (density = 3.3) and stirred. The minerals that sank were removed and washed with acetone. This heavy mineral separate was then heated at 150°C for 1/2 hour in 7N HNO₃ (reagent grade). This removes pyrite which is the major contaminant at this point. After the nitric acid wash the heavy mineral separates were rinsed thoroughly with demineralized water and warmed for 1/2 hour in the same water. The heavy minerals were then passed through the magnetic separator at 15° forward slope, 1.5 amps current and successively lower side slopes starting at 15°. The usual series of side slopes used were 15, 10, 5, 4, 3, 2, and 1 degrees. Most zircons were non-magnetic down to 5° where metamict zircons began to appear on the magnetic side. The only exception to this treatment were the zircons from R8311 which were very magnetic (magnetic at 20° side slope) and it was found easier to separate them by varying the current going through the magnet.

Each magnetic split was checked optically to gauge the efficiency of separation and the nature of the zircons and contaminating materials. Splits that were too small to use were mixed with the next higher or lower split. Splits that were large enough were further split into size fractions.

The zircon designations after the sample numbers iden-

tify the side slope and whether the split was magnetic (M) or non-magnetic (NM) at that side slope (e.g. 5M = magnetic at a 5° side slope). If the sample was further split according to size the upper and lower mesh sizes are given (e.g. -150+200).

Each split or portion of a split was then purified by hand picking out the contaminating minerals. Multiple grains and zircons with inclusions were also removed. When enough purified zircon sparate was obtained it was placed in a 5 ml Pyrex beaker, washed twice with warm ultrapure H₂O, dried and covered with Parafilm.

For samples rich in biotite and hornblende, the initial separation was somewhat different. Magnetite was first removed with a hand magnet. The sample was then passed through the magnetic separator at 40° forward slope, 25° side slope and successive magnet currents of 0.1, 0.2, 0.5, and 1.0 amps. This removed a significant portion of the biotite and hornblende which otherwise would make the initial heavy liquid separation very inefficient. After the magnetic separation, the least magnetic material that remained went through the procedure outlined above starting with the tetrabromide separation.

For the small samples used for Rb-Sr work, the sample was sieved to -60+325 mesh and the sized powder was placed in 50 ml centrifuge tubes filled with acetylene tetrabromide. The sample was stirred thoroughly and then centrifuged at mod-

erate speed for about 5 minutes. The acetylene tetrabromide and the minerals that floated were decanted off. The heavy mineral separate then followed the procedure given above beginning with the acetone washing after tetrabromide separation.

Sample Dissolution and U-Pb Separation

The procedure used followed essentially that described by Krogh (1973), so it will not be described in detail here. Some variations were made on Krogh's technique to meet the specific needs of this study. These variations are described below.

Variations of the Krogh Technique

Because of the small sample sizes and low Pb and U contents of most of the zircons, it was decided to reduce the amounts of reagents to 1/2 those used by Krogh. It made the chemistry somewhat more difficult to handle but it was thought that this would minimize contamination from the reagents, which were not as clean as those used by Krogh. Optical checks were made to insure that the zircons were completely dissolved and that solids did not appear during processing. In only three samples did solid appear (W-1, W-2 and Z-1 splits). These were re-processed with new purified zircon separates.

A change was also made in the spiking procedure. Normally

the sample is spiked with U^{235} prior to aliquoting and resealed in the bomb and returned to the oven. However, to increase bomb life by reducing the number of times the bombs are sealed and heated, it was thought best to do the spiking of U^{235} after aliquoting. This has an added advantage in that it is not necessary to know the precise amount of liquid in each aliquot since a Concordia point can be obtained directly from the spiked aliquot. Two replicates (described later) were made to test the efficacy of this procedure.

After the sample had been dissolved and the HF evaporated off, 1 ml of ultrapure 3N HCl was added to the Teflon capsule, the capsule cover was replaced and the solution allowed to sit overnight. This ensures that the sample dissolves completely. The solution was then split into two roughly equal aliquots. One of the aliquots was then spiked with accurately measured quantities of Pb^{208} and U^{235} . To insure equilibration of spike and sample, the spiked aliquot was then dried down and taken up again with 3 N HCl (1 ml) and warmed with a heat lamp to insure complete dissolution. The normal procedure was then followed.

All work, with the exception of resin column separation, was done in laminar flow hoods. Input of reagents was done either directly from the bottles holding the reagents or, in the case of very small amounts, with a 10 microliter pipette

with disposable plastic tips. The tips were cleaned by boiling in reagent grade 7 N HNO_3 and washing with demineralized and ultrapure H_2O .

Mass Spectrometry

Samples were loaded onto 0.0013" thick, 0.03" wide zone-refined rhenium filaments using the silica-gel + H_3PO_4 technique of Cameron et al. (1969). The samples were not loaded as nitrates but as chlorides in H_3PO_4 solution (Krogh, 1973). Filaments were previously outgassed at 1800 to 2000 °C at a pressure less than 10^{-6} torr for 30 to 45 minutes.

The general loading procedure started with 0.01 ml of silica gel solution placed on the rhenium filament. This was taken down almost, but not completely, to dryness with a heat lamp. Then 0.02 ml of H_3PO_4 (0.75 N) was added to the sample and mixed with the sample with the tip of the micropipette. A different clean plastic tip was used for the silica gel, the H_3PO_4 , and mixing and removing the sample solution. Next 0.01 ml of the sample - H_3PO_4 solution was removed from the Teflon beaker and loaded on the filament on top of the moist silica gel. The acid was evaporated off with a heat lamp and a small current passing through the filament. The final appearance of the sample is a dark, glassy, frothy bead on the filament.

The unspiked Pb, spiked Pb and spiked U samples are run separately on the programmable mass spectrometer system described in Appendix A. The same computer program used for

running the Rb was used to run the Pb and U analyses. The $\text{Pb}^{208}/\text{Pb}^{206}$, $\text{Pb}^{207}/\text{Pb}^{206}$ and $\text{Pb}^{204}/\text{Pb}^{206}$ ratios were measured for the unspiked lead. The $\text{Pb}^{208}/\text{Pb}^{206}$ and $\text{Pb}^{204}/\text{Pb}^{206}$ ratios were measured for the spiked lead. Both were corrected for contamination. In the spiked lead the Pb^{204} was assumed to come from contamination and spike. The spike Pb^{204} in the spiked lead run was corrected for. The corrected ratios were then used to calculate the amounts of Pb^{208} , Pb^{207} and Pb^{206} in the spiked aliquot.

The $\text{U}^{235}/\text{U}^{238}$ ratio was measured for uranium to calculate amounts of U^{235} and U^{238} in the spiked aliquot. These were combined with the lead data to give the Concordia points. Amounts of contamination were also calculated from the data.

Reagents and Reagent Blanks

Ultrapure HF, HNO_3 , and HCl: Prepared according to the procedures of Mattinson (1971, 1972). Blanks: HF, Pb = less than 0.2 ng/ml; HNO_3 , Pb = approximately 1-2 ng/ml; 6N HCl, Pb = less than 0.5 ng/ml; 3 N HCl, Pb blank is not detectable.

Ultrapure H_2O : Tap water distilled, then demineralized on resin column, then double distilled in quartz still. Lead blank not detectable.

Ultrapure 0.75 N H_3PO_4 : Prepared according to Krogh (1973). Blank: not determined but probably less than 0.2 ng/ml, based on specifications of ultrapure P_2O_5 and blank of ultrapure H_2O .

Silica gel: Prepared according to Cameron et al (1969). Blank: 300-400 ng/ml; highly variable.

No uranium reagent blanks were made.

It can be seen that essentially all of the contamination comes from the silica gel.

Standards

Three standards were run to check spectrometer operation and fractionation: NBS 983 and CIT PN-2 for lead and NBS 950a for uranium. Accepted values for the isotopic ratios of these standards are given by Doe (1970). Measurements were made over the period encompassed by the U-Pb work presented in Chapter 6. The average of all the measurements, the number of ratios measured and agreement with accepted values are shown below:

<u>Standard</u>	<u># of Ratios</u>	<u>Ratio</u>	<u>Average Value</u>	<u>% Error from Accepted Value</u>
NBS 983	32	Pb ²⁰⁷ /Pb ²⁰⁶	.07123 ±.00003	+ 0.034
	27	Pb ²⁰⁸ /Pb ²⁰⁶	.19082 ±.00005	- 0.239
	30	Pb ²⁰⁴ /Pb ²⁰⁸	.02773 ±.00007	+ 1.81
PN-2	16	Pb ²⁰⁸ /Pb ²⁰⁷	2.351 ±.001	+ 0.201
	25	Pb ²⁰⁷ /Pb ²⁰⁶	.9316 ±.0004	+ 0.015
	19	Pb ²⁰⁶ /Pb ²⁰⁴	16.558 ±.007	- 0.391
NBS 950a	14	U ²³⁵ /U ²³⁸	.00722 ±.00001	- 0.48

Taking into account the observed errors and the errors in the accepted values (Doe, 1970) all of the ratios except the Pb²⁰⁸/Pb²⁰⁷ and Pb²⁰⁶/Pb²⁰⁴ of PN-2 and the U²³⁵/U²³⁸ of 950a agree to within one standard deviation of the mean with the accepted value. The Pb²⁰⁸/Pb²⁰⁷ value of PN-2 agrees to within 2 standard deviations with the accepted value. Only the Pb²⁰⁶/Pb²⁰⁴ ratio of PN-2 and the U²³⁵/U²³⁸ ratio of 950a were more than 2 standard deviations off from the ac-

cepted values. An explanation for the low uranium value is that one set of data for the 950a standard was run using the Ta_2O_5 technique described by Krogh (1973). The average for this run was 0.00718, significantly lower than the accepted value of $0.007252 \pm .000007$ (Stacey and Stern, 1973). For this reason, plus other problems outlined by Montgomery (1977), all uranium samples were run using the silica gel technique. An analysis of 950a using silica gel gave a value of $0.007265 \pm .000011$, well within one standard deviation of the accepted value. Apparently the problem is extraneous peaks at the 235 and 238 mass positions, probably the result of production of complex tantalum phosphates.

These data for the standard indicate that fractionation of the isotopes during a mass spectrometer run is minor.

Spikes

Pb^{208} : Enriched Pb^{208} oxide dissolved with HF and HNO_3 and diluted to approximate concentration desired with 3 N HCl. All reagents were ultrapure. An aliquot of the spike was evaporated and loaded on a rhenium filament using the silica gel technique.

The observed isotopic ratios were:

$$Pb^{206}/Pb^{208} = 0.002275 \pm .000002$$

$$Pb^{204}/Pb^{206} = 0.008185 \pm .000112$$

Pb^{207} was not measured since it is not necessary for any of the calculations. The Pb^{208} in the spike was calibrated against a gravimetrically prepared solution of NBS 983 which had a concentration of $1.10577 \pm .00155 \times 10^{-7}$ moles Pb/g solution.

The calibration gave a value for the spike of:

$$\text{Pb}^{208} = 1.01150 \pm .00163 \times 10^{-7} \text{ moles/g solution.}$$

U^{235} : Enriched U^{235} oxide prepared and diluted in a similar manner to the lead spike. Analysis of an uncalibrated aliquot gave the following isotopic ratio:

$$\text{U}^{238}/\text{U}^{235} = 0.000755 \pm .000014$$

The U^{235} concentration was calibrated against a gravimetrically prepared solution of NBS 950a₋₇ with a concentration of $1.46026 \pm .00181 \times 10^{-7}$ moles U/g solution. The calculated concentration of the spike was:

$$\text{U}^{235} = 4.04459 \pm .00722 \times 10^{-8} \text{ moles/g solution.}$$

Procedure Blanks

Three procedure blanks were run by following the entire procedure but without a sample. Because the amount of lead in the unspiked aliquot was small, only one unspiked lead analysis ran well enough to give the isotopic ratios of the contamination. The isotopic ratios were:

$\text{Pb}^{208}/\text{Pb}^{206} = 1.95791 \pm 0.00078$	}	From procedure blank #2.
$\text{Pb}^{207}/\text{Pb}^{206} = 0.784296 \pm 0.000252$		
$\text{Pb}^{204}/\text{Pb}^{206} = 0.049567 \pm 0.000099$		

The behavior of the unknown samples (Chapter 6) and the replicates (below) suggest that these isotopic ratios for the contamination are close to the correct values.

The amounts of lead and uranium encountered in the blanks were:

<u>Blank #</u>	<u>Pb_{total} (ng)</u>	<u>U_{total} (ng)</u>
1	44.0	0.85
2	11.7	0.69
3	10.7	0.28

(These blanks are the total of the spiked plus unspiked aliquots.)

Two things are noticeable about the blanks: they are somewhat high and they are extremely variable. For the uranium blanks, although they are somewhat high, they still represent less than 0.25% of the total U in the sample. All the uranium data were corrected by subtracting off the average of the three blanks from the observed amounts of U²³⁵ and U²³⁸ in the unknown.

The only explanation for the variability in the blanks is that most of the contamination is coming from the silica gel. About 0.01 ml of silica gel are used for each load. As the reagent blanks show this is about 3 to 4 ng of Pb per load or 6 to 8 ng for the spiked plus unspiked runs. These values are close to the lowest of the procedure blanks. In practice the amount of silica gel loaded usually ranges between 0.01 and 0.02 ml. The amount of Pb contamination would be 6 to 16 ng as a maximum range. As the reagent blanks show the amount of contamination from the other reagents is negligible.

Since most of the contamination comes from the silica gel, it is not homogeneously distributed throughout the sample. Thus the amount of contamination calculated will de-

pend on the amount of sample loaded on the filament compared to the amount of silica gel. Since only one-half of the sample was usually loaded at any one time the contamination may appear as high as 32 ng. This is due to the fact that when the amounts of radiogenic and contamination lead are calculated, the total Pb^{208} from the spike which was added to the sample is used, even though only one-half of it may be loaded on the filament. This would make the $\text{Pb}^{204}/\text{Pb}^{208}$ ratio of the spiked sample look twice as large as it would be if the silica gel were mixed thoroughly with the sample.

In addition, another process is at work. The final Pb samples are in the form of chlorides. Lead chlorides are only slightly soluble in dilute HCl solutions. The sample is then dissolved in 0.75N H_3PO_4 . Lead phosphates are also insoluble. Even though one-half of the H_3PO_4 is loaded on the filament, less than one-half of the lead sample may be dissolved in the acid. This would make the contamination look larger than it really is. Of course, such an effect would only be seen where the loading blanks are large. For very small loading blanks (less than 1 ng) observed $\text{Pb}^{206}/\text{Pb}^{204}$ ratios would be very large. Variations in the amount of Pb* loaded on the filament would not change that ratio as markedly as they would if the loading blank were larger.

All of these processes taken together would explain

the wide variation and seemingly large amounts of contamination in the blanks and unknown samples. The same analysis would apply to the uranium samples.

That such processes may be at work is evidenced by the fact that in the microbomb analyses (Chapter 8), the samples ran better and with lower $\text{Pb}^{204}/\text{Pb}^{206}$ ratios when they were first converted to nitrates. The nitrates of lead (and most other cations) are usually soluble. As a nitrate, the lead dissolves more easily and efficiently so that more can be loaded on the filament in the same amount of liquid. This suggests that the Pb and U samples in the Krogh technique should first be converted to nitrates before loading as done by Cameron *et al.* (1969). Or, alternatively, some method of getting the Pb sample to dissolve more adequately in the H_3PO_4 could be tried, such as warming the acid with a heat lamp or leaving it overnight in contact with the sample. Since the H_3PO_4 is added to the Pb sample just prior to loading the filament, kinetic factors may be appreciable. Higher temperatures or longer contact time between the H_3PO_4 and the sample would improve the mixing.

Replicates

Replicate analyses of Z-1 2M and Z-1 1M -250 were made. The results were:

Sample	Run	261	
		Pb ²⁰⁶ /U ²³⁸	Pb ²⁰⁷ /U ²³⁵
Z-1 2M	1	0.0767 ± .0003	0.6089 ± .0039
	2	0.0615 ± .0003	0.4791 ± .0029
Z-1 1M -250	1	0.0705 ± .0003	0.5616 ± .0034
	2	0.0715 ± .0005	0.5704 ± .0050

The two replicates for Z-1 1M -250 agree quite well with one another. The two analyses are within 1.25 standard deviations of one another. The replicates for Z-1 2M, however, are about 20 standard deviations away from one another. The only explanation that can be advanced besides non-equilibrium problems between spike and sample during the chemistry is that the sample is non-sized. When the sample was first poured out of the sample vial the larger zircons would be the first to come out. In other words, the first replicate would have a higher proportion of larger zircons than the second replicate. Sample Z-1 1M -250 has a narrow range of sizes (-250 +325) so a sizing effect while pouring out the sample would not occur. Evidence for this is the fact that the first replicate of Z-1 2M is less discordant than the second one. The larger zircons would be expected to be less discordant. Also the corrected Pb²⁰⁷/Pb²⁰⁶ ratios of the two replicates are very different (0.05759 ± .00021 versus 0.05652 ± .00028); such an effect would not result from poor equilibration between spike and sample.

Constants

Decay constants (Jaffey et al., 1971):

$$U^{238} = 0.155125 \pm .000083 \times 10^{-9} \text{ y}^{-1}$$

$$U^{235} = 0.98485 \pm .000672 \times 10^{-9} \text{ y}^{-1}$$

Composition of natural uranium (AEC Report, 1962):

$$U^{238}/U^{235} = 137.88 \pm 0.14$$

Atomic weights of isotopes (Friedlander et al., 1964):

$$U^{238} = 238.0508 \pm .0005$$

$$U^{235} = 235.04393 \pm .00005$$

$$Pb^{208} = 207.97664 \pm .00005$$

$$Pb^{207} = 206.97590 \pm .00005$$

$$Pb^{206} = 205.97446 \pm .00005$$

$$Pb^{204} = 203.97307 \pm .00005$$

Appendix C

Sample Locations and Thin Section Descriptions

Because of the large number of samples involved in this work, only nineteen samples have been selected for thin section work. They cover all the formations studied as well as most of the relevant lithologies and geographic situations of the units. In this way a representative description of the units can be obtained without sacrificing time and space.

All of the samples collected specifically for zircon work are given. In addition, eleven Rb-Sr samples are described. They come from both isochrons (Chapter 7) and include some of the more questionable samples (e.g. R8443).

Amounts of minerals were estimated by rough point counts. No attempt was made to get accurate mineral counts or to determine precise compositions of minerals or accurate compositions of opaque minerals. Only general descriptions are given so that the reader can get an overall idea of mineralogy and petrology of the rocks sampled.

Westboro FormationW-1

Locality: Small lenticular body of sugary quartzite in fine grained volcanics and quartzites on northwest side of small hill along west side of Route 28 approximately 0.25 km south of Interchange 22 in the Middlesex Fells Reservation, west-central portion of Boston North Quadrangle.

Thin section: Quartz (90%), biotite (5%), magnetite (2%), unidentified (2%), feldspar and sericite (1%). Accessories: zircon, hornblende, calcite (as veins).

Quartz grains still show rounding in most places but are crushed, broken and occasionally embayed by surrounding grains. Most grains are surrounded by groundmass of fine grained biotite, magnetite and a very fine grained material composed of unidentified minerals. Occasionally the quartz grains occur in welded clumps where the groundmass is absent and the quartz grains are interlocked and angular.

W-2

Locality: Same as W-1 but from the east side of the small hill. Outcrop is large roadcut along Route 28.

Thin section: Mineralogy similar to W-1 although biotite and feldspar are more common (10-15%).

Feldspar is microcline that is badly weathered with clumps and patches of sericite and clay minerals. Quartz grains are angular and recrystallized and occur in large polycrystalline grains. Accessories are similar to W-1 although carbonates (calcite ?) are more common (about 1%).

Fishbrook Gneiss

Z-1

Locality: Southeast corner of South Groveland Quadrangle approximately 1 km north of Sharpners Pond. Outcrop is cleared area at the end of unnamed highway that turns right off Forest Street 0.5 km northwest of Sharpners Pond.

Thin section: Andesine (50%), quartz (40%), biotite, magnetite, chlorite (8%), hornblende, sericite, microcline (?) and epidote (2%). Accessories: zircon, apatite.

Texture is granoblastic; myrmekite is common; feldspar is mainly albite twinned with occasional Carlsbad twins. Biotite, magnetite and chlorite occasionally occur together, although separate grains of each are common. Crushed grains and shadowy extinction in quartz and feldspar common. Biotite is very poorly foliated, grains are occasionally bent.

Z-4

Locality: Southeast corner of Hudson Quadrangle 0.5 km south of Nutting Lake. Outcrop is roadcut along Route 3 (New Middlesex Turnpike) 0.2 km southeast of bridge over Route 3.

Thin section: Mineralogy similar to Z-1 but biotite is more common (10%) with very little chlorite or magnetite. Also, garnet is common as large hypidiomorphic grains.

Texture is granoblastic, shadowy extinction is common. Zircons occur mainly in biotite flakes; dark radiation damage halos in the biotite are common around the zircons. Feldspar is oligoclase-andesine in composition. Biotite shows no foliation but many grains are bent.

R8441

Locality: Same locality as Z-1.

Thin section: Similar to Z-1 but biotites show definite preferred orientation. Feldspars are more weathered also. Rims and patches of very fine grained clays are common on and around the feldspar grains.

R8443

Locality: Same as Z-1.

Thin section: Quartz and feldspar about equal at 45%; chlorite, magnetite and biotite make up most of the remaining 10%. Sericite common around and in feldspar grains, muscovite occasionally present. Small crystals of sillimanite also present. Other accessories include zircon, ilmenite and apatite (?).

Chlorite, magnetite and biotite are often associated. Zircons in biotite flakes often show radiation damage halos. Feldspar is andesine in composition. Quartz shows shadowy extinction. Albite and Carlsbad twinning common in feldspars.

Shawsheen Gneiss

Z-2

Locality: Northeast quadrant of Reading quadrangle, along Forest Street 2.1 km west of intersection of Forest St. and North Main St. at Wills Hill. Roadcut on north side of Forest St.

Thin section: Hornblende (35%), biotite (40%), chlorite (20%), plagioclase and hypersthene (5%). Accessories: magnetite, ilmenite, sphene, zircon, epidote.

Feldspars badly weathered, mostly polycrystalline ag-

gregates of clays and sericite. Composition approximately andesitic. Biotite and hornblende show preferred direction. Two biotites, brown and green in color. Some chlorite appears to be retrograde biotite and hornblende since relict cleavage traces are present, and the chlorite does not show a strong preferred direction. Grains of biotite and hornblende are bent and broken.

Z-3

Locality: Southeast corner of Billerica, Mass. along Middlesex Turnpike 0.1 km southeast of intersection with Lexington Road and Old Billerica Road.

Thin section: Quartz (30%), plagioclase (30%), microcline (15%), biotite (15%), magnetite and chlorite (8%), sillimanite (2%). Accessories: garnet, zircon, ilmenite.

Microcline extensively weathered to polycrystalline aggregates of sericite. Chlorite and magnetite mainly the result of breakdown of biotite; the three minerals occur almost exclusively together. Biotite shows preferred orientation. Plagioclase is andesine. Quartz gives shadowy extinction, biotite grains are bent and crushed. Interlocking al-
lotriomorphic texture.

R8399

Locality: Southeast side of Billerica and southwest corner of Wilmington Quadrangles, outcrops from along McKee Brook where it crosses the boundaries of the two quadrangles.

Thin section: Feldspar (badly weathered; 40%), quartz (35%), biotite (15%), magnetite (5%), hornblende, chlorite, sillimanite, muscovite (5%). Accessories: epidote, zircon, and ilmenite (?).

Feldspar composition is unknown because it is badly weathered to a fine grained mixture of sericite and clays. Biotites are oriented, quartz shows shadowy extinction. Biotite and hornblende also badly altered with occasional bent and broken grains.

Nashoba Formation

Z-5

Locality: Northwest corner of Billerica Quadrangle.

Ground level outcrops along dirt path that continues from the end of Gilford Street which is 0.4 km west of Westford Street along Abbot Lane. Outcrop is between the end of Gilford St. and Pine Hill Road just at the western border of the quadrangle.

Thin section: Quartz (30%), plagioclase (20%), biotite (20%), microcline (20%), magnetite and sillimanite (10%). Accessories: zircon (with occasional radiation damage halos in biotite), muscovite, kyanite.

Plagioclase is oligoclase in composition. Myrmekite well developed, texture is sheared and broken, especially evident in the quartz and feldspar grains. Cracks in grains are filled with quartz, possibly some carbonate. Feldspar and biotite are very fresh. Biotite has slight orientation and is segregated into biotite rich layers.

Z-6

Locality: West central part of Hudson Quadrangle, outcrop along Golden Run Road approximately 1.0 km southeast of intersection of Golden Run Road and Harvard Road. Sample is from rubble pile over outcrop.

Thin section: Quartz (40%), plagioclase (20%), biotite (10%), microcline (15%), sillimanite (10%), magnetite and chlorite (5%). Accessories: zircon, muscovite (?), kyanite.

Plagioclase is andesine. Sillimanite is elongate bent crystals often associated with sericite. Texture is highly cataclastic, crushed grains common. Strongly crystalline, with grains tightly interlocked; much interpenetration and embayment is evident, especially in the quartz. Myrmekitic texture well developed in many grains. Slight foliation in the biotite and sillimanite crystals.

R8381

Locality: Southwest corner of Hudson Quadrangle; roadcut on northeast corner of turnoff from Route 62 going east onto Route 495 north.

Thin section: Biotite (40%), quartz (30%), feldspar (25%), magnetite, apatite, chlorite, and sericite (5%).

Biotite shows well developed preferred orientation, many grains are bent and cracked. Quartz grains show shadowy extinction, cataclasis and recrystallization. Feldspar is microcline and oligoclase in about equal proportions. Chlor-

ite always associated with biotite and magnetite.

R8458

Locality: Southeast part of Billerica Quadrangle, along New Middlesex Turnpike (Route 3), 120 m south of the Concord River on the east side of the turnpike.

Thin section: Microcline and quartz (each about 40%), biotite (10%), sillimanite (8-10%), magnetite (about 1%).

All feldspar grains are weathered with the development of much sericite and unidentified clay minerals. Sillimanite occurs as fibrous aggregates usually within microcline grains. Quartz is strongly recrystallized and shows shadowy extinction. Quartz and feldspar grains are large and strongly interlocked. Texture is well developed crystalloblastic. Occasional myrmekite is seen.

Tadmuck Brook Schist

R8383

Locality: Southeast corner of Clinton Quadrangle, 230 m west of railroad crossing on Willow Road, West Berlin, Mass.

Thin section: Sillimanite (35%), quartz (30%), biotite (25%), magnetite, ilmenite, and unidentified fine grained groundmass (10%). Accessories include zircon (radiation damage halos observed in biotite), apatite, sphene (?) and pyrite.

Sillimanite occurs as single grains and fibrous masses that are well oriented. Quartz, sillimanite, magnetite and biotite occur in bands and lenses separated by masses of very fine grained material. This material probably consists of feldspar, carbonates (calcite?), quartz, and finely divided biotite, although definite identifications could not be made. Small folds occur in the bands and lenses. Texture is hypidiomorphic although the sillimanite crystals are well developed where aggregated.

R8455

Locality: Northeast corner of Westford Quadrangle 1300 m southeast of West Chelmsford. Approximately 50 m east of intersection of School Street and Old Westford Road. Exposure is in parking lot on southwest side of Old Westford Road.

Thin section: Quartz and oligoclase (each 40%), biotite and chlorite (15%), magnetite, ilmenite and pyrite (5%). Accessories include zircon, carbonate, and sillimanite (?).

Texture is crystalloblastic, well crystallized with no observable preferred orientation. Feldspars are badly weathered with extensive development of sericite and clays. Biotite, chlorite and magnetite almost always occur together. Quartz shows signs of strain.

Worcester Formation

R8395 - Unit 5

Locality: South face of quarry, 1660 m south-southwest of Lake Shirley, north-northwest of intersection of Fort Pond - Lunenburg Road and Route 2 in the Shirley Quadrangle.

Thin section: Quartz (50%), biotite (35%), feldspar (orthoclase ?; 10%), andalusite (3%), magnetite (1%), chlorite and sericite (1%). Accessories: zircon, carbonate, kyanite (?), sphene.

Biotites show distinct preferred orientation. Feldspars untwinned except for occasional Carlsbad twins. Feldspars show slight development of sericite. Most quartz grains show subrounded texture with moderate intergrowth, and some overgrowth of quartz is evident.

R8397 - Unit 3

Locality: From quarry near Cowdry Hill between Lake Shirley and Fort Pond, just off Leominster Road in Shirley Quadrangle.

Thin section: Very fine grained rock; mineralogy could not be definitely determined.

Very strong alignment of grains with superimposed micro-folding. Pseudo-foliation appears due to concentration of opaque minerals (carbon, magnetite, and ilmenite ?) at the noses of the folds. Extinction of mineral grains shows the true foliation to be at an angle to the folding. Very fine material is probably a combination of quartz, feldspar, sericite (muscovite), biotite and carbonate. Small veins of quartz and feldspar cut the section.

Middlesex Fells Volcanic ComplexR8422

Locality: Boston North Quadrangle, ledge just east of tennis courts 200 m northeast of Stoneham Junior High School.

Thin section: Large (1-2 mm) grains of Ca-oligoclase and Na-andesine in fine grained groundmass of quartz and feldspar (mainly oligoclase). Large biotite flakes (0.5 - 1 mm) now largely converted to chlorite and magnetite. Feldspar and biotite grains make up about 20% of rock. Feldspar makes up most of the groundmass with about 10-15% quartz. Accessories include zircon, apatite, microcline and hornblende (?).

Magnetite occurs as small grains sprinkled throughout the groundmass. Feldspars are badly weathered and sausseritized; sericite, clays and epidote are extensively developed. Very few feldspars are twinned. Large feldspar grains are corroded around the edges with large embayments. Groundmass is microcrystalline with strong interlocking of grains. Evidence of recrystallization of groundmass into larger grains is common.

R8450

Locality: Lexington Quadrangle, 1000 m northwest of Spy Pond in Menotomy Rocks Park.

Thin section: Large grains of feldspar, now almost completely converted to clays, sericite and epidote, in a fine grained groundmass of feldspar, quartz, biotite (largely converted to chlorite and magnetite), and magnetite.

Occasional large grains of biotite and magnetite are found. Some of the chlorite and epidote (about 35%) also appears to be the result of breakdown of hornblende and pyroxene although alteration is so intense that only relict traces remain.

Appendix D

Statistics and Errors

All measurements of a single parameter were assumed to be normally distributed. Parameters such as isotope ratios, spike concentrations and spike weights, which were directly used in the calculation of an isochron or Concordia point, were measured a number of times in order to determine statistics for the measurements. The standard deviation of an observation and the mean were calculated along with the mean value. Measurements outside of ± 2 standard deviations of an observation (95% confidence level) were then removed and a new mean and standard deviation calculated. For the uranium and lead isotopic ratios a slightly different procedure was used. Measurements outside of 1.4 standard deviations (85% confidence level) were removed and a new mean and standard deviation were calculated and the cleaning repeated. The procedure was terminated when no more ratios could be removed or when only 25% of the measurements remained. This course was followed because it was quite often observed with the lead and uranium data that ratios which were quite obviously bad - erratic and noisy chart readings, or spikes in the electrometer output - would still give ratios within two standard deviations of an observation. The 1.4 standard deviation level was low enough to remove many of these measurements without affecting the average to a large extent.

More measurements were made for more erratic observed data. On the average, mean isotopic ratios were based on 10 or more observed values after cleaning, although in a few cases a mean is based on as few as three measurements.

Measured values, such as sample weight, or constants, such as atomic weights, not directly involved in the calculation of isochron or Concordia diagram points, were not dealt with as accurately. Errors were either assumed based on past experience or not applied at all. The only case where errors were not attached to values used directly in isochron calculations are the constants used in Rb-Sr calculations in Appendix A. No limits of error could be found in the literature, so that it was thought better not to attach errors at all.

All errors quoted in this paper are plus or minus one standard deviation of the mean unless noted otherwise. The standard deviations of the mean for all parameters were then propagated through all calculations using the standard equations for error propagation. Thus, the errors attached to any individual isochron or Concordia point are the result of all the errors of all the measurements or constants used in calculating the point. These errors, of course, only give the quality of measurement for a point and not its overall accuracy, which depends on other factors, such as sample fractionation, sample homogeneity and equilibrium between sample and spike. Results from the replicates (Appendices A and B) sug-

gest that the true errors of the points are larger. The effects of larger errors for individual points on the regression analyses are given below.

Straight lines on isochron and Concordia diagrams were calculated using the linear least squares cubic regression equations of York (1966, 1967, 1969). For the Rb-Sr isochron diagrams, the York (1966, 1967) equations using uncorrelated errors for x and y values were used. This is reasonable since the errors in the $\text{Rb}^{87}/\text{Sr}^{86}$ and $\text{Sr}^{87}/\text{Sr}^{86}$ ratios are to a large extent independent of one another. The calculated errors in the slope and intercept using these equations (York, 1966, 1967) are independent of errors in the individual points. The slope and intercept errors are determined essentially by the scatter in the data. The errors for the individual points do affect the weighting of each point but this has a small effect on the slope and intercept and their errors. Increasing the errors on the $\text{Rb}^{87}/\text{Sr}^{86}$ and $\text{Sr}^{87}/\text{Sr}^{86}$ ratios to 4σ does not affect the slopes, intercepts and their errors discernably. The regression program is set up so that individual absolute errors for each point are not used; rather a single percentage error is attached separately to all x values and y values. For the Rb-Sr data an error of 1.0% was given to all $\text{Rb}^{87}/\text{Sr}^{86}$ ratios and an error of 0.05% was used for all $\text{Sr}^{87}/\text{Sr}^{86}$ ratios.

For the U-Pb data the regression equations using correlated errors (York, 1969) were employed. The error attached to

the $\text{Pb}^{206}/\text{U}^{238}$ ratios was 0.7%; that of the $\text{Pb}^{207}/\text{U}^{235}$ ratios was 1.4%. Because the number of replicates was small, an error correlation coefficient of 0.0 was used. The errors for the slopes and intercepts using these equations are highly dependent on the errors attached to the individual points. The changes in the upper and lower intercepts for the detrital and volcanic lines with changes in the errors of the individual points are given below.

Error correlation coefficient = 0

Errors in ages are $\pm 1\sigma$ error of the mean.

<u>Suite</u>	<u>Standard Deviation of Points</u>	<u>Upper Age (m.y.)</u>	<u>Lower Age (m.y.)</u>
Detrital	1 σ	1547 \pm 14	276.9 \pm 7.7
	2 σ	1547 \pm 28	276.9 \pm 15.5
	3 σ	1547 \pm 42	276.9 \pm 23.5
Volcanic	1 σ	741.8 \pm 43.5	271.6 \pm 21.9
	2 σ	741.8 \pm 90.7	271.6 \pm 47.3
	3 σ	741.8 \pm 141.5	271.6 \pm 76.3

Using the uncorrelated error regression equations the following results are obtained:

Detrital: Upper age = 1.55 \pm 0.06 b.y.

Lower age = 277 \pm 37 m.y.

Volcanic: Upper age = 742 \pm 93 m.y.

Lower age = 272 \pm 49 m.y.

Increasing the errors on the individual points to 4 σ does not affect these last four ages.

Next, the effect of correlation in the x and y errors must be considered. If the correlation between the $\text{Pb}^{207}/\text{U}^{235}$ and $\text{Pb}^{206}/\text{U}^{238}$ errors are 1.0 the following results are obtained (errors in both individual points and ages are $\pm 1\sigma$):

Detrital: Upper age = 1.409 ± 0.005 b.y.
Lower age = 231.8 ± 2.3 m.y.

Volcanic: Upper age = 617.1 ± 12.9 m.y.
Lower age = 189.3 ± 14.3 m.y.

For an error correlation coefficient of -1.0:

Detrital: Upper age = 1.554 ± 0.018 b.y.
Lower age = 278.9 ± 10.5 m.y.

Volcanic: Upper age = 750.4 ± 60.3 m.y.
Lower age = 275.1 ± 29.4 m.y.

For U-Pb analyses with small amounts of contamination the error correlation coefficient is approximately 1.0. However, rough calculations to determine how the error propagates through the equations used to calculate the $\text{Pb}^{207}/\text{U}^{235}$ and $\text{Pb}^{206}/\text{U}^{238}$ ratios suggests that for many of the analyses used in this paper the correlation coefficient (r) is low, approximately 0.10. This is due to the large amounts of contamination in many of the samples. Large amounts of contamination cause large errors in the corrected $\text{Pb}^{207}/\text{Pb}^{206}$ ratio. This causes a large error in the $\text{Pb}^{207}/\text{U}^{235}$ ratio while the $\text{Pb}^{206}/\text{U}^{238}$ ratio remains relatively unaffected.

Ideally, r should be determined by running enough replicate analyses to establish a trend in the x and y errors. In lieu of this it was decided to plot the percentage errors of $\text{Pb}^{207}/\text{U}^{235}$ against those of $\text{Pb}^{206}/\text{U}^{238}$ for the samples analyzed in this paper. The results are shown in Figure D-1. It can be seen that there are two trends in the data. One is a group of points with a small slope of about 0.08, while the other group has a high slope of 0.95. There is no particular correlation between various samples or zircon morphology (detrital versus volcanic) and these two groups. The correlation appears to be with the $\text{Pb}^{204}/\text{Pb}^{206}$ ratio of the unspiked aliquot. Samples with $\text{Pb}^{204}/\text{Pb}^{206}$ ratios in the unspiked aliquot of 0.002 or greater fall for the most part on the line of lower slope, while those with ratios less than 0.002 fall on the higher slope. There is some overlap but the trends and the correlation with $\text{Pb}^{204}/\text{Pb}^{206}$ ratio are fairly well defined.

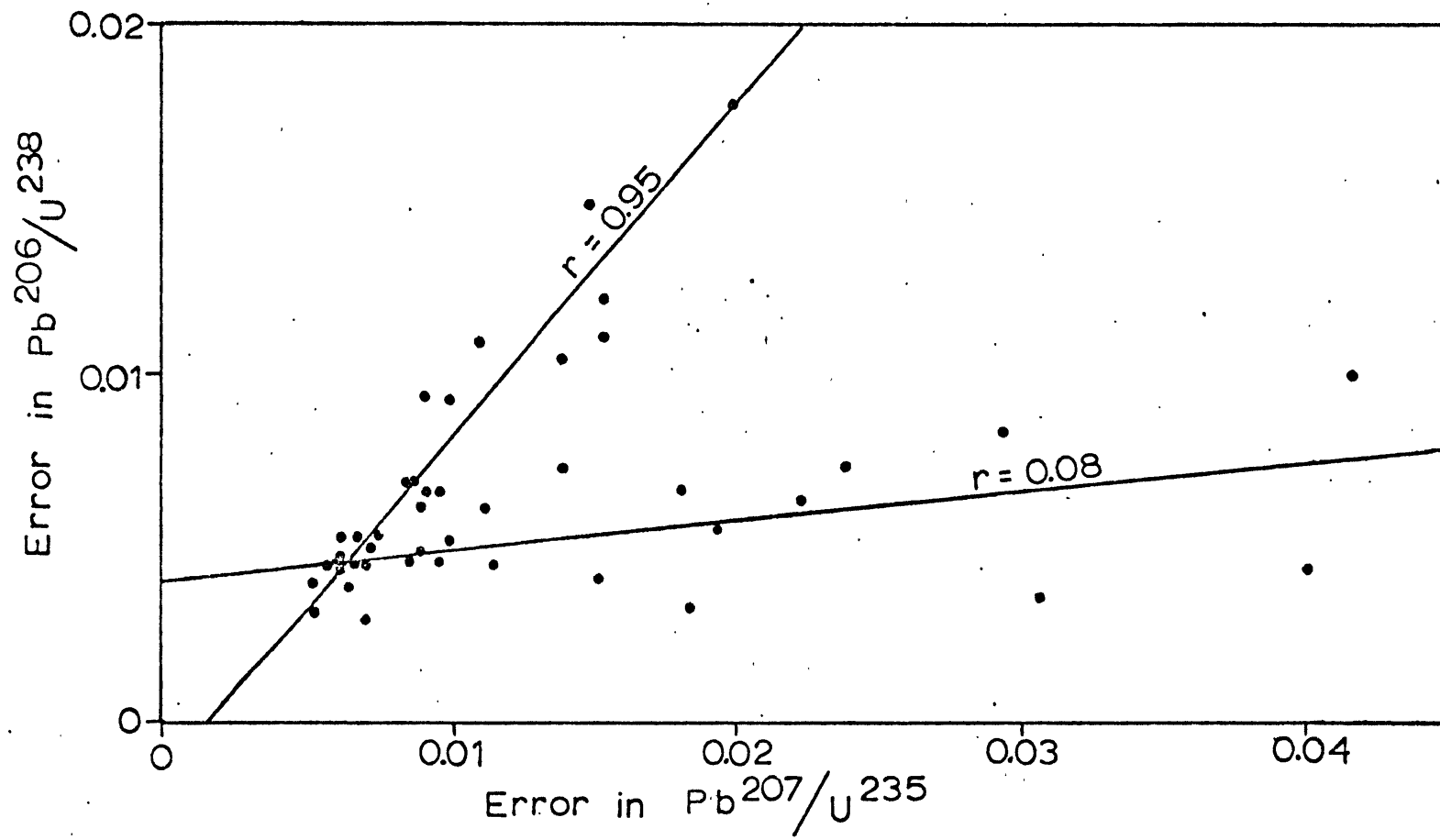
Figure D-1 suggests a way of assigning error correlation coefficients to the observed Concordia points. Samples that fall in the upper group are given an r value of 0.95. Those in the lower group are given an r value of 0.08. Using these r values for individual points and an error for the $\text{Pb}^{207}/\text{U}^{235}$ of 1.4% and an error for the $\text{Pb}^{206}/\text{U}^{238}$ of 0.7%, the correlated error regressions yield the following results:

Detrital: Upper age = 1.46 ± 0.01 b.y.

Lower age = 277 ± 4 m.y.

Figure D-1

Plot of fractional error in $\text{Pb}^{207}/\text{U}^{235}$ versus fractional error in $\text{Pb}^{206}/\text{U}^{238}$. Solid lines indicate two trends in the data, one with a slope of 0.08, the other with a slope of 0.95.



Volcanic: Upper age = 710 ± 22 m.y.
Lower age = 277 ± 11 m.y.

For the Rb-Sr isochrons the errors in age and intercepts are calculated in a straightforward manner. The error in the intercept comes directly from the regression analysis; the error in the age is simply due to the error in the slope which also comes directly from the regression data. Thus, the error in the age is simply the ages calculated at ± 1 standard deviation of the mean value of the slope. For the U-Pb data, the error in the age is more complicated. Strictly speaking, the error in the age is the point where the one standard deviation limits of the best fit line intercept Concordia. These limits are hyperbolas asymptotic to the lines representing the one standard deviation errors in the slope (Acton, 1959). These hyperbolas are difficult to calculate and it is even more difficult to calculate their intercepts with Concordia. Rough calculations show that the points of intersection, the hyperbolas and their asymptotes differ little - usually less than 1 m.y., always less than 2 m.y. So it was decided to calculate the errors in U-Pb ages using the intercepts with Concordia of lines representing $\pm 1\sigma$ errors in the mean slope. Since the value of the + deviation in age usually varied from the - deviation because of the curvature of Concordia, the highest value was taken and used as the \pm error in the age.

"When I use a word," Humpty Dumpty said, in rather a scornful tone, "it means just what I choose it to mean - neither more nor less."

"If I'd meant that, I'd have said it," said Humpty Dumpty.

"It seems very pretty," she said when she had finished it, "but it's rather hard to understand!" (You see she didn't like to confess, even to herself, that she couldn't make it out at all.)

"Somehow it seems to fill my head with ideas - only I don't exactly know what they are!"

- Lewis Carrol, Through the Looking-Glass and what Alice Found There

Long is the way, and hard,
That out of hell leads up to light.

- Milton, Paradise Lost

References Cited

- Abu-Moustafa, A.A., and Skehan, J.W., 1976. Petrography and geochemistry of the Nashoba Formation, east-central Massachusetts: in Lyons, P.C., and Brownlow, A.H. (eds.), Studies in New England Geology, Geol. Soc. Amer. Mem. 146, pp. 31-70.
- Acton, F.S., 1959. Analysis of Straight-Line Data: John Wiley and Sons, N.Y., 267 p.
- Alvord, D.C., Bell, K.G., Pease, M.H., Jr., and Barosh, P.J., 1976a. The aeromagnetic expression of bedrock geology between the Clinton-Newbury and Bloody Bluff Fault Zones, northeastern Massachusetts: U.S.G.S. J. Res., v. 4, #5, pp. 601-604.
- Alvord, D.C., Pease, M.H., Jr., and Fahey, R.J., 1976b. The pre-Silurian eugeosynclinal sequence bounded by the Bloody Bluff and Clinton-Newbury Faults, Concord, Billerica and Westford Quadrangles, Massachusetts: in Cameron, B. (ed.), Geology of Southeastern New England, N.E.I.G.C. Guidebook, 68th Ann. Mtg., Science Press, Princeton, N.J., pp. 315-333.
- Atomic Energy Commission Advisory Committee on Standards, 1962: Report #11, July.
- Ballard, R.D., and Uchupi, E., 1974. Geology of Gulf of Maine: Amer. Assn. Petrol. Geol. Bull., v. 58, #6, pp. 1156-1158.
- Barosh, P.J., 1972. Structural geology of Rhode Island and southeastern Massachusetts, as revealed by aeromagnetic data: Geol. Soc. Amer. Abstr. with Programs, v. 4, #7, pp. 444-445 (abs.).
- Barosh, P.J., 1976. Faults and related deformation in the Clinton-Newbury - Bloody Bluff Fault Complex of eastern Massachusetts: in Cameron, B. (ed.), Geology of Southeastern New England, N.E.I.G.C. Guidebook, 68th Ann. Mtg., Science Press, Princeton, N.J., pp. 301-314.
- Barosh, P.J., Fahey, R.J., and Pease, M.H., Jr., 1977. Preliminary Compilation of the Bedrock Geology of the Land Area of the Boston 2° Sheet, Massachusetts, Connecticut, Rhode Island, and New Hampshire: U.S.G.S. open file report 77-285, 142 p.
- Bell, K.G., 1967. Faults in eastern Massachusetts: Geol. Soc. Amer. Spec. Paper v. 115, p. 250 (abs.).

- Bell, K.G., and Alvord, D.C., 1976. Pre-Silurian stratigraphy of northeastern Massachusetts: in Page, L.R. (ed.), Contributions to the Stratigraphy of New England, Geol. Soc. Amer. Mem. 148, pp. 179-216.
- Berry, W.B.N., 1968. Ordovician paleogeography of New England and adjacent areas based on graptolites: in Zen, E-An et al. (eds.), Studies of Appalachian Geology, Wiley Interscience Publishers, N.Y., pp.23-34.
- Bescanson, J.R., Gaudette, H.E., and Naylor, R.S., 1977. Age of the Massabesic Gneiss, southeastern New Hampshire: Geol. Soc. Amer. N.E. Sect. Mtg., v. 9, #3, p. 242 (abs.).
- Bickel, C.E., 1976. Stratigraphy of the Belfast Quadrangle, Maine: in Page, L.R. (ed.), Contributions to the Stratigraphy of New England, Geol. Soc. Amer. Mem. 148, pp. 97-128.
- Bird, J.M., and Dewey, J.F., 1970. Lithosphere plate - continental margin tectonics and the evolution of the Appalachian Orogen: Geol. Soc. Amer. Bull., v. 81, pp. 1031 - 1060.
- Billings, M.P., 1976. Geology of the Boston Basin: in Lyons, P.C., and Brownlow, A.H. (eds.), Studies in New England Geology, Geol. Soc. Amer. Mem. 146, pp. 5-30.
- Bottino, M.L., 1963. Whole-rock Rb-Sr studies of volcanics and some related granites: in Variations in Isotopic Abundances of Strontium, Calcium, and Argon and Related Topics, M.I.T. Dept. of Geol. and Geophys. 11th Ann. Prog. Rept. to U.S.A.E.C., #NYO-10517, pp. 65-84.
- Bottino, M.L., and Fullagar, P.D., 1968. The effects of weathering on whole-rock Rb-Sr ages of granitic rocks: Amer. J. Sci., v. 266, #8, pp. 661-670.
- Bottino, M.L., Fullagar, P.D., Fairbairn, H.W., Pinson, W.H., Jr., and Hurley, P.M., 1970. The Blue Hills Igneous Complex, Massachusetts: whole-rock Rb-Sr open systems: Geol. Soc. Amer. Bull., v. 81, pp. 3739-3746.
- Boudette, E.L., and Boone, G.M., 1976. Pre-Silurian stratigraphic succession in central western Maine: in Page, L.R. (ed.), Contributions to the Stratigraphy of New England, Geol. Soc. Amer. Mem. 148, pp. 79-96.
- Brookins, D.G., 1976. Geochronologic contributions to the stratigraphic interpretation and correlation in the Penobscot Bay Area, eastern Maine: in Page, L.R. (ed.),

- Contributions to the Stratigraphy of New England, Geol. Soc. Amer. Mem. 148, pp. 129-145.
- Brookins, D.G., and Methot, R.L., 1971. Geochronological investigations in south-central Connecticut: I. Pre-Triassic basement rocks: Geol. Soc. Amer. Abstr. with Progs. N.E. Sect. Mtg., v. 3, #1, p. 20.
- Bullard, E., Everett, J.E., and Smith, A.G., 1965. The fit of the continents around the Atlantic: Phil. Trans. Roy. Soc. Lond., #A0258, pp. 41-51.
- Buma, G., Frey, F.A., and Wones, D.R., 1971. New England granites: trace element evidence regarding their origin and differentiation: Contrib. Mineral. and Petrol., v. 31, pp. 300-320.
- Cady, W.M., 1969. Regional Tectonic Synthesis of Northwestern New England and Adjacent Quebec: Geol. Soc. Amer. Mem. 120, 181 p.
- Cameron, A.E., Smith, D.H., and Walker, R.L., 1969. Mass spectrometry of nanogram-size samples of lead: Anal. Chem., v. 41, pp. 525-526.
- Cameron, B., and Naylor, R.S., 1976. General geology of southeastern New England: in Cameron, B. (ed.), Geology of Southeastern New England, N.E.I.G.C. Guidebook, 68th Ann. Mtg., Science Press, Princeton, N.J., pp. 13-27.
- Castle, R.O., 1964. Geology of the Andover Granite and Surrounding Rocks, Massachusetts: U.S.G.S. open file report, Boston, MA, 550 p.
- Castle, R.O., 1965a. A proposed revision of the subalkaline intrusive series of northeastern Massachusetts: U.S.G.S. Prof. Paper 525C, pp. C74-C80.
- Castle, R.O., 1965b. Gneissic rocks in the South Groveland Quadrangle, Essex County, Massachusetts: U.S.G.S. Prof. Paper 525C, pp. C81-C86.
- Charlot, R., 1976. The Precambrian of the Anti-Atlas (Morocco): a geochronological synthesis: Precamb. Res., v. 3, pp. 273-299.
- Clapp, C.H., 1921. Geology of the Igneous Rocks of Essex County, Massachusetts: U.S.G.S. Bull. 704, 132 p.
- Cordani, U.G., Kawashita, K., and Filho, A.T., 1976. The applicability of the rubidium strontium method to shales

and related rocks: Proc. 25th Int. Geol. Cong.,
Sydney, Australia.

- Cormier, R.F., 1969. Radiometric dating of the Coldbrook Group of southern New Brunswick, Canada: Can. J. Earth Sci., v. 6, pp. 393-398.
- Currier, L.W., 1937. The problem of the Chelmsford, Massachusetts Granite: Trans. Amer. Geophys. Union, v. 18, pp. 260-261 (abs.).
- Dalrymple, G.B., and Lanphere, M.A., 1969. Potassium-Argon Dating: W.H. Freeman and Company, San Francisco, 258 p.
- Dennen, W.H., 1976. Plutonic series in the Cape Ann area: in Cameron, B. (ed.), Geology of Southeastern New England: N.E.I.G.C. Guidebook, 68th Ann. Mtg., Science Press, Princeton, N.J., pp. 265-278.
- Dixon, H.R., 1976. Summary discussion of stratigraphy of eastern Massachusetts and Connecticut: in Page, L.R. (ed.), Contributions to the Stratigraphy of New England, Geol. Soc. Amer. Mem. 148, pp. 277-284.
- Doe, B.R., 1970. Lead Isotopes: Springer-Verlag, N.Y., 137 p.
- Eckelman, F.D., and Kulp, J.L., 1956. The sedimentary origin and stratigraphic equivalence of the so-called Cranberry and Henderson Granites in western North Carolina: Amer. J. Sci., v. 254, pp. 288-315.
- Emerson, B.K., 1917. Geology of Massachusetts and Rhode Island: U.S.G.S. Bull. 597, 289 p.
- Fairbairn, H.W., and Hurley, P.M., 1957. Radiation damage in zircon and its relation to ages of Paleozoic igneous rocks in northern New England and adjacent Canada: Trans. Amer. Geophys. Union, v. 38, pp. 99-107.
- Fairbairn, H.W., and Hurley, P.M., 1970. Northern Appalachian geochronology as a model for interpreting ages in older orogens: Eclog. Geol. Helv., v. 63, pp. 83-90.
- Fairbairn, H.W., Bottino, M.L., Pinson, W.H., Jr., and Hurley, P.M., 1966. Whole-rock age and initial $^{87}\text{Sr}/^{86}\text{Sr}$ of volcanics underlying fossiliferous lower Cambrian in the Atlantic Provinces of Canada: Can. J. Earth Sci., v. 3, pp. 509-521.

- Fairbairn, H.W., Hurley, P.M., Pinson, W.H., Jr., and Handford, L.S., 1966. Rb-Sr age of intrusives near Salem, Massachusetts: M.I.T. Geochronology Lab. 14th Ann. Prog. Rept. to U.S.A.E.C., 1381-14, pp. 173-174.
- Fairbairn, H.W., Bottino, M.L., Handford, L.S., Hurley, P.M., Heath, M.M., and Pinson, W.H., Jr., 1967a. Radiometric ages of igneous rocks in northeastern Massachusetts: Geol. Soc. Amer. Spec. Paper 115, p. 260 (abs.).
- Fairbairn, H.W., Moorbath, S., Ramo, A.O., Pinson, W.H., Jr., and Hurley, P.M., 1976b. Rb-Sr age of granitic rocks of southeastern Massachusetts and the age of the lower Cambrian at Hoppin Hill: Earth and Plan. Sci. Lett., v. 2, pp. 321-328.
- Faure, G. and Hurley, P.M., 1963. The isotopic composition of strontium in oceanic and continental basalts: J. Petrol., v. 4, pp. 31-50.
- Faure, G., and Powell, J.L., 1972. Strontium Isotope Geology: Springer-Verlag, N.Y., 188 p.
- Friedlander, G. Kennedy, J.W., and Miller, J.M., 1964. Nuclear and Radiochemistry (2nd ed.): John Wiley and Sons, N.Y., 585 p.
- Gastil, L.G., DeLisle, M., and Morgan, G., 1967. Some effects of progressive metamorphism on zircons: Geol. Soc. Amer. Bull., v. 78, pp. 879-906.
- Gates, R.M., and Martin, C.W., 1976. Pre-Devonian stratigraphy of the central section of the Western Connecticut Highlands: in Page, L.R. (ed.), Contributions to the Stratigraphy of New England: Geol. Soc. Amer. Mem. 148, pp. 301-336.
- Gebauer, D., and Grünenfelder, M., 1974. Rb-Sr whole-rock dating of late diagenetic to anchimetamorphic Paleozoic sediments in southern France (Montagne Noire): Contrib. Mineral. and Petrol., v. 47, pp. 113-130.
- Gheith, M.A., 1958. Tabulated index and bibliography of published age measurements of North America: in Variations in Isotopic Abundances of Strontium, Calcium, and Argon, and Related Topics: M.I.T. Dept. of Geol. and Geophys., 5th Ann. Prog. Rept. to U.S.A.E.C., NYO-3938, pp. 61-68.
- Goldsmith, R., 1964. Geologic map of New England - (1) general geology, (2) metamorphic zones, (3) radiometric ages: U.S.G.S. open file report, Boston, MA.

- Goldsmith, R., 1976. Pre-Silurian stratigraphy of the New London area, southeastern Connecticut: in Page, L.R. (ed.), Contributions to the Stratigraphy of New England, Geol. Soc. Amer. Mem. 148, pp. 271-275.
- Gore, R.Z., 1976a. Cataclastic and plutonic rocks within and west of the Clinton-Newbury Fault Zone, east-central Massachusetts: in Cameron, B. (ed.), Geology of Southeastern New England, N.E.I.G.C. Guidebook, 68th Ann. Mtg., Science Press, Princeton, N.J., pp. 335-344.
- Gore, R.Z., 1976b. Ayer Crystalline Complex at Ayer, Harvard and Clinton, Massachusetts: in Lyons, P.C. and Brownlow, A.H. (eds.), Studies in New England Geology, Geol. Soc. Amer. Mem. 146, pp. 103-124.
- Grew, E.S., 1971. Stratigraphy of the Worcester area of Massachusetts: Geol. Soc. Amer. Abstr. with Progs., N.E. Sect., v. 3, pp. 33-34 (abs.).
- Grew, E.S., 1976. Pennsylvanian rocks of east central Massachusetts: in Cameron, B. (ed.), Geology of Southeastern New England, N.E.I.G.C. Guidebook, 68th Ann. Mtg., Science Press, Princeton, N.J., pp. 383-404.
- Hall, B.A., Pollock, S.G., and Dolan, K.M., 1976. Lower Devonian Seboomook Formation and Matagamon Sandstone, northern Maine: a flysch basin - margin delta complex: in Page, R.L. (ed.), Contributions to the Stratigraphy of New England, Geol. Soc. Amer. Mem. 148, pp. 57-63.
- Hall, L.M., 1976. Preliminary correlation of rocks in southwestern Connecticut: in Page, R.L. (ed.), Contributions to the Stratigraphy of New England, Geol. Soc. Amer. Mem. 148, pp. 337-349.
- Handford, L.S., and staff, 1965. Rb-Sr whole rock age study of the Andover and Chelmsford Granites, Massachusetts: M.I.T. Geochronology Lab. 13th Prog. Rept. to U.S.A.E.C., 1381-13, pp. 11-14.
- Hansen, W.R., 1956. Geology and Mineral Resources of the Hudson and Maynard Quadrangles, Massachusetts: U.S.G.S. Bull 1038, 104 p.
- Heath, M.M.M., 1965. Geochronology of the Ayer Granite in the Wachusett - Marlborough Tunnel, Clinton, Massachusetts: unpubl. S.M. Thesis, M.I.T. Dept. of Geol. and Geophys., 18 p.

- Hepburn, J.C., 1976. Lower Paleozoic rocks west of the Clinton-Newbury Fault Zone, Worcester area, Massachusetts: in Cameron, B. (ed.), Geology of Southeastern New England, N.E.I.G.C. Guidebook, 68th Ann. Mtg., Science Press, Princeton, N.J., pp. 366-382.
- Hofmann, A.W., and Giletti, B.J., 1970. Diffusion of geochronologically important nuclides in minerals under hydrothermal conditions: Eclog. Geol. Helv., v. 63, #1, pp. 141-150.
- Hull, M.W., 1976. Microtechniques in Pb-U Dating of Moroccan Zircons: unpubl. S.M. Thesis, M.I.T. Dept. of Earth and Plan. Sci., 28 p.
- Hurley, P.M., 1974. Pangaeic orogenic system: Geol., v. 2, #8, pp. 373-376.
- Hurley, P.M., Boudda, A., Kafes, W.H., and Nairn, A.E.M., 1974. A plate tectonics origin for late Precambrian - Paleozoic orogenic belt in Morocco: Geol., v. 2, #7, pp. 343-344.
- Hurley, P.M., Fairbairn, H.W., Kanes, W.H., and Boudda, A., 1976. Rb-Sr whole rock age dating in the Anti-Atlas and Meseta of Morocco: M.I.T. Geochronology Lab. 21st Ann. Prog. Rept., pp. 115-126.
- Hurley, P.M., Fairbairn, H.W., Pinson, W.H., Jr., and Faure, G., 1970. K-Ar and Rb-Sr minimum ages for the Pennsylvanian section in the Narragansett Basin: Geochim. et Cosmochim. Acta, v. 18, pp. 247-258.
- Hurley, P.M., Fairbairn, H.W., Pinson, W.H., Jr., and Faure, G., 1965. Radioactive decay of Rb⁸⁷ to Sr⁸⁷ in geological science exclusive of age dating: M.I.T. Dept. of Geol. and Geophys. 13th Ann. Prog. Rept., pp. 191-194.
- Hurley, P.M., and Rand, J.R., 1969. Pre-drift continental nuclei: Science, v. 164, pp. 1229-1242.
- Jaffey, A.H., Flynn, K.F., Gelninen, L.E., Bentley, W.C., and Essling, A.M., 1971. Precision measurement of half-lives and specific activities of ²³⁵U and ²³⁸U: Phys. Rev. C, v. 4, p. 1889.
- Jäger, E., 1970. Rb-Sr systems in different degrees of metamorphism: Eclog. Geol. Helv., v. 63, pp. 163-172.

- Jahns, R.H., Willard, M.E., and White, W.S., 1959. Preliminary Bedrock Geologic Map of the Lowell - Westford area, Massachusetts: U.S.G.S. open file map, Boston, MA.
- Kaktins, U., 1976. Stratigraphy and petrography of the volcanic flows of the Blue Hills area, Massachusetts: in Lyons, P.C., and Brownlow, A.H. (eds.), Studies in New England Geology, Geol. Soc. Amer. Mem. 146, ;;. 125-141.
- Kollar, F. Russel, R.D., and Ulrych, T.J., 1960. Precision intercomparisons of lead isotope ratios, Broken Hill and Mount Isa: Nature, v. 187, pp. 754-756.
- Köppel, V., and Grünenfelder, M., 1971. A study of inherited and new formed zircons from paragneisses and granitized sediments of the Strona-Ceneri Zone (Southern Alps): Schweiz. Mineral. Petro. Mitt., v. 5, pp. 385-409.
- Kovach, A., Hurley, P.M., and Fairbairn, H.W., 1977. Rb-Sr whole rock age determinations of the Dedham Granodiorite, eastern Massachusetts: Amer. J. Sci., v. 277, pp. 905-912.
- Krogh, T.E., 1973. A low-contamination method for hydrothermal decomposition of zircon and extraction of U and Pb for isotopic age determinations: Geochim. et Cosmochim. Acta, v. 37, pp. 485-494.
- LaForge, L., 1932. Geology of the Boston area, Massachusetts: U.S.G.S. Gull. 839, 105 p.
- LeRoux, L.J., and Glendedin, L.L., 1963. Half-life of thorium-232: Proc. Nat. Conf. on Nucl. Energy, Praetoria.
- Lancelot, J.R., Vitrac, A., and Allègre, C.J., 1973. Dation U-Th-Pb des zircons grain par grain, par dilution isotopique - conséquences géologiques: Comptes Rend. Acad. Sci. Paris, Sér. D., v. 277, #20, pp. 2117-2120.
- Lancelot, J., Vitrac, A., and Allègre, C., 1976. Uranium and lead isotopic dating with grain-by-grain zircon analysis: a study of complex geological history with a single rock: Earth and Plan. Sci. Lett., v. 29, pp. 357-366.
- Ludman, A., 1976. Fossil-based stratigraphy in the Merrimack Synclinorium, central Maine: in Page, L.R. (ed.), Contributions to the Stratigraphy of New England, Geol. Soc. Amer. Mem. 148, pp. 65-78.

- Lyons, J.B., and Faul, H., 1968. Isotopic geochronology of the northern Appalachians: in Zen, E-An et al. (eds.), Studies of Appalachian Geology: Northern and Maritime, Wiley Interscience Publishers, N.Y., pp. 305-318.
- Lyons, P.C., and Krueger, H.W., 1976. Petrology, chemistry, and age of the Rattleshake Pluton and implications for other alkalic granite plutons of southern New England: in Lyons, P.C., and Brownlow, A.H. (eds.), Studies in New England Geology, Geol. Soc. Amer. Mem. 146, pp. 71-102.
- Lyons, P.C., Tiffney, B., and Cameron, B., 1976. Early Pennsylvanian age of the Norfolk Basin, southeastern Massachusetts, based on plant megafossils: in Lyons, P.C., and Brownlow, A.H. (eds.), Studies in New England Geology, Geol. Soc. Amer. Mem. 146, pp. 181-197.
- Mattinson, J.M., 1971. Preparation of ultrapure HF, HCl, and HNO₃: Carnegie Inst. Wash. Yrbk., v. 70, pp. 266-268.
- Mattinson, J.M., 1972. Preparation of hydrofluoric, hydrochloric and nitric acids at ultralow lead levels: Anal. Chem., v. 44, pp. 1715-1716.
- Montgomery, C.P.W., 1977. Uranium-Lead Isotopic Investigation of the Archean Imataca Complex, Guayana Shield, Venezuela: unpubl. Ph.D. Thesis, M.I.T. Dept. of Earth and Plan. Sci., 261 p.
- Montgomery, C.W., Hurley, P.M., Fairbairn, H.W., and Gaudette, H.E., 1977. Equilibrated domains and combined Rb-Sr and U-Pb systematics in the history of a granulite: M.I.T. Geochronology Lab. 21st Prog. Rept., pp. 1-25.
- Naylor, R.S., 1968. Origin and regional relationships of the core-rocks of the Oliverian domes: in Zen, E-An, et al., (eds.), Studies in Appalachian Geology: Northern and Maritime, Wiley Interscience Publishers, N.Y., pp. 231-240.
- Naylor, R.S., 1976. Isotopic dating and New England stratigraphy: in Page, L.R. (ed.), Contributions to the Stratigraphy of New England, Geol. Soc. Amer. Mem. 148, pp. 419-425.
- Naylor, R.S., Boone, G.H., Boudette, E.L., Ashenden, D.D., and Robinson, P., 1973. Pre-Ordovician rocks in the

- Bronson Hill and Boundary Mountain anticlinoria, New England, U.S.A.: Trans. Amer. Geophys. Union, v. 54, p. 495 (abs.).
- Naylor, R.S., Gates, T.M., and Fryer, B.J., 1969. Basement rocks in the northern Appalachians - preliminary data on the Massabesic Gneiss, Manchester area, New Hampshire: M.I.T. Geochronology Lab. 17th Ann. Prog. Rept. to U.S.A.E.C., 1381-17, pp. 21-22.
- Naylor, R.S., and Sayer, S., 1976. The Blue Hills Igneous Complex, Boston area, Massachusetts: in Cameron, B. (ed.), Geology of Southeastern New England, N.E.I.G.C. Guidebook, 68th Ann. Mtg., Science Press, Princeton, N.J., pp. 135-146.
- Nelson, A.E., 1974. Changes in nomenclature of upper Pre-cambrian to lower Paleozoic (?) formations in the Natick Quadrangle, eastern Massachusetts and their tentative correlations with rocks in Rhode Island and Connecticut: U.S.G.S. Bull. 1395-E, 15 p.
- Norton, S.A., 1976. Hoosac Formation (early Cambrian or older) on the east limb of the Berkshire Massif, western Massachusetts: in Page, L.R. (ed.), Contributions to the Stratigraphy of New England, Geol. Soc. Amer. Mem. 148, pp. 357-371.
- Oleksyshyn, J., 1976. Fossil plants of Pennsylvanian age from northwestern Narragansett Basin: in Lyons, P.C., and Brownlow, A.H. (eds.), Studies in New England Geology, Geol. Soc. Amer. Mem. 146, pp. 143-180.
- Ostic, R.G., Russel, R.D., and Stanton, R.L., 1967. Additional measurements of the isotopic composition of lead from stratiform deposits: Can. J. Earth Sci., v. 4, pp. 245-269.
- Page, L.R., 1968. Devonian plutonic rocks in New England: in Zen, E-An et al. (eds.), Studies of Appalachian Geology: Northern and Maritime, Wiley Interscience Publishers, N.Y., pp. 371-383.
- Page, L.R., 1976. Introduction and Summary: in Page, L.R. (ed.), Contributions to the Stratigraphy of New England, Geol. Soc. Amer. Mem. 148, pp. 1-24.
- Pankiowskyj, K.A., Ludman, A., Griffin, J.R., and Berry, W.B. N., 1976. Stratigraphic relationships on the southeast limb of the Merrimack Synclinorium in central and west-central Maine: in Lyons, P.C., and Brownlow, A.H. (eds.),

- Studies in New England Geology, Geol. Soc. Amer. Mem. 146, pp. 263-280.
- Peck, J.H., 1976. Silurian and Devonian stratigraphy in the Clinton Quadrangle, central Massachusetts: in Page, L.R. (ed.), Contributions to the Stratigraphy of New England, Geol. Soc. Amer. Mem. 148, pp. 241-252.
- Peper, J.D., and Pease, M.H., Jr., 1976. Summary of stratigraphy in the Brimfield area, Connecticut and Massachusetts: in Page, L.R. (ed.), Contributions to the Stratigraphy of New England, Geol. Soc. Amer. Mem. 148, pp. 253-270.
- Peterman, Z.E., Hedge, C.E., and Tourtelot, H.A., 1970. Isotopic composition of Sr in sea water throughout Phanerozoic time: Geochim. et Cosmochim. Acta, v. 34, pp. 105-120.
- Pidgeon, R.T., Köppel, V., and Grünenfelder, M., 1970. U-Pb isotopic relationships in zircon suites from a para- and ortho-gneiss from the Ceneri Zone, southern Switzerland: Contrib. Mineral. and Petrol., v. 26, pp. 1-11.
- Poldervaart, A., 1955. Zircons in Rocks: 1 - Sedimentary Rocks: Amer. J. Sci., v. 253, pp. 433-461.
- Poldervaart, A., 1956. Zircons in Rocks: 2 - Igneous Rocks: Amer. J. Sci., v. 254, pp. 521-544.
- Quinn, A.W., 1971. Bedrock Geology of Rhode Island: U.S.G.S. Bull. 1295, 68 p.
- Ratcliffe, N.M., and Zartman, R.E., 1976. Stratigraphy, isotopic ages, and deformational history of basement and cover rocks of the Berkshire Massif, southwestern Massachusetts: in Page, L.R. (ed.), Contributions to the Stratigraphy of New England: Geol. Soc. Amer. Mem. 148, pp. 373-412.
- Rodgers, J., 1952. Absolute ages of radioactive minerals from the Appalachian Region: Amer. J. Sci., v. 250, pp. 411-427.
- Rodgers, J., 1970. The Tectonics of the Appalachians: Wiley Interscience Publishers, N.Y., 271 p.
- Saxena, S.K., 1966. Evolution of zircons in sedimentary and metamorphic rocks: Sedimentology, v. 6, pp. 1-33.

- Schenk, P.E., 1971. Southeastern Atlantic Canada, northwestern Africa, and continental drift: Can. J. Earth Sci., v. 8, pp. 1218-1251.
- Schnabel, R.W., 1976. Pre-Silurian stratigraphy in south-central Massachusetts and north-central Connecticut: in Page, L.R. (ed.), Contributions to the Stratigraphy of New England, Geol. Soc. Amer. Mem. 148, pp. 285-299.
- Schutts, L.D., Brecher, A., Hurley, P.M., Montgomery, C.W., and Krueger, H.W., 1976. A case study of the time and nature of paleomagnetic resetting in a mafic complex in New England: Can. J. Earth Sci., v. 13, pp. 898-907.
- Semenenko, N.P., 1970. Geochronological aspects of stabilization of continental Precambrian platforms: Eclog. Geol. Helv., v. 63, pp. 301-310.
- Shride, A.F., 1976a. Stratigraphy and structural setting of the Newbury Volcanic Complex, northeastern Massachusetts: in Cameron, B. (ed.), Geology of Southeastern New England, N.E.I.G.C. Guidebook, 68th Ann. Mtg., Science Press, Princeton, N.J., pp. 291-300.
- Shride, A.F., 1976b. Stratigraphy and correlation of the Newbury Volcanic Complex, northeastern Massachusetts: in Page, L.R. (ed.), Contributions to the Stratigraphy of New England, Geol. Soc. Amer. Mem. 148, pp. 147-177.
- Silver, L.T., 1963. The relation between radioactivity and discordance in zircons: Nucl. Geophys., NAC-NRC Publ. 1075, Rept #38, pp. 34-42.
- Silver, L.T., and Deutsch, S., 1963. Uranium-lead isotopic variations in zircons: a case study: J. Geol., v. 71, pp. 721-758.
- Skehan, J.W., 1968. Fracture tectonics of southeastern New England as illustrated by the Wachusett - Marlborough Tunnel, east-central Massachusetts: in Zen, E-An, et al., (eds.), Studies of Appalachian Geology: Northern and Maritime, Wiley Interscience Publishers, N.Y., pp. 281-290.
- Skehan, J.W., 1969. Tectonic framework of southern New England and eastern New York: in Kay, M. (ed.), North Atlantic - Geology and Continental Drift: A Symposium, Amer. Assoc. Petrol. Geol. Mem. 12, pp. 793-814.
- Skehan, J.W. and Abu-Moustafa, A.A., 1976. Stratigraphic analysis of rocks exposed in the Wachusett - Marlborough

- Tunnel, east-central Massachusetts: in Page, L.R. (ed.), Contributions to the Stratigraphy of New England, Geol. Soc. Amer. Mem. 148, pp. 217-240.
- Stacey, J.S., and Stern, T.W., 1973. Revised Tables for the Calculation of Lead Isotope Ages: U.S.G.S. Rept. #GD-73-016, 37 p.
- Stockwell, C.H., 1968. Geochronology of stratified rocks of the Canadian Shield: Can. J. Earth Sci., v. 5, pp. 693-698.
- Theokritoff, G., 1968. Cambrian biogeography and biostratigraphy in New England: in Zen, E-An, et al., Studies of Appalachian Geology: Northern and Maritime, Wiley Interscience Publishers, N.Y., pp. 9-22.
- Thompson, J.B., Jr., and Norton, S.A., 1968. Paleozoic regional metamorphism in New England and adjacent areas: in Zen, E-An, et al., (eds.), Studies of Appalachian Geology: Northern and Maritime, Wiley Interscience Publishers, N.Y., pp. 319-327.
- Thompson, J.B., Jr., and Robinson, P., 1976. Geologic setting of the Harvard Conglomerate, Harvard, Massachusetts: in Cameron, B. (ed.), Geology of Southeastern New England, N.E.I.G.C. Guidebook, 68th Ann. Mtg., Science Press, Princeton, N.J., pp. 345-351.
- Thompson, J.B., Jr., Robinson, P., Clifford, T.N., and Trask, N.J., Jr., 1968. Nappes and gneiss domes in west-central New England: in Zen, E-An, et al. (eds.), Studies of Appalachian Geology: Northern and Maritime, Wiley Interscience Publishers, N.Y., pp. 203-218.
- Tilton, G.R., 1960. Volume diffusion as a mechanism for discordant lead ages: J. Geophys. Res., v. 65, pp. 2933-2945.
- Tilton, G.R., 1965. Compilation of Phanerozoic geochronological data for eastern North America: in Wetherill, G. W. (ed.), Geochronology of North America, NAS-NRC, Nucl. Sci. Serv., Rept. #41, Publ. 1276, pp. 181-220.
- Toulmin, P., III, 1964. Bedrock Geology of the Salem Quadrangle and Vicinity, Massachusetts: U.S.G.S. Bull. #1163-A, pp. A1-A79.
- Turner, F.J., 1968. Metamorphic Petrology, Mineralogical and Field Aspects: McGraw-Hill, N.Y., 403 p.

- United States Geological Survey, 1967. Age of plutonism in eastern Massachusetts: U.S.G.S. Prof. Paper 575A, pp. A166-A167.
- Veizer, J., and Compston, W., 1974. $^{87}\text{Sr}/^{86}\text{Sr}$ composition of seawater during the Phanerozoic: Geochim. et Cosmochim. Acta, v. 38, pp. 1461-1484.
- Veizer, J., and Compston, W., 1976. $^{87}\text{Sr}/^{86}\text{Sr}$ in Precambrian carbonates as an index of crustal evolution: Geochim. et Cosmochim. Acta, v. 40, pp. 905-914.
- Wasserburg, G.J., 1963. Diffusion processes in lead-uranium systems: J. Geophys. Res., v. 68, pp. 4823-4846.
- Webber, G.R., Hurley, P.M., and Fairbairn, H.W., 1956. Relative ages of eastern Massachusetts granites by total lead ratios in zircon: Amer. J. Sci., v. 254, pp. 574-583.
- Wetherill, G.W., 1956. Discordant uranium-lead ages: Trans. Amer. Geophys. Union, v. 37, pp. 320-326.
- Whitney, P.R. and Hurley, P.M., 1964. The problem of inherited radiogenic strontium in sedimentary age determinations: Geochim. et Cosmochim. Acta, v. 28, pp. 425-436.
- Whitney, P.R., and staff, 1961. Authigenic versus allogenic Rb-bearing components in shales by growth of Sr^{87} : in Variations in Isotopic Abundances of Strontium, Calcium, and Argon and Related Topics, M.I.T. Dept. of Geol. and Geophys. 9th Ann. Prog. Rept. to U.S.A.E.C., NYO-3942, pp. 259-262.
- Williams, H., 1964. The Appalachian in northeastern Newfoundland - a two-sided symmetrical system: Amer. J. Sci., v. 262, pp. 1137-1158.
- Wilson, J.T., 1966. Did the Atlantic close and then re-open?: Nature, v. 211, pp. 676-681.
- York, D., 1966. Least-squares fitting of a straight line: Can. J. Earth Sci., v. 44, pp. 1079-1086.
- York, D., 1967. The best isochron: Earth and Plan. Sci. Lett., v. 2, pp. 479-482.
- York, D., 1969. Least squares fitting of a straight line with correlated errors: Earth and Plan. Sci. Lett., v. 5, pp. 320-324.

- Zartman, R.E., 1965. The isotopic composition of lead in microclines from the Llano uplift, Texas: J. Geophys. Res., v. 70, pp. 965-975.
- Zartman, R.E., Hurley, P.M., Krueger, H.W., and Giletti, B.J., 1970. A Permian disturbance of K-Ar radiometric ages in New England - its occurrence and cause: Geol. Soc. Amer. Bull., v. 81, pp. 3359-3373.
- Zartman, R.E., and Marvin, R.F., 1971. Radiometric age (late Ordovician) of the Quincy, Cape Ann and Peabody Granites from eastern Massachusetts: Geol. Soc. Amer. Bull., v. 82, pp. 937-958.
- Zartman, R.E., and Naylor, R.S., 1972. Structural implications of some U-Th-Pb zircon isotopic ages of igneous rocks in eastern Massachusetts: Geol. Soc. Amer. Abstr. with Progs., N.E. Sect., v. 4, pp. 54-55 (abs.).
- Zartman, R.E., Snyder, G., Stern, T.W., Marvin, R.F., and Buckman, R.C., 1965. Implications of new radiometric ages in eastern Connecticut and Massachusetts: U.S.G.S. Prof. Paper 525D, pp. D1-D10.
- Zen, E-An, 1968. Introduction: in Zen, E-An, et al. (eds.), Studies of Appalachian Geology: Northern and Maritime, Wiley Interscience Publishers, N.Y., pp. 1-5.
- Zen, E-An, 1972. The Taconide Zone and the Taconide Orogeny in the Western Part of the Northern Appalachian Orogen: Geol. Soc. Amer. Spec. Paper 135, 72 p.
- Zen, E-An, 1976. Taconic "room problem", North Adams gap, and time of formation of basement-related nappes in southwestern New England: Discussion of papers by Harwood, Norton, and Ratcliffe and Zartman: in Page, L.R. (ed.), Contributions to the Stratigraphy of New England, Geol. Soc. Amer. Mem. 148, pp. 413-417.